Short Papers in Geology and Hydrology, Articles 60–119

GEOLOGICAL SURVEY RESEARCH 1962

GEOLOGICAL SURVEY PROFESSIONAL PAPER 450-C

Scientific notes and summaries of investigations prepared by members of the Geologic and Water Resources Divisions in the fields of geology, hydrology, and allied sciences

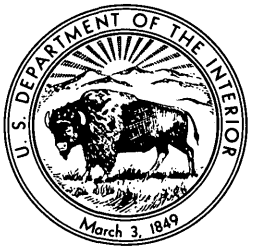

UNITED STATES GOVERNMENT PRINTING OFFICE, WASHINGTON : 1962

UNITED STATES DEPARTMENT OF THE INTERIOR

STEWART L. UDALL, *Secretary*

GEOLOGICAL SURVEY

Thomas B. Nolan, *Director*

For sale by the Superintendent of Documents, U.S. Government Printing Office
Washington 25, D.C.

FOREWORD

This collection of 60 short papers on subjects in the fields of geology, hydrology, and related sciences is the second of a series to be released during the year as chapters of Professional Paper 450. The papers in this chapter report on the scientific and economic results of current work by members of the Geologic and Water Resources Divisions of the United States Geological Survey. Some of the papers announce new discoveries or present observations on problems of limited scope; other papers draw conclusions from more extensive or continuing investigations that in large part will be discussed in greater detail in reports to be published in the future.

Chapter A of this series, to be published later in the year, will present a synopsis of results from a wide range of work done during the present fiscal year.

Thomas B. Nolan

THOMAS B. NOLAN,
Director.

CONTENTS

GEOLOGICAL SURVEY RESEARCH 1962

SHORT PAPERS IN GEOLOGY AND HYDROLOGY, ARTICLES 60–119

GEOLOGIC STUDIES

ECONOMIC GEOLOGY

60. EOCENE TOPOGRAPHY OF THE CENTRAL EAST TINTIC MOUNTAINS, UTAH

By HAL T. MORRIS and JAMES A. ANDERSON, Menlo Park, Calif., and Bear Creek Mining Co., Salt Lake City, Utah

Geologic mapping, mine workings, and drill holes have disclosed a partly exhumed surface of strong relief, which is carved on Paleozoic sedimentary rocks, underlying the volcanic rocks of the Tintic, East Tintic, and North Tintic mining districts in central Utah. At Long Ridge, a few miles southeast of the Tintic district, Muessig (1951) has shown that these volcanic rocks interfinger with limestones, shales, and bentonitic tuffs which he assigned to the upper part of the Green River Formation, of early and middle Eocene age. The topography of the prevolcanic surface thus gives some indication of the geomorphic conditions that existed along the western margin of the Eocene Lake Uinta (Bradley, 1929, 1931). Detailed knowledge of the configuration of the prevolcanic surface and of its displacement by postvolcanic faulting is useful, also, in mineral exploration and mine development. Large silver-lead-zinc replacement ore bodies commonly occur in the rocks below the erosion surface, and they can be reached at least expense where the cover of barren lavas is relatively thin.

Contours of the prevolcanic surface (fig. 60.1) indicate that it is similar to the present surface in general relief, and that the ridges and peaks of Paleozoic rocks that now rise above the lavas are Eocene topographic prominences from which the less resistant, commonly altered tuffs and lavas have been removed by erosion.

Most of the prevolcanic surface was drained by several valleys that unite near the Homansville shaft to form a major drainage course that trends eastward through the area between the Copper Leaf and North Lily shafts. Shorter valleys that also drain eastward parallel to the main drainage course have been recognized north and south of Pinyon Peak and south of the Tintic Standard No. 2 shaft. None of these valleys have breached their headlands, and all are V-shaped, with moderate to steep walls, indicating that erosion at the time of the eruptions of the Eocene volcanic rocks was in the middle youthful stage. All the major valleys drained eastward with moderately steep gradients, indicating that the basin occupied by ancient Lake Uinta was bordered on the west by a considerably higher area. The total relief of this highland within the contoured area was at least 4,400 feet and probably much greater. This is indicated by the great thickness of lava 1.4 miles southeast of the Independence shaft, where a drill hole was bottomed in lava at an elevation of about 3,100 feet, 1,300 feet below the lowest contour shown on figure 60.1.

The present configuration of the prevolcanic surface (fig. 60.2) has been greatly affected by faults, some of them older and some of them younger than the volcanic rocks. Many of the larger tributary valleys are alined with major faults that terminate at the base of the volcanic rocks. The steep side slopes of several of these valleys, including the unusually steep surface near the Chief No. 2 shaft, were probably formed by rapid erosion of the sheared and brecciated rocks adjacent to these faults before the eruption of the lavas.

The maximum postvolcanic displacement, estimated to be at least 1,400 feet, occurred on the system of linked faults near the Selma shaft, in the north-central part of the map area. South of the intersection of the Selma fault with the prevolcanic

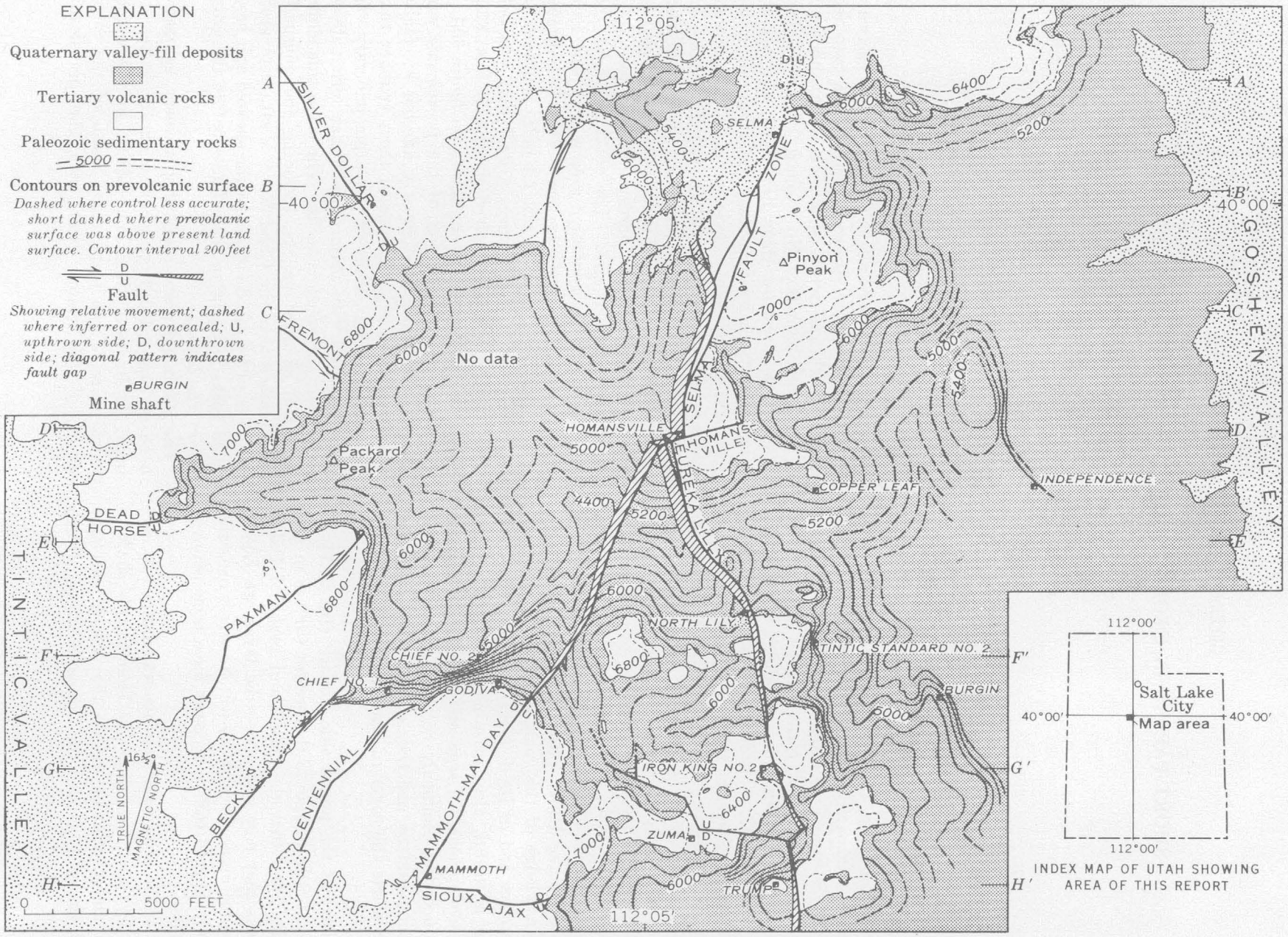

FIGURE 60.1.—Simplified geologic map of the central East Tintic Mountains, Utah, showing topography of the prevolcanic surface. Postvolcanic intrusive rocks not shown. Datum is sea level.

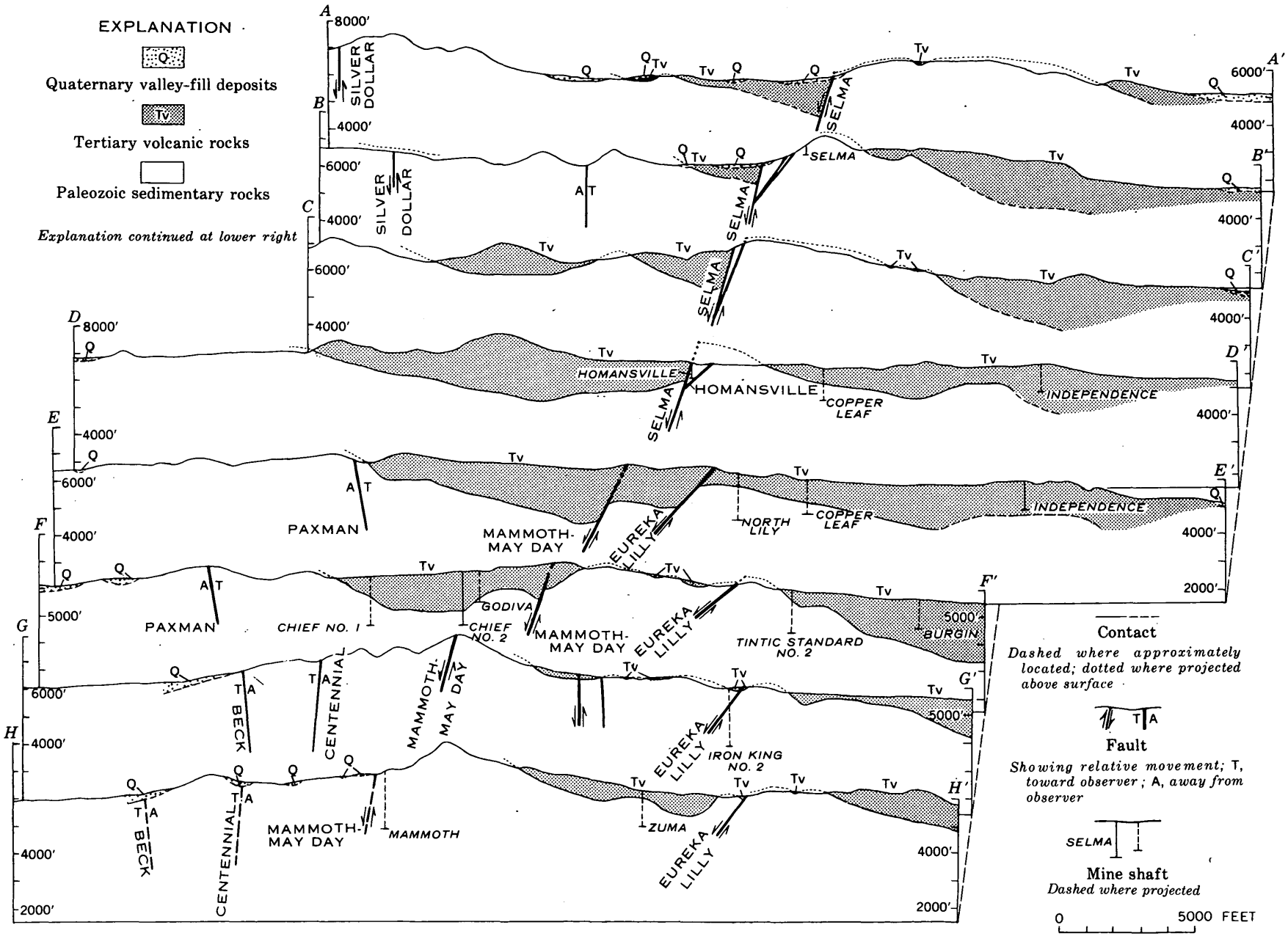

FIGURE 60.2.—Simplified geologic sections of the central East Tintic Mountains, Utah. Datum is sea level.

Homansville fault, this displacement is distributed on the Mammoth-May Day and Eureka Lilly faults. The postvolcanic displacement on both of these faults also diminishes southward from the vicinity of the Homansville fault. On the Mammoth-May Day fault the displacement decreases from about 800 feet near the Homansville fault to about 100 feet near the Godiva shaft, and on the Eureka Lilly fault it decreases from about 600 feet near the Homansville shaft to less than 50 feet near the Iron King No. 2 shaft, but the displacement on a southerly continuation of the Eureka Lilly fault increases southward from the vicinity of the Trump shaft.

Ore bodies deposited during the final stages of volcanism are not appreciably displaced by the Selma, Mammoth-May Day, and Eureka Lilly faults. This relationship suggests that these faults were chiefly formed during the early and perhaps most violent parts of the volcanic interval and probably became essentially inactive before the latest lava flows were erupted.

The most important concealed ore bodies in the East Tintic Mountains were mined or developed through the Chief No. 1, Godiva, North Lily, Tintic Standard No. 2, and Burgin shafts. These ore deposits, excepting the Burgin, are overlain by altered volcanic rocks near the edge of the lava field (Lovering and others, 1949) and were found in geological environments that were reasonably well known from nearby exposures of the sedimentary host rocks. The Burgin ore bodies were discovered recently as a result of studies of hydrothermal alteration, geochemical exploration, and an analysis of concealed geologic structures in favorable sedimentary host rocks beneath the barren volcanic rocks (Bush, Cook, Lovering, and Morris, 1960). Exploration for other concealed deposits like the Burgin will continue to be based on these methods, but engineering and economic considerations are likely to prohibit exploration of target areas overlain by a thick cover of volcanic rocks. The areas in which the volcanic cover is thin consist chiefly of buried extensions of the prevolcanic ridges and include the area north-northwest of the Independence shaft, the vicinity of the Copper Leaf shaft, the areas east of the Tintic Standard No. 2 shaft and south of the Burgin shaft, and that around the Trump shaft. Areas near the central parts of deep prevolcanic valleys, on the other hand, such as those between the Chief No. 2 and Homansville shafts, between the North Lily and Copper Leaf shafts, and the one generally east of the Burgin shaft, can be explored only at great economic risk by probing through a thick cover of barren volcanic rocks.

REFERENCES

Bradley, W. H., 1929, The varves and climate of the Green River epoch: U.S. Geol. Survey Prof. Paper 158–E, p. 87–110.

——— 1931, Origin and microfossils of the oil shale of the Green River formation of Colorado and Utah: U.S. Geol. Survey Prof. Paper 168.

Bush, J. B., Cook, D. R., Lovering, T. S., and Morris, H. T., 1960, The Chief Oxide-Burgin area discoveries, East Tintic district, Utah; a case history: Econ. Geology, v. 55, no. 6, p. 1116–1147, and no. 7, p. 1507–1540.

Lovering, T. S., and others, 1949, Rock alteration as a guide to ore—East Tintic district, Utah: Econ. Geology Mon. 1, 65 p.

Muessig, Siegfried, 1951, Eocene volcanism in central Utah: Science, v. 114, no. 2957, p. 234.

61. A RARE SODIUM NIOBATE MINERAL FROM COLORADO

By Raymond L. Parker, John W. Adams, and Fred A. Hildebrand, Denver, Colo.

A rare sodium niobate mineral with perovskite-type structure has been found at the old vermiculite mine at Gem Park, Colo., about 3½ miles east of Hillside, Fremont County. The discovery of the mineral was incidental to an examination of a radioactive sample submitted by Messrs. R. R. Gresham and L. C. Knobbe of Westcliffe, Colo. Subsequent to the identification of sodium niobate in the sample, the discovery locality was visited and a sufficient quantity of the niobium-bearing rock was collected for detailed study.

The sodium niobate mineral at Gem Park is the first reported occurrence in the United States and appears to be the third known occurrence in the world. The same mineral, or a nearly identical one, was found previously in Greenland and was given the name igdloite (Danø and Sørensen, 1959). Sodium niobate was found also in the Republic of the

Congo and was assigned the name lueshite (Safiannikoff, 1959). The use of either proposed mineral name is purposely avoided in this preliminary report because the nomenclature is in dispute. A more comprehensive report is being prepared in which the nomenclature of the mineral is discussed.

The identification of the Colorado sodium niobate was made by comparison of its X-ray powder data with powder data of the mineral from the Republic of the Congo.

The sodium niobate mineral at Gem Park occurs in a friable, altered mafic rock composed principally of "vermiculite," with smaller amounts of asbestiform actinolite-tremolite, magnetite, ilmenite, sericitized feldspar(?), barite, calcite, pyrochlore, and unidentified minerals containing thorium and uranium. The rock is radioactive and is apparently a part of a mafic (alkalic?) complex of unknown extent.

Sodium niobate at Gem Park occurs mostly as euhedral cube-shaped crystals. Optical and X-ray examinations show that the mineral is orthorhombic (pseudocubic). Some crystals are as large as 1 mm across, but most of them are less than ½ mm. The crystals appear black and opaque, but the edges of fragments are translucent and are reddish brown. The powdered mineral is light gray. Many crystals are striated parallel to pseudocube face-diagonals and some show crude cubic cleavage. Some crystals contain inclusions of actinolite-tremolite that are oriented parallel to the striae. Interpenetrating cube twins are common.

The physical properties of the Gem Park mineral are summarized in table 61.1. A spectrographic analysis and X-ray powder data are presented in tables 61.2 and 61.3 respectively. The close correspondence

TABLE 61.1.—*Physical properties of the sodium niobate mineral from Gem Park, Fremont County, Colo.*

Color	Crystals opaque, black; fragments reddish brown; powder light gray; in thin section violet brown, in polished section light gray.
Luster	Vitreous.
Properties in transmitted light.	Extinction parallel; $2V(+) \approx 45°$; birefringence low; relief very high.
Properties in reflected light.[1]	Reflection pleochroism (weak) slightly bluish in one direction in air, gray to purplish gray in oil; anisotropism weak; internal reflection variable; hardness—scratches with needle; nonreactive with HNO_3, HCl, KCN, $FeCl_3$, KOH, $HgCl_2$, or aqua regia; $\bar{R}_{orange}=13.2$ percent in air, ≈ 3 percent in oil; indices of refraction calculated from reflectivity measurements—$nZ'_{calc} \approx 2.16$ and $nX'_{calc} \approx 2.13$ (absorption coefficient is neglected, true indices of refraction are possibly greater than those calculated).
Other	Nonmagnetic.

[1] Determined by B. F. Leonard, U.S. Geological Survey.

TABLE 61.2.—*Semiquantative spectrographic analysis, in percent, of sodium niobate from Gem Park, Colo.*

[Analyst: Nancy M. Conklin, U.S. Geological Survey]

Nb	Major constituent.	Mg	0.5
Na	Major constituent.	Sr	.5
Ti	7	Pb	.15
Th	5	Pr	.1
Ce	2	Sm	<.1
Ca	1.5	Zr	<.1
La	1	Al	<.1
Si	≈.5	Mn	.05
Fe	.7	Ba	.015
Nd	.7	Y	<.01

Looked for but not found: K, P, Ag, As, Au, B, Be, Cd, Co, Cr, Cu, Ga, Ge, Hf, Hg, In, Mo, Ni, Pd, Pt, Re, Sb, Sc, Sn, Ta, Te, Tl, U, V, W, Yb, Zn, Gd, Tb, Dy, Ho, Er, Tm, Lu.

TABLE 61.3.—*X-ray powder diffraction data for sodium niobate from Gem Park, Colo., and Lueshe, Republic of the Congo, compared with synthetic sodium niobate*

Gem Park, Colo.[1]		*Lueshe, Republic of the Congo*[2]		*Synthetic $NaNbO_3$*[3]	
d(A)	*I*	*d*(A)	*I*	*d*(A)	*I*
3. 90	84	3. 91	100	3. 93	90
				3. 85	90
2. 76	100	2. 77	69	2. 77	90
				2. 74	100
				2. 59	5
				2. 44	20
				2. 37	10
				2. 34	10
		2. 26	3	2. 25	20
				2. 24	20
1. 949	70	1. 96	34	1. 96	80
		1. 955	43	1. 94	60
				1. 78	5
1. 746	35	1. 748	19	1. 75	50
				1. 74	90
				1. 66	20
				1. 653	5
1. 594α_1	70	1. 596	30	1. 598	50
				1. 583	90+
				1. 537	5
				1. 523	15
1. 379α_1	25	1. 385	3	1. 389	40
		1. 382	12	1. 377	80
1. 300α_1	11	1. 302	7	1. 302	50
				1. 295	60
				1. 265	10
				1. 242	20
1. 235α_1	15	1. 236	7	1. 236	70
		1. 234	8		
1. 176α_1	2	1. 178	2		
1. 128α_1	3	1. 127	2. 5		
1. 083α_1	2	1. 083	2		
1. 044α_1	15	1. 043	8		
. 9768α_1	2	. 977	1		
		. 976	2		
. 9473α_1	4	. 948	2		
		. 946	3		
. 9210α_1	6	. 921	3		
		. 918	4		
. 8958α_1	2	. 895	. 5		
. 8736α_1	4	. 874	2		
		. 871	3		
. 8527α_1	2	. 852	2		
		. 850	2. 5		
. 8331α_1	3	. 832	2. 5		
. 7976α_1	4	. 796	2		

[1] Sodium niobate mineral from Gem Park, Fremont County, Colo. Film D. 6298; 114.59-mm diameter camera, CuKα (Ni filter), λ=1.5418 A, λ for Kα_1=1.5405 A; shrinkage correction applied; intensities by calibrated, successive steps ($\sqrt{2}$) film strips.

[2] Sodium niobate mineral (Lueshite) from Lueshe, 150 km north of Goma, Republic of the Congo (Safiannikoff, 1959, p. 1254).

[3] Synthetic sodium niobate from ASTM card 9-103 from data furnished by Elizabeth A. Wood (Wood, 1951).

of X-ray powder data of the minerals from Gem Park, Colo., and the Republic of the Congo to the synthetic sodium niobate shows that they are identical, barring minor impurities and minor elements in isomorphous substitution. Rare earths, titanium, and calcium are believed to be a compositional part of the Gem Park mineral because no mineral phase other than sodium niobate was detectable in the powder patterns of the purified mineral. Substitution of rare earths and calcium in the sodium position in the mineral with corresponding substitution of Ti for Nb would indicate a trend in composition toward perovskite ($CaTiO_3$) with which $NaNbO_3$ is isostructural. Thorium may or may not be a compositional part of the mineral.

REFERENCES

Danø, M., and Sørensen, H., 1959, An examination of some rare minerals from the nepheline syenites of southwest Greenland: Medd. om Grønland, v. 162, no. 5, p. 25–27.

Safiannikoff, A., 1959, Un nouveau mineral de niobium: Acad. royale sci. d'outre-mer, Bull. 5, p. 1251–1255.

Wood, E. A., 1951, Polymorphism in potassium niobate, sodium niobate, and other ABO_3 compounds: Acta Cryst., v. 4, p. 353–362.

62. LOCALIZATION OF THE URAVAN MINERAL BELT BY SEDIMENTATION

By Daniel R. Shawe, Denver, Colo.

Work done in cooperation with the U.S. Atomic Energy Commission

Uranium-vanadium deposits were localized in the Uravan mineral belt at least partly by favorable lithology in the Salt Wash Member of the Morrison Formation of Late Jurassic age. Perhaps structural deformation in southwestern Colorado and southeastern Utah during deposition of the Salt Wash induced differences in sedimentation that account for the favorable lithology.

Most of the uranium-vanadium deposits in the Salt Wash Member are elongate tabular bodies oriented parallel to sedimentary structures. Uranium and vanadium minerals impregnate the thicker parts of sandstone layers. The deposits are most abundant in the upper part ("ore-bearing sandstone") of the member.

The Uravan mineral belt is an arcuate zone about 75 miles long, concave to the west, in western Colorado and eastern Utah (Fischer and Hilpert, 1952). The belt is characterized by abundant closely spaced deposits, many of which are larger than deposits in the Salt Wash elsewhere in the Colorado Plateau. Ore bodies within the mineral belt show a striking radial orientation through the arc of the belt (Fischer and Hilpert, 1952, pl. 2), reflecting a similar orientation of sedimentary structures.

The Salt Wash Member was deposited as a broad fan-shaped alluvial plain or apron by aggrading streams (Craig and others, 1955, p. 150–151). The source area as indicated by orientation of sedimentary structures, by facies changes, and by the position of the apex of the alluvial apron probably lay in west-central Arizona and southeastern California. The configuration of the alluvial apron of the Salt Wash is shown in figure 62.1*A*.

The Salt Wash Member consists of interlayered fluvial sandstone and flood-plain-type mudstone strata. In the vicinity of the Uravan mineral belt, a thick and extensive layer of sandstone—the ore-bearing sandstone—makes up the upper part of the member. This layer is notable for the abundance of fluvial crossbedding, cut-and-fill structures, and carbonaceous material (carbonized plant remains). West of the mineral belt, the sandstone is crossbedded and contains abundant cut-and-fill bedding, but carbonaceous material disappears abruptly along the west edge of the belt (John E. Motica, oral communication). Where carbonaceous material is present locally farther west, ore deposits also occur. East of the mineral belt, strata at the horizon of the ore-bearing sandstone appear to be more flat bedded and contain a higher proportion of mudstone, suggestive of deposition under conditions of quieter water (Fischer and Hilpert, 1952, p. 6; McKay, 1955, p. 272 and pl. 13).

The orientation of sedimentary structures and the distribution of lithologies in the vicinity of the Uravan mineral belt suggest a smaller alluvial fan superimposed on the larger alluvial plain of the Salt Wash.

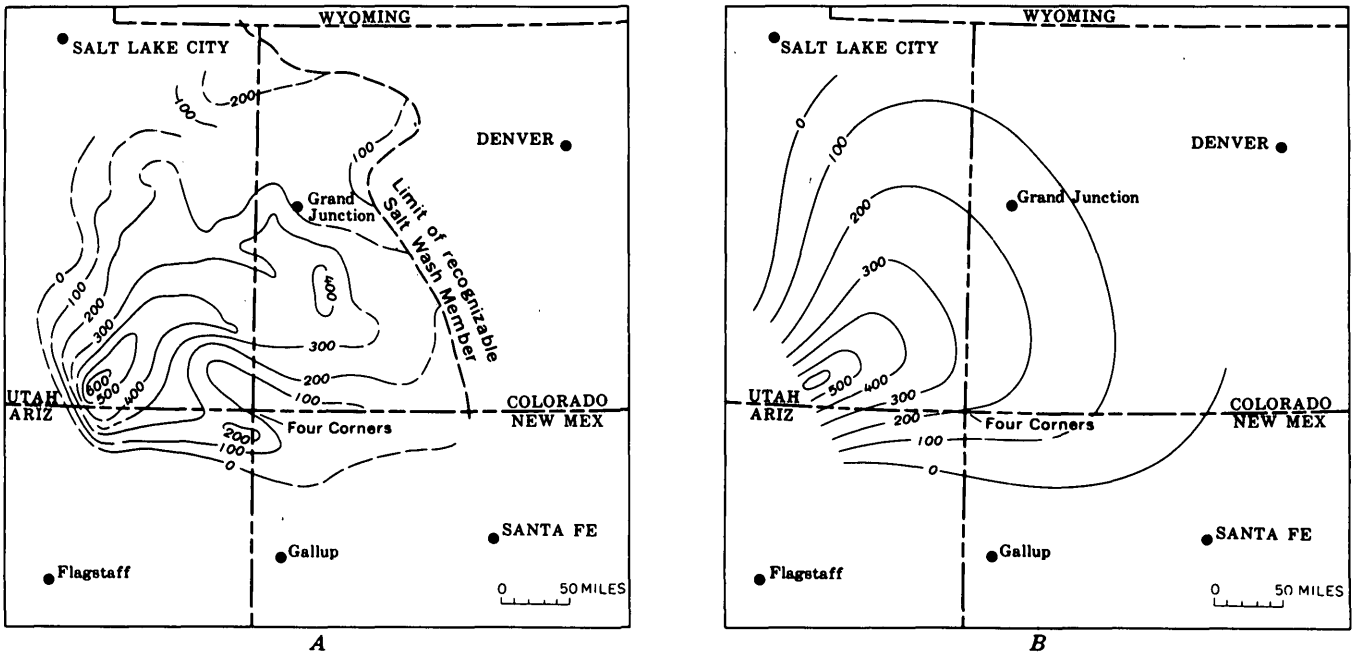

FIGURE 62.1.—Isopach maps of actual and idealized alluvial fans or aprons of the Salt Wash Member of the Morrison Formation. *A*, Actual fan (from Craig and others, 1955, fig. 21); *B*, idealized fan, based on actual fan. Isopach interval 100 feet; isopachs dashed where inferred.

It seems likely that the smaller fan was a result of warping during Salt Wash deposition.

Before the Salt Wash Member was deposited, the area must have been virtually a flat plain underlain by horizontal strata of the Summerville Formation of Late Jurassic age, which were deposited in a shallow marginal marine and tidal-flat environment. As interpreted from the data of Craig and others (1955), uplift of land in west-central Arizona and southern California caused movement of detritus northward, northeastward, and eastward into the area of the Salt Wash, forming a great aggrading alluvial apron with its apex near the source area. Irregularities in the alluvial apron in places where stratigraphic complications are absent probably reflect structural modifications of the area of accumulation during the period of deposition. Evidence that post-Salt Wash erosion was negligible precludes the possibility that structural modification of the area of accumulation took place immediately after the member was deposited.

In order to determine the amount and location of structural modification of the Salt Wash, an isopach map of an idealized alluvial fan or apron (fig. 62.1*B*) was constructed by using the general configuration of the actual fan. The differences in thickness between this idealized fan and the actual fan may represent structural deformation of the area of Salt Wash deposition. The differences in thickness are shown in figure 62.2. The uplift in southeastern Utah and the small basin south of the Four Corners may be explained by stratigraphic changes and may reflect the relations of the Salt Wash Member to other earlier and synchronous stratigraphic units. The basin in southwestern Colorado, however, seems clearly the result of structural deformation.

The large basin shown in figure 62.2 overlaps part of the Paradox basin of Pennsylvanian age and part of the Uncompahgre element of the ancestral Rocky Mountains of Pennsylvanian and Permian time. The position of the Uravan mineral belt and data on direction of sediment transport are also plotted on figure 62.2. From this diagram it appears that subsidence of the large basin could have caused the development of a lobe or smaller alluvial fan upon the much larger apron of the Salt Wash Member. The apex of the small fan is in a position that may have permitted deflection or "capture" of a considerable part of the distributary streams of Salt Wash time. The Uravan mineral belt forms the toe of the fan. The area east of the Uravan mineral belt is interpreted to contain sediments of flood-plain and perhaps lacustrine type; those in the mineral belt and westward to the end of the basin are interpreted to be fluvial deposits.

Carbonaceous material originally may have been abundant throughout the fluvial deposits, but it was subsequently destroyed except locally. R. P. Fischer

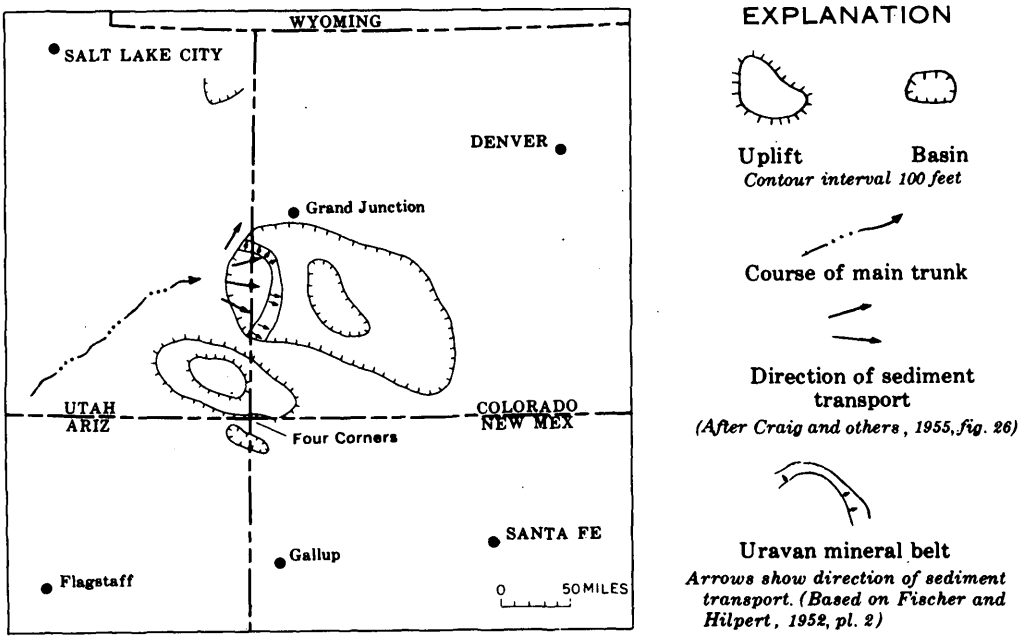

FIGURE 62.2.—Basins and uplift formed during Salt Wash deposition (based on differences in thickness between idealized and actual alluvial fans of the Salt Wash Member), general course of the interpreted main trunk of the distributary system during Salt Wash time, the position of the Uravan mineral belt, and direction of sediment transport in the vicinity of the mineral belt.

(oral communication, March 1961) has suggested that places where carbonaceous material survived were below the water table at the time of deposition and indefinitely thereafter, as at the foot of an aggrading slope at the edge of a body of water. Upslope above the water table, aeration caused oxidation and destruction of carbonaceous material. Such a mechanism fits the conditions pictured for the small alluvial fan, the toe of which may have been close to or under the water table that occupied the basin depicted in figure 62.2. Upper reaches of the fan, being alternately wet and dry, lost most of the original carbonaceous material by oxidation. In addition, possibly the toe of the alluvial fan adjacent to a flood plain or body of water may have been a favorable environment of abnormally abundant vegetation, which could account in part for abundant plant remains in the sediments in this area.

The envisaged smaller alluvial fan or lobe was an aberrant environment of deposition in which abundant cut-and-fill fluvial sandstone and carbonaceous material were deposited. Unusual sedimentation partly controlled later deposition of uranium-vanadium ores; the configuration of the alluvial fan determined the shape and extent of the Uravan mineral belt.

REFERENCES

Craig, L. C., and others, 1955, Stratigraphy of the Morrison and related formations, Colorado Plateau region, a preliminary report: U.S. Geol. Survey Bull. 1009–E, p. 125–168.

Fischer, R. P., and Hilpert, L. S., 1952, Geology of the Uravan mineral belt: U.S. Geol. Survey Bull. 988–A, p. 1–13.

McKay, E. J., 1955, Criteria for outlining areas favorable for uranium deposits in parts of Colorado and Utah: U.S. Geol. Survey Bull. 1009–J, p. 265–282.

63. CRITERIA FOR THE RECOGNITION OF JASPEROID ASSOCIATED WITH SULFIDE ORE

By T. G. Lovering and J. C. Hamilton, Denver, Colo.

Silicified carbonate rocks, commonly called jasperoid, have been reported from more than 70 mining districts in the United States. Jasperoids closely associated spatially with sulfide replacement deposits are referred to in this report as "productive." Jasperoids apparently unrelated to such deposits, although they may occur in the same general area, are referred to here as "barren."

The distinction between barren and productive jasperoid was made on the basis of spatial association with ore deposits. Samples taken from, or adjacent to, mine workings were called productive; those taken more than a quarter of a mile from any known ore bodies were called barren. This arbitrary distinction is not entirely valid because barren jasperoid could be related to undeveloped ore bodies, and productive jasperoid could be fortuitously located in the vicinity of an ore body to which it is completely unrelated. However, in most of the districts from which samples were collected, the criterion of spatial association of jasperoid with ore was the only one available for segregating samples into the two groups. The color, texture, mineralogy, and chemical composition of all the samples in both groups were tabulated and the resulting distributions compared statistically to determine those attributes that show a significantly greater association with productive jasperoid than with barren jasperoid.

A suite of 95 samples of productive jasperoid, representing 23 districts, has been compared with 53 samples of barren jasperoid representing 20 districts; most of these districts are represented by both types. The districts sampled are all in Western Conterminous United States and are distributed as follows: Nevada, 11; Utah, 7; Colorado, 5; Arizona, 4; Washington, 1; Oklahoma, 1; New Mexico, 1; South Dakota, 1. The number of samples per district varies from 1 to more than 20.

The majority of samples came from within 20 feet of the surface. Although the number of samples studied is far too small to represent adequately the jasperoid populations from which they were drawn, the results of this study suggest some real differences between barren and productive jasperoids; furthermore, the methods presented for the appraisal of jasperoid characteristics should be universally applicable, even though their application to other sample suites may considerably modify the list of diagnostic criteria.

The characteristics studied are divided into three groups as follows: (1) characteristics visible in hand specimen, (2) characteristics visible in thin section, and (3) chemical composition as determined by semiquantitative spectrographic analysis. Group 1 includes color, described according to the National Research Council color chart (Goddard and others, 1948); coarse grain (grains visible); brecciation; and prominent vugs. Group 2 includes three subdivisions: texture, including size range of quartz grains, xenomorphic texture (interlocking grains), jigsaw puzzle texture (highly irregular interlocking grains with boundaries resembling the pieces of a jigsaw puzzle), granular texture (equant grains with smooth boundaries), reticulated texture (abundant randomly oriented elongated grains with a length-to-width ratio of >3:1); associated hypogene minerals; and associated supergene minerals. Group 3 includes all elements except Si detected by semiquantitative spectrographic analysis in more than 10 percent of the samples.

Table 63.1 shows the number of samples and the proportion of samples of productive and barren jasperoid that exhibit the indicated characteristics of groups 1 and 2. The significance of the observed differences in the distribution, as tested by chi square (Siegel, 1956, p. 104 and 111), is shown in the last two columns.

The distribution of elements (group 3) is classified, for both productive and barren samples, into 3 classes for each order of magnitude of element concentration (for example, 0.15, 0.3, 0.7 for the range from 0.1 percent to 1 percent). The number of samples in each such class has been converted into the corresponding proportion of the total number of productive or barren samples, and these proportions have been cumulated successively from the lowest concentration observed for each element to the highest. The concentration showing the greatest discrepancy between cumulative totals for productive and barren samples is noted for each element, and the magnitude of this discrepancy has been tested statistically to determine whether the distributions differ significantly. The statistical test used is the Kolmogorov-Smirnov two-sample test (Siegel, 1956, p. 127–135). Data for all

TABLE 63.1.—*Distribution of observable characteristics between barren and productive jasperoid samples*

[n=number of samples; χ^2=chi square]

Characteristics	Productive samples		Barren samples		χ^2 [1]	Significance [1]
	n	Percent	n	Percent		
VISIBLE IN HAND SPECIMEN						
Color [2] [3]						
Light red (5R 6-8/2-6).	0	0	3	5½	3.01	Possibly significant (0.10).
Moderate red (5R 4-5/2-6).	1	1	8	15	9.41	Highly significant (0.01).
Dark red (5R 2-3/2-6).	8	8½	5	9½	.01	Not significant.
Reddish orange (10R 6-8/2-6).	0	0	1	2	.09	Do.
Reddish brown (10R 4-5/2-6).	4	4	6	11	1.72	Do.
Dark reddish brown (10R 2-3/2-6).	6	6½	4	7½	<.01	Do.
Light brown (5YR 6-8/2-4).	8	8½	0	0	3.21	Possibly significant (0.10).
Moderate brown (5YR 4-5/2-6).	27	28½	9	17	1.84	Not significant.
Dark brown (5YR2-3/2-4).	23	24	4	7½	5.27	Significant (0.05).
Yellowish orange (10YR 7-8/2-6).	20	21	10	19	.01	Not significant.
Yellowish brown (10YR 5-6/2-6).	33	35	19	36	<.01	Do.
Dark yellowish brown (10YR 2-4/2).	5	5	5	9½	.39	Do.
White to light gray (N 7-9).	40	42	18	34	.64	Do.
Medium gray (N 4-6).	29	30½	12	22½	.70	Do.
Dark gray to black (N 1-3).	15	16	11	21	.29	Do.
Texture						
Phaneritic	66	69½	22	41½	9.91	Highly significant (0.01).
Brecciated	33	35	23	43	.74	Not significant.
Vuggy	55	58	18	34	6.87	Highly significant (0.01).
VISIBLE IN THIN SECTION						
Texture						
Size range of quartz grains [4]	57	60	17	32	9.52	Highly significant (0.01).
Xenomorphic	63	66	35	66	.02	Not significant.
Jigsaw puzzle	48	50½	40	75½	7.78	Highly significant (0.01).
Granular	15	16	5	9½	.69	Not significant.
Reticulated	31	32½	5	9½	8.73	Highly significant (0.01).
Associated hypogene [5] minerals						
Barite	15	16	3	5½	2.39	Not significant
Calcite	12	12½	8	15	.03	Do.
Carbonate dust	26	27½	16	30	.03	Do.
Chalcedony	9	9½	7	13	.18	Do.
Chlorite or biotite	3	3	2	4	.08	Do.
Clay (kaolinite group)	33	35	12	23	1.82	Do.
Clay (montmorillonite group).	0	0	3	5½	3.01	Possibly significant (0.10).
Dolomite	5	5½	1	2	.32	Not significant.
Hematite	11	11½	8	15	.13	Do.
Pyrite	29	30½	6	11	5.93	Significant (0.05).
Sericite or hydromica	25	26	22	41½	2.96	Possibly significant (0.10).
Tourmaline	4	4	0	0	.97	Not significant.
Zircon	2	2	0	0	.10	Do.
Associated supergene [6] minerals						
Calcite	15	16	17	32	4.41	Significant (0.05).
Chalcedony	7	7½	3	5½	<.01	Not significant.
Clay (kaolinite group)	4	4	0	0	.97	Do.
Clay (montmorillonite group).	1	1	1	2	.10	Do.
Fluorite	5	5½	0	0	1.50	Do.
Goethite	45	47½	12	23	7.77	Highly significant (0.01).
Hematite	20	21	14	26½	.29	Not significant.
Jarosite	23	24	3	5½	6.85	Highly significant (0.01).
Brown limonite	22	23	12	23	.02	Not significant.
Yellow-orange limonite	1	1	5	9½	4.18	Significant (0.05).
Opal	3	3	0	0	.49	Not significant.

[1] Siegel (1956, p. 104–111).
[2] Many samples exhibit more than 1 color.
[3] Goddard and others (1948).
[4] Ratio of largest quartz grain diameter to smallest quartz grain diameter >10.
[5] Older than or contemporaneous with jasperoid silica.
[6] Younger than jasperoid silica.

elements detected in more than 10 percent of the samples are summarized in table 63.2.

Some elements that were not detected in most of the samples, and failed to show a significant difference between the distributions for productive and barren samples, might show such a difference if a more sensitive analytical method were used.

TABLE 63.2.—*Maximum difference in cumulative distribution of elements between barren and productive jasperoid samples*

[ΣP=cumulative proportion; ΣP_p=cumulative proportion, productive samples; ΣP_b=cumulative proportion, barren samples]

Element	Concentration C (percent) at which maximum $\lvert\Sigma P_p - \Sigma P_b\rvert$ occurs	$\Sigma P \leq$ Concentration, C		Difference, D $\lvert\Sigma P_p - \Sigma P_b\rvert$	Significance [1]
		Productive	Barren		
Al	0.3	0.725	0.515	0.210	Not significant.
Fe	1.5	.605	.905	.300	Significant (0.01).
Mg	.015	.375	.130	.245	Possibly significant (0.05).
Ca	.15	.560	.450	.110	Not significant.
Na	.3	1.000	.950	.050	Do.
Ti	.015	.450	.540	.090	Do.
Mn	.007	.370	.275	.095	Do.
Ag	.00015	.355	.920	.565	Highly significant (0.001).
As	≤.15	.775	.980	.205	Not significant.
B	≤.003	.840	.815	.025	Do.
Ba	.007	.535	.440	.095	Do.
Be	≤.00015	.800	.720	.080	Do.
Bi	≤.0007	.670	1.000	.330	Highly significant (0.001).
Cr	.0007	.395	.535	.140	Not significant.
Cu	.003	.355	.830	.475	Highly significant (0.001).
Ga	≤.00007	.780	.925	.145	Not significant.
In	≤.0007	.790	1.000	.210	Do.
Mo	≤.0007	.480	.870	.390	Highly significant (0.001).
Ni	.0003	.420	.350	.070	Not significant.
Pb	≤.0015	.210	.760	.550	Highly significant (0.001).
Sb	≤.015	.810	.905	.095	Not significant.
Sn	≤.0015	.760	1.000	.240	Possibly significant (0.05).
Sr	.0015	.505	.595	.090	Not significant.
V	≤.0007	.460	.280	.180	Do.
Y	.0015	.970	.890	.080	Do.
Yb	[2].00007	.810	.725	.085	Do.
Zn	≤.015	.340	.820	.480	Highly significant (0.001).
Zr	≤.0015	.235	.350	.115	Not significant.

[1] Siegel, 1956, p. 127–136.
[2] Element detected.

The interpretation of table 63.2 may be illustrated by the following example. For the element Fe, the greatest difference between the cumulative distribution for productive and barren samples comes at a concentration of 1.5 percent; 0.605 (60½ percent) of the productive samples have an iron content less than or equal to 1.5 percent; 0.905 (90½ percent) of the barren samples have an iron content less than or equal to 1.5 percent. This great a discrepancy in the observed sample distributions could occur by chance less than once in a hundred times if there were no real difference in the distribution of iron in the two types represented by the samples; the difference is significant at the 0.01 level. A sample containing more than 1.5 percent iron is thus considerably more likely to be productive than it is to be barren.

The significant criteria that are suggestive of productive and barren jasperoid samples are summarized in table 63.3 and are listed in the order of significance for each group.

An individual sample is likely to exhibit both productive and barren characteristics. No single criterion, regardless of its statistical significance, can be relied upon to distinguish barren from productive samples; however, if all of the observed characteristics in a given sample are weighted according to their significance (+ for productive, − for barren, 4 for highly significant, 2 for significant, and 1 for possibly significant), a large majority of productive samples will have positive scores >5, and a majority of barren samples will have zero or negative scores. A low positive score suggests a sample from a mineralized area, but not closely associated with an ore deposit. The distribution of the scores obtained on samples used in this study is given in table 63.4.

If the cutoff between barren and productive samples is taken at +5, it appears that approximately 1 out of every 5 barren samples studied was incorrectly classified as productive, and approximately 1 out of every 12 productive samples was incorrectly classified as barren, assuming that the field classification was correct.

These criteria are derived from small groups of samples taken from many localities. Intensive study of jasperoid samples from any individual district would probably show some valid criteria that are not generally significant, and some generally significant criteria that are not locally applicable. Nevertheless we feel that these criteria will prove useful for the recognition of jasperoid bodies that are closely associated with sulfide ore bodies, and the elimination of those that are not.

TABLE 63.3.—*Criteria for the recognition of productive and barren jasperoid samples*

Characteristics	Significance
CHARACTERISTICS VISIBLE IN HAND SPECIMEN	
Productive jasperoid	
Phaneritic texture	Highly significant (0.01).
Abundant vugs	Do.
Dark-brown color (5*YR* 2-3/2-4)	Significant (0.05).
Light-brown color (5*YR* 6-8/2-4)	Possibly significant (0.10).
Barren jasperoid	
Moderate-red color (5*R* 4-5/2-6)	Highly significant (0.01).
Light-red color (5*R* 6-8/2-6)	Possibly significant (0.10).
CHARACTERISTICS VISIBLE IN THIN SECTION	
Productive jasperoid	
Size range of quartz grain >10 [1]	Highly significant (0.01).
Reticulated texture	Do.
Crystalline orange goethite	Do.
Jarosite	Do.
Pyrite or its pseudomorph	Significant (0.05).
Barren jasperoid	
Jigsaw-puzzle texture	Highly significant (0.01).
Supergene calcite	Significant (0.05).
Yellow limonite	Do.
Hypogene clay (montmorillonite group)	Possibly significant (0.10).
Hypogene sericite or hydromica	Do.
CHEMICAL COMPOSITION BY SEMIQUANTITATIVE SPECTROGRAPHIC ANALYSIS	
Productive jasperoid	
Ag >0.00015 percent	Highly significant (0.001).
Pb >.0015 percent	Do.
Zn >.015 percent	Do.
Cu >.003 percent	Do.
Mo >.0007 percent	Do.
Bi >.0007 percent	Do.
Fe >1.5 percent	Significant (0.01).
Sn >.0015 percent	Possibly significant (0.05).
Barren jasperoid	
Mg >0.015 percent	Possibly significant (0.05).

[1] Ratio of largest quartz grain diameter to smallest quartz grain diameter >10.

TABLE 63.4.—*Frequency distribution of scores of barren and productive jasperoid samples studied*

Field classification	Number of samples		With indicated scores		
	<+1	+1 to +5	+6 to +10	>+10	Total
Barren jasperoid	28	13	9	3	53
Productive jasperoid	2	6	8	79	95

REFERENCES

Goddard, E. N., chm, and others, 1948, Rock color chart: Washington, D.C., Natl. Research Council.

Siegel, Sidney, 1956, Nonparametric statistics for the behavioral sciences: New York, McGraw-Hill Book Co., 312 p.

639466 O - 62 - 2

64. BEACH PLACERS CONTAINING RADIOACTIVE MINERALS, BAY OF BENGAL, EAST PAKISTAN

By Robert G. Schmidt and S. Ali Asad, Quetta, West Pakistan

Work done in cooperation with the Geological Survey of Pakistan

Beach placers containing monazite, ilmenite, zircon, and other heavy minerals extend 100 miles southeastward along the Bay of Bengal from Chittagong to the Burma border. The placers were first noted at Cox's Bazar by geologists of the Pakistan Industrial Development Corporation in 1960. Six samples were submitted to the Geological Survey of Pakistan, and a memorandum on these was prepared by R. A. Khan Tahirkehli (written communication, 1961). The sands were first studied by the authors early in 1961. A comprehensive survey of the placers, including an airborne radiometric survey of the entire beach, was begun in November 1961 and is continuing.

The placers consist of sands generally containing 10 to 30 percent heavy minerals with local lenses that contain as much as 96 percent of minerals exceeding 2.80 specific gravity. The principal placers are at 10 localities randomly distributed along the coast within the area surveyed. Small concentrations of heavy minerals are present at many places along the coast, as well as on St. Martin's Island, 7 miles offshore (fig. 64.1). Three of the major placers are on Sonadia and Kutubdia Islands. No observations were made north of Chittagong nor on the islands west of Chittagong. Each placer is tens or hundreds of feet wide and several hundreds to thousands of feet long. At least one extends for several miles.

Most of the beach placers are above normal high tide and, where dunes are present, along the seaward edge of the dune tracts. Otherwise the placers generally appear to end near the seaward edge of the vegetation cover. Only placers near enough to the surface to be detected by radiation-detection instruments were studied. In 11 prospect pits extending to as much as 4½ feet below the surface no heavy-mineral layers were noted below the surficial layer. More deeply buried heavy-mineral layers may be present, however, and generalizations regarding the mode of occurrence are limited to the near-surface layers.

The heavy minerals are in layers that are most commonly about 1 foot thick, but layers as thick as 2½ feet have been measured. In places the layers are exposed on the surface of the beach; elsewhere they are beneath a blanketing layer of white sand. Within the dune areas, the heavy minerals generally form a semiconsolidated surface over which the small shore dunes move; less commonly, the heavy minerals make up parts or, locally, almost all of some dunes.

The very rich layers containing as much as 96 percent heavy minerals form rather discrete lenses on the open beach. One extends well below the high-tide mark. No lenses are over a foot in thickness and all are, at most, a few tens of feet wide and a thousand feet long. One lens was traced by test pits from the discovery point about 6 inches below the beach surface to a depth of about 4 feet. The lens dipped seaward more steeply than the beach surface.

The very rich placer layers on the open beach are probably formed almost entirely by wave action, perhaps during a period of erosion of the beach.

The placers of the higher beach appear to have formed by a combination of wave action, perhaps mostly by storm waves, and wind sorting. The enrichment of surficial heavy-mineral layers by removal of lighter particles is noticeable during strong winds and appears to be a very rapid process. This deflation is particularly effective downwind of creeks that enter the ocean across the beach. Quartz sand and blowing along the beach is trapped by the streams; therefore only deflation occurs on the downwind side, and sizeable tracts so located are enriched in heavy minerals to depths of several inches to a foot.

The heavy-mineral layers within the dunes are wind deposited, but the layer under the dunes may have been formed partly by storm waves, and the dunes may have formed on top at a later time.

The heavy-mineral suite and the grain size and sorting are different in placers with a moderate concentration of heavy-mineral layers as compared to those with a high concentration; also there may be distinct differences in the suites from different placer areas along the coast. W. C. Overstreet (written communication, 1961) has described the following mineral suite from beach placers at Cox's Bazar that contain 10 to 30 percent poorly sorted heavy minerals:

Abundant	*Common*	*Sparse*
Quartz	Tourmaline	Amphibole
Magnetite	Staurolite	Kyanite
Pyroxene	Zircon	Muscovite
Ilmenite(?)	Rutile	Biotite
Epidote		Monazite
Garnet		

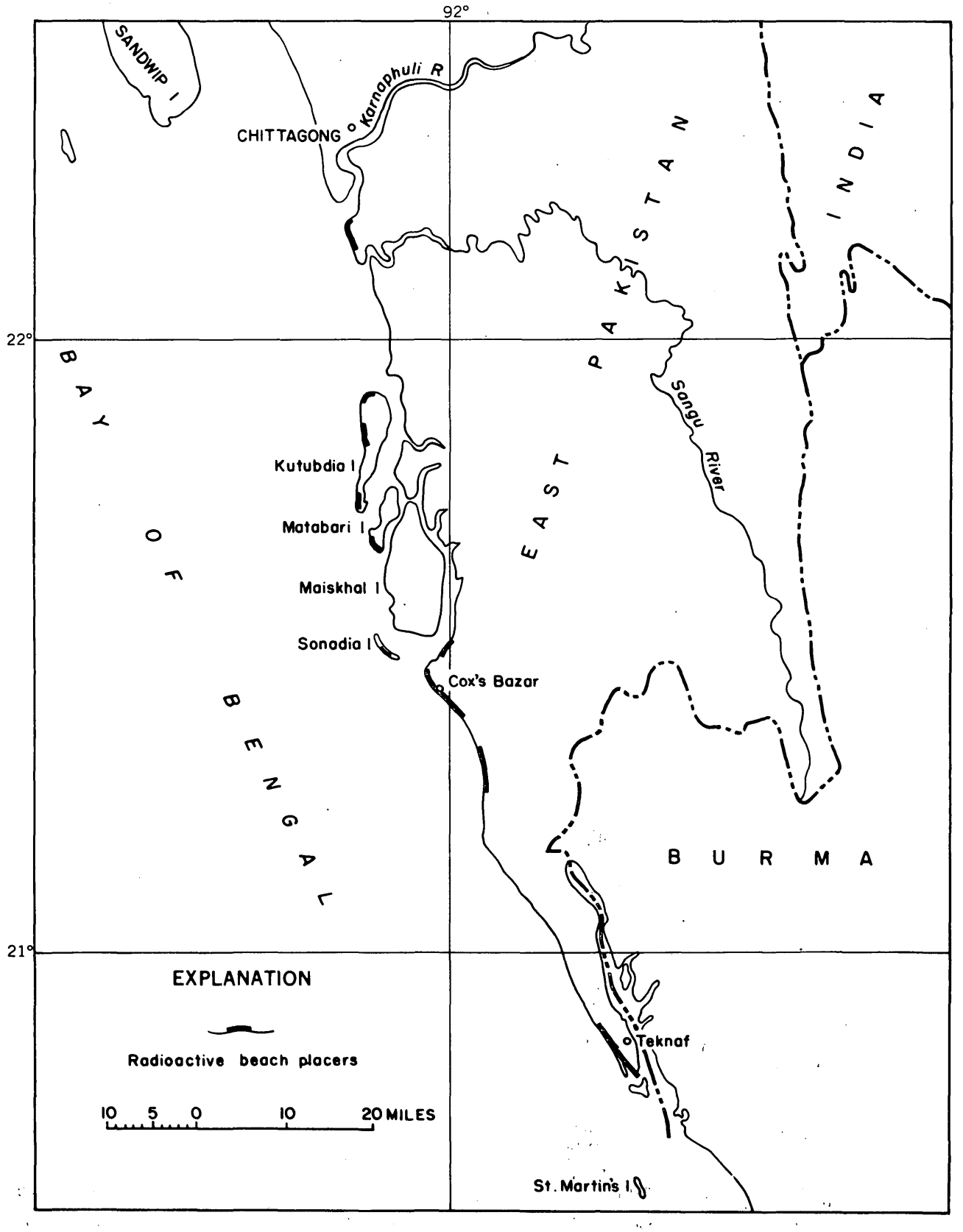

FIGURE 64.1.—Location of beach placers containing radioactive minerals, Bay of Bengal, East Pakistan.

The sand in lenses consisting almost entirely of heavy minerals is finer grained, better sorted, and better rounded than that in beach placers of moderate concentration, and magnetite makes up about half of the heavy minerals. According to Overstreet very little pyroxene or amphibole was found in such lenses, and far less epidote than in the ordinary beach placers. The magnetite is angular and includes a few nearly perfect octahedra. Garnet is abundant but staurolite and tourmaline are sparse, and biotite, kyanite, and muscovite are lacking.

The sand in the placers at the northernmost tip of Kutubdia Island appears to be different from either of the types described above. Relatively coarse, the sand is almost entirely black, with virtually no associated white sand, and rests on a compact mud platform. It is relatively less radioactive than equally dark colored sands farther south on Kutubdia Island.

The richest natural sands examined contained 0.63 percent equivalent thorium, but there appears to be too little monazite in the sample to account for this much thorium. Monazite isolated from this sand is less radioactive than the residual fraction of the sample in which the radioactive mineral is believed to be black and opaque.

65. VARIATION IN RANK OF TERTIARY COALS IN THE COOK INLET BASIN, ALASKA

By F. F. Barnes, Menlo Park, Calif.

Tertiary coals in the Cook Inlet basin of south-central Alaska range in rank from lignite to anthracite. Until recently all the coals sampled had been limited to a relatively narrow stratigraphic range and were at or near the present surface. In 1960 the writer obtained core samples of coals from several wells in the recently developed Kenai oil field from depths of as much as 11,000 feet, and in 1961 he collected samples of lignite from a bed on the Chuitna River, west of Anchorage, that probably is considerably younger than those in other parts of the basin. Proximate analyses (on the as-received basis) and rank of coals from the Kenai wells and of representative samples from other parts of the Cook Inlet basin are given in the table below, and the sampled localities are shown in figure 65.1.

Analyses of coals on the as-received basis in the Cook Inlet basin, Alaska

[Analyses by U.S. Bureau of Mines]

Sample No.	Sampled locality	Rank [1]	Laboratory No.	Moisture (percent)	Volatile matter (percent)	Fixed carbon (percent)	Ash (percent)	Sulfur (percent)	Heating value (Btu)	Moist mineral-matter-free (Btu)
	Kenai field									
1	Outcrop 14 miles north of Ninilchik.	Lig	D–51010	27. 1	31. 8	25. 4	15. 7	0. 2	6, 640	8, 000
2	Outcrop 2 miles north of Ninilchik.	Subc	D–49805	27. 1	36. 5	28. 4	8. 0	. 3	7, 730	8, 460
	Core samples from Kenai oil wells:									
	Well *Depth (feet)*									
3	SRU 14–4 5, 500	Subb	G–89425	13. 2	30. 1	24. 6	32. 1	. 8	6, 360	9, 740
4	SRU 34–10 10, 200	Hvcb	A–49	9. 1	38. 1	41. 3	11. 5	. 3	10, 650	12, 150
5	SRU 34–10 10, 230	Hvcb	G–89428	7. 6	29. 9	37. 4	25. 1	. 3	8, 630	11, 845
6	SRU 32–33 10, 680	Hvcb	G–89424	7. 7	37. 2	42. 3	12. 8	. 4	11, 190	12, 990
7	SRU 12–27 10, 720	Hvbb	G–89426	5. 9	38. 7	48. 7	6. 7	. 5	12, 150	13, 100
8	SRU 34–16 11, 110	Hvbb	G–89429	5. 6	41. 7	45. 7	7. 0	. 3	12, 360	13, 350
9	SRU 34–10 11, 360	Hvcb	G–89427	4. 9	30. 3	35. 4	29. 4	. 2	8, 800	12, 900

See footnotes at end of table.

Analyses of coals on the as-received basis in the Cook Inlet basin, Alaska—Continued

[Analyses by U.S. Bureau of Mines]

Sample No.	Sampled locality	Rank [1]	Laboratory No.	Moisture (percent)	Volatile matter (percent)	Fixed carbon (percent)	Ash (percent)	Sulfur (percent)	Heating value (Btu)	Moist mineral-matter-free (Btu)
			Matanuska field							
10	Houston strip mine, Little Susitna district.	Subb	D–51894	20. 3	31. 6	38. 9	9. 2	0. 4	9, 210	10, 250
11	Evan Jones mine, Wishbone Hill district.	Hvbb	A–98201	5. 2	34. 7	41. 4	18. 7	. 4	10, 860	13, 620
12	Chickaloon mine, Chickaloon district.	Lvb	85740	1. 3	16. 2	66. 4	16. 1	. 6	12, 690	[2] 81. 8
13	Outcrop, Anthracite Ridge district.	An	12746	2. 9	7. 8	77. 3	12. 0	. 6	12, 730	[2] 92. 7
			Susitna field							
14	Outcrop on Chuitna River, Beluga district.	Lig	H–17384	33. 1	32. 9	27. 6	6. 4	0. 1	7, 260	7, 800

[1] In accordance with American Society for Testing Materials (1939). Ranks were determined from calculated moist mineral-matter-free Btu or dry mineral-matter-free fixed carbon.
[2] Calculated dry mineral-matter-free fixed carbon, in percent.

Several factors have been considered by different writers to be primarily responsible for increasing the rank of coals (Hendricks, 1945, p. 14–19). Chief among these are: (a) length of time since burial of vegetation, (b) depth of burial (load metamorphism), (c) heat from compression by or from intrusion of igneous rocks (thermal metamorphism), and (d) pressure from horizontal stress (regional metamorphism).

The coals in outcrops in the Kenai field are lowest in rank and those in the core samples from this field show a general increase in rank with depth (fig. 65.2). As available data indicate that all these coals originated during one general period of continental deposition, it seems unlikely that difference in age alone could account for the difference in rank. The enclosing Kenai Formation has not been intruded by

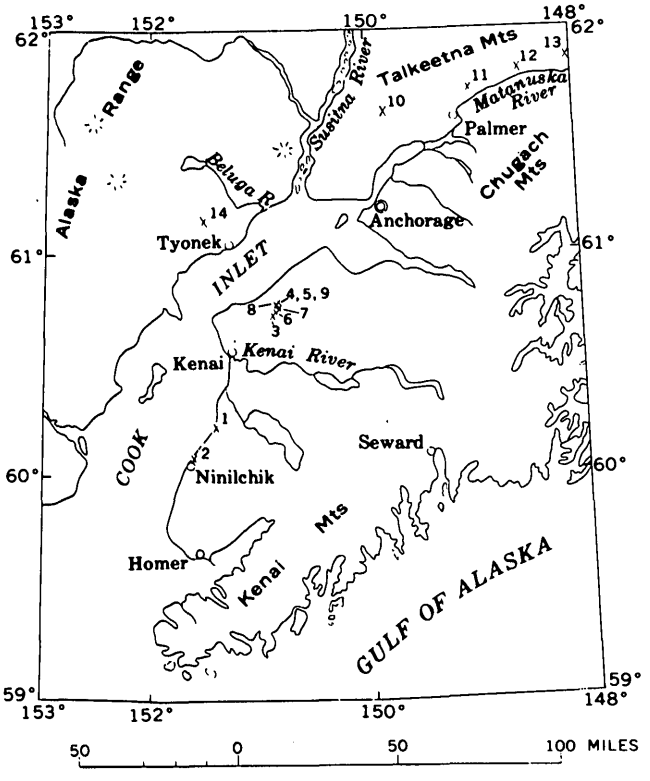

FIGURE 65.1.—Index map of Cook Inlet basin, showing sampled coal localities listed in table.

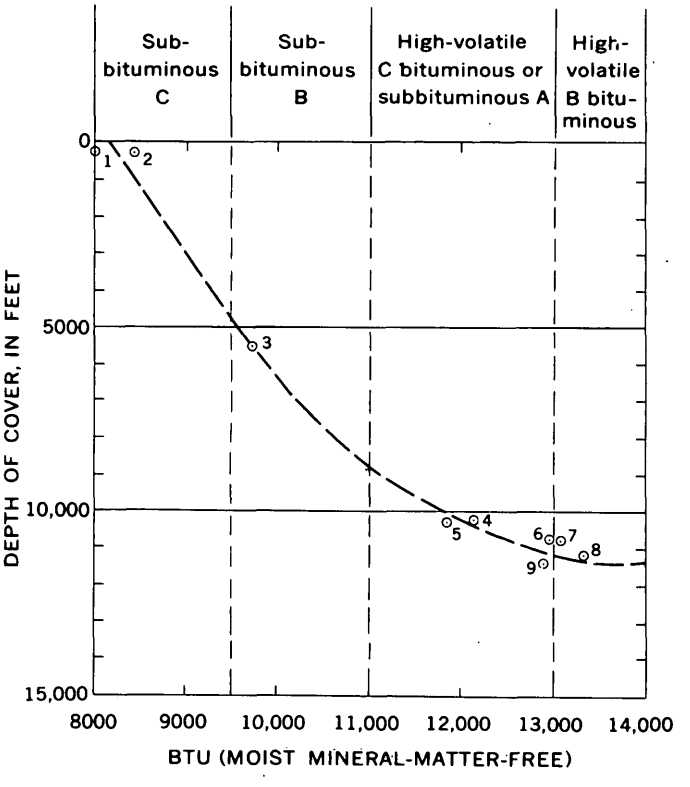

FIGURE 65.2.—Relation of rank to present depth of cover of Kenai coals. See table and figure 65.1 for localities sampled.

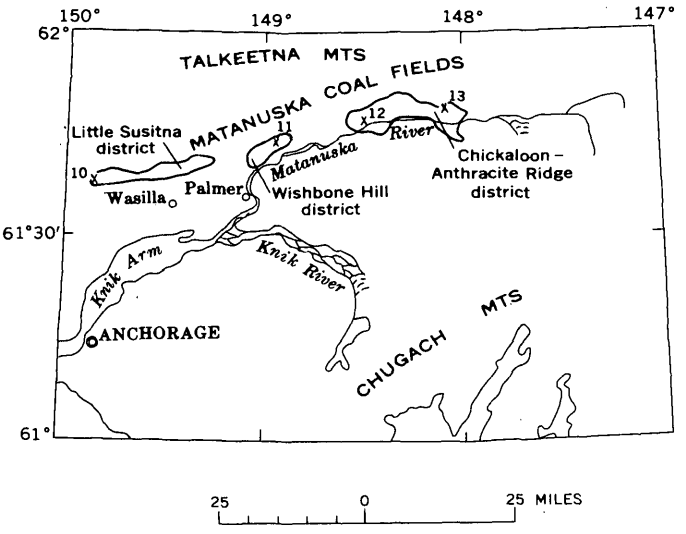

FIGURE 65.3.—Index map of Anchorage quadrangle, showing sampled coal localities in the Matanuska coal field.

igneous rocks and has undergone only mild folding and normal faulting, so that both thermal and regional metamorphism probably can be safely ruled out as dominant factors in increasing the rank of the coals. It therefore seems probable that load metamorphism was chiefly responsible for increasing the rank of the deeper Kenai coals.

In the Matanuska coal field, at the head of Cook Inlet north of Anchorage, coals of the Chickaloon Formation, of early Tertiary age, increase progressively in rank from subbituminous at the west end of the field, through high-volatile bituminous in the central part, to low-volatile bituminous and anthracite at the east end of the field (see fig. 65.3 and table). Although the coals in the different parts of the field have not been closely correlated, available evidence indicates that they are all part of the same general sequence and hence do not differ greatly in geologic age. Also, no evidence is known to indicate that the coals of the eastern end of the field were more deeply buried than those to the west. The degree of deformation changes markedly, however, from slight folding and faulting in the western part of the field (Barnes and Sokol, 1959, p. 125–126) to extremely complex folding and faulting in the eastern part (Capps, 1927, p. 51–55). Furthermore, intrusive dikes, sills, and stocks are abundant in the eastern part of the field, of minor occurrence in the central part, and totally lacking in the western part. These relations strongly suggest that the dominant factors in increasing the rank of the coals were heat and pressure resulting from regional deformation accompanied by igneous intrusion.

In 1961 the writer sampled a 30-foot coal bed on the Chuitna River in the Susitna field west of Anchorage; analysis has shown this coal to be considerably lower in rank than typical Kenai coal (see table). The enclosing rocks are similar to those of the Kenai field and, like them, have undergone only slight deformation and are free of intrusive rocks. However, they contain fossil leaves that, according to Jack A. Wolfe (written communication, 1962), may be considerably younger than the typical Kenai flora and are of probable early or middle Miocene age. This coincidence of lower rank with probable younger age suggests that length of time since burial is the dominant factor affecting the rank of the Chuitna River coal.

In summary, evidence indicates that several factors have played a part in advancing the rank of Tertiary coals in the Cook Inlet basin, and that no single factor was universally dominant. The following conclusions appear to be warranted:

1. Age and a moderate depth of burial have been sufficient to advance to subbituminous rank all coals deposited in early Tertiary time. Relatively undisturbed coals of probable middle Tertiary age have not passed beyond the lignite stage.

2. Load metamorphism has raised to bituminous rank the deeper coals in the Kenai field, but so far as is known it had little effect on coals in other parts of the basin. Deep drilling may reveal higher rank coals at depth in other areas, for example in the western part of the Matanuska field.

3. Regional metamorphism resulting from horizontal stresses, possibly aided by heat from igneous intrusions, has raised coals to bituminous and higher ranks in the Matanuska field but has not been an important factor elsewhere in the Cook Inlet basin.

REFERENCES

American Society for Testing Materials, 1954, Standard specification for classification of coals by rank, *in* ASTM standards on coal and coke, D388–38, p. 79–81.

Barnes, F. F., and Sokol, Daniel, 1959, Geology and coal resources of the Little Susitna district, Matanuska coal field, Alaska: U.S. Geol. Survey Bull. 1058–D, p. 121–138.

Capps, S. R., 1927, Geology of the upper Matanuska Valley, Alaska: U.S. Geol. Survey Bull. 791, 92 p.

Hendricks, T. A., 1945, The origin of coal, *in* Lowry, H. H., ed., Chemistry of coal utilization: Natl. Research Council Committee on Chemical Utilization of Coal, New York, John Wiley and Sons, v. 1, p. 1–24.

ENGINEERING GEOLOGY

66. POSSIBLE ENGINEERING USES OF SUBSIDENCE INDUCED BY CONTAINED UNDERGROUND NUCLEAR EXPLOSIONS

By F. N. Houser and Edwin B. Eckel, Denver, Colo.

Work done in cooperation with the U.S. Atomic Energy Commission

Nearly circular depressions have been formed in the level floor of Yucca Flat, Nevada Test Site, Nev., by subsidence over the sites of several of the recent underground nuclear tests. This method of creating depressions—by contained underground nuclear explosions—has the advantage of being free of radioactive throwout debris and might be applicable for creating harbors or for consolidating ground much closer to populated regions than has previously been thought possible.

The depressions over the Yucca test areas have been referred to as craters, but because this term obscures the essential factor of subsidence in their formation the term should be discarded in favor of the more appropriate term "sink," thereby emphasizing the mechanics involved.

The sinks in Area 3, Yucca Flat, are as much as several hundred feet in diameter and 100 feet in depth, and were formed as a result of subsidence of alluvial material into cavities formed by nuclear explosions of relatively small yield. All explosions were in filled holes that had been drilled in alluvium. The alluvium consists of sand, gravel, and clay, some of which is moderately to well consolidated. A microscopic analysis of the sand- and gravel-size fractions of this material was made by T. Cole, of the U. S. Geological Survey (written communication, 1962). The material has an average composition of 75 percent zeolitized and welded tuff fragments, 10 percent quartz and feldspar grains, and 16 percent miscellaneous rock fragments including volcanics, carbonates, quartzite, chert, granite, argillite, and siltstone. The coherence of the alluvium cored to date has been so weak that only fragments of core have been available for analysis. The average density, porosity, and water content of 10 core samples taken prior to testing are as follows:

Porosity ---------- percent	36
Sample-state bulk density ---------- g per cc	1.92
Sample-state water content by volume g per cc	0.32
Sample-state water content percent by weight	16.6
Dry bulk density ----------	1.61
Grain density ----------	2.51

An explosion of a nuclear device in such material creates a markedly unstable cavity by fusion and compaction. As soon as the initial pressures have sufficiently dissipated, the alluvial material overlying the cavity subsides in mass or progressively. As it lacks any significant coherence and as its original porosity is very high, the net result of explosion and subsidence is a large reduction in volume. This is contrary to the volume increase, or "swell," that usually results from blasting or other disturbance of more consolidated and less porous rocks. If the original explosion-produced cavity is large enough, the subsidence progresses to the surface and causes a sink.

In some regions along the sea coast such sinks on a considerably larger scale would have enormous economic potential as harbors. The advantage of harbor formation by the subsidence method is that, in being free of radioactive throwout debris, it could be accomplished much closer to populated areas where there are practical uses for harbors. Elimination of fallout is one of the major problems in formation of a harbor by cratering techniques.

Except for differences in water content, the structurally homogeneous alluvium in Yucca Flat probably is similar to materials that underlie coastal plains on which many major cities of the world are built. This analogy suggests another possible engineering application for contained nuclear explosions—the preconsolidation of alluvium before construction. For example, investigations of the recent Chilean earthquakes have shown that major damage to several towns and ports resulted from differential consolidation of alluvium by earthquake tremors. This consolidation caused subsidence and large-scale incursion of sea or estuary water (Dobrovolny and Lemke, 1961). It seems reasonable that preconsolidation (subsidence) of alluvial materials by contained nuclear explosions might alleviate or prevent similar problems in other areas where extensive new or heavy construction is planned. The explosion-induced subsidence method, if applicable at all, need not be confined to seismically active areas. Indeed, it might be even more promising in stable areas, where alluvium

has had no chance to be partly consolidated by prior earthquake shocks.

As the study of cavity stability and chimney formation before and after nuclear explosions progresses in more complicated media than the Yucca Valley alluvium, an increasing degree of precision will be attained in prediction of effects. Such data would be required in the use of the subsidence method in an area underlain by moderately complex geologic terrane where essential differences in physical properties and water content of the rocks are involved. For most areas, thick deposits of alluvium at the surface would be an asset to subdue venting and to promote subsidence. Much has to be known also of the effects of nuclear explosions in saturated media such as would be found in coastal regions, and of the potential water-contamination problems.

REFERENCE

Dobrovolny, Ernest, and Lemke, R. W., 1961, Engineering geology and the Chilean earthquakes of 1960: Art. 276 *in* U.S. Geological Survey Prof. Paper 424–C, p. C357–C359.

STRUCTURAL GEOLOGY

67. A REGIONAL ULTRAMAFIC SHEET IN EASTERN KLAMATH MOUNTAINS, CALIFORNIA

By William P. Irwin and Peter W. Lipman, Menlo Park, Calif., and Denver, Colo.

Work done in cooperation with the California Division of Mines and Geology

Ultramafic rocks crop out over large irregular areas in the eastern part of the Klamath Mountains of northern California, generally along the boundary between the rocks of the central metamorphic belt on the west and strata of the eastern Paleozoic belt (Irwin, 1960). The structural relations of these rocks were studied in detail by Irwin in the Weaverville quadrangle and by Lipman [1] in the southeastern Trinity Alps. Based chiefly on these studies, and on the general pattern of distribution of these rocks mapped by others elsewhere in the eastern Klamath Mountains (fig. 67.1), the ultramafic rocks are considered to be parts of a great, once-continuous subhorizontal sheet that separated the rocks of the central metamorphic belt from the structurally overlying rocks of the eastern Paleozoic belt.

The central metamorphic belt includes the Abrams Mica Schist and Salmon Hornblende Schist of Hershey (1901). In the Trinity Alps, rocks formerly called Abrams have been divided into two mappable rock units by Davis and Lipman (1962). Although long considered to be Precambrian or pre-Silurian, the age designations of the rocks of the central metamorphic belt have been based chiefly on the high degree of recrystallization compared to the weakly and nonmetamorphosed strata of the eastern Paleozoic belt. In the Trinity Alps the schists are tightly folded with steep east-dipping axial planes, but in the Weaverville quadrangle the folds generally are open. The schists have been through more than one episode of folding and metamorphism, and in the Trinity Alps both the complexity of deformation and intensity of metamorphism increase with proximity to the ultramafic rock.

The eastern Paleozoic belt includes strata of Ordovician(?) and Silurian age, the Copley Greenstone of Devonian age, the Kennett Formation and Balaklalla Rhyolite of Devonian(?) age, the Bragdon Formation of Mississippian age, and other still younger formations of Paleozoic age. The strata of Ordovician(?) and Silurian age are known only in the northern part of the belt, where they predominate, whereas the Copley Greenstone and Bragdon Formation predominate in the central and southern parts of the belt. The younger Paleozoic formations lie east of the Bragdon Formation. Thus the rocks of the eastern Paleozoic belt that crop out adjacent to the ultramafic sheet are chiefly the strata of Ordovician(?) and Silurian age in the northern part and the Copley Greenstone and Bragdon Formation in the central and southern part. The structure of the rocks

[1] Lipman, P. W., 1962, Geology of the southeastern Trinity Alps, northern California: Stanford Univ. PhD. thesis.

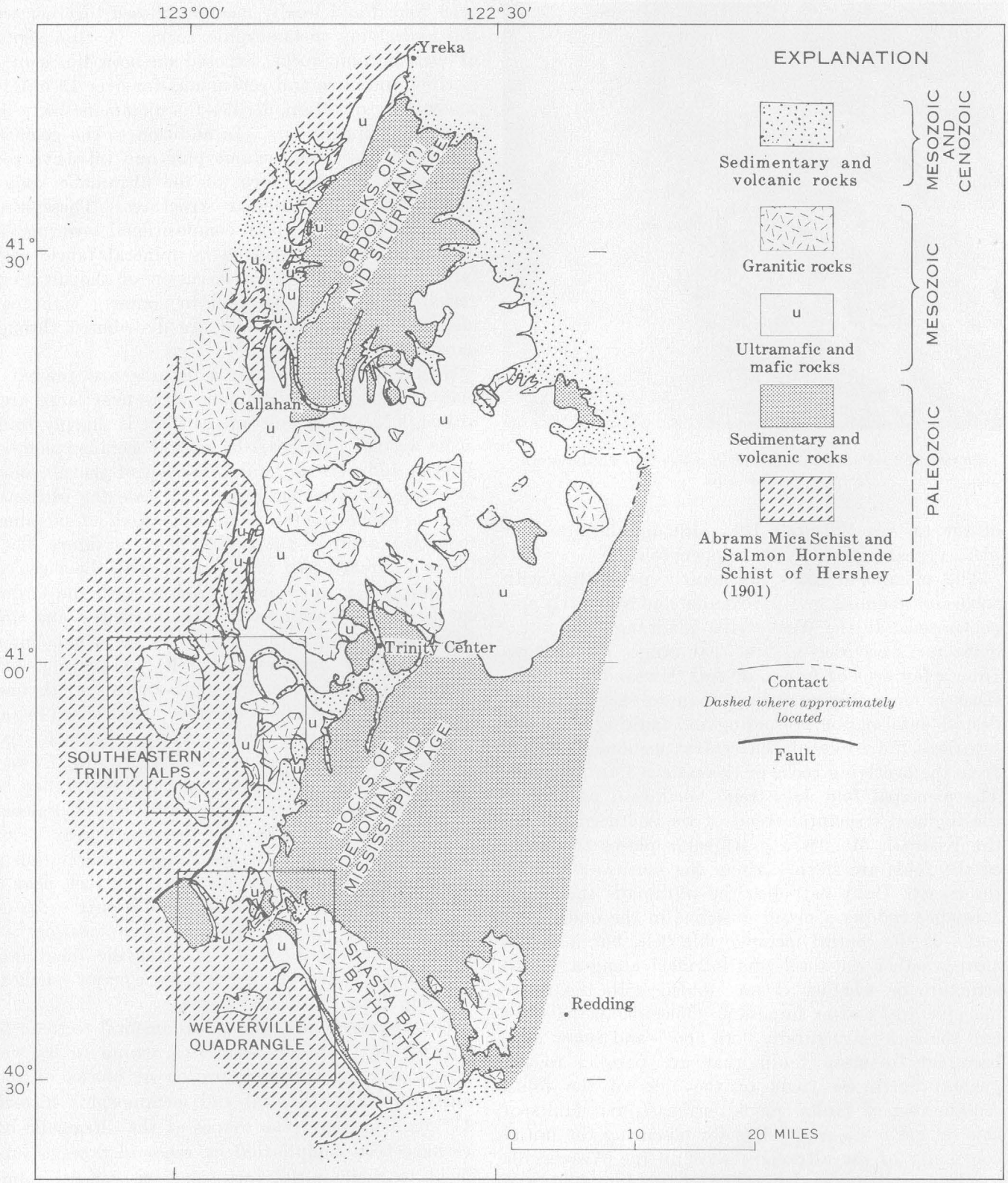

FIGURE 67.1.—Map showing distribution of rocks in eastern Klamath Mountains. (Generalized and modified after unpublished Redding and Weed 2-degree sheets compiled by the California Division of Mines and Geology.)

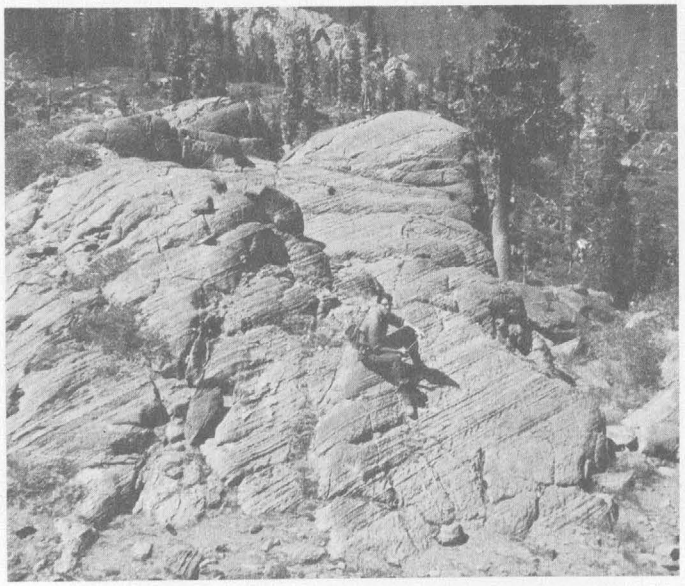

FIGURE 67.2.—Pyroxenite layers in peridotite, southeastern Trinity Alps.

of the eastern Paleozoic belt, although locally complex, appears generally to be open folds.

The ultramafic rocks are mostly peridotite, with subordinate dunite and pyroxenite, and are partly serpentinized. In the Weaverville quadrangle the ultramafic rocks occur as a sheet that ranges in thickness from a few tens of feet to several thousand feet. The sheet is more disrupted here than to the north, but despite deformation by folding and faulting, it clearly separates the rocks of the central metamorphic belt from the overlying rocks of the eastern Paleozoic belt. The principal fold axes trend northwest, parallel to the regional structural trend of the southern part of the Klamath Mountains. At some places the limbs of the folds are steep. Along the southwest side of the Shasta Bally batholith the ultramafic sheet conformably follows a major anticline in the underlying rocks of the central metamorphic belt, but it is not clear whether the sheet was intruded along a folded structure or whether it was folded with the metamorphic rocks after intrusion. The ultramafic sheet and the rocks structurally both above and below have been cut by steep faults that are parallel to the general northwest trend of the axes of the folds. Another set of faults trends northeast, and faults of this set are more responsible for obscuring the initial continuity of the ultramafic sheet in the Weaverville quadrangle than are the northwest-trending folds and faults.

The ultramafic rocks in the southeastern Trinity Alps have the shape of a multiple sill intrusive into rocks of the central metamorphic belt, and they have been folded and locally metamorphosed together with the underlying metamorphic rocks. A thin septum of metamorphic rocks, exposed on both limbs of an isoclinal anticline and continuous for over 15 miles in a northerly direction, divides the ultramafic body into lower and upper units. In addition to the geometry of contacts between metamorphic and intrusive rock, the folded sheetlike form of the ultramafic body is shown by internal planar structures. These structures, which include both compositional layering (fig. 67.2) and foliation defined by mineral fabric orientation, originated during intrusion of the ultramafic rocks, for they are parallel to contacts with metamorphic country rocks and are distributed throughout the ultramafic sheet.

Gently dipping planar structures are present at many places in the ultramafic rocks over large areas, although locally the ultramafic sheet is sharply folded in its western part near the central metamorphic belt. This in addition to the distribution of the ultramafic rock suggests that on a regional scale the ultramafic sheet is subhorizontal. The large area of ultramafic rock that occupies the central part of figure 67.1 is likely an arched part of the sheet, with the sheet continuing as a broad synclinorium beneath the Ordovician(?) and Silurian rocks to the northwest and again emerging at the surface along the eastern boundary of the central metamorphic belt. A large positive magnetic anomaly over the southern part of this area supports the concept that the Ordovician(?) and Silurian strata are underlain by ultramafic rock (Irwin and Bath, 1962, profile *G–G′*). Northwest of Callahan, ultramafic rocks crop out along valley bottoms and clearly are structurally below Paleozoic strata on the hill crests. Farther south near Trinity Center, small patches of the Bragdon Formation are found within the terrane of ultramafic rock near the eastern boundary of the sheet, and appear to be outliers. A large outlier of Bragdon Formation is in the northwest part of the Weaverville quadrangle, where it is limited to the north by a major northeast-trending fault.

The ultramafic sheet is a fundamental tectonic feature of the Klamath Mountains, owing to its widespread and consistent separation of blocks of rocks with differing structural and metamorphic histories. Although in places the shapes of the ultramafic bodies have been complicated by renewed flowage subsequent to their initial intrusion, the general tabular form and recurrent appearance at the same structural horizon suggest that the sheet, prior to disruption by folding and faulting, had an areal extent of more than a thousand square miles. The root zone of the

sheet probably lies to the east, for in that direction the ultramafic rocks disappear beneath the Paleozoic strata, whereas at its western edge the sheet has been upturned and eroded. Large tabular masses of ultramafic rock crop out at many places in the Klamath Mountains west of the central metamorphic belt, but although some of them appear to be subhorizontal, and they separate rocks of grossly different ages, their relation to the great ultramafic sheet of the eastern Klamath Mountains remains to be established.

The structural control of emplacement of the ultramafic sheet is not clear. The sheet may have intruded along a depositional unconformity between the Paleozoic rocks and presumably older metamorphic rocks. On the other hand, the present distribution of the Paleozoic strata above metamorphic rocks may have resulted from thrusting before, during, or after intrusion of the sheet. Thrusting, whether before or after intrusion, is suggested by a stratigraphic discordance of the Paleozoic strata with the ultramafic sheet. In the southern part of the map area (fig. 67.1), the Bragdon Formation on the west locally rests on the ultramafic sheet and at some places is separated from it by a thin layer of Copley Greenstone, but to the east the Bragdon is underlain by a thick section of Copley and other Devonian strata. Exposed strata older than Devonian lie on the ultramafic sheet only in the northern part of the map area.

The age of the ultramafic sheet and of the possible thrust is Late Jurassic (Tithonian) or older, as the ultramafic sheet as well as the Paleozoic strata and rocks of the central metamorphic belt are cut by the Shasta Bally batholith. Inclusions of ultramafic rock have been found (J. Albers, written communication, 1961) in the batholith where it is exposed in the Paleozoic strata east of the Weaverville quadrangle, and these likely were broken off from the ultramafic sheet and carried upward during intrusion of the batholith. No significant displacement of either the batholith or its contact aureole is seen where the batholith crosses into the inferred thrust zone and essentially cuts out the ultramafic sheet in the northern part of the Weaverville quadrangle. The age of the Shasta Bally batholith, determined by the potassium-argon method, is 134 million years (Curtis, Evernden, and Lipson, 1958), and this age is compatible with a Late Jurassic (Tithonian) age for the batholith based on relations between the batholith and the sequence of Late Jurassic and Cretaceous fossiliferous strata of the Sacramento Valley (Irwin, 1960, p. 58).

REFERENCES

Curtis, G. H., Evernden, J. F., and Lipson, J., 1958, Age determination of some granitic rocks in California by the potassium-argon method: California Div. Mines Spec. Rept. 54, 16 p.

Davis, G. A., and Lipman, P. W., 1962, Revised structural sequence of pre-Cretaceous metamorphic rocks in the southern Klamath Mountains, California: Geol. Soc. America Bull. (In press.)

Hershey, O. H., 1901, Metamorphic formations of northwestern California: Am. Geologist, v. 27, p. 225–245.

Irwin, W. P., 1960, Geologic reconnaissance of the northern Coast Ranges and Klamath Mountains, California: California Div. Mines Bull. 179, 80 p.

Irwin, W. P., and Bath, G. D., 1962, Magnetic anomalies and ultramafic rock in northern California: Art. 25 *in* U.S. Geol. Survey Prof. Paper 450–B, B65–B67.

68. TECTONIC FRAMEWORK OF AN AREA WITHIN THE SIERRA MADRE ORIENTAL AND ADJACENT MESA CENTRAL, NORTH-CENTRAL MEXICO

By Cleaves L. Rogers; Zoltan de Cserna, Jesús Ojeda Rivera, Eugenio Tavera Amezcua; and Roger van Vloten: Denver, Colo.; Mexico, D.F.; Washington, D.C.

Work done in cooperation with Consejo de Recursos Naturales no Renovables under the auspices of International Cooperation Administration, U.S. Department of State

Reconnaissance geologic mapping, in connection with a study of marine phosphorites, has been completed in an area of about 26,000 square kilometers that lies mainly in northern Zacatecas and southern Coahuila but extends eastward into the States of Nuevo León and San Luis Potosí. Some aspects of this work have been reported previously (Rogers and others, 1956; Rogers and others, 1961; Vloten, 1955),

but little has been published in English [1] concerning the regional tectonics, which are of considerable interest.

The area contains a thick section of marine sedimentary rocks that range in age from Late Jurassic to Late Cretaceous and include three distinct lithologic sequences. In the greater part of the area mapped (fig. 68.1) these rocks have an average thickness of 3,000 to 4,000 meters, but they are several times as thick along the northern margin of the area. The lower sequence was deposited in the Late Jurassic and at the beginning of Early Cretaceous time and is composed predominantly of limestone, with subordinate amounts of calcareous siltstone, sandstone, shale, phosphorite, and chert. It was deposited in the subsiding Mexican geosyncline (Imlay, 1938). The middle sequence is mainly limestone, in part a reef facies, with smaller amounts of clastic material, and was deposited in the widespread late Early Cretaceous sea that covered all of northeastern Mexico. The upper sequence, which contains about two-thirds of the total section, consists largely of shale and sandstone deposited in the shrinking Late Cretaceous sea, which in some areas acquired a foredeep character. It constitutes a clastic wedge.

The sedimentary rocks unconformably overlie a basement complex containing schists and phyllites of possible late Paleozoic age and red beds of Early and Middle Jurassic(?) age. The basement rocks are exposed only along the southwestern margin of the area mapped, in the Teyra-Candelaria section (fig. 68.1).

The area is a part of the major belt of folded mountains that occupies the site of the Mexican geosyncline and that dates from the Eocene orogeny. The position and orientation of the Late Jurassic geosynclinal belt in this part of Mexico, and its departure from a normal northwesterly trend, can be explained by the presence in Jurassic time of the Coahuila Peninsula in the area lying to the north. This southward extension of the North American Mesozoic continent formed a land area that was a major source of sediments in Late Jurassic and Early Cretaceous time. It was covered by shallow seas in late Early and Late Cretaceous time but continued to form a relatively high and stable mass, and during the early Tertiary orogeny served as a buttressing element. Forces acting from the west-southwest compressed the sediments that filled the geosyncline into a series of narrow elongated folds, most of which lay parallel to the borders of the old land mass and were overturned toward the north and east. The deformation also produced many fan structures and some overturning toward the south and west.

Different fold and fault characteristics, and the distribution of the igneous rocks and related mineralization, serve as a logical basis for the division of the mapped area into three geologic provinces (fig. 68.1). These are designated, from north to south, as the valley and ridge belt, the plain and range belt, and the mineral belt, and represent a progression from simple folding to folding with some faulting, and finally to folding with common normal and reverse faulting and igneous activity.

The valley and ridge belt is in the Cross Ranges portion of the Sierra Madre Oriental and is characterized by a series of long, narrow ridges, arcuate toward the east, which form a nearly unbroken mountain barrier with few transverse canyons. The ridges are the topographic expressions of deeply eroded anticlines, and the equally narrow intervening valleys are the topographic expressions of deeply eroded synclines. The close spacing may be the result of crowding of the folds in the vicinity of the foreland mass. Faulting is rare and generally of small magnitude, although low-angle overthrusts are found to the east, along or close to the eastern front of the Sierra Madre Oriental. The limits of the geosyncline in that area were controlled by the presence of another foreland mass, which is generally referred to as the Tamaulipas Peninsula.

The valley and ridge belt is bounded on the north by the Parras Basin, or Bolsón de Coahuila, a large synclinorium on the site of a deep trough that existed in Late Cretaceous time along the margin of the submerged Coahuila Peninsula. The trough was filled with a great thickness of Upper Cretaceous sediments. Geologic mapping did not extend into this belt.

The plain and range belt lies along the boundary between the Sierra Madre Oriental and the Mesa Central and represents a transition from the valley and ridge belt to the mineral belt. The ridges are more widely spaced than in the valley and ridge belt. The relatively broad alluviated valleys not only reflect the presence of more open synclinal structures but have formed partly at the expense of the anticlines, by means of faulting. Thrust faults have not been found within the belt, but normal faults are common. The major structures are (a) longitudinal faults, which appear to have formed contemporaneously with the folding and are an integral part of the fold pattern, and (b) block faults, which belong to two distinct periods and are prominent in several areas.

The mineral belt lies within the Mesa Central, a

[1] A paper in Spanish on the tectonics of the Sierra Madre Oriental between the cities of Torreón and Monterrey was prepared by de Cserna (1956) for the 20th International Geological Congress.

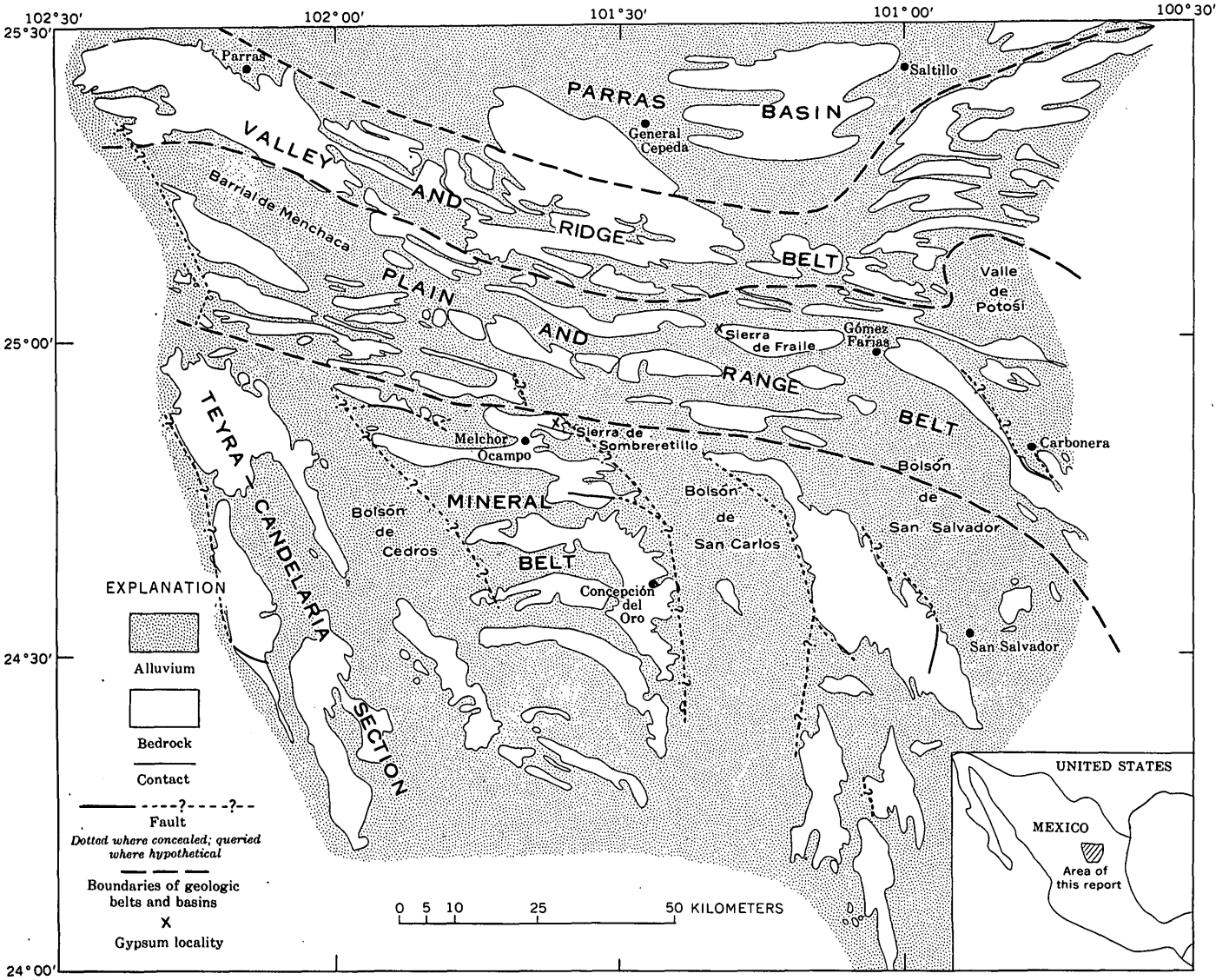

FIGURE 68.1.—Sketch map showing geologic provinces, block faulting, and gypsum localities within the area studied. Approximately 85 percent of the area was mapped by the authors. Most of the remainder is based on mapping by Imlay (1936, 1937, 1938), with some modification by the authors.

major physiographic province resembling the Basin and Range province of the United States. Its most obvious characteristic is the relatively great development of bolsons and the smaller area occupied by the mountain ranges. Block faulting is of major importance, and in addition the belt is characterized by fairly common reverse faults, some of which are low-angle thrusts, and by the wide distribution of igneous rocks, both intrusive and extrusive, with related mineralization. The distribution of the volcanic rocks seems to be related, at least in part, to the block faults, which intermittently bound the large intermontane basins. The faults probably served as conduits for the basaltic magma.

The northwest to north-northwest-trending folds in the Teyra-Candelaria section appear to be somewhat anomalous tectonically. They lie at a sharp angle to the regional trend of this segment of the cordillera, which is westerly, and they differ from all other structures in the area in that the basement rocks were intimately involved with the overlying rocks in the folding and faulting, and have been widely exposed by erosion. It is believed that the explanation for these basement folds lies in the distribution of the Minas Viejas Gypsum, an Upper Jurassic unit that in the region to the east of the map area conformably underlies the thick-bedded limestones at the base of the carbonate sequence. The Minas Viejas is not exposed

within the area under discussion, but it is believed to underlie all except the Teyra-Candelaria section, for the structural pattern to the north and east of that section is typical of shallow folding above abnormally mobile beds; the gypsum has acted as a slip plane and permitted widespread décollement. More direct evidence for the presence of the Minas Viejas Gypsum is found at two localities shown in figure 68.1. One occurs at the west end of the Sierra de Fraile, where a large gypsum mass has been squeezed upward along a normal fault. The other lies near the east end of the Sierra de Sombreretillo, where, in an area of fracturing and mineralization, abundant gypsum was brought up in solution from a lower horizon and deposited in the Upper Jurassic La Caja Formation.

Since gypsum was not present in the Teyra-Candelaria section, deeper folds involving the basement rocks were formed. The northwest orientation of these deep-seated folds may mean that they formed perpendicular to the lateral force that was responsible for the deformation, whereas the shallow folds having a west or west-northwesterly trend formed obliquely to that force.

REFERENCES

Cserna, Zoltan de, 1956, Tectónica de la Sierra Madre Oriental de México, entre Torreón y Monterrey: Internat. Geol. Cong., 20th, Mexico City, 1956, 87 p.

Imlay, R. W., 1936, Geology of the western part of the Sierra de Parras, Coahuila, Mexico: Geol. Soc. America Bull., v. 47, p. 1091–1152.

——— 1937, Geology of the middle part of the Sierra de Parras, Coahuila, Mexico: Geol. Soc. America Bull., v. 48, p. 587–630.

——— 1938, Studies of the Mexican geosyncline: Geol. Soc. America Bull., v. 49, p. 1651–1694.

Rogers, C. L., Cserna, Zoltan de, and others, 1956, General geology and phosphate deposits of Concepción del Oro district, Zacatecas, Mexico: U.S. Geol. Survey Bull. 1037–A, 102 p.

Rogers, C. L., Tavera, Eugenio, and others, 1961, Marine phosphorites of north-central Mexico: Art. 369 *in* U.S. Geol. Survey Prof. Paper 424–D, p. D222–D224.

Vloten, Roger van, 1955, Geology of the border region between Coahuila and Zacatecas, Mexico: Leidse Geologische Mededelingen, v. 19, p. 111–166.

69. PRECAMBRIAN BASEMENT STRUCTURE AND LITHOLOGY INFERRED FROM AEROMAGNETIC AND GRAVITY DATA IN EASTERN TENNESSEE AND SOUTHERN KENTUCKY

By JOEL S. WATKINS, Washington, D.C.

Interpretations of buried basement rocks are made from aeromagnetic and Bouguer gravity anomaly maps in eastern Tennessee and southern Kentucky. The buried Precambrian basement beneath the Paleozoic rocks of the Cumberland Plateau and the Valley and Ridge province has been divided into 5 lithologic units, and 1 major basement fault has been recognized. There is no evidence to suggest that the thrust faults of the Valley and Ridge province extend into the basement.

The interpretations are based on an aeromagnetic survey flown in 1959 by the U.S. Geological Survey. The flight lines are oriented northwest-southeast and are spaced approximately 1 mile apart. Over 900 gravity observations were made along roads in the area during the fall of 1961. About two-thirds of the gravity observations were made at 1-mile intervals along roads which cross the regional structures of the area. The remainder were made at intervals of 1 to 2 miles along roads parallel to regional structure. The observations were made at bench marks and other points of known elevation.

The area of investigation and the major geologic structures are shown in figure 69.1. In the north-

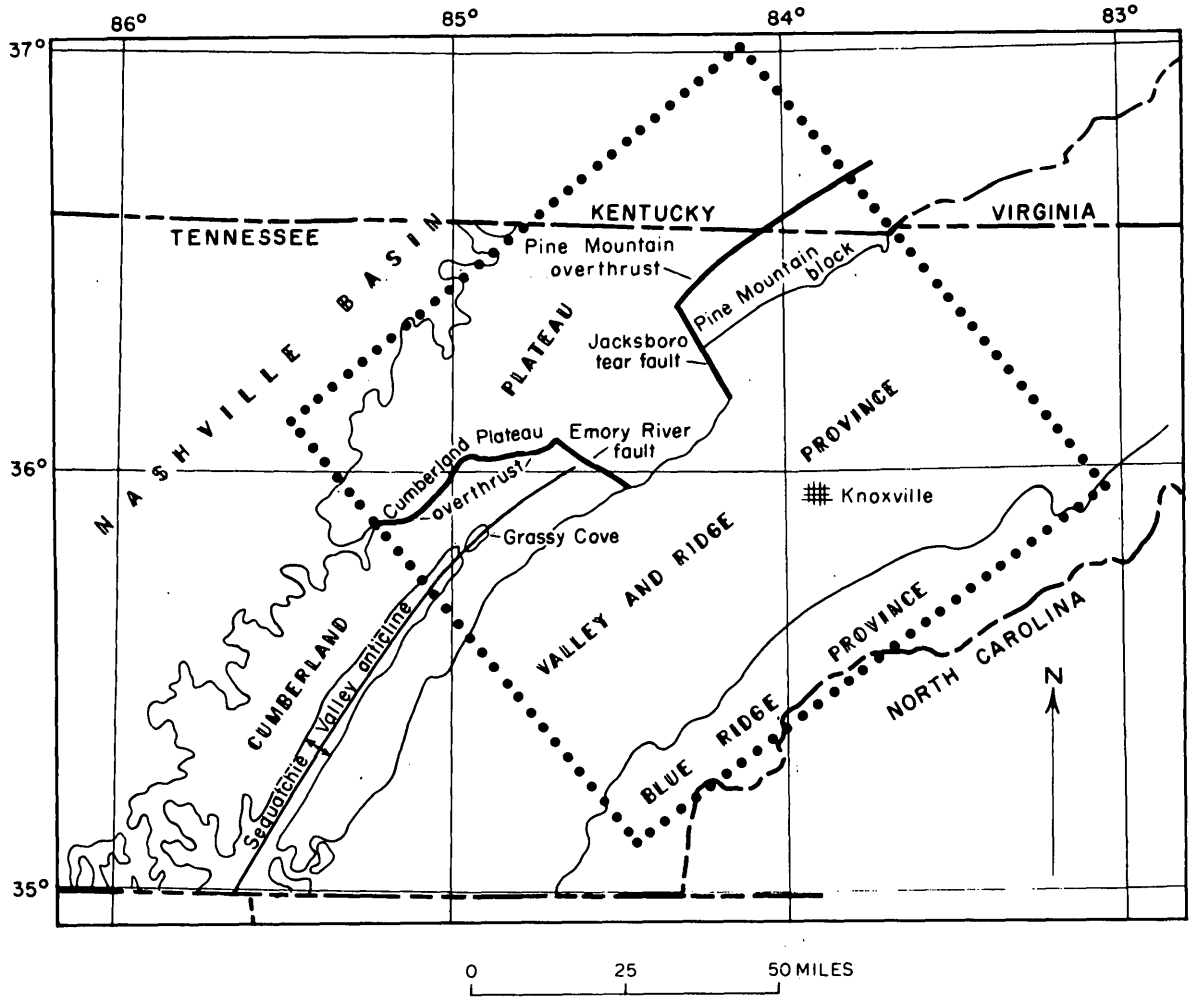

FIGURE 69.1.—Location of aeromagnetic and gravity surveys in eastern Tennessee and southern Kentucky. Generalized structural geology based on Rodgers (1952), Wilson and others (1956), and Wilson and Stearns (1958). Dotted lines enclose area of this report (fig. 69.2).

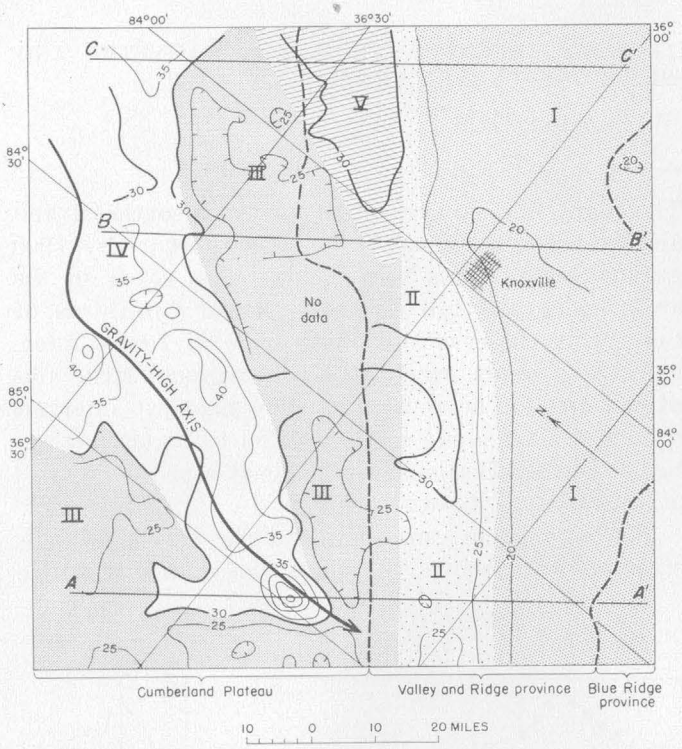

FIGURE 69.2.—Generalized aeromagnetic map of a part of eastern Tennessee and southern Kentucky showing inferred lithologic units of basement, identified by Roman numerals I through V. Contour interval is 500 gammas, and numbers show hundreds of gammas. *A-A'*, *B-B'*, and *C-C'* are the lines of profiles shown in figure 69.3.

western part of the area, the Cumberland Plateau is capped by essentially horizontal Pennsylvanian clastic rocks. The rocks are broken in the southwestern part by the Cumberland Plateau overthrust and the Emory River fault (Wilson and others, 1956) and in the northeastern part by the Pine Mountain overthrust and the Jacksboro tear fault. Displacement is relatively small along the Cumberland Plateau and Emory River faults, but may exceed 10 miles along the Pine Mountain and Jacksboro faults (Wilson and Stearns, 1958). One major fold, the Sequatchie Valley anticline, extends into the southwest margin of the area and dies out near the Emory River fault.

The Valley and Ridge province consists of Paleozoic rocks thrust from southeast to northwest along many thrust planes which are commonly parallel to bedding. Folding with axes parallel to the strike of the thrust faults is common. No attempt is made to show the many fault traces on figure 69.1. The Pine Mountain block resembles the Valley and Ridge province structurally, but it is usually included in the Cumberland Plateau because of its Pennsylvanian cap rock (Wilson and Stearns, 1958).

Rocks of the Blue Ridge Province consist of Late Precambrian and Early Cambrian clastic sedimentary rocks thrust northwestward over the Paleozoic rocks of the Valley and Ridge province (King, 1959).

Interpretation of basement lithologies is possible because sedimentary rocks are essentially nonmagnetic. Magnetic anomalies are therefore the result of variations in magnetic susceptibility in the Precambrian basement. Gravity anomalies, on the other hand, can result from density variations in either the basement or the overlying sedimentary rocks. Sources of gravity anomalies in this study are attributed to the basement only when gravity and magnetic anomalies are coincident over a substantial area or when the observed gravity anomaly is too large to be attributed to density variations within the sedimentary section. The density of many rocks of the sedimentary section has been measured, and calculations show that local anomalies in excess of 10 mgals are probably due to density variations in the basement.

Five lithologic units inferred from gravity and magnetic anomalies are shown in figures 69.2 and 69.3. Unit I is characterized by the near absence of either gravity or magnetic anomalies. The lowest gravity anomaly values on the map are associated with unit II, but the magnetic anomaly values are 500 to 750 gammas higher than in unit I and the magnetic gradients are steeper. Unit III differs from unit II only in that the gravity anomalies are higher and the gravity gradients are steeper. The magnetic anomalies are essentially unchanged across the boundary of units II and III. Unit IV is composed of dense and strongly magnetic rocks. R. W. Johnson, Jr. (written communication, 1961) has shown strong similarities between anomalies in the northward extension of this unit and upward continuations (Henderson and Zietz, 1949) of anomalies of the Lake Superior iron-formations. Unit V is characterized by a small increase in the gravity anomalies (when corrected for regional gravity gradient) and a substantial magnetic anomaly.

Units I and II are separated by a steep magnetic gradient having 500 to 700 gammas of relief (figs. 69.2–69.4). This gradient is interpreted as the magnetic expression of a fault because of (1) the linearity of the anomaly across the map area, (2) the contrast in character of the magnetic contours on either side of the gradient, and (3) the truncation of flattening of anomalies which approach the gradient from either side but do not cross it.

A magnetic anomaly with 2,000–2,500 gammas of relief is located at Grassy Cove near the center of the southwest boundary of the area (near the middle of

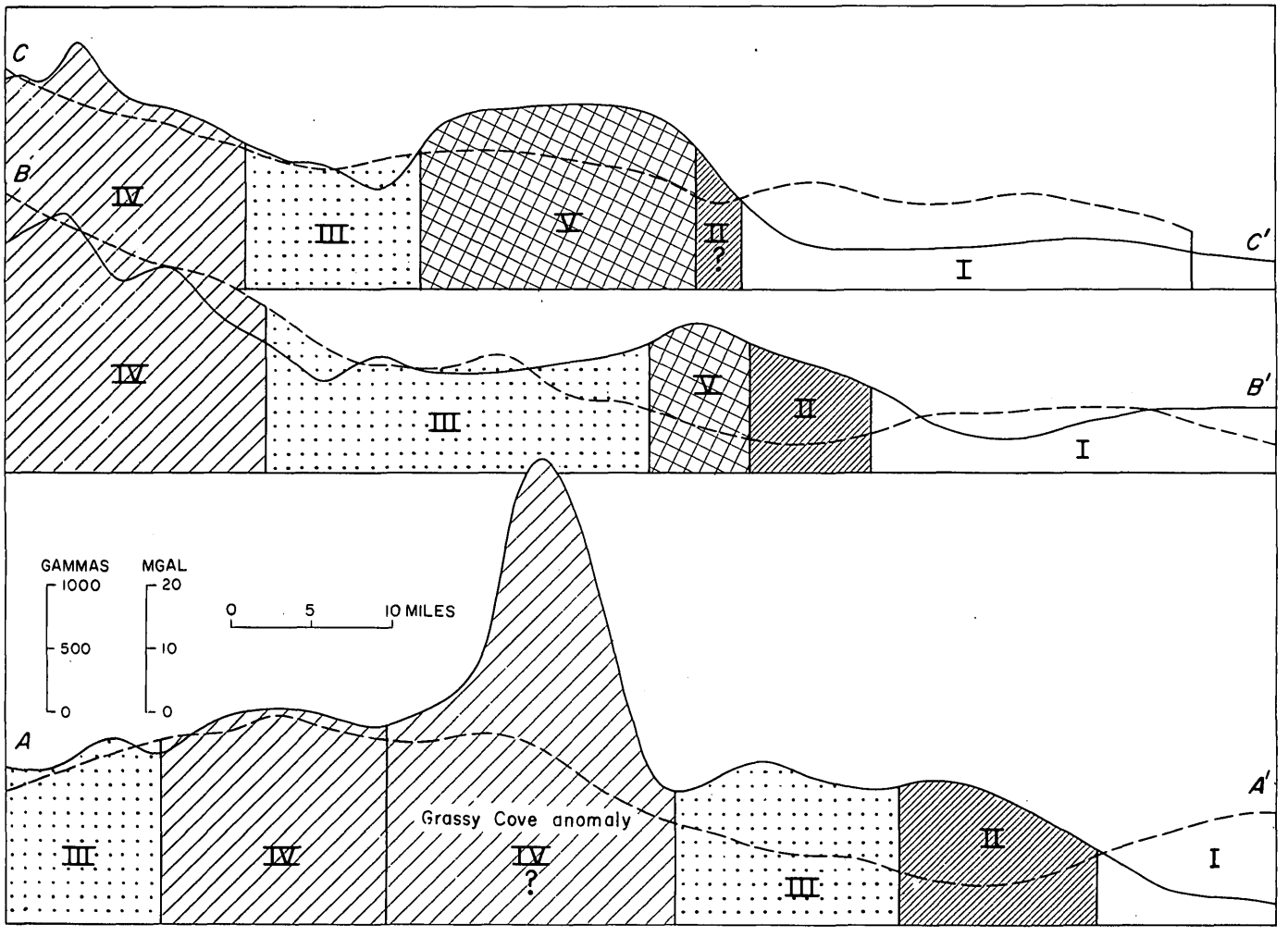

FIGURE 69.3.—Aeromagnetic and Bouguer gravity anomaly profiles. Solid lines represent magnetic intensities and dashed lines represent Bouguer gravity anomalies. Basement lithologic units inferred from the geophysical anomalies are indicated by Roman numerals. Lines of profiles are shown on figure 69.2.

profile A–A'). A major gravity anomaly coincides with the magnetic anomaly. These anomalies are interpreted as representing a plug or stock of dense ultramafic material. This anomaly resembles, in amplitude, the Pea Ridge anomaly in southeast Missouri which is associated with economic iron-ore deposits (Allingham, 1960).

Rocks of the Blue Ridge Province have a distinctive magnetic pattern which makes them easily identifiable even though the amplitudes of the associated anomalies are small. This distinctive pattern is most obvious in the southern corner of figure 69.4. Blue Ridge rocks are not included in the five previously mentioned lithologic zones.

The orientation of the lithologic units suggests that pre-Appalachian structures have a more northerly trend than structures of the Valley and Ridge and the Blue Ridge provinces. Kay (1942) and Woodward (1961) came to similar conclusions concerning the orientation of basement structures in Kentucky and Ohio.

The presence of local magnetic anomalies in all regions of the map area implies that all major basement rock units are at least in part susceptible to magnetization. If a surface thrust fault extends into the basement, then the block of magnetically susceptible basement rock upthrown into nonsusceptible sedimentary rocks should create a linear anomaly parallel to the strike of the fault, with a higher magnetic intensity on the southeast. The fact that no such anomalies exist beneath the Valley and Ridge province implies that the thrust faults do not extend into the basement.

639466 O - 62 - 3

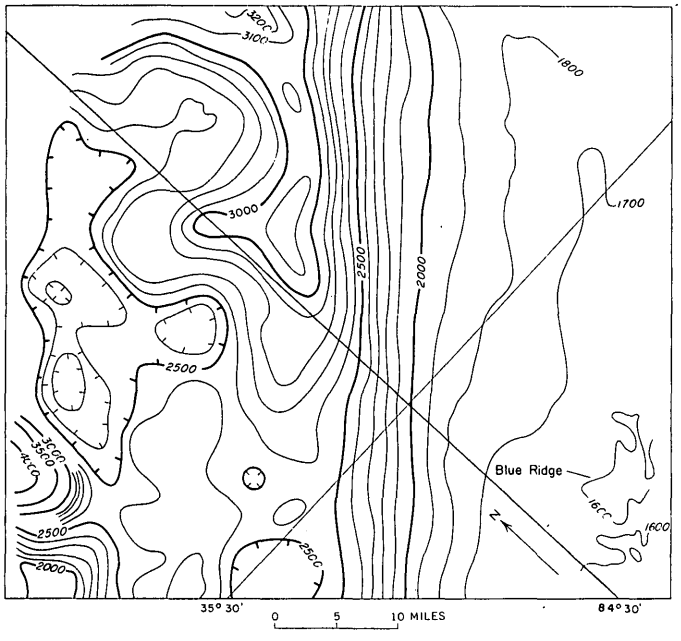

FIGURE 69.4.—Detail of aeromagnetic anomalies southwest of Knoxville, Tenn., in part of the area shown in figure 69.2. Contour interval is 100 gammas.

REFERENCES

Allingham, J. W., 1960, Interpretation of aeromagnetic anomalies in southeast Missouri: Art. 95 *in* U.S. Geol. Survey Prof. Paper 400–B, p. B216–B219.

Henderson, R. G., and Zietz, Isidore, 1949, The upward continuation of anomalies in total magnetic intensity fields: Geophysics, v. 14, p. 517–534.

Johnson, R. W., Jr., 1960, Basement magnetic and gravity anomalies in southeastern Kentucky [abs.]: Geol. Soc. America Bull., v. 71, no. 11, p. 2017–2018.

Kay, G. M., 1942, Development of the northern Allegheny synclinorium and adjoining regions: Geol. Soc. America Bull., v. 53, no. 11, p. 1601–1658.

King, P. B., 1959, The evolution of North America: Princeton, N.J., Princeton Univ. Press, 189 p.

Rodgers, John, 1952, Geologic map of east Tennessee: Tennessee Div. Geology Bull. 58, pls. 1–15.

Wilson, C. W. Jr., Jewell, J. W., and Luther, E. T., 1956, Pennsylvanian Geology of the Cumberland Plateau: Tennessee Div. Geology Folio, 21 p.

Wilson, C. W. Jr., and Stearns, R. G., 1958, Structure of the Cumberland Plateau, Tennessee: Geol. Soc. America Bull. v. 69, no. 10, p. 1283–1296.

Woodward, H. P., 1961, Preliminary subsurface study of southeastern Appalachian interior plateau: Am. Assoc. Petroleum Geologists Bull., v. 45, no. 10, p. 1634–1655.

70. STRUCTURAL EFFECTS RELATED TO HYDRATION OF ANHYDRITE, COPIAPÓ AREA, CHILE

By KENNETH SEGERSTROM, Santiago, Chile

Work done in cooperation with the Instituto de Investigaciones Geológicas

The Gamma Member, 1 to 125 m thick, is the upper member of the Nantoco Formation and immediately underlies the Totoralillo Formation (Biese, 1942). These formations, of Early Cretaceous age, are in the middle part of the Chañarcillo Group, which has a total thickness of about 2,000 m. Despite its thinness, the Gamma Member is exceptionally persistent: it extends 62 km in a sinuous outcrop belt from lat 27°20′ S. to lat 27°56′ S. (fig. 70.1). Rocks of the same lithology in the Corral Quemado manganese district at about lat 30° S., more than 300 km farther south, are probably correlative with the Gamma Member (G. E. Ericksen, oral communication, March 1962). The member is more resistant to erosion than the strata above and below it.

Rocks of the Gamma Member are cliff-forming, cavernous-weathering, massive gray gypsiferous limestone breccia and limestone (fig. 70.2), with several intercalated lenses of dark-gray calcareous shale. In places the rock is partly replaced by hematite and manganese oxide, and it contains irregular pods and stringers of calcite, gypsum, and barite. Breccia zones within the member are made up of platy fragments of shale in a matrix of calcite and gypsum (fig. 70.3).

The underlying and overlying beds are poorly resistant, thin- and medium-bedded calcareous siltstone and limestone with thick lenses of graywacke, which is glauconitic in part. The underlying beds are yellowish gray and are interbedded with thin lenses of black chert. The overlying beds are reddish gray in part, are interbedded with calcareous shale, and contain well-preserved ammonites.

The age of the rocks corresponds to the Hauterivian stage of Neocomian (Early Cretaceous) time, as established by the occurrence of the large ammonite *Crioceras andinum* Gerth in both the Nantoco and Totoralillo Formations (Corvalán and Pérez, 1958).

The Gamma Member of the Nantoco Formation

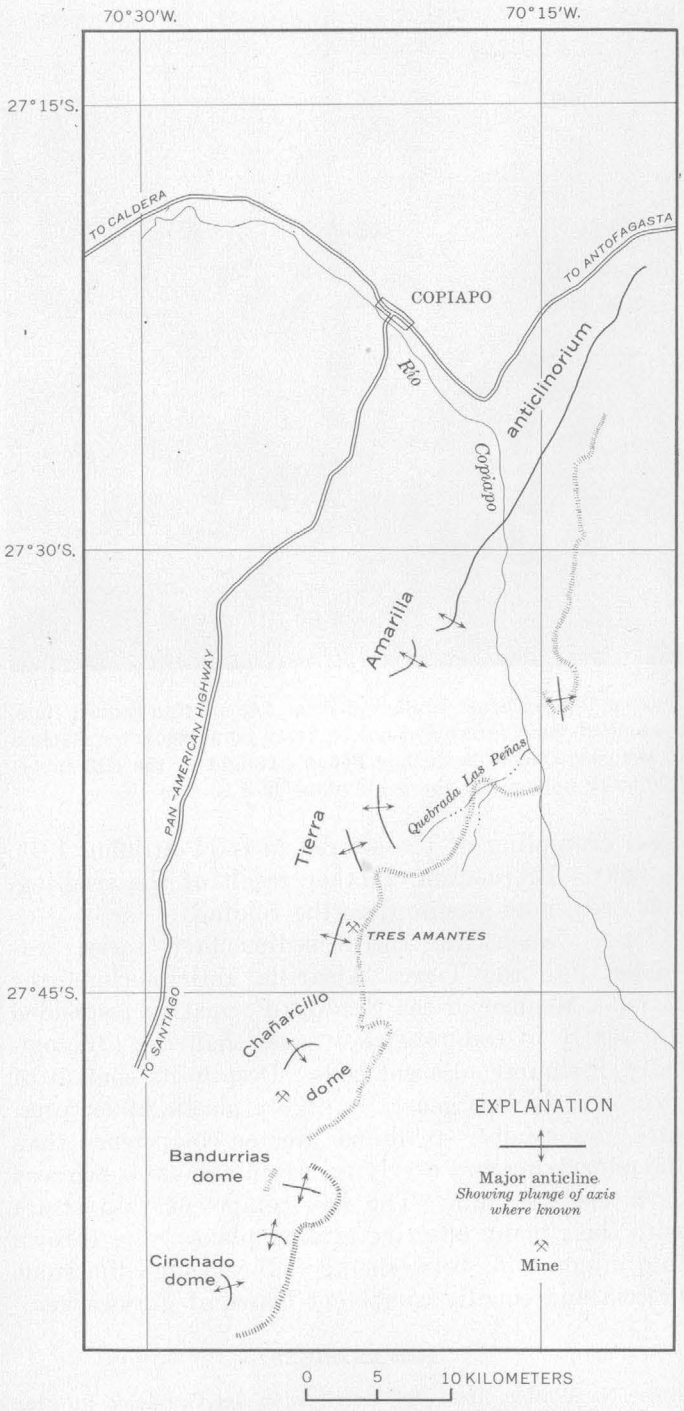

FIGURE 70.1.—Map of an area south of Copiapó, Atacama Province, Chile, showing the location of major anticlines and the outcrop area of the Gamma Member (hachured) of the Nantoco Formation.

crops out on the eastern limb of the Tierra Amarilla anticlinorium (Segerstrom, 1960) and on domes at the south end of this major fold. In places the eastern limb has been deformed by open folds whose axial planes are more or less parallel to that of the anticlinorium, producing repetition of the Gamma Member. Wavelengths of these folds are from several hundred meters to a kilometer or more. In addition, the lenses of calcareous shale are crinkled by minor folds with wavelengths ranging from a few millimeters to 10 centimeters, and the enclosing limestone breccia contains numerous fragments of the crinkled shale.

The thin beds directly underlying and overlying the member have been deformed into innumerable minor

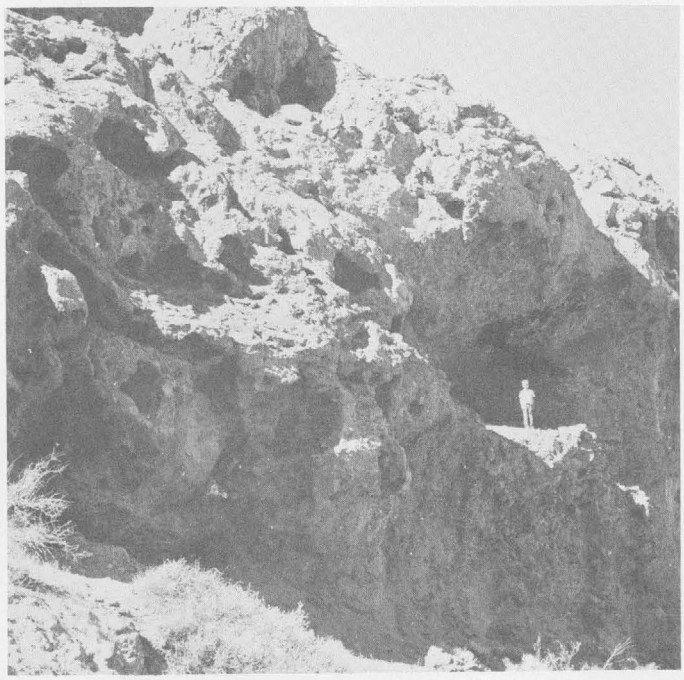

FIGURE 70.2.—Massive gypsiferous limestone breccia and limestone of the Gamma Member of the Nantoco Formation, Quebrada de Las Peñas, Atacama Province, Chile.

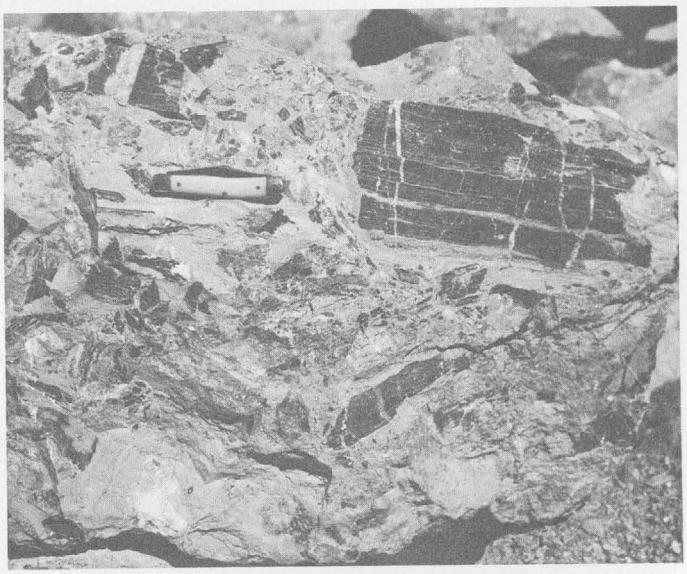

FIGURE 70.3.—Breccia in the Gamma Member made up of platy fragments of shale in a matrix of calcite and gypsum.

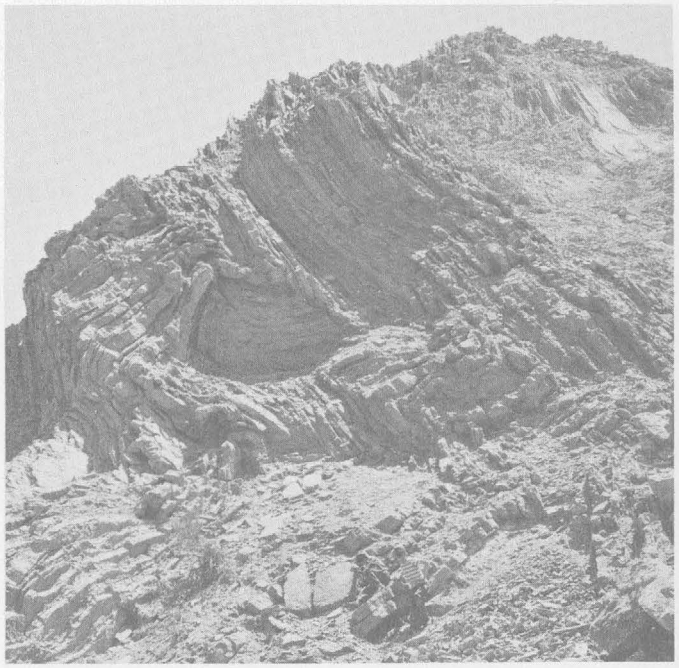

FIGURE 70.4.—Complex folding of thin-bedded limestone of the Totoralillo Formation immediately overlying the Gamma Member of the Nantoco Formation, Quebrada de las Peñas. Amplitude of the central fold (in shadow) is about 10 m.

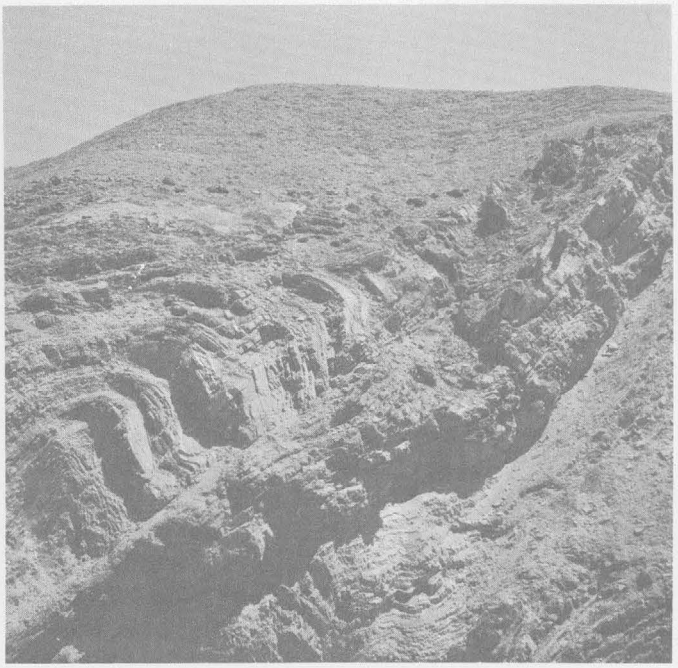

FIGURE 70.5.—Thrust fault and drag fold of thin-bedded limestone of the Nantoco Formation about 50 m below the Gamma Member, Quebrada de Las Peñas. Height of the cliff immediately underlying the fault plane is 3 to 8 m.

synclines and anticlines, most of them of the chevron type, with amplitudes of 2 to 10 m and with axial planes normal to the limbs of the larger open folds. Axes of these minor folds generally plunge down the dip of the limb of the major fold. Axial planes of asymmetric, overturned, and recumbent synclines and anticlines (fig. 70.4), which are also present among the minor folds, are subparallel to those of the major folds. Overthrusting of the folded beds for distances as great as 20 to 30 m has also taken place (fig. 70.5). The minor folds die out below and above the Gamma Member at distances ranging up to about 100 m. Deformation of the beds is further expressed by closely spaced fracture cleavage which is more or less parallel to axial planes of minor folds, and by boudinage. At most places the crinkled and fractured zone of limestone and argillaceous beds is abruptly terminated by relatively undeformed lenses of graywacke, and the rest of the Chañarcillo Group, both above and below the Gamma Member, is neither brecciated nor deformed by minor folds, overthrusts, or fracture cleavage.

Deformation of the Gamma Member may have been due in the first place to its content of gypsum. The gypsum was probably produced by hydration of the original evaporite, anhydrite, which involves an increase in volume of 30 to 50 percent, resulting in local crumpling of the altered beds (Pettijohn, 1949, p. 356). Brecciation, another result of the swelling, was even more intense than the folding.

Later, when the entire sedimentary series was folded into the Tierra Amarilla anticlinorium, the Gamma Member of the Nantoco Formation responded differently to compressive stresses than the lithologically dissimilar adjacent beds. Despite its content of gypsum, which is generally highly plastic under pressure, the member exhibited greater competence than the underlying and overlying strata because it behaved as a massive unit. The less competent thin strata with their many effective gliding planes were thrown into minor folds between the well-cemented limestone breccia and equally competent lenses of graywacke.

REFERENCES

Biese N., Walter, 1942, La distribución del Cretácico inferior al sur de Copiapó: Santiago, Anales del Primer Congreso Panamericano de Ingeniería de Minas y Geología, v. 2, p. 429–466.

Corvalán, José, and Pérez D., Ernesto, 1958, Fósiles guías chilenos (Titoniano-Neocomiano): Santiago, Inst. Inv. Geol. Manual 1, 48 p.

Pettijohn, F. J., 1949, Sedimentary rocks: New York, Harper Bros., 526 p.

Segerstrom, Kenneth, 1960, Structural geology of an area east of Copiapó, Atacama Province, Chile: Internat. Geol. Congr., 21st, Copenhagen 1960, Proc., pt. 18, p. 14–20.

STRATIGRAPHY

71. SEDIMENTARY ROCKS OF TRIASSIC AGE IN NORTHEASTERN MASSACHUSETTS

By ROBERT N. OLDALE, Boston, Mass.

Work done in cooperation with the Massachusetts Department of Public Works

Fragments of unmetamorphosed red arkosic sandstone and conglomerate and red micaceous shale are found in Wisconsin Drift, in both younger and older tills and in glaciofluvial deposits, throughout the northern part of the Salem quadrangle (fig. 71.1). The fragments range in size from boulders to red silt and clay, and are very easily distinguished from the igneous and metamorphic rocks that make up the rest of the drift in this area.

Fragments of arkose and shale in a red matrix form red lenses in the older till. The fragments are disseminated through the typical yellow-brown or olive-brown older till, and are irregularly distributed through the younger till and associated glaciofluvial deposits. At locality 6 (fig. 71.2) a bed of red silty clay was found at the base of the glaciofluvial deposits. A red flowtill layer 6 inches to 1 foot thick and 60 to 80 feet long was interbedded with typical yellow-brown glaciofluvial deposits at locality 7.

The highest concentration of unmetamorphosed arkose and shale fragments in the drift is at localities 2, 3, 4, and 5. To the south and east of this area the arkose and shale fragments in the drift decrease in abundance; in the southern part of the quadrangle they are almost or completely absent. To the north and west the frequency of arkose and shale in the drift appears to decrease rapidly. Exposures are few, however, and accurate estimates of the frequency of arkose and shale fragments were not made.

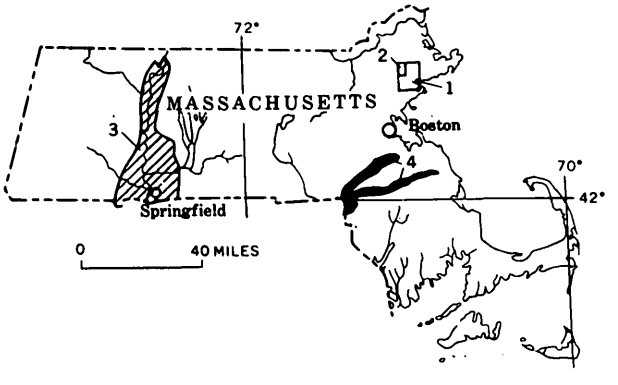

FIGURE 71.1.—Index map of Massachusetts showing (1) location of the Salem quadrangle, (2) area of figure 71.2, (3) approximate distribution of the Connecticut Valley Triassic sediments, and (4) the approximate distribution of the Carboniferous Wamsutta Formation.

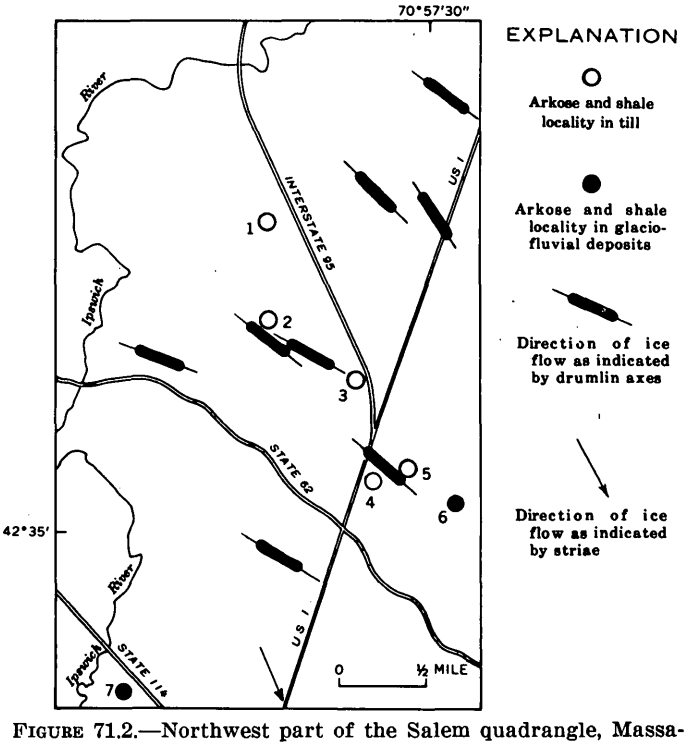

FIGURE 71.2.—Northwest part of the Salem quadrangle, Massachusetts, showing localities where fragments of unmetamorphosed arkose and shale have been found in glacial drift.

The abundance of arkose and shale fragments in both tills may indicate that the outcrop was overrun and eroded by both advances of the ice. The high concentration of arkose and shale in the drift in the northwestern part of the quadrangle suggests that the bedrock source is near this area. Directions of striations and drumlin axes indicate that at least the last ice sheet moved from the north-northwest or northwest. The direction of motion of the earlier ice advance was probably little different from that of the last. Therefore, the bedrock source of the fragments in the drift is probably north or west of the northwest corner of the Salem quadrangle.

Unmetamorphosed conglomerates, sandstones, and shales similar in appearance are found in Triassic

sediments in the Connecticut Valley, and somewhat similar slightly metamorphosed red sedimentary rocks occur in the Carboniferous Wamsutta Formation in southeastern Massachusetts (fig. 71.1; Emerson, 1917, p. 54 and p. 89–96). Slightly metamorphosed light-yellow conglomerates of probable late Paleozoic age have been reported in the northeastern corner of the Georgetown quadrangle, immediately north of the Salem quadrangle (N. P. Cuppels, oral communication, 1962). In all places these rocks rest unconformably upon the underlying igneous and metamorphic rocks.

A comparison of thin sections from the rock fragments found in the drift, from sedimentary rocks from the northeastern part of the Georgetown quadrangle, and from Triassic arkoses and shales from the Connecticut Valley showed that the drift fragments most closely resemble the Triassic rocks in composition, texture, and in lack of metamorphism. The rocks from the Georgetown quadrangle, which appear to be the closest possible source of the fragments, are different in composition and texture and are slightly metamorphosed. Thus the fragments in the drift appear to be Triassic in age and to come from a body of Triassic rocks now buried beneath the glacial deposits, located northwest of the Salem quadrangle.

REFERENCE

Emerson, B. K., 1917, Geology of Massachusetts and Rhode Island: U.S. Geol. Survey Bull. 597.

72. SUBDIVISION OF THE CATSKILL FORMATION IN THE WESTERN PART OF THE ANTHRACITE REGION OF PENNSYLVANIA

By Harold H. Arndt, Gordon H. Wood, Jr.; and J. Peter Trexler: Washington, D.C.; Ann Arbor, Mich.

The Catskill Formation of Late Devonian and Early Mississippian age (Art. 73) is subdivided into various members between the Pocono plateau and the Allegheny front in Pennsylvania. The members, for the most part, are based on differences in lithology within the formation, which in northeastern Pennsylvania consists chiefly of a thick sequence of continental red beds that grade laterally westward into and intertongue with successively younger marine rocks.

Detailed mapping in Schuylkill, Northumberland, Lebanon, Dauphin, and Columbia Counties (fig. 72.1) has shown that the lower part of the Catskill intertongues from east to west with the Trimmers Rock Sandstone of Late Devonian age, and that the upper part of the formation is unconformably overlain by the Pocono Formation of Early Mississippian age (Trexler, Wood, and Arndt, 1961). The lower part of the formation consists of interbedded marine and continental rocks and the upper part consists predominantly of continental rocks with a few marine tongues. Thus the Catskill represents a transitional phase of sedimentation that separates wholly marine Middle and lower Upper Devonian rocks from continental Carboniferous rocks.

The Catskill Formation is 5,000 to 9,400 feet thick in the western part of the Anthracite region. The Spechty Kopf Member, consisting of 0 to 2,400 feet of gray and olive conglomerate, sandstone, siltstone, and shale interbedded with lesser amounts of red sandstone, siltstone, and shale, is at the top of the formation (fig. 72.2) in most of the area of detailed mapping. It is successively underlain in the southern part of the area by 700 to 1,800 feet of dominantly red sandstone, siltstone, and shale here designated the Cherry Ridge Member; 0 to 700 feet of gray to pink conglomerate, sandstone, siltstone, and shale, here designated the Honesdale Sandstone Member; 2,300 to 4,700 feet of dominantly red sandstone, siltstone, and shale, here designated the Damascus Member; and a previously unnamed sequence of red and olive-hued sandstone, siltstone, and shale transitional between Trimmers Rock lithology and typical Catskill red bed lithology which comprises the lower 200 to 2,250 feet of the formation. The Cherry Ridge, Honesdale Sandstone, and Damascus Members are so designated here because the authors believe they are correlative with the Cherry Ridge red beds, Honesdale sandstone, and Damascus red shale subdivisions of the Catskill Formation of eastern and northeastern Pennsylvania described by Willard and others (1939).

Subdivision of the Catskill Formation in the southern part of the area of detailed mapping is based largely on the occurrence of the recognizable Hones-

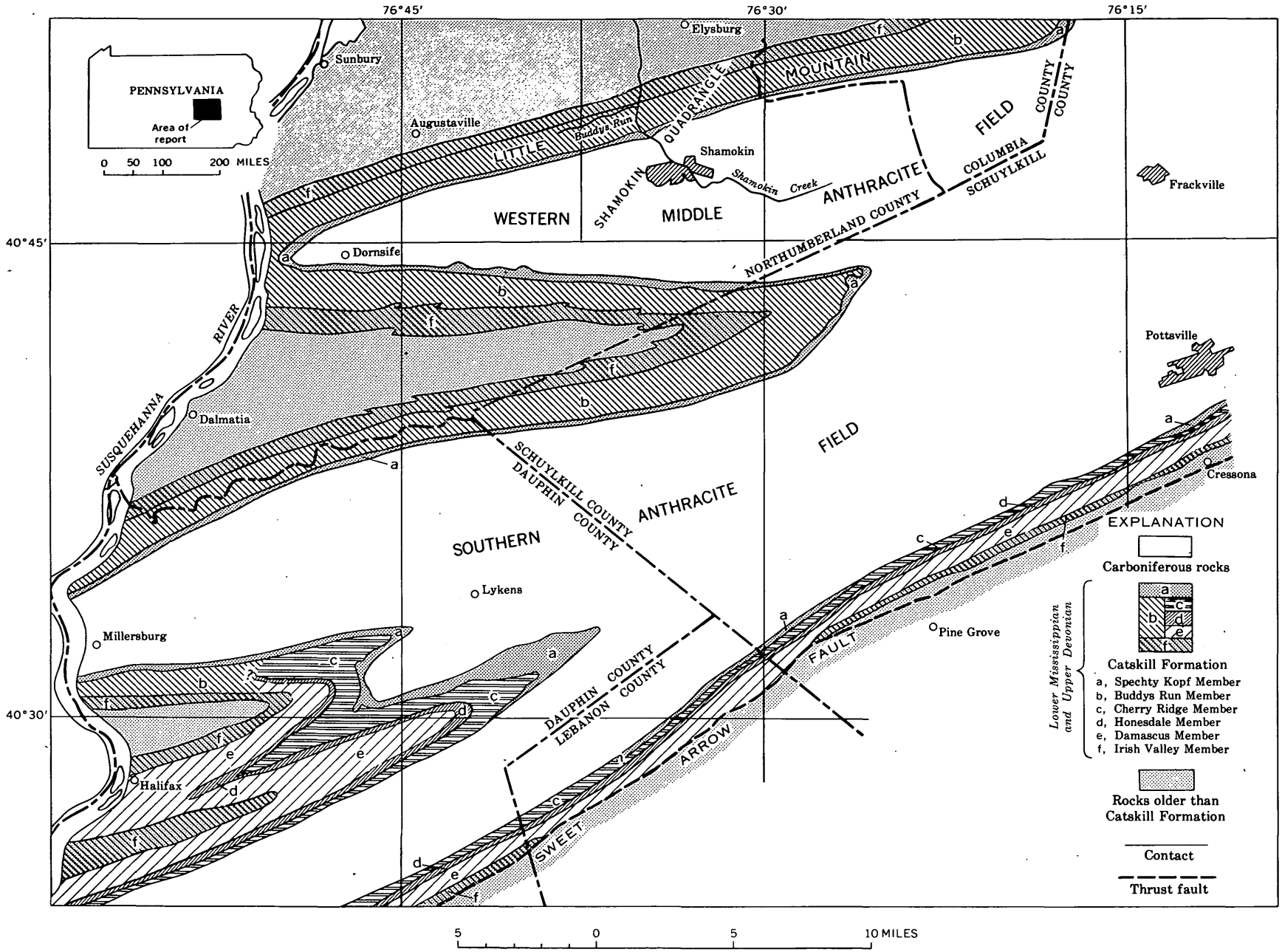

FIGURE 72.1.—Map showing subdivisions of the Catskill Formation in the western part of the Anthracite region, Pennsylvania.

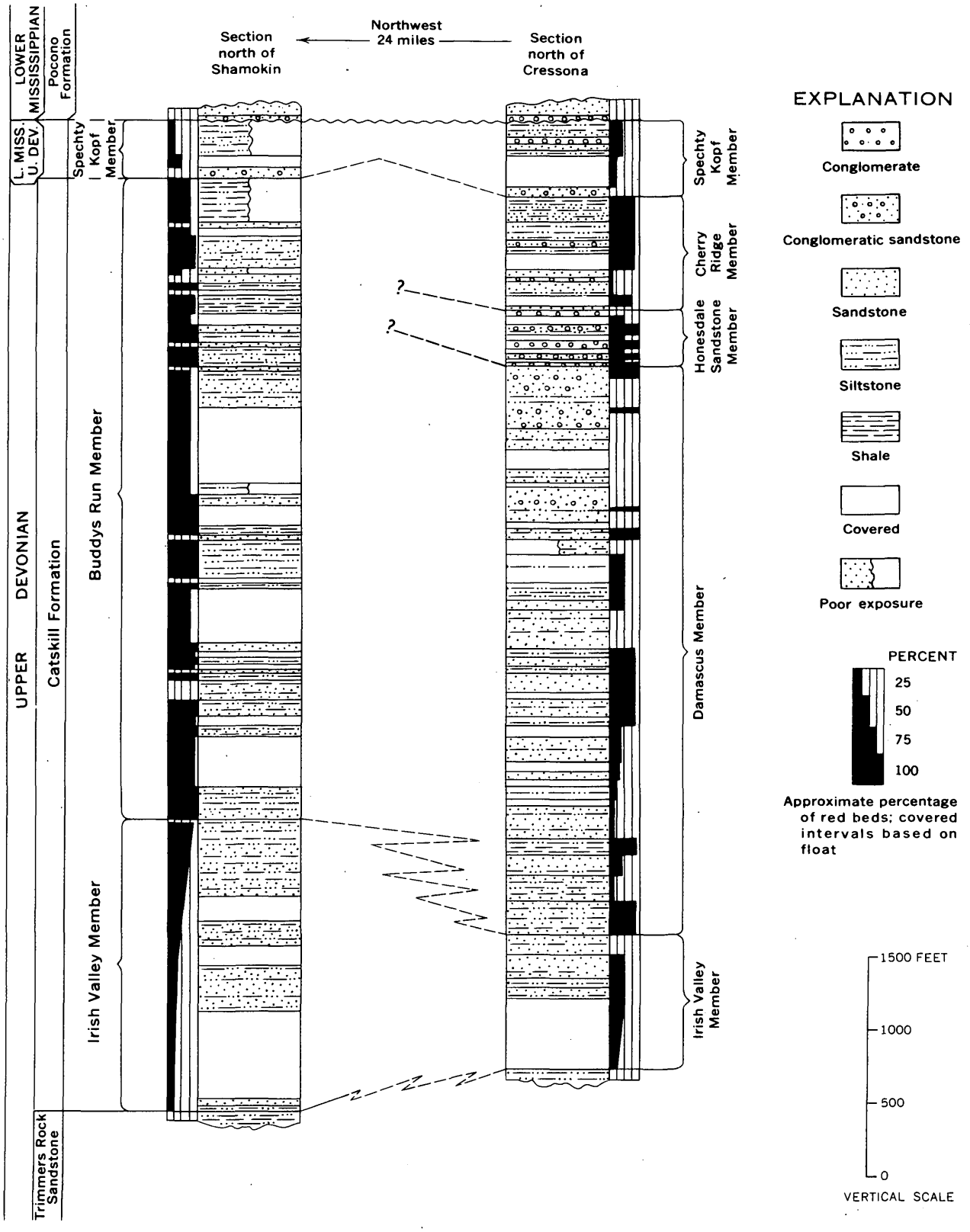

FIGURE 72.2.—Generalized stratigraphic sections showing approximate percentages of red beds and subdivisions of the Catskill Formation in the western part of the Anthracite region, Pennsylvania.

dale Sandstone Member. Where the Honesdale is absent or not recognizable, as in the west-central part of the area, the Cherry Ridge Member and the Damascus Member cannot be differentiated. Thus, except for the Spechty Kopf Member at the top of the formation, 4,000 to 8,200 feet of Catskill rocks in the west-central part of the area was not subdivided prior to this report.

In the west-central part of the Anthracite region where the Honesdale Sandstone Member is absent or not recognizable, the catskill Formation contains few widespread key units by which it may be subdivided. Because of the lack of good exposures, stratigraphic units commonly cannot be correlated for any distance from the locality where first observed. The upper two-thirds of the Catskill below the Spechty Kopf Member consists of grayish-red predominantly continental facies. The lower third of the formation, however, is composed of intercalated grayish-red, olive-gray, and olive-brown marine and continental facies and, because of its transitional nature and varicolored aspect, forms a widely mappable stratigraphic unit in the Catskill Formation.

The lower varicolored sequence of intertonguing continental and marine facies of the Catskill Formation in the western part of the Anthracite region is here named the Irish Valley Member, and the upper dominantly red continental facies beneath the Spechty Kopf Member is here designated the Buddys Run Member. Both the newly recognized members are named from the same locality in the Shamokin quadrangle, Northumberland County, Pa.; the Irish Valley Member for the valley which lies north of Little Mountain, between Augustaville and Shamokin Creek, and the Buddys Run Member for the small stream which flows east through Irish Valley to Shamokin Creek. Both members are best exposed at their type section at the mouth of Irish Valley on the west side of Shamokin Creek along the Reading Railroad north of Shamokin. The top of the Buddys Run along these tracks is in the water gap in Little Mountain, about 1½ miles northwest of the Shamokin city limits, and the base of the Irish Valley is about 3¼ miles north of the city limits.

The Buddys Run Member is 4,400 feet thick at the type section (fig. 72.2). It consists of about 75 percent red beds, chiefly grayish-red to pale-brown and brownish-gray sandstone, siltstone, and shale, and 25 percent gray to light-olive-gray and dusky-yellow sandstone, siltstone, and shale. Gray and olive-hued rocks are thinly dispersed in this dominantly red-bed succession and only in very restricted stratigraphic sequences do gray or olive-hued rocks predominate over the red beds.

Thin-bedded micaceous siltstone forms about 40 percent of the section. Thin- to medium-bedded quartzose sandstone, which forms about 30 percent of the member, is common throughout the section but is more prevalent among the gray and olive-hued rocks. Most of the sandstone is fine to medium grained, but several beds of moderate-yellowish-brown coarse-grained sandstone occur in the upper part of the section. Platy and moderately fissile shale forms the other 30 percent of the member.

Crossbedding is common, particularly in the upper part of the member. The middle part is fairly evenly bedded and somewhat flaggy, whereas the lower part is generally more evenly bedded and blocky. Mudcracks are preserved in many of the red beds, and oscillation ripple marks are common in the red beds as well as in the gray and olive-hued rocks. Fragmentary plant fossils occur throughout the member without regard to rock color, and at several localities they are associated with what appear to be poorly preserved brachiopods or pelecypods.

The top of the Buddys Run Member is arbitrarily placed at the horizon where gray and greenish-gray beds characteristic of the Spechty Kopf Member predominate over red beds characteristic of the main body of the Catskill. The basal beds of the Buddys Run Member intertongue with the upper beds of the Irish Valley Member. The contact is arbitrarily placed at the horizon where the dominantly red-bed sequence comprising the main body of the Catskill Formation is, in the lower part, noticeably replaced by olive and gray beds.

The Buddys Run Member crops out in a continuous belt that surrounds the western end of the Western Middle anthracite field and the northern prong or "fishtail" of the Southern anthracite field. South of the "fishtail," about 8 miles southeast of Millersburg, a thin sequence of pinkish-gray sandstone and conglomeratic sandstone gradually wedges into the grayish-red siltstone and sandstone in the upper part of the member. This sequence is the northwesternmost known occurrence of the Honesdale Sandstone Member. South and east of that locality the upper part of the Catskill Formation is subdivided into the Cherry Ridge Member, Honesdale Sandstone Member, and Damascus Member instead of the Buddys Run Member.

The Irish Valley Member is about 2,000 feet thick at the type section (fig. 72.2). In contrast to the Buddys Run Member, it contains less than 50 percent red beds. Grayish-red to brownish-gray and greenish-

gray sandstone, siltstone, and shale predominate in the upper part of the member. However, the proportion of olive-gray to olive-brown and dusky-yellow sandstone, siltstone, and shale steadily increases downward in the section.

The sandstones are fine to very fine grained, quartzitic, and commonly micaceous. They occur in tabular, thin-bedded sequences in almost equal abundance with siltstone and shale. Weathered surfaces of the sandstone and siltstone commonly have a hackled appearance, and at a few localities spheroidal weathering has developed.

Fossil plant fragments are rare and appear to be restricted to the upper two-thirds of the member. Although not abundant, invertebrate marine fossils occur throughout the Irish Valley Member.

The Irish Valley Member conformably overlies the Trimmers Rock Sandstone of Late Devonian age. The contact between them is drawn at the base of the lowest red bed in the section; however, because of intertonguing, individual red beds wedge out along the strike and the base of the Catskill Formation becomes progressively younger westward.

The Irish Valley Member occurs throughout the area of detailed mapping, ranging from 200 to 2,250 feet in thickness. Within the member are sequences of varicolored rocks that individually are not sufficiently distinctive to be mapped widely. Collectively these sequences comprise a marine and continental sedimentational unit, the so-called "transition beds" of the Catskill Formation. The main distinction between the Irish Valley and Buddys Run Members of the Catskill Formation is the dominant red hue of the Buddys Run in contrast to the varicolored rocks of the Irish Valley. The sedimentary features of the Catskill rocks in the western part of the Anthracite region are not plentiful or diagnostic enough everywhere to indicate clearly the environmental conditions in which the rocks were deposited. Therefore, it is not practical to attempt subdivision of the Catskill strictly on the basis of marine versus continental rocks.

REFERENCES

Trexler, J. P., Wood, G. H., Jr., and Arndt, H. H., 1961, Angular unconformity separates Catskill and Pocono Formations in western part of Anthracite region, Pennsylvania: Art. 38 *in* U.S. Geol. Survey Prof. Paper 424–B, p. B84–B88.

Willard, Bradford, and others, 1939, The Devonian of Pennsylvania: Pennsylvania Geol. Survey, 4th ser., Bull. G–19, 481 p.

73. UPPERMOST DEVONIAN AND LOWER MISSISSIPPIAN ROCKS OF THE WESTERN PART OF THE ANTHRACITE REGION OF EASTERN PENNSYLVANIA

By J. Peter Trexler; Gordon H. Wood, Jr., and Harold H. Arndt: Ann Arbor, Mich.; Washington, D.C.

The uppermost Devonian and Lower Mississippian rocks adjacent to the western part of the Southern Anthracite field and to most of the Western Middle Anthracite field are herein defined to include the Spechty Kopf Member of the Catskill Formation and the Beckville and Mount Carbon Members of the overlying Pocono Formation. The three members are named herein, and their lithology and lateral stratigraphic relations are described.

The Catskill Formation, which is 5,000 to 9,400 feet thick and consists in large part of red beds, has until recently been considered to be of Late Devonian age. During the 1960 field season the authors determined, however, that the uppermost beds of the Catskill Formation in the western part of the Anthracite region are of Early Mississippian age. These beds constitute a sequence of gray and olive-gray sandstone, conglomerate, shale, and siltstone, with interbeds of red sandstone and shale, that is so distinctive that the sequence can be mapped separately. This sequence was informally named the gray member of the Catskill by Trexler, Wood, and Arndt (1961, p. B84). The Catskill Formation is unconformably overlain by the Pocono Formation of Early Mississippian age, which consists of 550 to 1,800 feet of gray conglomerate, sandstone, siltsone, and shale.

SPECHTY KOPF MEMBER OF THE CATSKILL FORMATION

The beds previously included by the authors in the gray member of the Catskill Formation are included in a unit here named the Spechty Kopf Member after

Spechty Kopf, a small hill about 3.5 miles south-southeast of the town of Lykens in Dauphin County. Spechty Kopf hill, which is underlain by the lower part of the member (fig. 73.1), is near the locality

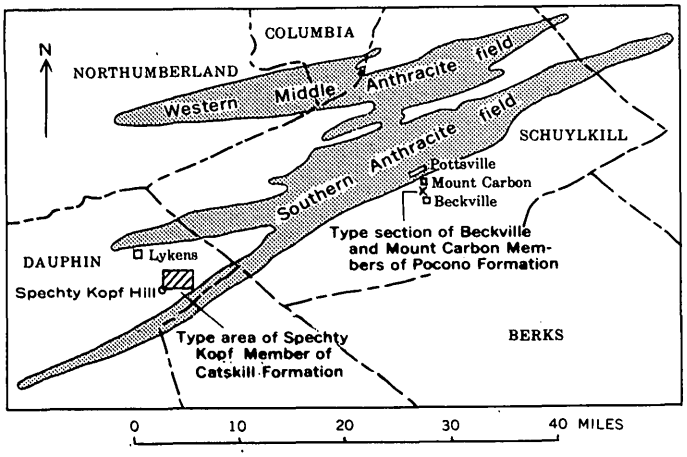

FIGURE 73.1.—Map showing the Southern and Western Middle Anthracite fields, Pennsylvania, location of the type section of the Beckville and Mount Carbon Members of the Pocono Formation, and type locality of the Spechty Kopf Member of the Catskill Formation. (See Art. 74, fig. 74.1, for map showing the location of anthracite fields in eastern Pennsylvania.)

where the member was first recognized and is where the member is apparently thickest and contains the youngest beds. Exposures of the Spechty Kopf Member are poor, and the authors have not been able to find a complete or nearly complete section. The member is defined, therefore, without a type section, but the type locality is here designated as being to the east and northeast of Spechty Kopf hill in the headwaters of Powell Creek, Stone Cabin Run, and the East Branch of Rattling Creek, all of which are located in the Lykens 7½-minute quadrangle.

The maximum thickness of the Spechty Kopf Member in the type locality is about 2,400 feet. The lower 500± feet consists chiefly of gray and gray-green sandstone, shale, and fine to coarse quartz-pebble conglomerate with a few intercalated thin red beds. The lithology of the gray beds in this part of the member is similar to that of beds in the younger Pocono Formation, and previous workers have included the lower 500 feet of the Spechty Kopf in the Pocono at many places in the western part of the Anthracite region where the overlying beds of the member are missing. The upper 1,900± feet of the member consists of almost equal amounts of the gray and olive-gray sandstone and fine conglomerate, and red beds. Beds of gray and olive-gray sandstone and fine conglomerate are concentrated largely in the upper 1,000 feet.

The lower contact of the Spechty Kopf Member with red beds of the underlying main body of the Catskill Formation is not well-exposed in the type area. It is gradational and is placed arbitrarily at the horizon where gray- and olive-hued beds characteristic of the Spechty Kopf predominate over red beds characteristic of the main body of the Catskill. This horizon commonly lies only a few feet below a gray to olive-gray fine to coarse quartz-pebble conglomerate. An unconformity separates the Spechty Kopf Member from the overlying Pocono Formation in the type area and throughout the western part of the Anthracite region (Trexler, Wood, and Arndt, 1961). On Peters Mountain south and east of the type area and on Broad Mountain west of the type area, the upper beds of the member are beveled gradually by the unconformity, and the overlying basal conglomerate of the Pocono rests upon successively older beds of the Spechty Kopf and in some places upon the main body of the Catskill.

In 1961 the authors (p. B87) cited paleobotanical evidence which indicates that the gray member of the Catskill (Spechty Kopf Member of this article) is Late Devonian and Early Mississippian in age. This age determination was made by S. H. Mamay (oral communication, 1960) on the basis of a sparse fossil flora collected by the authors about 500 feet above the base of the member at the juncture of Line and Little Mountains in the Sunbury 7½-minute quadrangle. In addition, Read (1955, p. 8) included beds in the lower part of the Pocono Formation which the authors recognize as the lower part of the Spechty Kopf Member. These beds contain fossil plants which Read assigned to his Early Mississippian zone of *Adiantites*. These data show that much of the Spechty Kopf is of Early Mississippian age.

The Spechty Kopf Member has been mapped and correlated throughout most of the western part of the Anthracite region (Trexler, Wood, and Arndt, 1961, fig. 38.1), where it ranges in thickness from 0 to about 2,400 feet. The Spechty Kopf probably correlates with beds in northeastern Pennsylvania that were included by Willard and others (1939, p. 283–284) in the Elk Mountain Sandstone and the Mount Pleasant Red Shale. The Spechty Kopf may also be correlative with the marine Oswayo Formation of north-central Pennsylvania, which is considered to be Devonian but which may contain Lower Mississippian beds in its upper part.

BECKVILLE AND MOUNT CARBON MEMBERS OF THE POCONO FORMATION

During field mapping and stratigraphic studies in the vicinity of the Southern Anthracite field, the authors divided the Pocono Formation into two mappable stratigraphic units. Each unit consists, at the base, of a fine to coarse quartz-pebble conglomerate that is overlain by intercalated beds of fine pebble conglomerate, conglomeratic sandstone, quartzose sandstone, subgraywacke, siltstone, shale, and a few thin lenses of anthracite. The authors here name the lower of these stratigraphic units the Beckville Member and the upper the Mount Carbon Member.

The type section of the members of the Pocono Formation (fig. 73.1) is on the east side of the water gap cut in Second Mountain by the West Branch of the Schuylkill River in the Pottsville 7½-minute quadrangle of Schuylkill County. The rocks in the type section are slightly overturned to the north and are moderately to well-exposed on the east side of the paved road connecting the villages of Beckville and Mount Carbon. The base of the formation and of the Beckville Member lies a few feet north of the paved road junction 1 mile north of Beckville. The contact between the 2 members is 0.15 mile north of this road junction, and the upper contact of the formation (the contact also of the Mount Carbon Member with red beds of the overlying Mauch Chunk Formation) is 0.25 mile north of this road junction.

The Beckville Member is named after the village of Beckville, Schuylkill County. At the type section the member is 544 feet thick and is well exposed. The basal unit of the member is 18 feet thick and consists of a very-light-gray to light-olive-gray quartz-pebble conglomerate that rests disconformably upon a 30-foot unit of light-olive-gray dark-brown-weathering shale and siltstone of the Spechty Kopf Member of the Catskill Formation. This 30-foot unit is underlain by 101 feet of contorted shale and siltstone also assigned to the Spechty Kopf.

The pebbles in the basal conglomerate of the Beckville are as much as 3 inches in diameter. The upper contact of the Beckville is located at the top of a 1.5-foot medium- to dark-gray coaly shale which contains abundant plant remains. The basal bed of the overlying Mount Carbon Member is a conglomerate and coarse sandstone, 30 feet thick, which rests conformably upon the shale. The succession and lithology of beds in the member are shown on figure 73.2.

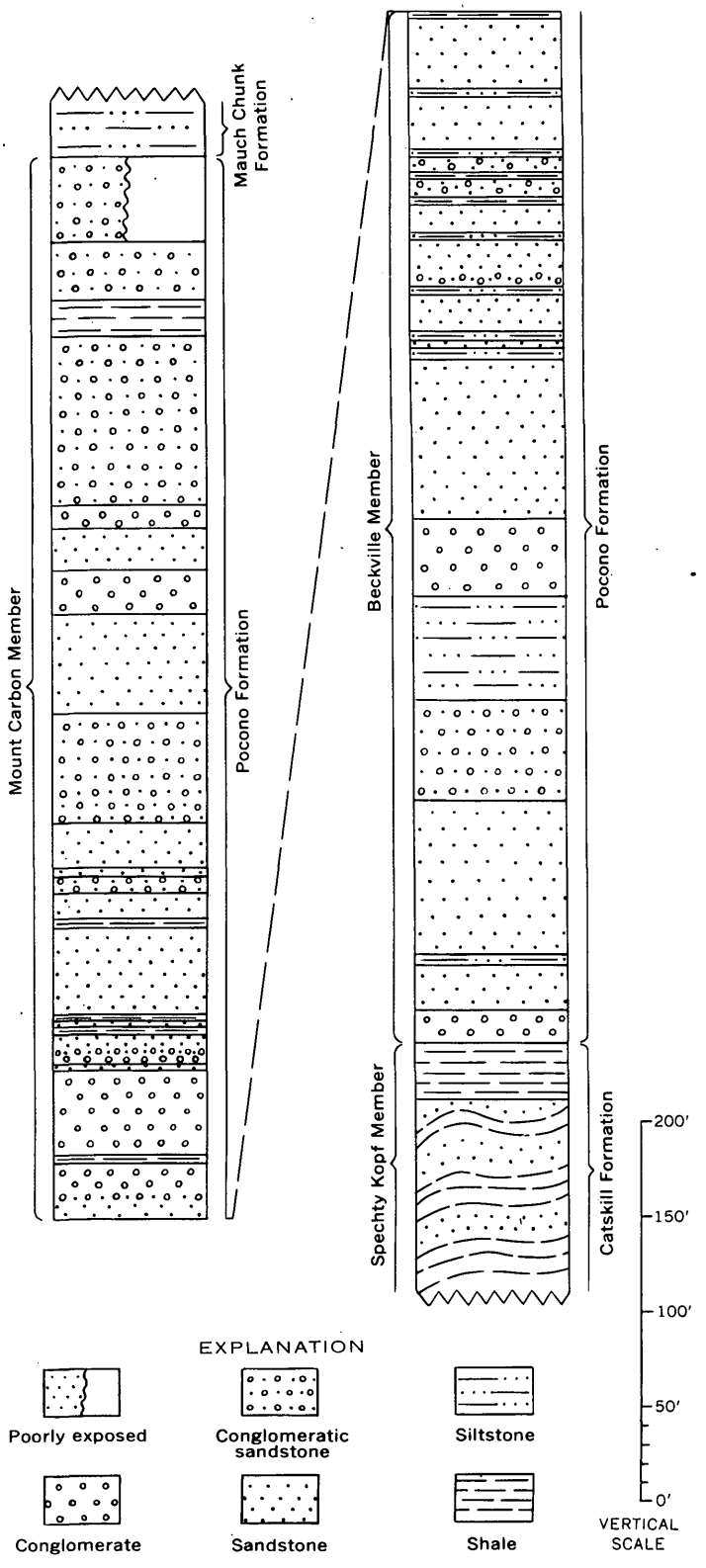

FIGURE 73.2.—Stratigraphy of the Beckville and Mount Carbon Members of the Pocono Formation at their type section.

The Mount Carbon Member is named from Mount Carbon, a village on the southern outskirts of the city of Pottsville in Schuylkill County. The member is 560 feet thick at the type section. Except for the upper 45 feet, the member is fairly well exposed in the type section. The basal unit of the member is a 30-foot-thick light-olive-gray to light-gray quartz-pebble conglomerate which grades downward into a thin coarse sandstone, below which the contact is placed. The quartz pebbles range from ¼ to ¾ inch in diameter. The upper unit of the member in the type section is a poorly exposed light-gray conglomeratic sandstone about 45 feet thick. It is overlain by about 30 feet of grayish-red siltstone of the Mauch Chunk Formation. The lithologic succession of the member is shown on figure 73.2.

The Beckville and Mount Carbon Members of the Pocono Formation contain a fossil flora which Read (1955, p. 8–15) considered to be Early Mississippian in age. The two members thin irregularly northward and northwestward and thicken irregularly southwestward across the western part of the Anthracite region. Both appear to attain their maximum thickness in the vicinity of Lykens, where the Beckville is about 800 feet thick and the Mount Carbon is about 1,000 feet thick. The members have been traced around the Southern Anthracite field. To the north and to the west of this field the basal conglomerate of the Mount Carbon gradually loses its conglomeratic character and it is increasingly difficult, and in many places impossible, to distinguish the two members. The conglomerate at the base of the Beckville Member, however, is recognizable throughout the western part of the Anthracite region and may be correlative with the Griswold Gap Conglomerate of White (1881, p. 56–57). Reconnaissance stratigraphic studies by the authors indicate that the Beckville and Mount Carbon Members may be recognizable over considerable areas northeast of the Southern Anthracite field. The authors recommend that, until additional stratigraphic work is done on the Pocono Formation, the members be recognized as stratigraphic units only in the region surrounding the Southern Anthracite field.

REFERENCES

Read, C. B., 1955, Floras of the Pocono Formation and Price Sandstone in parts of Pennsylvania, Maryland, West Virginia, and Virginia: U.S. Geol. Survey Prof. Paper 263, 32 p., 20 pls.

Trexler, J. P., Wood, G. H., Jr., and Arndt, H. H., 1961, Angular unconformity separates Catskill and Pocono Formations in western part of Anthracite region, Pennsylvania: Art. 38 *in* U.S. Geol. Survey Prof. Paper 424–B, p. B84–B88.

White, I. C., 1881, The geology of Susquehanna County and Wayne County: Pennsylvania Geol. Survey, 2d, Rept. G5, 243 p.

Willard, Bradford, and others, 1939, The Devonian of Pennsylvania: Pennsylvania Topog. and Geol. Survey, 4th ser., Bull. 19–G, 481 p.

74. PENNSYLVANIAN ROCKS OF THE SOUTHERN PART OF THE ANTHRACITE REGION OF EASTERN PENNSYLVANIA

By Gordon H. Wood, Jr., J. Peter Trexler, and Harold H. Arndt, Washington, D.C., Ann Arbor, Mich., Washington, D.C.

Pennsylvanian rocks in the Southern and Western Middle Anthracite fields (fig. 74.1) are herein defined to include part of the upper member of the Mauch Chunk Formation, the Pottsville Formation, and the Llewellyn Formation. The name Llewellyn Formation is herein defined and assigned.

In the southern part of the Anthracite region the Mauch Chunk Formation, classically considered to be of Late Mississippian age, consists of a sequence of red beds 2,400± to 6,000± feet thick that is overlain by a sequence of alternating red sandstone and shale beds and gray conglomerate and sandstone beds 300 to 600 feet thick. The upper sequence is a transition zone in which red beds typical of the underlying main body of the Mauch Chunk are interbedded with gray beds typical of the overlying Pottsville Formation. White (1900, p. 832) arbitrarily placed the upper boundary of the Mauch Chunk at the top of the uppermost red bed in the transition zone, whereas other geologists have arbitrarily placed this boundary

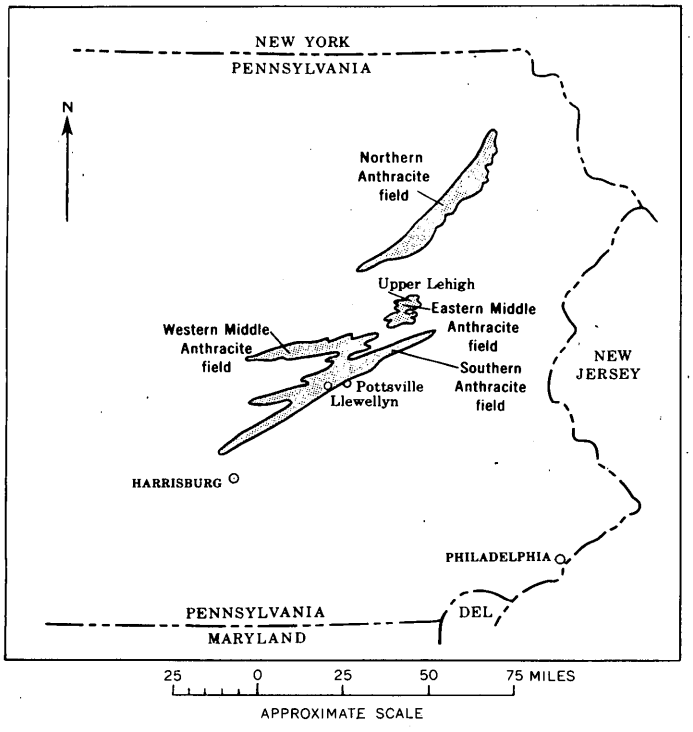

FIGURE 74.1.—Map showing the location of the anthracite fields in eastern Pennsylvania.

at various places in the transition sequence or at the base of the lowest conglomerate typical of the Pottsville. The authors (Wood and others, 1956, p. 2673) followed White's usage rather than one of those of the other geologists because the uppermost red bed generally is more easily located on the talus-covered slopes surrounding the anthracite fields than is (a) some indeterminate bed in the midst of the transition zone or (b) the base of the lowest conglomerate typical of the Pottsville. The transition zone is here termed informally the upper member of the Mauch Chunk Formation because it is easily distinguished lithologically from both the main body of the Mauch Chunk and from the Pottsville. Its top is the same as the top of the Mauch Chunk, and its base, which is usually difficult to locate because of talus, is at the base of the lowest conglomerate, sandstone, siltstone, or shale lithologically typical of the Pottsville.

The overlying Pottsville Formation in the southern part of the Anthracite region consists, from the base, of the Tumbling Run, Schuylkill, and Sharp Mountain Members (Wood and others, 1956, p. 2671). All three members are composed of conglomerate, quartzose sandstone, subgraywacke, siltstone, shale, and anthracite. The formation ranges in thickness from about 1,400 feet to the west of Pottsville on the southern margin of the Southern Anthracite field to about 600 feet in the western part of the Western Middle Anthracite field. Plant fossils indicate that the formation is of Early and Middle Pennsylvanian age (Read and Mamay, 1960, p. B381).

The Pottsville Formation has been defined heretofore as the lowest unit of the Pennsylvanian System in the type area of the system—the Commonwealth of Pennsylvania. The base of the formation at the type and reference sections at Pottsville (Wood and others, 1956, p. 2670–2671) therefore has been designated as the horizon of the time boundary separating the Mississippian and Pennsylvanian Periods (Moore and others, 1944, p. 665).

INCLUSION OF PART OF THE MAUCH CHUNK FORMATION IN THE PENNSYLVANIAN SYSTEM

Detailed stratigraphic studies and geologic mapping by the authors and their associates show that beds of the upper member of the Mauch Chunk Formation intertongue with and laterally replace the lower beds of the Pottsville Formation from south to north. To illustrate the effect and magnitude of the tonguing, the following example is cited. At the reference section of the Pottsville on the southern margin of the Southern Anthracite field at Pottsville, the Tumbling Run Member is about 535 feet thick (Wood and others, 1956, p. 2683) (fig. 74.2), whereas about 27

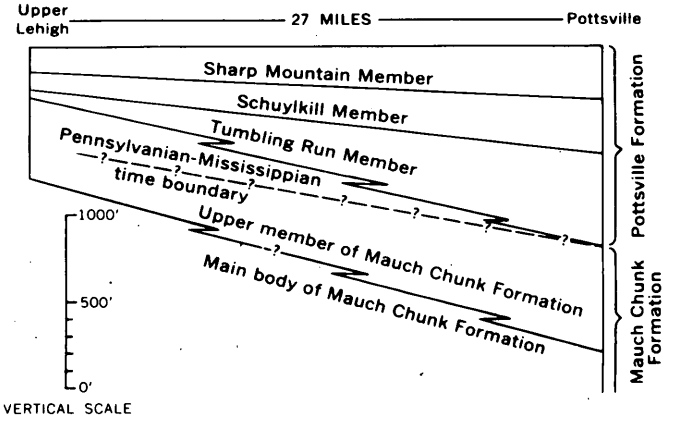

FIGURE 74.2.—Diagram showing tonguing between the upper member of the Mauch Chunk Formation and the Tumbling Run Member of the Pottsville Formation. The time boundary between the Mississippian and Pennsylvanian Periods as defined at Pottsville is in the Mauch Chunk Formation at Upper Lehigh.

miles to the north-northeast in the Eastern Middle Anthracite field, near Upper Lehigh, the member is about 45 feet thick. Thus, between these 2 localities the member thins 490 feet. Mapping and stratigraphic studies indicate that the thinning results from tonguing of gray sandstones and conglomerates of the Tumbling Run Member with laterally equivalent gray sandstones, conglomerates, and red beds of the upper member of the Mauch Chunk. Because of the tonguing, the time boundary between the Mississippian and Pennsylvanian Periods as defined at Pottsville must lie in the upper member of the Mauch Chunk Formation in much of the southern part of the Anthracite region. Therefore, the age of the Mauch Chunk Formation is necessarily Late Mississippian and Early Pennsylvanian rather than Late Mississippian as previously classified.

SUMMARY OF THE STRATIGRAPHIC NOMENCLATURE OF UPPER PENNSYLVANIAN ROCKS

The Pennsylvanian rocks which overlie the Pottsville Formation in the southern part of the Anthracite region have produced much of the anthracite for which Pennsylvania is famous. These rocks, despite their economic importance, however, for many years have been neglected in regional stratigraphic studies of the Pennsylvanian System. For almost three-quarters of a century they were referred to simply as "coal measures." Stevenson (1906, p. 216–221), with considerable uncertainty, correlated the "coal measures" with the Allegheny and Conemaugh Formations of western Pennsylvania on the basis of scanty paleontologic data, and stratigraphic interval and position. White (*in* Willis, 1912, p. 439–442), using paleobotanical evidence, correlated the Allegheny and Conemaugh Formations with the coal-bearing rocks of the Anthracite region but retained the name "coal measures." He noted, however, that the rocks of the Anthracite region were considerably more arenaceous and less calcareous than were those of eastern Pennsylvania. Lohman (1937, p. 46), after consulting with White, abandoned the term "coal measures" and on the basis of White's paleobotanical correlations extended the usage of the names Allegheny and Conemaugh into the Anthracite region. Rothrock, Wagner, and Haley (1950) and others accepted Lohman's nomenclature in reports of the U. S. Geological Survey on the Western Middle Anthracite field. Read (1955, written communication) and Read and Mamay (1960, p. B381) correlated the upper part of the type Pottsville Formation with the lower part of the type Allegheny Formation by refinement of paleobotanical evidence.

The authors confirmed White's observation that the strata included in the Allegheny and Conemaugh Formations of the region and those of the formations bearing the same names in western Pennsylvania were lithologically dissimilar. This dissimilarity, the great distance between outcrops of Pennsylvanian rocks in western Pennsylvania and the Anthracite region, and the apparent time overlap of type Allegheny and type Pottsville strata as indicated by Read prompted the authors and their associates (1956, p. 2678 and 1958) to discontinue using the terms Allegheny and Conemaugh for these strata in the southern part of the Anthracite region and to use instead the informal term "post-Pottsville rocks" for all Pennsylvanian strata younger than the Pottsville Formation. Post-Pottsville rocks appear to be thickest and to contain the youngest beds in the general vicinity of Llewellyn, a small town in Schuylkill County about 5 miles west of Pottsville (fig. 74.1).

DEFINITION OF THE LLEWELLYN FORMATION

The strata heretofore informally termed "post-Pottsville rocks" in the Southern and Western Middle Anthracite fields are here named the Llewellyn Formation after the aforementioned town of Llewellyn. The Llewellyn Formation is composed of gray- and brown-hued beds of conglomeratic sandstone, quartzose sandstone, subgraywacke, and siltstone with lesser amounts of conglomerate, shale, and anthracite (fig. 74.3). Except for coal beds, the Llewellyn does not contain widespread lithologic units that permit stratigraphic subdivision. A type section of the formation cannot be designated because exposures are discontinuous and structurally complex in the vicinity of Llewellyn. The contact of the Llewellyn with the Pottsville is at the base of the shale bed that underlies the Buck Mountain coal bed. The formation is overlain by Recent stream alluvium, talus, and mine waste at many places. Although the original thickness cannot be determined because of erosion, and although structural complications prevent accurate measurement, the

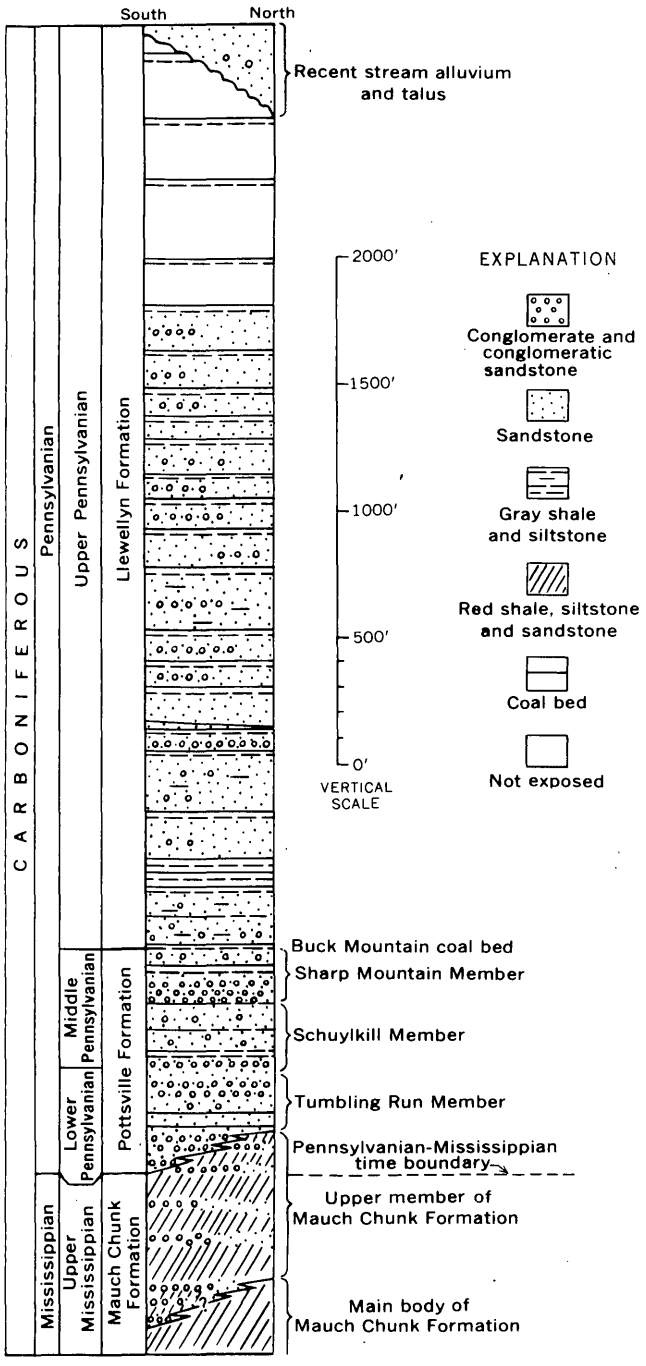

FIGURE 74.3.—Generalized stratigraphic section of Pennsylvanian rocks in the southern part of the Anthracite region.

authors estimate that the maximum preserved thickness near Llewellyn is about 3,500 feet.

The rocks included in the Llewellyn Formation contain a fossil flora similar to that in the upper part of the Allegheny Formation and the lower part of the Conemaugh Formation (Read and Mamay, 1960, p. B381). The age of the formation based upon the floral zonation of Read and Mamay is Late Pennsylvanian.

Rocks believed by the authors to be correlative with the Llewellyn crop out in the Eastern Middle and Northern Anthracite fields. These rocks, however, are not connected by outcrop with the Llewellyn in the Southern and Western Middle Anthracite fields and are, therefore, not included in the formation at this time.

REFERENCES

Lohman, S. W., 1937, Ground water in northeastern Pennsylvania: Pennsylvania Topog. and Geol. Survey, 4th ser., Bull. W–4, 312 p.

Moore, R. C., and others, 1944, Correlation of Pennsylvanian formations of North America: Geol. Soc. America Bull., v. 55, no. 6, p. 657–706.

Read, C. B., and Mamay, S. H., 1960, Upper Paleozoic floral zones of the United States: Art. 176 *in* U.S. Geol. Survey Prof. Paper 400–B, p. B381–B383.

Rothrock, H. E., Wagner, H. C., and Haley, B. R., 1950, Geology of anthracite in the west-central part of the Mt. Carmel quadrangle, Pennsylvania: U.S. Geol. Survey Coal Inv. Map C–3. (3 sheets)

Stevenson, J. J., 1906, Carboniferous of the Appalachian basin: Geol. Soc. America Bull., v. 17, no. 5, p. 65–228.

White, C. D., 1900, The stratigraphic succession of the fossil floras of the Pottsville Formation in the Southern Anthracite coal field, Pennsylvania: U.S. Geol. Survey 20th Ann. Rept., pt. 2 (1898–1899), p. 749–930.

Willis, Bailey, 1912, Index to the stratigraphy of North America: U.S. Geol. Survey Prof. Paper 71, p. 439–442.

Wood, G. H., Jr., and others, 1956, Subdivision of Pottsville Formation in Southern Anthracite field, Pennsylvania: Am. Assoc. Petroleum Geologists Bull., v. 40, no. 11, p. 2669–2688.

Wood, G. H., Jr., and others, 1958, Geology of the northern half of the Minersville quadrangle and a part of the northern half of the Tremont qualrangle, Schuylkill County, Pennsylvania: U.S. Geol. Survey Coal Inv. Map C–43. (2 sheets).

75. REVISED STRATIGRAPHIC NOMENCLATURE FOR UPPER PENNSYLVANIAN AND LOWER PERMIAN ROCKS, WASHINGTON COUNTY, PENNSYLVANIA

By HENRY L. BERRYHILL, JR., and VERNON E. SWANSON, Denver, Colo.

Work done in cooperation with the Pennsylvania Topographic and Geologic Survey

Current geologic mapping in southern Washington County, Pa. (fig. 75.1), has yielded data that permit the establishment of a revised nomenclature and classification for the Pennsylvanian and Permian rocks. The existing nomenclature and classification (fig. 75.2, left side) were first proposed by Stevenson (1876) and have since been modified by Clapp (1907), Griswold and Munn (1907), Stevenson (1907), Shaw and Munn (1911), and Munn (1912); the reader is referred to Wilmarth (1938) for the history of names, definitions, and type localities of the named units. The revised classification described here meets mapping requirements in Washington County and is consistent with the concept of cyclic sedimentation.

The coal-bearing strata of Washington County are cyclic sequences of coal or carbonaceous shale, mudstone, impure sandstone and siltstone, impure limestone, and clay (fig. 75.2, columnar section). Coal beds and carbonaceous layers are the most persistent units. Fresh-water limestone beds occupy much or all of the intervals between some coal beds in the lower and upper parts of the section, and thin, lenticular fresh-water limestone beds are interbedded with the sandstone and siltstone in other parts of the section. The limestone was deposited in a predominantly lacustrine-marsh environment; the sandstone and finer grained clastic units were laid down in a fluvial–delta plain environment. Sandstone becomes increasingly abundant southward in West Virginia where the environment of deposition was predominantly deltaic (Arkle, 1959, p. 122–123).

FIGURE 75.1.—Location of Washington County, Pa.

These rocks were originally classified on the basis of the presence or absence of minable coals. Names were first given to the minable coal beds, and subsequently to most of the thicker and more persistent limestone units and to a few of the sandstone units. Most of the sandstone, siltstone, and mudstone units have not been named. Elsewhere in southwestern Pennsylvania and in eastern Ohio and West Virginia, more than 80 names have been applied at one place or another to the strata shown in the generalized geologic section on figure 75.2. Continued use of this multitude of names would tend to perpetuate many names of units that cannot be mapped or correlated; and it also would violate article 11(c) of the code of the American Commission on Stratigraphic Nomenclature (1961), which prohibits the use of the same geographic name for more than one lithologic unit in the same area. "Waynesburg," for example, has been assigned to 6 different stratigraphic units, including rocks of 3 different lithologies.

Mapping in Washington County has demonstrated that coal beds are the most distinctive and most easily correlated units; further, the many intervening sandstone and limestone units are so monotonously similar that they can be correlated only when related to an underlying or overlying coal bed. Therefore, the basic mapping unit for field classification includes the several rock types between coal beds, and the basic unit represents a sedimentary cycle. This unit is defined as the rock sequence from the base of a coal bed or carbonaceous layer to the base of the next overlying carbonaceous unit. Because many of the units thus defined represent relatively thin or incomplete cycles, and because facies changes are common within many of the coal-to-coal sequences, these units are designated as members rather than as formations. Where

639466 O - 62 - 4

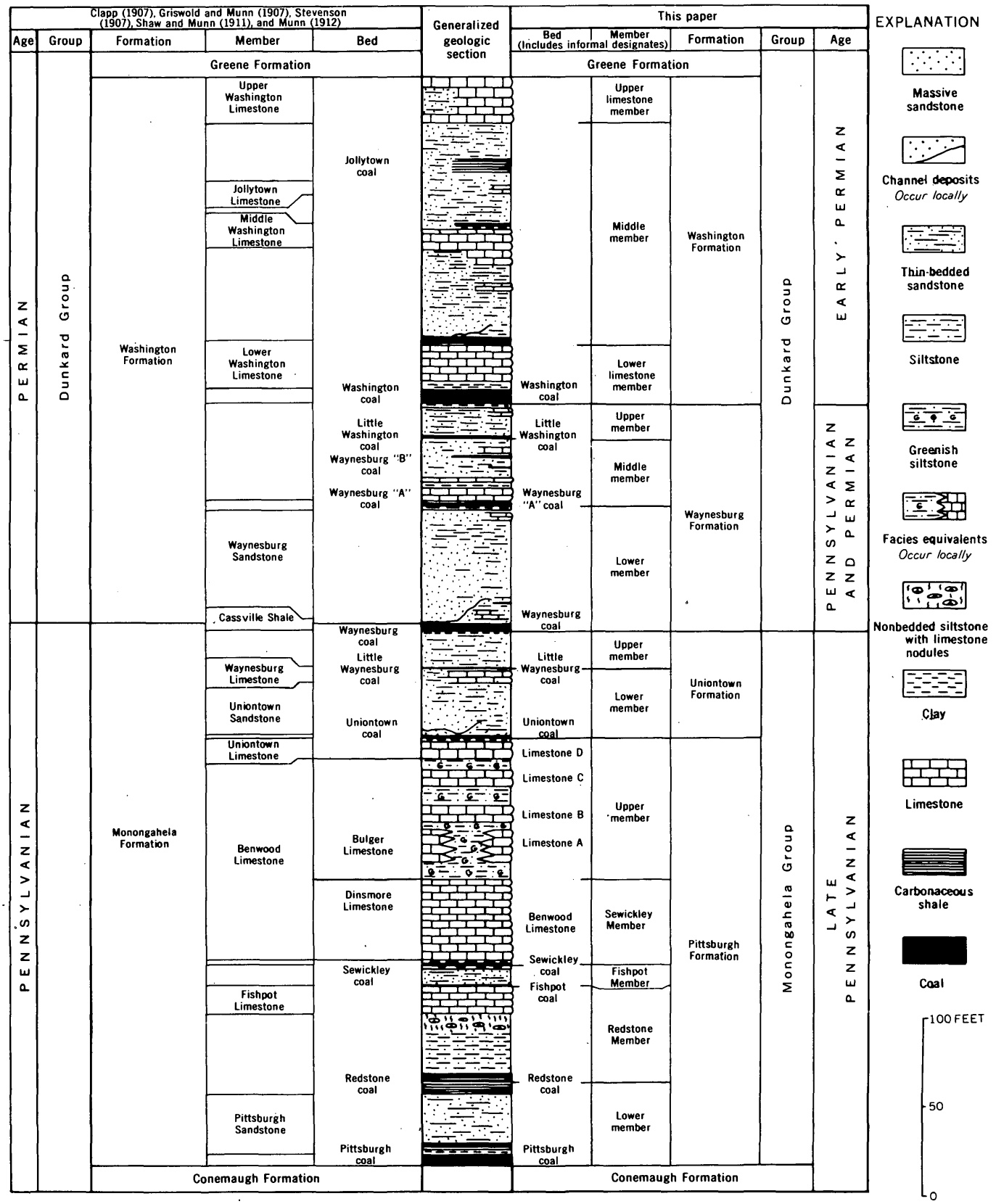

FIGURE 75.2.—Revision of stratigraphic nomenclature for Upper Pennsylvanian (Carboniferous) and Lower Permian rocks, Washington County, Pa.

possible, the member has been assigned the name of the coal bed at its base, thus retaining long-established names and relating the member name to its most easily mapped unit. These changes eliminate the confusing duplication of geographic names. Where coal beds are nonpersistent or where rapid facies changes preclude positive correlation, members have not been named but are informally designated as upper, middle, or lower members.

Because the basal unit of a member as here defined is a coal bed, it follows that the basal unit of a formation must also be a coal bed. In Washington County, the formation boundaries are placed at the base of the most important and persistent thick coal beds, and the name assigned to the formation is that of the major coal bed at its base. Further, the formation includes two or more members that represent sets of similar and related sedimentary cycles.

On the basis of the above principles, the Monongahela Formation in Washington County has been divided into two formations and raised to group rank. The lower, predominantly limestone part of the Monongahela, which represents lacustrine deposition, is here named the Pittsburgh Formation; the upper, predominantly clastic part, which represents fluvial–delta plain deposition, is named the Uniontown Formation.

Similarly, the basal part of the Dunkard Group can be divided into two mappable formations. The Waynesburg Formation at the base includes the Waynesburg coal bed and overlying rocks to the base of the Washington coal bed. The overlying Washington Formation includes the Washington coal and overlying rocks to the base of the Greene Formation.

In summary, all names of stratigraphic units shown on the left side of figure 75.2 have been redefined and their usage restricted to southwestern Pennsylvania; the names Dinsmore and Bulger are hereby abandoned. The revised nomenclature and stratigraphic classification are shown on the right side of figure 75.2.

PITTSBURGH FORMATION

The Pittsburgh Formation is named for the general area of Pittsburgh, Pa. The reference section for the formation is just west of Elco, Washington County, Pa. (California quadrangle) along the north bank of the Monongahela River and in road cuts of State Route 88. Previously the name "Pittsburgh" has been applied to several thin lithologic units in the basal part of this sequence. As redefined, the Pittsburgh Formation includes a sequence of beds 230 to 250 feet thick that extends from the base of the Pittsburgh coal bed to the base of the Uniontown coal bed, or to the top of the brecciated limestone beneath the coal horizon in areas where the Uniontown coal bed is represented by carbonaceous shale or clay. The formation includes five members (fig. 75.2): an unnamed lower member; the Redstone, Fishpot, and Sewickley members, named after the basal coal beds; and an unnamed upper member.

The Pittsburgh Formation is a cyclic sequence in which fresh-water limestone beds and clay beds occupy much of the intervals between coal beds. The Benwood Limestone Bed of the Sewickley Member has an aggregate thickness of 45 to 60 feet. Farther west, in western Washington County, Pa., in the panhandle area of West Virginia, and in east-central Ohio, limestone beds extend down to the Pittsburgh coal. The upper member of the Pittsburgh Formation is characterized by several persistent greenish siltstone layers, of which the lowest is the most conspicuous; locally, as in the section at Elco, the two lowest green siltstone layers merge to form a greenish massive sandstone.

UNIONTOWN FORMATION

The Uniontown Formation is named for the general area of Uniontown, Pa., where the name was originally applied to a coal bed, to a sandstone member, and to a limestone member. The name is retained because of its long established usage, but is redefined to describe a formation comprised of an upper and a lower member representing two sedimentary cycles. The formation is 55 to 70 feet thick and includes strata from the base of the Uniontown coal bed to the base of the Waynesburg coal bed.

The Uniontown Formation typically has two persistent layers of thin-bedded sandstone and siltstone separated by a limestone and a thin coal bed; the coal bed, long known as the Little Waynesburg, is the basal bed of the unnamed upper member. The Waynesburg coal bed, formerly included as the uppermost bed in the Monongahela Formation, is now considered as the basal bed in the overlying Waynesburg Formation to conform to the principles of classification adopted for this area.

WAYNESBURG FORMATION

The rocks from the base of the Waynesburg coal bed to the base of the Washington coal bed, formerly included in the basal part of the Washington Formation, are here redefined as the Waynesburg Formation. The type area is Waynesburg, Pa., and its environs.

The Waynesburg Formation in southern Washington County is 100 to 130 feet thick and is divided into 3 members. A thick, locally massive sandstone (for-

merly Waynesburg Sandstone Member) is the main unit in the lower member; several lenticular impure coal beds and patchy fresh-water limestone beds comprise the middle member; and a persistent plant-bearing sandy siltstone-sandstone unit with a thin impure coal bed (Little Washingon) at its base comprises the upper member.

In the past the strata above the Waynesburg coal bed have been dated Early Permian, based on floral studies by Fontaine and White (1880). The lenticular shales above the Waynesburg coal bed contain many plant fossils with Permian affinities, but they also contain all Pennsylvanian species characteristic of sediments below the Waynesburg coal bed. The diagnostic Permian plant form, *Callipteris conferta*, has not been found below the Washington coal. Because the floral evidence indicates a transition in plant forms from Pennsylvanian to Permian time, and because there is no profound lithologic change above the Waynesburg coal bed as claimed by Fontaine and White, the age of the strata between the Waynesburg and Washington coal beds is redesignated as Pennsylvanian and Permian.

WASHINGTON FORMATION

As redefined in this report, the Washington Formation includes the sequence of beds 160 to 180 feet thick between the base of the Washington coal bed and the top of the upper limestone member. This sequence represents the upper part of the Washington Formation as formerly described. The Washington Formation, particularly the lower limestone member with the Washington coal bed at its base and the upper limestone member, is well exposed in and near the city of Washington, which is the type area. The middle unnamed member consists of several impure sandstone beds, a unit of highly impure limestone beds near the middle, several lenticular thin limestone beds, and three impure coal and carbonaceous shale beds.

The Washington coal bed at the base of the formation is stratigraphically the highest persistent thick coal in the Pennsylvanian-Permian sequence of Eastern United States. The Washington coal and the overlying rocks are probably of Early Permian age.

REFERENCES

American Commission on Stratigraphic Nomenclature, 1961, Code of stratigraphic nomenclature: Am. Assoc. Petroleum Geologists Bull., v. 45, p. 645–665.

Arkle, Thomas, Jr., 1959, Monongahela series, Pennsylvanian system, and Washington and Green series, Permian system of the Appalachian Basin, *in* Guidebook for field trips, Pittsburgh meeting, Geol. Soc. America: 203 p.

Clapp, F. G., 1907, Description of the Amity quadrangle (Pennsylvania): U.S. Geol. Survey Geol. Atlas, Folio 144.

Fontaine, W. M., and White, I. C., 1880, The Permian or Upper Carboniferous flora of West Virginia and southwestern Pennsylvania: Pennsylvania Geol. Survey, 2d, Rept. PP, 143 p.

Griswold, W. T., and Munn, M. J., 1907, Geology of oil and gas fields in Steubenville, Burgettstown, and Claysville quadrangles, Ohio, West Virginia, and Pennsylvania: U.S. Geol. Survey Bull. 318, 196 p.

Munn, M. J., 1912, Description of the Claysville quadrangle (Pennsylvania): U.S. Geol. Survey Geol. Atlas, Folio 180.

Shaw, E. W., and Munn, M. J., 1911, Description of the Burgettstown-Carnegie Folio: U.S. Geol. Survey Geol. Atlas, Folio 177.

Stevenson, J. J., 1876, Report of progress in Greene and Washington district of the bituminous coal fields of western Pennsylvania: Pennsylvania Geol. Survey, 2d, Rept. K, 419 p.

——— 1907, Carboniferous of the Appalachian basin: Geol. Soc. America Bull., v. 18, p. 29–178.

Wilmarth, M. G., 1938, Lexicon of geologic names of the United States: U.S. Geol. Survey Bull. 896, pts. 1 and 2, 2396 p.

76. THE FROZEN SANDSTONE, A NEW MEMBER OF THE BREATHITT FORMATION OF EASTERN KENTUCKY

By WALLACE R. HANSEN, EDWIN V. POST, and GEORGE E. PRICHARD, Denver, Colo.

Work done in cooperation with Commonwealth of Kentucky, University of Kentucky, Kentucky Geological Survey

A new member of the Breathitt Formation of Middle Pennsylvanian age is here named the Frozen Sandstone Member for exposures 0.3 mile north-northeast of the Frozen Creek Post Office (fig. 76.1). The member is well exposed in parts of at least five 7½-minute quadrangles in Breathitt and Wolfe Counties, Ky. Its total areal extent is not yet known but must be appreciably larger than its outcrop area be-

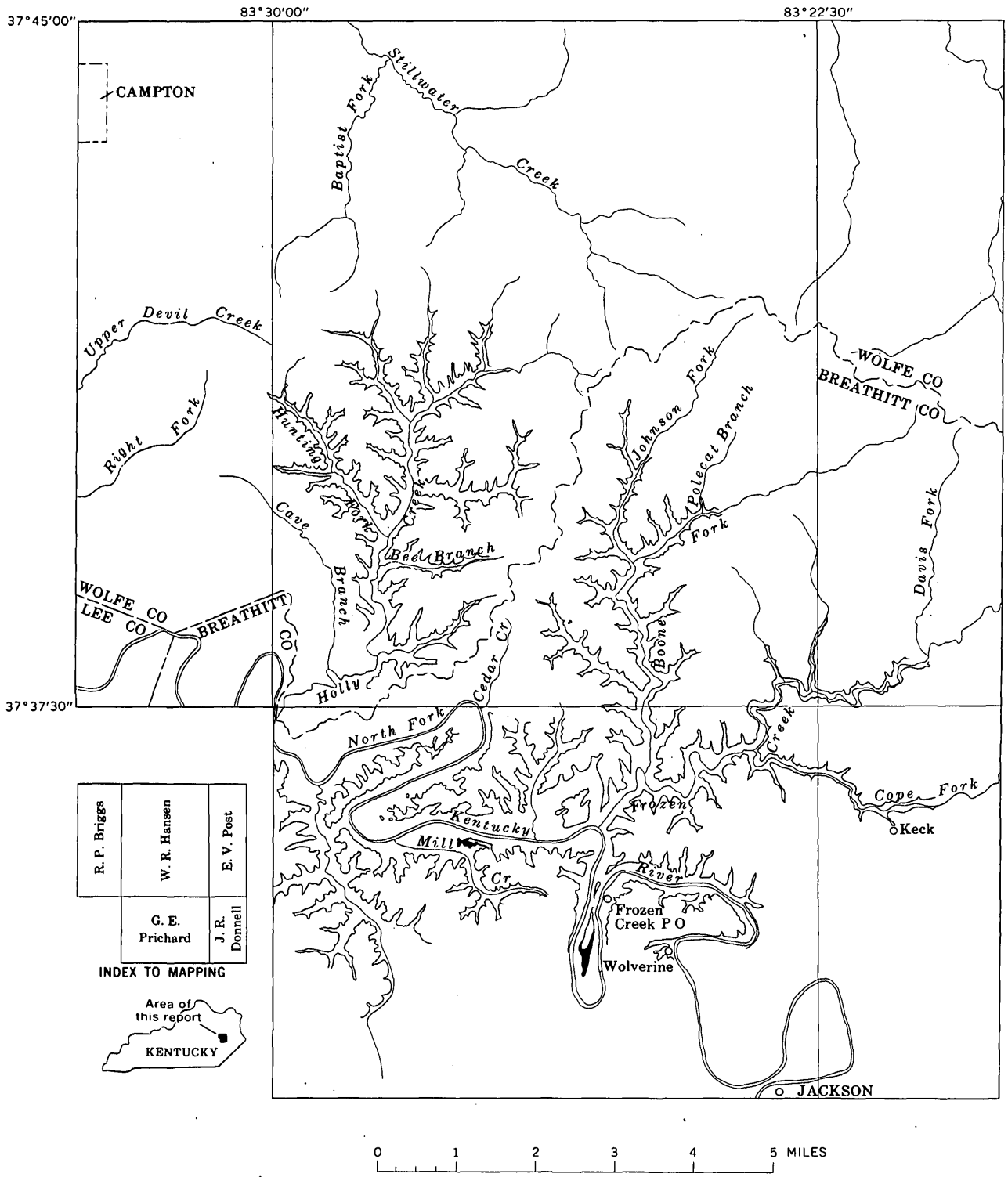

FIGURE 76.1.—Map showing line of outcrop of Frozen Sandstone Member of Breathitt Formation.

cause it passes below drainage. Commonly, the member forms low buff-colored cliffs or ledges; locally it forms near-vertical cliffs 40 to 60 feet high. Its widespread exposure and ready recognition—in an area of generally poor outcrops—make it an excellent marker unit in the Breathitt Formation.

Possibly the best and most complete sections of the Frozen Sandstone Member, together with several tens of feet of beds below and above the sandstone, crop out in newly opened highway cuts along the right bank of the North Fork of the Kentucky River just north of the Frozen Creek Post Office. These sections, therefore, may be regarded as containing the type section of the Frozen Sandstone Member.

The following stratigraphic section of a part of the Breathitt Formation, including the type section of the Frozen Sandstone Member, was measured by Prichard in a deep roadcut 0.3 mile north-northeast of the Frozen Creek Post Office, Breathitt County, Kentucky.

Top of section, elevation 926 feet above mean sea level.
Breathitt Formation (top eroded):

	Thickness (feet)
Sandstone, light-gray	13
Covered; probably siltstone and shaly siltstone	19
Coal, lower split of Vires coal bed	1
Shale, fissile to platy, slightly carbonaceous	1
Siltstone and interbedded thin sandstone beds	19
Frozen Sandstone Member, very light gray, fine- to medium-grained, quartzose, massive to very thick bedded, crossbedded; forms ledge	55
Shale, silty, dark-gray, fissile to platy; contains *Lingula*, zones of ironstone concretions, scattered pyrite crystals	62+
Sandstone, mostly covered; appears to be medium to very thick bedded	15
Vancleve coal bed. Elevation of base, 738 feet	2+
Siltstone and silty shale interbedded; contains thin to very thin sandstone beds	15+
	202+

Base of section (base of Breathitt Formation concealed).

Sandstone in the streambed of Baptist Fork of Stillwater Creek is identified tentatively as the Frozen Sandstone Member.

The Frozen Sandstone Member generally is about 40 feet thick and ranges from about 25 to 60 feet. Along Cave Branch of Holly Creek and along Cedar Creek, however, it thins to less than 15 feet, and grades into siltstone that forms a mere break in an otherwise uniform hill slope.

The Frozen Sandstone Member consists chiefly of medium- to light-gray (*N*5 to *N*7 on the rock-color chart, Goddard, 1948) fine- to medium-grained calcareous micaceous highly crossbedded sandstone that contains scattered carbonized plant fragments, especially along bedding planes. It also contains interbeds of shaly siltstone that thicken locally.

The base of the Frozen Sandstone Member is about 80 to 100 feet above the base of the Breathitt Formation in the vicinity of Jackson. In that area the base of the Breathitt Formation is marked by a gradational but rapid change from the highly crossbedded sandstone of the underlying Lee Formation to dark-gray clay shale. The Frozen Sandstone Member is overlain by a thick sequence of shale, sandstone, clay, and interbedded coals. On the average, the top of the member is about 325 feet stratigraphically below the Magoffin Beds of Morse (1931, p. 302) and about 260 feet below the base of the Fire Clay coal zone, although the thickness of the interposed beds varies considerably from place to place.

A discontinuous coal bed about 4 inches thick at the base of the Frozen Sandstone Member is channeled out in many places. The overlying channel sandstone commonly contains coal fragments and stringers. The sandstone member as a whole exhibits a great deal of scour and fill structure, indicating a dominantly fluviatile depositional environment. Locally, however, long, steeply inclined foresets, which resemble the crossbedding of the Lee Formation, suggest a littoral environment.

Two representative specimens examined in thin section were found to be rather poorly sorted fine-grained impure sandstone that contains considerable calcite cement and appreciable clay and silica cement. Clastic grains are chiefly quartz, minor amounts of quartzite and chert, feldspar (both microcline and plagioclase), muscovite, and biotite. Most of the biotite is highly altered to chlorite, rutile or brookite, and leucoxene. Quartz, quartzite, and feldspar grains are subangular to angular and have low sphericity. Many grains are suspended in a matrix of calcite. Angularity of the clastic grains is due partly to corrasion and partly to replacement of the grain margins by calcite. Some of the replaced silica seems to have been redeposited in the matrix along with clay minerals. The following modes, in percent, were obtained:

	Sample 1	*Sample 2*
Quartz	47	25
Feldspar	6	5
Muscovite	1	3
Biotite	1	1
Altered biotite	4	14
Quartzite and chert	7	4
Calcite (matrix)	16	48
Clay and silica (matrix)	18	
Total	100	100

Semiquantitative spectrographic analyses of sandstones from the Breathitt and Lee Formations, Breathitt and Lee Counties, Ky.

[Analyses by Maurice De Valliere]

Sample No.	Percent				Parts per million														
	Fe	Mg	Ca	Ti	Mn	B	Ba	Be	Co	Cr	Cu	Ga	Ni	Pb	Sc	Sr	V	Y	Zr
1	0.3	0.15	1	0.2	500	10	150	<5	<5	10	<5	<5	5	5	<10	70	20	15	70
2	.7	.2	5	.1	300	<10	150	<5	<5	7	<5	<5	<5	5	<10	200	15	<10	30
3	.5	.1	7	.15	500	10	100	<5	<5	15	<5	<5	<5	<5	<10	150	15	10	50
4	1.5	.2	.3	.3	300	50	150	<5	<5	30	10	10	5	10	<10	50	20	20	700
5	2	.3	.05	.2	300	30	300	<5	7	30	10	15	10	10	5	70	30	15	150
6	1.5	.1	.05	.15	150	<5	100	<5	<5	20	5	7	5	<5	<10	50	20	7	30
7	1	.3	.2	.3	150	30	300	<5	5	30	5	10	7	10	5	30	30	15	300
8	1.5	.2	.02	.2	200	15	200	<5	5	20	10	7	7	15	<10	70	20	7	300
9	1.5	.5	.3	.2	300	30	150	<5	<5	30	7	7	7	10	<10	50	30	15	300
10	1.5	.1	.03	.3	200	10	200	<5	5	70	<5	10	10	7	<10	50	30	10	500
11	1	.07	.02	.2	100	15	150	<5	7	20	<5	7	10	<5	<10	50	30	10	150
12	.5	.2	7	.2	100	15	500	<5	<5	20	<5	<5	<5	10	<10	150	20	10	100
13	1.5	.03	.01	.2	1,000	10	150	<5	7	20	5	<5	7	5	<10	<50	20	<10	300
14	.15	.01	<.01	.07	50	<10	70	<5	<5	5	<5	<5	<5	<5	<10	<50	10	<10	150

NOTE.—The following elements were not present in quantities within the limits of detection of the spectrograph, and are reported as follows in parts per million: Ag<5, As<1,000, Bi<10, Ge<20, In<10, La<50, Mo<5, Sb<200, Sn<10, Ta<100, W<100, Zn<100.

1, 2. Frozen Sandstone Member, deep roadcut 1½ miles due east of Frozen Creek Post Office.
3. Frozen Sandstone Member, outcrop along Kentucky Highway 15 in Cope Fork, Quicksand quadrangle.
4, 5. Frozen Sandstone Member, outcrop along Frozen Creek road, Lee City quadrangle.
6–11. Sandstone in Breathitt Formation between Frozen Sandstone Member and Magoffin Beds of Morse (1931) along Frozen Creek road, Lee City quadrangle.
12. Sandstone in upper part of Magoffin Beds of Morse (1931) near head of Frozen Creek, Lee City quadrangle.
13. Sandstone in Breathitt Formation above Magoffin Beds of Morse (1931) near head of Frozen Creek, Seitz quadrangle.
14. Lee Formation, outcrop on Kentucky Highway 52, about 10 miles west of Beattyville, Lee County, Ky.

Semiquantitative spectrographic analyses of the above two samples are compared above with analyses of samples of other sandstones from the Breathitt and Lee Formations.

Statistical comparison of the average content for several elements in the Frozen Sandstone Member with other sandstones of the Breathitt Formation, based on the above analyses, show no significant difference in their composition. Thus, there probably was no distinctive change in the geochemical environment during deposition and diagenesis of the Frozen Sandstone Member as compared with the environment of other sandstones of the Breathitt Formation.

To the northwest, the Frozen Sandstone Member seems to merge laterally with the Lee Formation. This supposition cannot be demonstrated with the data at hand, however, because both the Frozen Sandstone Member and the Lee Formation are covered by younger rocks in the area of supposed merger. The top of the Lee Formation south of Campton, along Upper Devil Creek and Right Fork (Briggs, 1957), is at the same altitude as the top of the Frozen Sandstone Member 1½ miles east at Hunting Fork of Holly Creek. In the event that subsurface data eventually become available for the intervening area, the Frozen Sandstone Member may prove to be a tongue of the Lee Formation, rather than a member of the Breathitt.

REFERENCES

Briggs, R. P., 1957, Coal resources of the Campton quadrangle, Wolfe, Lee, and Breathitt Counties, Kentucky: U.S. Geol. Survey Coal Inv. Map C–42.

Goddard, E. N., chm., and others, 1948, Rock color chart: Washington, D.C., Natl. Research Council.

Morse, W. C., 1931, Pennsylvanian invertebrate fauna: Kentucky Geol. Survey, ser. 6, v. 36, p. 293–348.

77. THE RALSTON CREEK(?) FORMATION OF LATE JURASSIC AGE IN THE RATON MESA REGION AND HUERFANO PARK, SOUTH-CENTRAL COLORADO

By Ross B. JOHNSON, Denver, Colo.

A thin mappable sequence of distinctive beds that probably is of intermixed fresh-water, evaporite-basin, and possibly shallow-water marine origin conformably overlies the Entrada Sandstone (Gilluly and Reeside, 1928, p. 76) of Late Jurassic age and conformably underlies the Morrison Formation (Emmons, Cross, and Eldridge, 1896, p. 60–62) of Late Jurassic age throughout the Raton Mesa region and

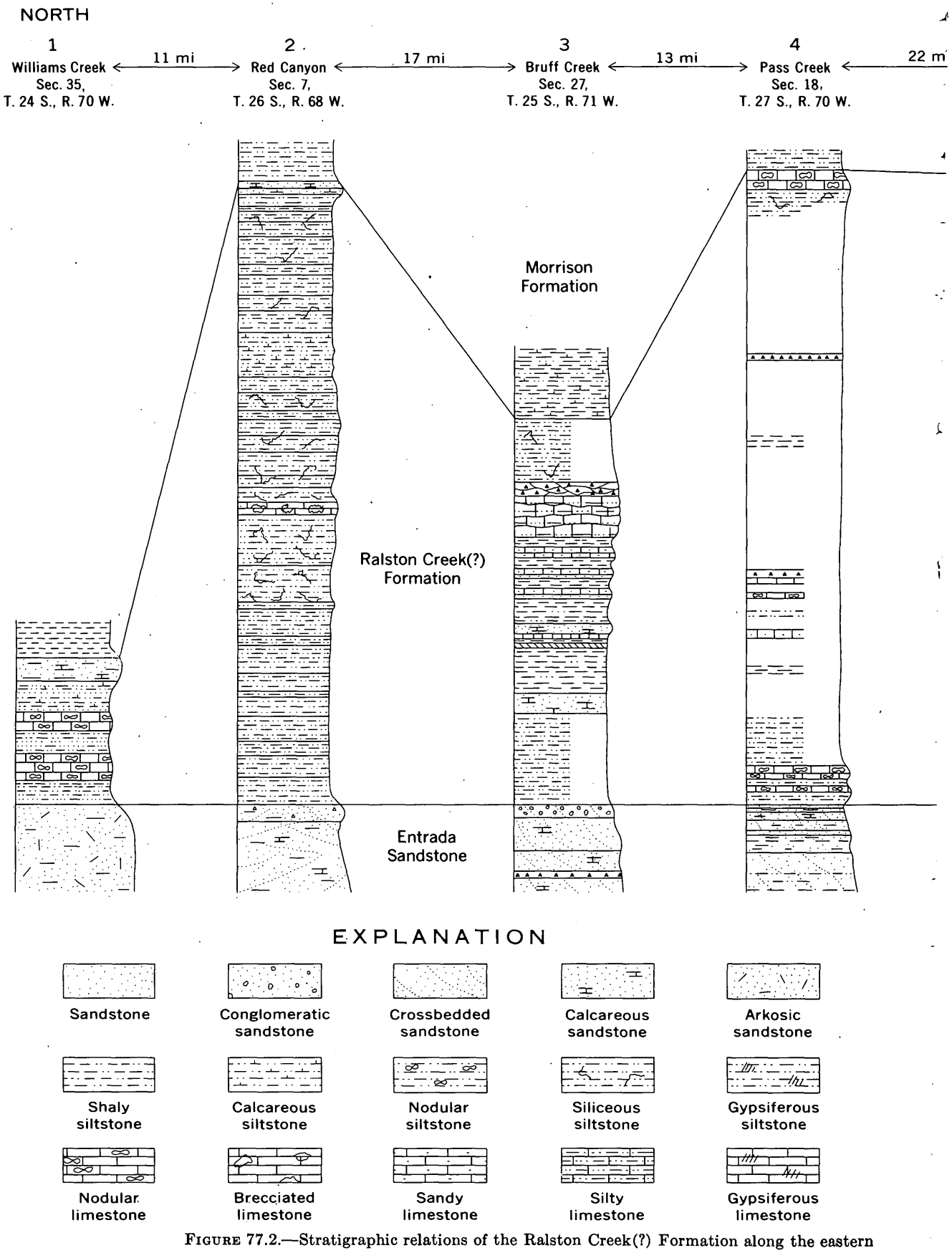

FIGURE 77.2.—Stratigraphic relations of the Ralston Creek(?) Formation along the eastern

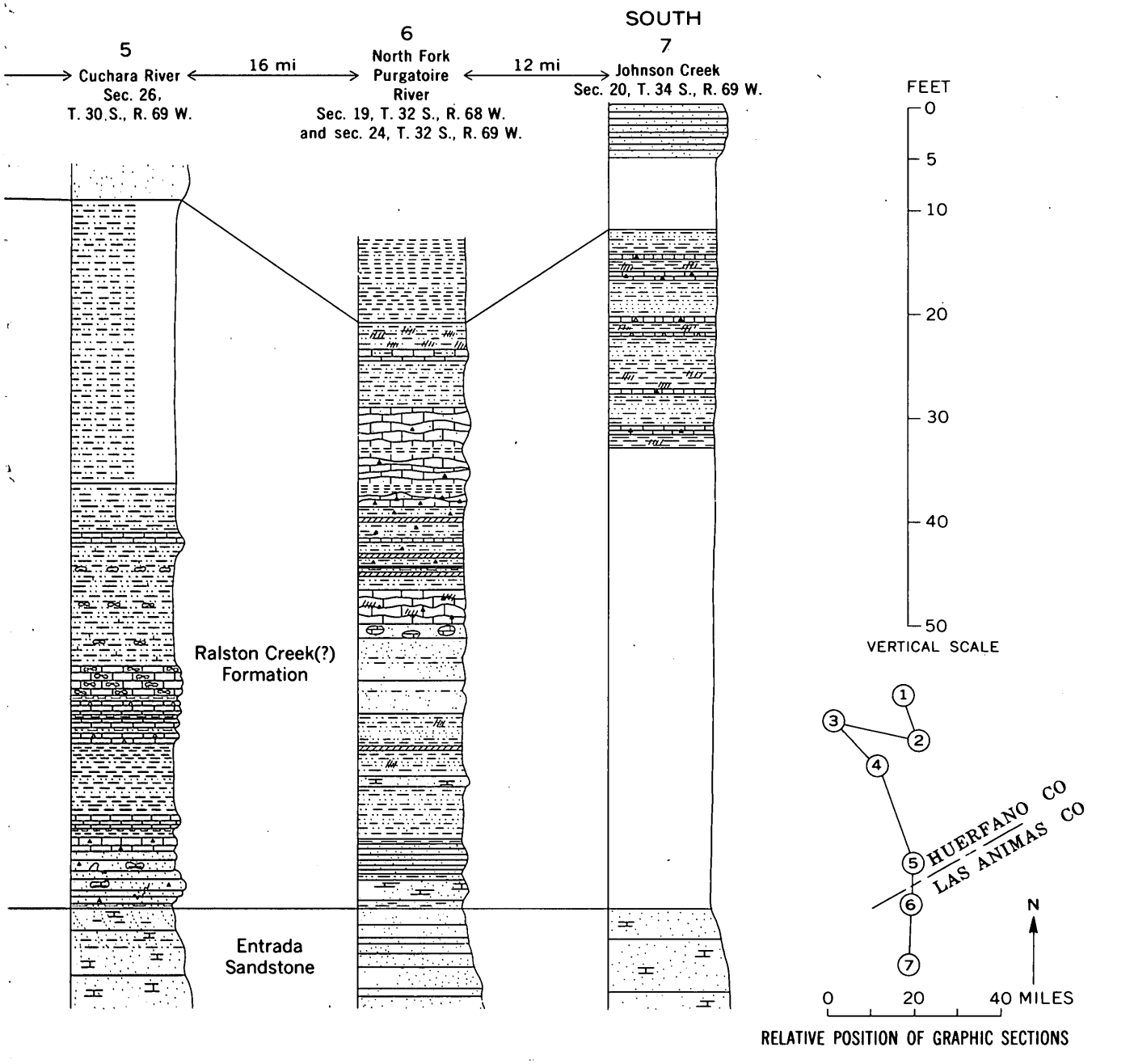

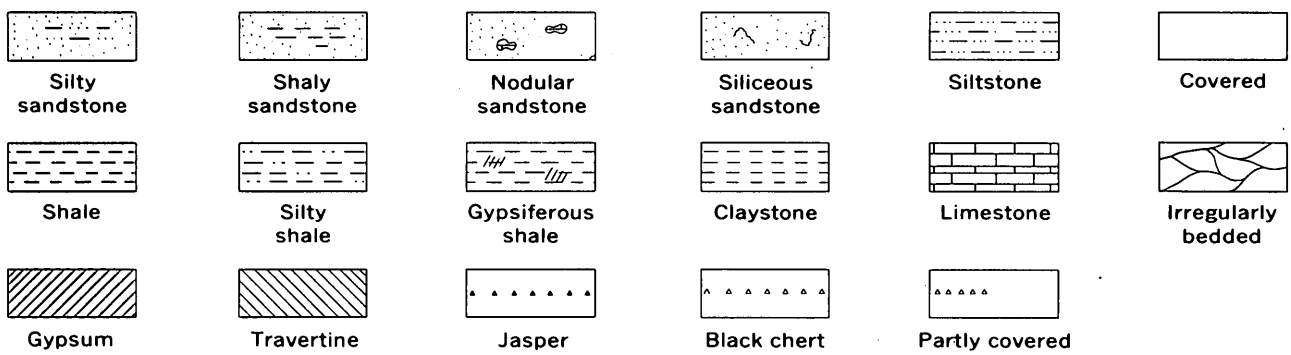

front of the Sangre de Cristo Mountains and Huerfano Park, south-central Colorado.

Le Roy, L. W., 1946, Stratigraphy of the Golden-Morrison area, Jefferson County, Colorado: Colorado School Mines Quart., v. 41, no. 2, 115 p.

Oriel, S. S., and Mudge, M. R., 1956, Problems of lower Mesozoic stratigraphy in southeastern Colorado, *in* Rocky Mtn. Assoc. Geologists, Guidebook to geology of Raton basin, Colorado: p. 19–24.

Van Horn, Richard, 1957, Ralston Creek formation, new name for Ralston formation of Le Roy (1946): Am. Assoc. Petroleum Geologists Bull., v. 41, no. 4, p. 755–756.

Wood, G. H., Jr., Johnson, R. B., and Dixon, G. H., 1956, Geology and coal resources of the Gulnare, Cuchara Pass, and Stonewall area, Huerfano and Las Animas Counties, Colorado: U.S. Geol. Survey Coal Inv. Map C–26.

——— 1957, Geology and coal resources of the Starkville-Weston area, Las Animas County, Colorado: U.S. Geol. Survey Bull. 1051, 68 p.

78. LANEY SHALE MEMBER AND TOWER SANDSTONE LENTIL OF THE GREEN RIVER FORMATION, GREEN RIVER AREA, WYOMING

By William C. Culbertson, Denver, Colo.

Mapping of parts of two 15-minute quadrangles in the Green River area of southwest Wyoming (fig. 78.1) shows that the rocks called Tower Sandstone Lentil in previous reports are resistant lenticular bodies of tuffaceous sandstone and siltstone that occur at many different horizons, principally the lower 400 feet, in the Laney Shale Member of the Eocene Green River Formation. The name Tower Sandstone Lentil is herein abandoned.

Powell (1876, p. 40–45) introduced the name Tower Sandstone (fig. 78.2) for the irregular ferruginous masses of rock that cap both the erosional remnants called "The Towers" just north of the town of Green River and the cliffs along the Green River. Schultz (1920, p. 27) introduced the name Laney Shale Member for the white-weathering beds lying unconformably below the Tower Sandstone, and Bradley (1926, p. 123) introduced the name Morrow Creek Member for the buff-weathering beds above the Laney, designating the Tower Sandstone as a lentil at the base. Bradley (1959, p. 1073) later observed that the unit previously called the Laney Shale Member in this area is older than the type Laney. Thus he renamed the white-weathering beds the Wilkins Peak Member, and substituted the name Laney Shale Member for the overlying buff beds previously called Morrow Creek, with the notable difference that the base of the Laney was placed at the top of the white-weathering beds, not at the base of the Tower Sandstone Lentil. The Tower Sandstone was defined as a lentil in the

Powell (1876, p. 40, 45)		Schultz (1920, p. 26, 49)		Bradley (1926, p. 123)	Bradley (1959, p. 1073)	This report
Upper Green River Group	Plant beds	Upper Green River Group	Plant beds	Morrow Creek Member	Laney Shale Member	Laney Shale Member
	Tower Sandstone		Tower Sandstone	Tower Sandstone Lentil	Tower Sandstone Lentil	
Lower Green River Group		Laney Shale and Tipton Shale Members		Laney Shale Member	Wilkins Peak Member	Wilkins Peak Member
				Tipton Shale Member	Tipton Shale Member	Tipton Shale Member

FIGURE 78.2.—Nomenclature of Green River Formation in the Green River area, Wyoming.

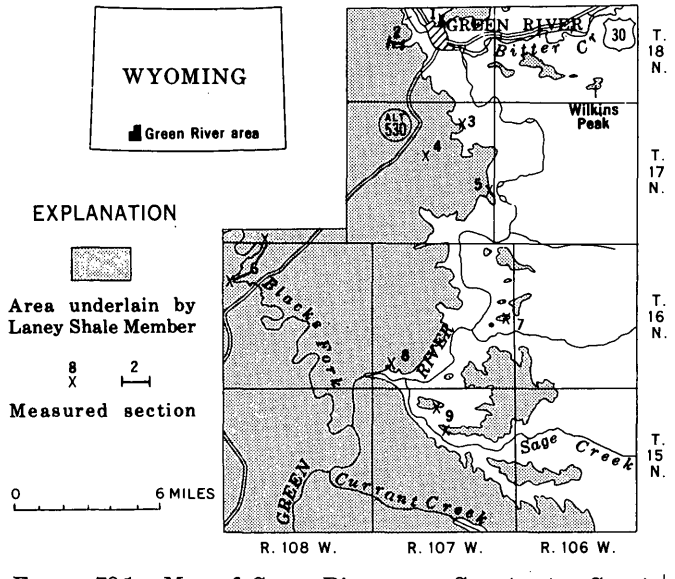

FIGURE 78.1.—Map of Green River area, Sweetwater County, Wyo. Measured sections shown on figure 78.3.

lower part of the Laney that only locally coincided with the base.

The Laney Shale Member is easily distinguished from the underlying Wilkins Peak Member but it is gradational upward with the Bridger Formation, whose lower boundary has not been defined in this area. The Laney is divisible into two lithologic parts, a lower sequence of oil shale and organic marlstone as much as 265 feet thick, and an upper sandy sequence (fig. 78.3). The oil-shale sequence can be further subdivided at most places into the following 4 units, from the base: (1) oil shale 22 to 38 feet thick that forms ledges, weathers brown, contains fish and ostracodes, and is predominantly varved, and that contrasts with the slope-forming white-weathering nonfossiliferous marlstone, oil shale, and limestone of the underlying Wilkins Peak Member, (2) marlstone or lean oil shale 6 to 35 feet thick, thickening southeastward, that weathers to a yellowish-orange recess along many of the outcrops, (3) a unit similar to unit 1, 22 to 35 feet thick, and (4) oil shale and marlstone as much as 200 feet thick that are predominantly slope forming and nonvarved. The entire sequence contains numerous thin analcitized tuff beds, several of which are persistent and recognizable throughout the area. The oil yields shown on figure 78.4 are probably representative of the oil-shale sequence in the northern part of the area. The upper part of the sequence is somewhat richer in the southern part of the area, where a zone of oil shale 20 to 30 feet thick at about 160 feet above the base of the Laney probably will yield about 25 gallons of oil per ton.

The upper sequence consists predominantly of fine- to medium-grained sandstone and marly siltstone, with lesser amounts of marlstone, oil shale, and shale, and a few beds, less than 3 feet thick, of ostracodal limestone, algal, and oolitic limestone (fig. 78.3). Several of the beds of white-weathering oil shale and resistant ostracodal limestone form persistent marker beds in the area. The sandstone and siltstone are of three types: (1) rocks called the Tower Sandstone Lentil; (2) thin-bedded gray very fine to fine-grained sandstone and siltstone; and (3) massive to poorly bedded moderate-yellowish-brown sandstone that is friable,

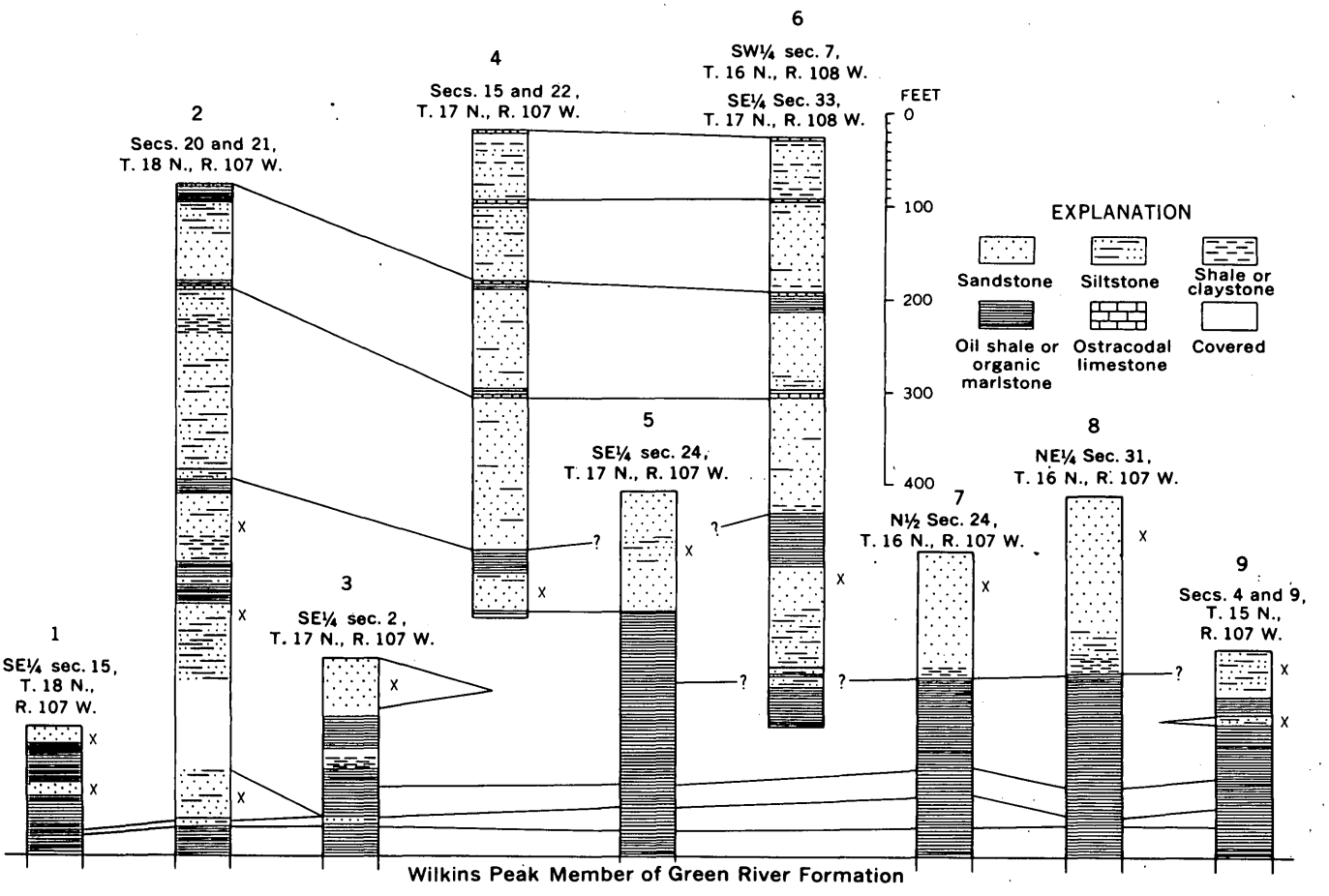

FIGURE 78.3.—Columnar sections of the lower part of Laney Shale Member in the Green River area, Wyoming. Location of sections shown on figure 78.1. x, well-cemented sandstone with characteristics similar to the Tower Sandstone Lentil.

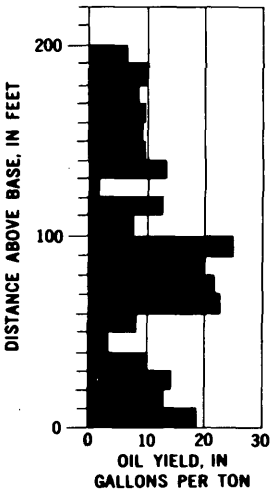

FIGURE 78.4.—Oil yield of 10-foot samples of rotary cuttings drilled through the lower 220 feet of the Laney Shale Member in the Allied Chemical Co. Perkins No. 3 well, sec. 8, T. 17 N., R. 107 W., Sweetwater County, Wyo. Assays by U.S. Bureau of Mines Laramie Petroleum Research Center, Laramie, Wyo.

fine to coarse grained, and conglomeratic in part, and that locally fills channels in underlying beds. The channel-fill sandstones are apparently more numerous westward and are as much as 60 feet thick near locality 4.

The conspicuous rock masses called Tower Sandstone Lentil are well-indurated bodies of pale-yellowish-brown to grayish-orange limonite-stained very fine to medium-grained sandstone and siltstone that crop out as cliffs in contrast to the predominantly slope-forming beds of the rest of the Laney Shale Member. Near the town of Green River they occur as lenses or lenticular beds, 5 to 100 feet thick, some of which fill channels in the underlying beds. Some are linear bodies only a few yards wide; others crop out for a mile or more and vary greatly in thickness and degree of cementation. An unusual feature of these rock masses is that most of them have chaotically tilted bedding, or even rolled bedding, that suggests postdepositional slumping, but others are even bedded to cross bedded. Oscillation ripple marks were found on one steeply tilted bedding plane in a lenticular sandstone body in the NW ¼ sec. 34, T. 18 N., R. 107 W. In places, sandstone dikes project downward from these bodies into the oil shale. The overlying oil-shale beds tend to drape over the smaller lenses.

The many rock masses called Tower Sandstone Lentil are not, however, part of a single bed. Near the town of Green River and as far south as locality 3 (fig. 78.1) they occur at many horizons in the lower 400 feet of the Laney Shale Member, only a few of which are shown in columns 1 and 2 (fig. 78.3). Southward from locality 3, the lower lenses abruptly disappear from the lower oil-shale sequence and do not reappear (fig. 78.3). The rock masses capping the bluffs overlooking Green River and extending northwestward up Blacks Fork and into the subsurface range in stratigraphic position from 170 to 265 feet above the base of the Laney Shale Member (fig. 78.3, columns 6, 7, 8, and 9). In general, these rocks differ from the lower lenses of sandstone near the town of Green River in that they are thicker, more continuous, and show less tilted bedding. At most exposures these rocks consist of a capping of fine- to medium-grained sandstone that grades downward to siltstone and in places to shale, and they show little or no evidence of predepositional erosion. These rock masses are apparently remnants of a once-continuous bed but, if so, the bed probably represents a coalescing of many lenses or tongues. Along the outcrop this bed thickens and thins abruptly, locally splits into two beds, and in places contains large lenses of organic marlstone or oil shale. At locality 5, for example, the 130-foot bluff-forming fine-grained sandstone called Tower Sandstone by Winchester (1923, p. 124) interfingers westward with oil shale (fig. 78.3, columns 4 and 5), and at locality 4 only the lower 40 feet is bluff forming. The rocks equivalent to the upper part of this bed consist of slope-forming siltstone and sandstone indistinguishable from many higher units.

At a few places, particularly along the Green River south of locality 8, higher beds locally form bluffs that resemble the Tower Sandstone Lentil. At the southern margin of T. 15 N., R. 108 W., for example, a thick resistant bed along the Green River is probably the bed called Tower Sandstone by Powell (1876, p. 45), and it may be the bed used in mapping the basal contact of the Morrow Creek Member of former usage (fig. 78.2) on the geologic map of Wyoming by Love and others (1955). A nearby test hole shows that this bed is more than 700 feet above the base of the Laney Shale Member.

A study of thin sections and X-ray analyses indicate that the rocks called the Tower Sandstone Lentil consist mostly of angular grains, up to medium-grain size, of plagioclase, quartz, hornblende, and biotite, with 10 to 40 percent of interstitial dolomite or calcite and a small amount of analcite and limonite. These rocks may represent the reworking of a crystal tuff with the admixture of varying amounts of subrounded grains of other origin, the amount in general increasing upward in the section.

Because the name Tower Sandstone Lentil has been applied to many different lenses and beds, and because no bed at the type locality is sufficiently different from similar beds at other horizons to warrant retaining a special name for it, the name Tower Sandstone Lentil is hereby abandoned.

A possible explanation of the characteristics of the lenses and beds that were called Tower Sandstone Lentil near the town of Green River is that they were laid down as a marginal deposit of a fluctuating fresh-water lake that was accumulating organic material. During each retreat of the lake, bogs of sapropelic ooze were exposed, or were only thinly covered with water. Upon these gel-like bogs adjacent streams dumped clastic debris in linear channels and in small deltas with only superficial scouring of the surface. These masses tended to sink into the bog, thereby partially preserving their shape during succeeding expansions of the lake which then covered them with more organic material. The tilting of bedding probably was caused in part by the sinking of the sand bodies into the bog and in part by the subsequent squeezing of these bodies during the differential compaction of the bog material and sand (see also J. R. Rapp, Art. 91). This compaction would also cause overlying oil-shale beds to drape over the relatively incompactible sand bodies. Tilted and rolled bedding may also have formed as the result of violent earthquakes that caused parts of the deltas to slump into deeper water. Sandstone dikes probably were formed at a later time by the squeezing of sand into earthquake-caused fractures in the adjacent beds. The thick sandstone lenses became better cemented than higher beds because they were preferential routes for the movement of carbonate-bearing water squeezed out of the adjacent oil shale.

The bed that forms the main bluff along the Green River and Blacks Fork, and that caps Wilkins Peak, probably represents a time in which the lake shrank steadily. The marginal deposits then encroached on the old lakebed in an irregular pattern and eventually coalesced into one bed. In the later part of Laney time the lake spasmodically expanded and deposited oil shale and thin limestone over a large area, but during much of the time the deposition was predominantly fluviatile.

REFERENCES

Bradley, W. H., 1926, Shore phases of the Green River formation in northern Sweetwater County, Wyoming: U.S. Geol. Survey Prof. Paper 140, p. 121–131.

——— 1959, Revision of stratigraphic nomenclature of Green River formation of Wyoming: Am. Assoc. Petroleum Geologists Bull., v. 43, no. 5, p. 1072–1075.

Love, J. D., Weitz, J. L., and Hose, R. K., 1955, Geologic map of Wyoming: U.S. Geol. Survey.

Powell, J. W., 1876, Report on the geology of the eastern portion of the Uinta Mountains: U.S. Geol. and Geog. Survey Terr., 2d div:, 218 p.

Schultz, A. R., 1920, Oil possibilities in and around Baxter Basin in the Rock Springs Uplift, Sweetwater County, Wyoming: U.S. Geol. Survey Bull. 702, 107 p.

Winchester, D. E., 1923, Oil shale of the Rocky Mountain region: U.S. Geol. Survey Bull. 727, 204 p.

79. VARIABLE FACIES OF THE CHAINMAN AND DIAMOND PEAK FORMATIONS IN WESTERN WHITE PINE COUNTY, NEVADA

By JOHN H. STEWART, Menlo Park, Calif.

The Chainman Shale and overlying Diamond Peak Formation of Late Mississippian age consist of several thousand feet of siltstone, sandstone, conglomerate, and minor amounts of limestone. The sequence of units and the lithologic types in these formations vary markedly from area to area, as has previously been noted by Hague (1883, p. 266), Nolan and others (1956, p. 56), Humphrey (1960, p. 33–35), and Brew (1961). In order to study the lithologic character and facies of these formations, the writer mapped two areas, one in Packer Basin in the southern Diamond Mountains and the other in the northern Pancake Range (fig. 79.1), where these strata are well exposed. Also he measured a stratigraphic section in each area. Both sections were measured in areas of general homoclinal structure and, although considerable local faulting and squeezing of the strata occur, the thicknesses of units are considered to be fairly accurate.

Strata equivalent to the upper part of the Diamond

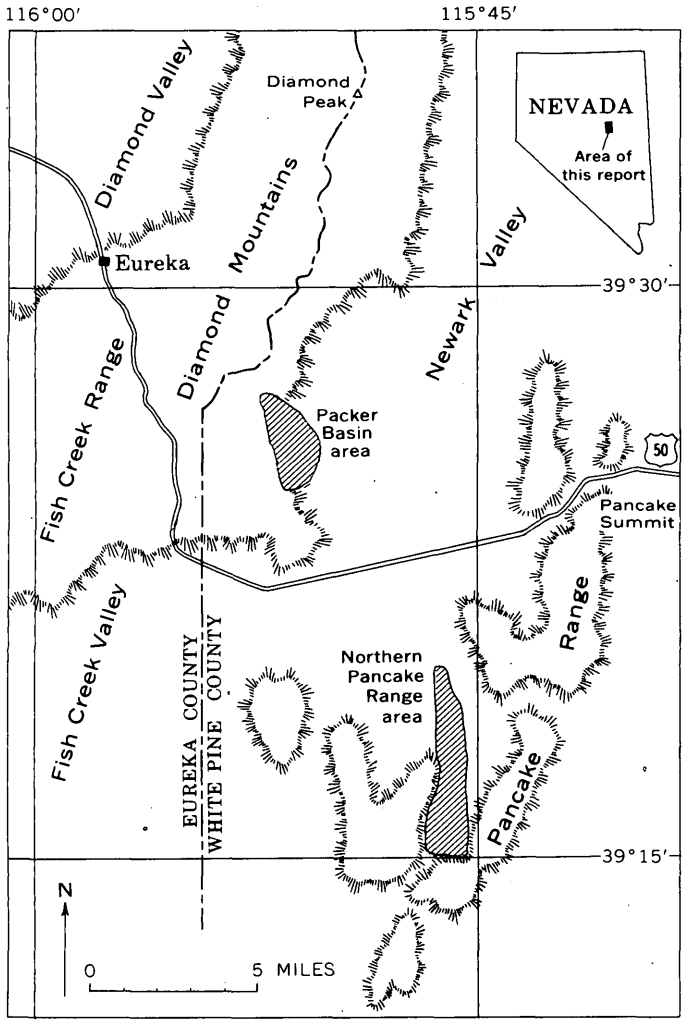

FIGURE 79.1.—Map of part of White Pine and Eureka Counties, Nev., showing the location of the areas studied (cross-ruled).

Peak Formation are not exposed in the areas studied. Thicknesses of the Chainman Shale and Diamond Peak Formation elsewhere in the region, however, indicate that lateral equivalents to the Chainman Shale as well as the lower part of the Diamond Peak Formation should be present in the areas mapped. No lithologic distinction could be made, however, between the Chainman Shale and the Diamond Peak Formation where studied, and the strata will be referred to here as the "Chainman and Diamond Peak Formations undifferentiated," a terminology previously used by Nolan and others (1956, p. 54) in the vicinity of Eureka in areas where these formations could not be separated.

In Packer Basin, slightly over 4,700 feet of the Chainman and Diamond Peak Formations undifferentiated is exposed in an area covering several square miles (fig. 79.1). In this area, the Chainman and Diamond Peak are underlain by the Joana Limestone of Early Mississippian age; the contact is probably an erosion surface (Nolan and others, 1956, p. 55). Three major lithologic units (fig. 79.2) are recognized in the undifferentiated Chainman and Diamond Peak in Packer Basin and each can be mapped to the limits of the exposure in the area.

The lower unit is about 1,750 feet thick and is composed of dark-gray siltstone and approximately 17 percent sandstone and 1 percent conglomerate. The sandstone is pale yellowish brown or olive gray and ranges in grain size from very fine to very coarse. The coarser grains are generally gray chert whereas the finer ones are quartz and feldspar. The conglomerate consists generally of granules and small pebbles of chert, and minor quartzite, in a sand matrix. The sandstone and conglomerate occur together in units ranging in thickness from a few feet to more than 40 feet. Commonly, individual beds grade from granule conglomerate at the base to coarse-grained sandstone at the top, suggesting that they were deposited by turbidity currents.

The middle unit of the Chainman and Diamond Peak sequence in Packer Basin is about 2,100 feet thick and consists of dark-gray siltstone and about 5 percent thin beds of dark-yellowish-brown very fine grained sandstone.

The upper unit of the Chainman and Diamond Peak sequence is at least 860 feet thick and consists of dark-gray siltstone and about 37 percent sandstone and 7 percent conglomerate. The sandstone and conglomerate are similar to those in the lower unit, except that no graded bedding was noted; the conglomerate is commonly coarser, and a thick conglomerate bed at the top contains cobbles as large as 3 inches in diameter. Carbonaceous material and, in a few places, crinoid columnals occur in some sandstone layers in all three of the units.

In the northern Pancake Range, slightly more than 3,500 feet of the undifferentiated Chainman and Diamond Peak Formations is exposed in a northward-trending belt about 5 miles long and 1 mile wide (fig. 79.1). The Chainman and Diamond Peak sequence is underlain by the Joana Limestone, which is discontinuous and probably separated from the overlying units by an erosion surface. Here the Chainman and Diamond Peak sequence is divided into four major lithologic units (fig. 79.2), each of which can be mapped to the limits of the exposure in the area.

The lower siltstone unit, the lowest unit, is about 1,070 feet thick and consists of olive-gray to dark-gray siltstone to silty claystone. A prominent 10-foot-thick dark-gray silty limestone, which weathers gray-

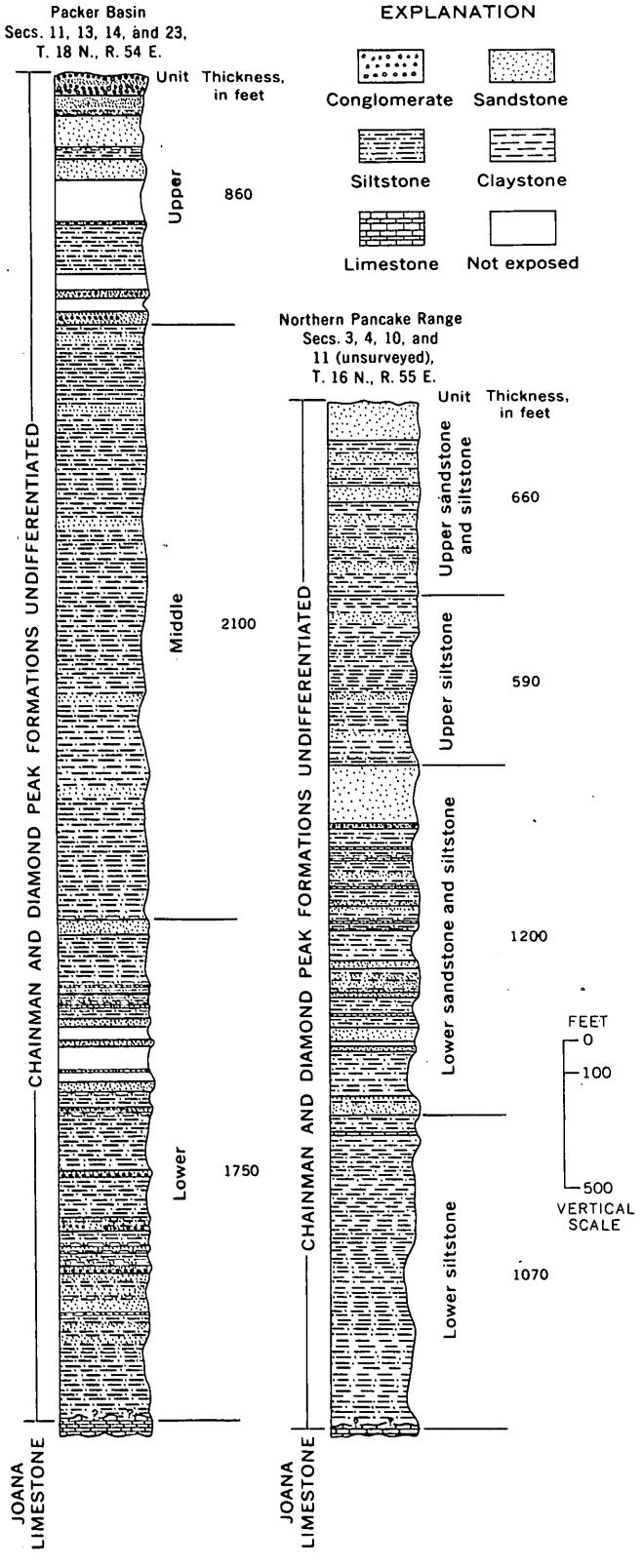

FIGURE 79.2.—Incomplete columnar sections of the Chainman and Diamond Peak Formations undifferentiated in Packer Basin and the northern Pancake Range, White Pine County, Nev.

639466 O - 62 - 5

ish orange, occurs 60 feet below the top of the lower siltstone unit.

The lower sandstone and siltstone unit, the second unit, is about 1,200 feet thick and consists of olive-gray siltstone and 40 percent sandstone, 1 percent silty limestone, and less than 1 percent conglomerate. The sandstone is pale yellowish brown and ranges in grain size from very fine to very coarse. The coarser grains are generally chert, whereas the finer ones are quartz and feldspar. The sandstone occurs in layers from a few feet to more than 200 feet thick. Sole marks, consisting of small groove casts and of irregular knobs, occur locally at the base of the sandstone layers. The silty limestone is similar to that in the lower siltstone unit and occurs in beds from ½ to 2 feet thick. One conglomerate layer occurs near the top of the unit; it contains granules and pebbles of chert as large as 1 inch in diameter.

The upper siltstone unit, the third unit, is about 590 feet thick and consists of dark-gray to olive-gray silty claystone to clayey siltstone and about 5 percent sandy siltstone and 2 percent sandstone. The sandy siltstone is poorly exposed and consists of a mixture of coarse silt and very fine grained sand. The sandstone is similar to that in the lower sandstone and siltstone unit.

The upper sandstone and siltstone unit, the highest unit, is at least 660 feet thick and consists of light-olive-gray sandy siltstone to silty claystone and 40 percent sandstone, 1 percent silty limestone, and less than 1 percent conglomerate. The sandstone, silty limestone, and conglomerate are similar to those occurring elsewhere in the Chainman and Diamond Peak sequence in the area. A few sole marks, similar to those in the lower sandstone and siltstone unit, were noted in the upper sandstone and siltstone unit. Carbonaceous material and crinoid columnals are common in some sandstone layers in the lower and upper sandstone and siltstone units, although not generally in association with one another. Brachiopods, corals, and cephalopods also occur at a few places in all four units.

A considerable difference can be noted between the section in Packer Basin and that in the northern Pancake Range, and, in addition, these two sections differ quite markedly from other sections of the Chainman and Diamond Peak Formations in eastern Eureka County and western White Pine County. The Packer Basin section contains three well-defined units, the lowest of which commonly contains conglomerate units. The section in the northern Pancake Range consists of four major lithologic units, in which conglomerate is nowhere an important constituent. Pos-

sibly the lower unit in Packer Basin could correlate with the lower sandstone and siltstone unit in the northern Pancake Range, but such a correlation would imply considerable variation in the lithology of the lowermost part of the Chainman and Diamond Peak Formations between the two areas. The sections in Packer Basin and the northern Pancake Range are both distinguished by the presence of thick pale-yellowish-brown sandstone beds, locally containing carbonaceous debris and crinoid columnals. This lithologic type is not common in other sections in eastern Eureka County and western White Pine County described by Nolan and others (1956, p. 56–61), Humphrey (1960, p. 33-38), Rigby (1960), and Brew (1961).

The variation in facies in the Chainman and Diamond Peak Formations suggests rapidly changing conditions in the basin of deposition, perhaps as a result of tectonic instability. As has been proposed by Roberts and others (1958), the Chainman and Diamond Peak Formations may represent, at least in part, deposits to the east of an active orogenic belt. In such an unsettled tectonic environment, particularly if movement took place in the basin of deposition as well as in the source area, abrupt lateral changes in lithologic type are expectable. In addition, the marked lithologic variability of these formations from place to place may be emphasized by thrusting of unrelated facies over one another, as Brew (1961) has suggested to explain the juxtaposition of unrelated facies of the Chainman Shale in the southern Diamond Mountains.

REFERENCES

Brew, D. A., 1961, Relation of Chainman Shale to Bold Bluff thrust fault, southern Diamond Mountains, Eureka and White Pine Counties, Nevada: Art. 191 *in* U.S. Geol. Survey Prof. Paper 424–C, p. C113–C115.

Hague, Arnold, 1883, Abstract of report on the geology of the Eureka district, Nevada: U.S. Geol. Survey 3d Ann. Rept., p. 237–272.

Humphrey, F. L., 1960, Geology of the White Pine Mining District, White Pine County, Nevada: Nevada Bureau of Mines Bull. 57, 119 p.

Nolan, T. B., Merriam, C. W., and Williams, J. S., 1956, The stratigraphic section in the vicinity of Eureka, Nevada: U.S. Geol. Survey Prof. Paper 276, 77 p.

Rigby, J. K., 1960, Geology of the Buck Mountain-Bald Mountain area, southern Ruby Mountains, White Pine County, Nevada, *in* Guidebook to the geology of east-central Nevada, Intermountain Assoc. of Petroleum Geologists, 11th Ann. Field Conf., 1960; p. 173–180.

Roberts, R. J., and others, 1958, Paleozoic rocks of north-central Nevada: Am. Assoc. Petroleum Geologists Bull., v. 42, no. 12, p. 2813–2857.

80. OAK SPRING GROUP OF THE NEVADA TEST SITE AND VICINITY, NEVADA

By F. G. Poole and F. A. McKeown, Denver, Colo.

Work done in cooperation with the U.S. Atomic Energy Commission

The Oak Spring Formation was defined by Johnson and Hibbard (1957, p. 367–369) to include all volcanic rocks in the eastern part of the Nevada Test Site (fig. 80.1). As a result of quadrangle mapping in the northern part of the test site, the formation was subdivided into eight members by Hinrichs and Orkild (1961). Recent mapping, however, in nine additional 7½-minute quadrangles in the southern and western parts of the test site has required subdividing thick sections of volcanic rocks, part of which are stratigraphically above and part of which are stratigraphically below the eight members defined by Hinrichs and Orkild. The sequence includes a wide variety of rocks that are complexly intercalated; they differ in composition, mode of deposition, and source. Superposed rock units that are similar in composition, mode of deposition, and source form major lithogenetic units that are given formational rank. Continued application of formational rank to all volcanic rocks in the test site is no longer feasible. Therefore, in this paper the Oak Spring Formation is raised to the rank of group and the two formations comprising it in the northern part of the test site are named, in ascending order, Indian Trail and Piapi Canyon (fig. 80.2).

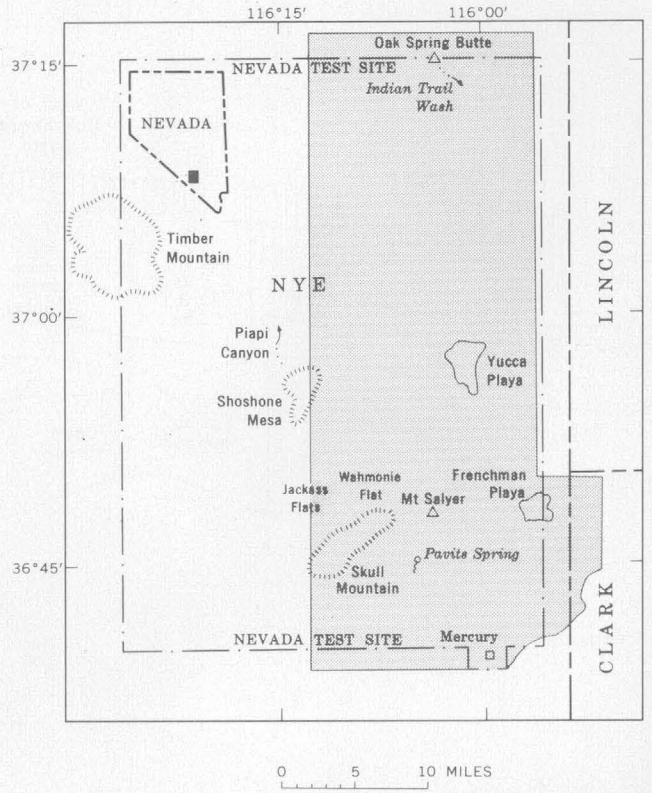

FIGURE 80.1.—Map of Nevada Test Site and vicinity showing localities referred to in text. Area mapped by Johnson and Hibbard (1957) shown by stipple.

The Indian Trail Formation includes the lowest three members described by Hinrichs and Orkild (1961) in the former Oak Spring Formation. These members are, in ascending order: lower, Tub Spring, and Grouse Canyon. The type locality of the formation is Indian Trail Wash on the southeast flank of Oak Spring Butte (fig. 80.1). The lower member consists predominantly of rhyolitic ash-flow tuffs, some of which are welded;[1] ash-fall tuff; and reworked tuff. The source of these rocks is believed to be many nearby vents. The Tub Spring and Grouse Canyon Members are multiple-flow simple cooling units[2] of rhyolitic welded and nonwelded ash-flow tuff and associated ash-fall tuff. These units wedge out southward from the Oak Spring Butte area, whereas northward they thicken and become more densely welded. They are probably related to a volcanic center located north of the test site.

The Piapi Canyon Formation includes the following members of Hinrichs and Orkild (1961), in ascending order: Survey Butte, Stockade Wash, Topopah Spring, Tiva Canyon, and Rainier Mesa. The type locality of this formation is in the vicinity of Piapi Canyon, which is located about 2 miles northwest of Shoshone Mesa (fig. 80.1). All members except the Survey Butte are multiple-flow simple or compound cooling units of rhyolitic welded and nonwelded ash-flow tuff and associated ash-fall tuff. The Survey Butte Member consists predominantly of ash-fall tuff, some of which appears to be reworked by water and possibly by wind, and of a minor amount of nonwelded ash-flow tuff. The tuffs of this member are believed to be genetically related to those of the other four members of the Piapi Canyon Formation. In many areas thick sections of dominantly ash-fall tuff adjacent to the other members of the Piapi Canyon Formation are included in the Survey Butte Member because the rocks in this interval cannot be differentiated without further study. The volcanic center from which the tuffs in this formation were ejected is believed to be in the vicinity of Timber Mountain (fig. 80.1), which is inferred to be the uplifted center of a caldera.

The Oak Spring Formation as defined by Johnson and Hibbard specifically included the volcanic rocks at Mount Salyer, Skull Mountain, and other localities (Johnson and Hibbard, 1957, p. 368) in the southern part of the Nevada Test Site. Most of these volcanic rocks are pre-Piapi Canyon as is shown in figure 80.2, but they cannot be physically correlated with the Indian Trail Formation. As the correlation of them to the Indian Trail Formation is uncertain, they are tentatively divided into several major informal units, in ascending order: a limestone, tuff, and conglomerate unit that may be equivalent to the Horse Spring Formation of Longwell (1921, p. 53); a tuffaceous sandstone, siltstone, and subordinate tuff and conglomerate unit exposed in the vicinity of Pavits Spring and south of Skull Mountain, Pavits Spring, and Frenchman Playa (fig. 80.1); a volcanic breccia and subordinate lithic tuff, tuffaceous sandstone, siltstone and claystone unit typically exposed in the Mount Salyer area; and an andesitic lava flow and associated ash-fall tuff unit typically exposed in the vicinity of Wahmonie Flat.

The only post-Piapi Canyon volcanic rocks exposed within the area mapped by Johnson and Hibbard are the basalt on Skull Mountain (fig. 80.2) and several small basalt flows in the Jackass Flats area north of Skull Mountain.

The age of the Oak Spring Group, as indicated by fossil evidence, ranges from Eocene to Pliocene. D. W. Taylor identified the snail, *Pleurocera tenerum* (Hall), collected from the base of the volcanic sequence south of Frenchman Playa. He considers this

[1] The terminology for pyroclastic rocks is that of Ross and Smith (1961).

[2] The terminology for ash-flow cooling units is that of Smith (1960).

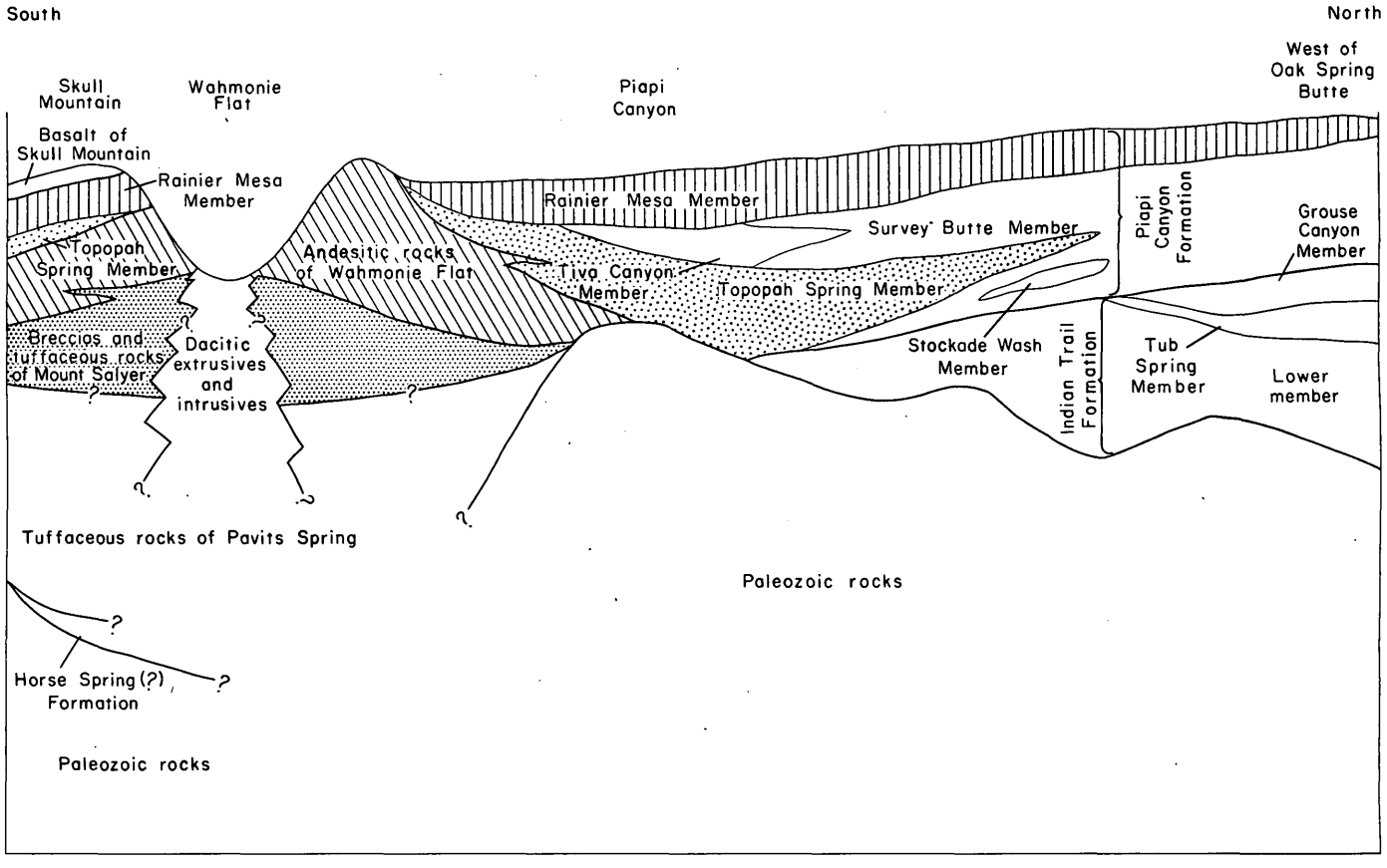

FIGURE 80.2.—Schematic diagram of the Oak Spring Group.

form as probably Eocene in age. G. E. Lewis (written communication, April 11, 1962) identified vertebrate remains collected from the basal part of the Piapi Canyon Formation and from pre-Piapi Canyon rocks in the vicinity of Pavits Spring as camel foot and toe bones of an age between Miocene and Pleistocene. Horse remains from pre-Piapi Canyon rocks east of Yucca Playa were identified by Lewis as *Merychippus* sp. and considered by him to be late Miocene or early Pliocene in age. The ages of the Indian Trail and Piapi Canyon Formations are believed to be late Miocene or early Pliocene, and early Pliocene or younger, respectively. The thick section of post-Piapi Canyon rocks in the western part of the test site are probably Pliocene and may be as young as Pleistocene in age. The youthful topography developed on these volcanic rocks also suggests a late Cenozoic age.

REFERENCES

Hinrichs, E. N., and Orkild, P. P., 1961, Eight members of the Oak Spring Formation, Nevada Test Site and vicinity, Nye and Lincoln Counties, Nev.: Art. 327 *in* U.S. Geol. Survey Prof. Paper 424–D, p. D96–D103.

Johnson, M. S., and Hibbard, D. E., 1957, Geology of the Atomic Energy Commission Nevada Proving Grounds area, Nevada: U.S. Geol. Survey Bull. 1021–K, p. 333–384.

Longwell, C. R., 1921, Geology of the Muddy Mountains, Nevada, with a section to the Grand Wash Cliffs in western Arizona: Am. Jour. Sci., 5th ser., v. 1, no. 1, p. 39–62.

Ross, C. S., and Smith, R. L., 1961, Ash-flow tuffs: their origin, geologic relations, and identification: U.S. Geol. Survey Prof. Paper 366, 81 p.

Smith, R. L., 1960, Zones and zonal variations in welded ash flows: U.S. Geol. Survey Prof. Paper 354–F, p. 149–159.

81. STRATIGRAPHY AND ORIGIN OF LAKE LAHONTAN DEPOSITS OF THE HUMBOLDT RIVER VALLEY NEAR WINNEMUCCA, NEVADA

By PHILIP COHEN, Carson City, Nev.

Work done in cooperation with the Nevada Department of Conservation and Natural Resources

Russell (1885) described the deposits of Lake Lahontan, a large Pleistocene lake that covered much of northwestern and north-central Nevada, and Morrison (1961) described the Lake Lahontan deposits in the Carson Desert near Fallon, Nev. However, only the youngest Lake Lahontan deposits are exposed in the Winnemucca area (fig. 81.1) and little was known about the geology of the Lake Lahontan deposits except for a few details about the uppermost units.

As part of a hydrogeologic investigation, test holes ranging in depth from about 15 to 120 feet were drilled in 1959 and 1960 at 175 locations in the area shown on figure 81.1. The drilling program yielded considerable information about the geology of the Lake Lahontan deposits. Five major lithologic units were recognized (three in the subsurface); the character and distribution of these units give a fairly clear picture of the history of Lake Lahontan within the area. The stratigraphic relations among most of these units are shown diagrammatically in figure 81.2.

The oldest Lake Lahontan deposit, recognized only in the subsurface in the study area, is termed the Lahontan lower silt and clay (fig. 81.2 Qll). This unit is correlated with the lower lacustral clays of Russell and the Eetza Formation of Morrison. It was penetrated with certainty in only two wells in Grass Valley. One of the wells was drilled with a cable-tool drill and this afforded an opportunity to examine fairly sizable fragments of the unit. The unit is about 20 feet thick and consists of alternating beds of silt, clayey silt, and silty clay. The beds of clayey silt and silty clay are gray to dark gray, blocky, and contain ostracodes.

A second unit of Lake Lahontan age, recognized only in the subsurface in Grass Valley, interfingers with upper beds of the Lahontan lower silt and clay.

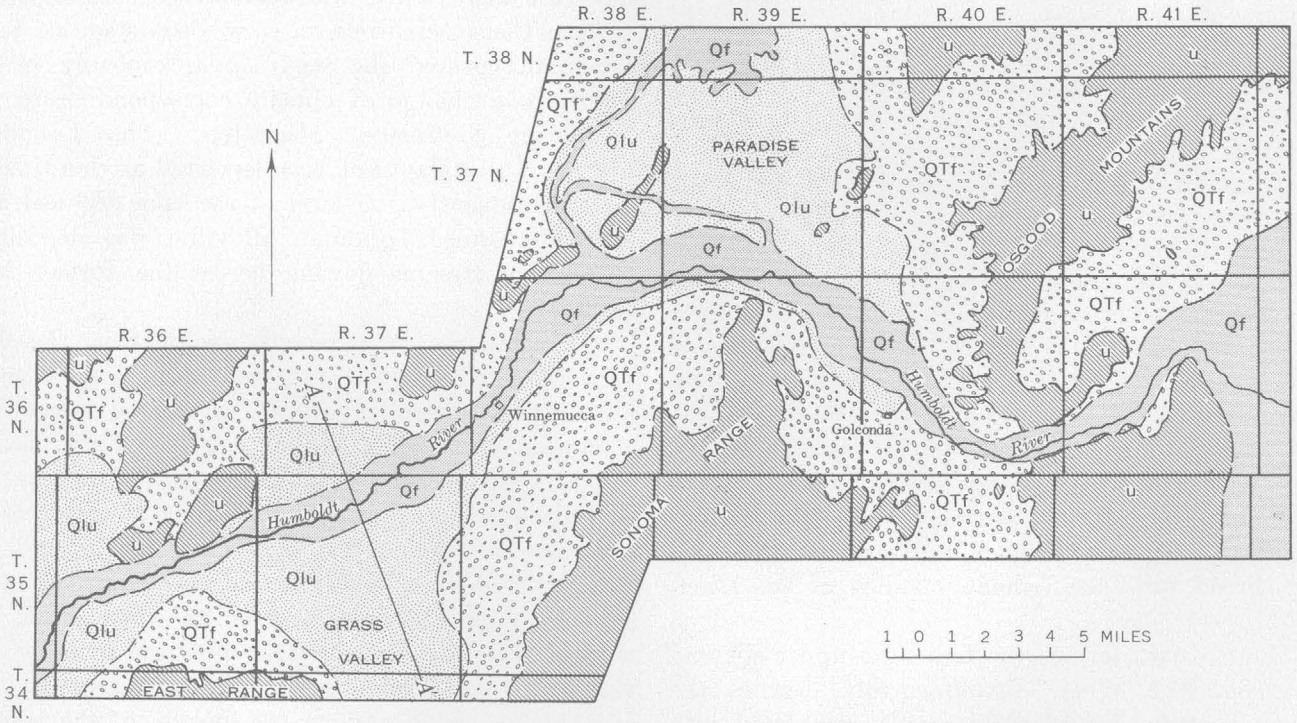

FIGURE 81.1.—Generalized geologic map of a segment of the Humboldt River valley, Humboldt and Pershing Counties, Nev. U, undifferentiated consolidated rocks ranging in age from Cambrian to Pleistocene(?). QTf, undifferentiated Tertiary and Quaternary alluvial-fan and lacustrine deposits. Qlu, Lahontan upper silt and clay. Qf, fluviatile and lacustrine deposits of post-Lake Lahontan age.

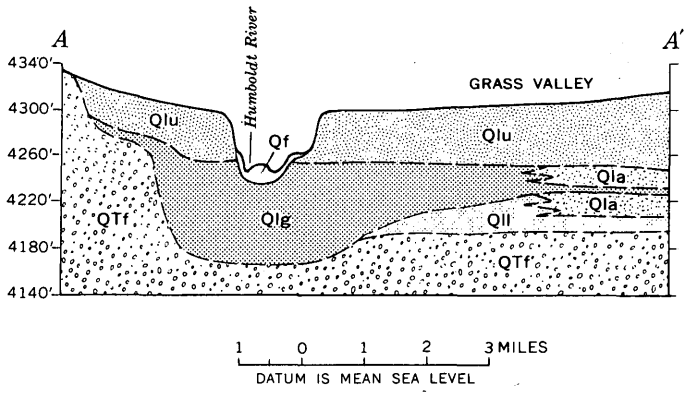

FIGURE 81.2.—Diagrammatic geologic cross section of the Humboldt River valley near the mouth of Grass Valley. QTf, undifferentiated Tertiary and Quaternary alluvial-fan and lacustrine deposits. Qll, Lahontan lower silt and clay. Qla, Lahontan alluvium. Qlg, Lahontan medial gravel. Qlu, Lahontan upper silt and clay. Qf, fluviatile and lacustrine deposits of post-Lake Lahontan age.

This unit, termed Lahontan alluvium (fig. 81.2, Qla), is tentatively correlated with the upper part of the Eetza Formation and the lower part of the Wyemaha Formation as described by Morrison (1961, p. 111–112). Its maximum thickness is about 35 feet, and it consists of interfingering fluviatile and windblown deposits of gravel, sand, silt, and clay.

The upper part of the Lahontan alluvium interfingers with the thickest Lake Lahontan unit, which is termed Lahontan medial gravel (fig. 81.2, Qlg). This unit is correlated with Russell's medial gravels and Morrison's Wyemaha Formation. More details are known about the character and distribution of this unit than the two previously described units because it was penetrated by more than 50 test holes and wells in the area. It ranges in thickness from a few inches to about 150 feet and consists of lenses of moderately to well-sorted gravel and coarse to medium sand. It extends from the western margin of the area eastward to the vicinity of Golconda and perhaps as far eastward as the eastern margin of the study area. The deposit probably is thickest beneath the flood plain of the Humboldt River, having filled a deep, broad pre-Lake Lahontan valley of the Humboldt River.

A fourth unit, termed the Lahontan upper silt and clay (fig. 81.2, Qlu), disconformably overlies the Lahontan medial gravel. This unit is correlated with Russell's upper lacustral clays and Morrison's Sehoo Formation. It is exposed throughout much of the area, and thick sections of the unit are exposed along river-cut scarps bordering the flood plain of the Humboldt River (fig. 81.1). The unit consists of beds of clay, silty clay, clayey silt, and very fine to medium sand. Individual beds, which range in thickness from a few inches to about 10 feet, can be traced for as much as 10 miles along the scarps bordering the Humboldt River, and the contacts between beds commonly are sharp. The thickness of the unit ranges from a few inches to about 60 feet. Although it contains silty and sandy beds throughout the area, the percentage of coarse-grained material tends to increase markedly upstream from Winnemucca and along the margins of Grass Valley and Paradise Valley.

The fifth lithologic unit of Lake Lahontan age is termed Lahontan gravel-bar deposits. It interfingers with and is partly of the same age as the Lahontan upper silt and clay. The gravel-bar deposits commonly are covered by a thin layer of the upper silt and clay and are exposed chiefly in gravel pits, where they commonly consist of steeply dipping beds of sand and gravel. Cobbles up to 6 inches in diameter and imbricate structure are common. The lateral and vertical extent of this unit is small, and it is not shown on figures 81.1 and 81.2.

The following history of Lake Lahontan is inferred from the distribution and character of the deposits:

1. In Pleistocene time an early deep stage of Lake Lahontan covered the study area, probably in response to a change of climate corresponding to the Wisconsin continental glaciation. The Lahontan lower silt and clay unit was deposited at this time.

2. Subsequently, the level of the lake declined and the unit termed Lahontan alluvium was deposited, largely by streams flowing across the former lake bottom.

3. In response to increased precipitation, the flow of the Humboldt River increased, and the river probably carried large volumes of coarse sediments that channeled underlying deposits. Most of the medial gravel was deposited in this manner. The level of the lake rose slowly, and fluctuations of the level of the lake resulted in rapidly transgressing and regressing shorelines. Beaches and bars associated with shifting shorelines were formed as wave action reworked the sediments brought into the area by the river. In addition, waves reworked some of the alluvial-fan deposits along the margin of the lake.

4. As the level of the lake rose, the medial gravel was covered by the upper silt and clay. The gravel-bar deposits were formed near the shore of this deep stage of the lake.

5. Probably at the end of Wisconsin time the climate became more arid. Lake Lahontan receded from the study area, and the Humboldt River cut into the upper silt and clay. The present terraces along the Humboldt River probably were formed during pauses in the decline of the level of the lake downstream from the study area.

REFERENCES

Morrison, R. B., 1961, Lake Lahontan stratigraphy and history in the Carson Desert (Fallon) area, Nevada: Art. 329 *in* U.S. Geol. Survey Prof. Paper 424–D, p. D111–D114.

Russell, I. C., 1885, Geological history of Lake Lahontan, a Quaternary lake of northwestern Nevada: U.S. Geol. Survey Mon. 11, 228 p.

82. SUBSURFACE STRATIGRAPHY OF LATE QUATERNARY DEPOSITS, SEARLES LAKE, CALIFORNIA: A SUMMARY

By GEORGE I. SMITH, Menlo Park, Calif.

Work done in cooperation with the California Division of Mines and Geology

Searles Lake, Calif., lies near the southwestern corner of the Basin and Range physiographic province and just north of the Mojave Desert. It is about 9 miles long and 7 miles wide, and has a surface area of about 40 square miles. Mud forms much of the surface, although nearly pure halite crops out over about 12 square miles in the center of the lake (Haines, 1959).

The late Quaternary deposits beneath the surface consist of interbedded saline and mud layers that lie nearly flat. Knowledge of this part of the basin fill is based almost entirely on core logs and samples from cores. The upper 150 feet of fill is known from many logs of cores obtained by the companies that extract chemicals from the deposit (Flint and Gale, 1958, figs. 2–4), and from logs of 41 cores described by Haines (1959). The deposits below 150 feet have been sampled by 6 core holes, 1 that extends to 875 feet (Smith and Pratt, 1957), 1 that extends to 628 feet (Gale, 1914, p. 289), and 4 that extend to about 300 feet (Flint and Gale, 1958, figs. 3, 4).

The major subsurface stratigraphic units in Searles Lake are described by Flint and Gale (1958). The purpose of this article is to describe 19 newly recognized subdivisions of 2 of their units, to redefine the stratigraphic relation between the youngest 2 units, and to summarize the evaporite-mineral suites that characterize each stratigraphic unit within the deposit.

As shown in figure 82.1, the major stratigraphic units have the following descriptive names: Mixed Layer, Bottom Mud, Lower Salt, Parting Mud, Upper Salt, and Overburden Mud. These names have been used for years as informal stratigraphic terms by company engineers and others working on the deposit (Flint and Gale, 1958, p. 694; Haines, 1959, p. 144–146), and their usage is continued in this paper. The 19 new stratigraphic subdivisions are in the Mixed Layer and Lower Salt, and letters or letters and numbers are assigned to them as shown in figure 82.1. In the Mixed Layer, the units are designated A, B, C, etc., from the highest unit downward. In the Lower Salt, which actually consists of interbedded layers of salines (S) and muds (M), the units are designated S–1, M–2, S–2, M–3, etc., from the lowest unit upward. The Bottom Mud is equivalent to M–1, but its descriptive name is retained.

The stratigraphic subdivisions of the Lower Salt are discrete beds of muds and salines that can be recognized throughout most of the deposit. At any given locality, each bed has a relatively constant thickness, and together the beds form a sequence that is recognizable in most nearby cores. The sequence changes from one part of the deposit to the next, but the changes are gradual. In general, the mud beds are more constant in thickness than the saline beds, and for this reason are more reliable markers. Toward the edges of the deposit, though, the saline beds pinch out, and the overlying and underlying mud beds are not distinguishable. Except for the basic distinction between muds and salines, lithology and mineralogy are not used as criteria for stratigraphic

correlation because the several mud layers are too similar to be distinguished from each other, and the saline beds change in composition laterally.

The stratigraphic subdivisions of the Mixed Layer are thicker units characterized by the dominance of muds in some units and of salines in others, or by changes in saline-mineral content that indicate significant differences in the chemical nature of the lake in which the units were deposited.

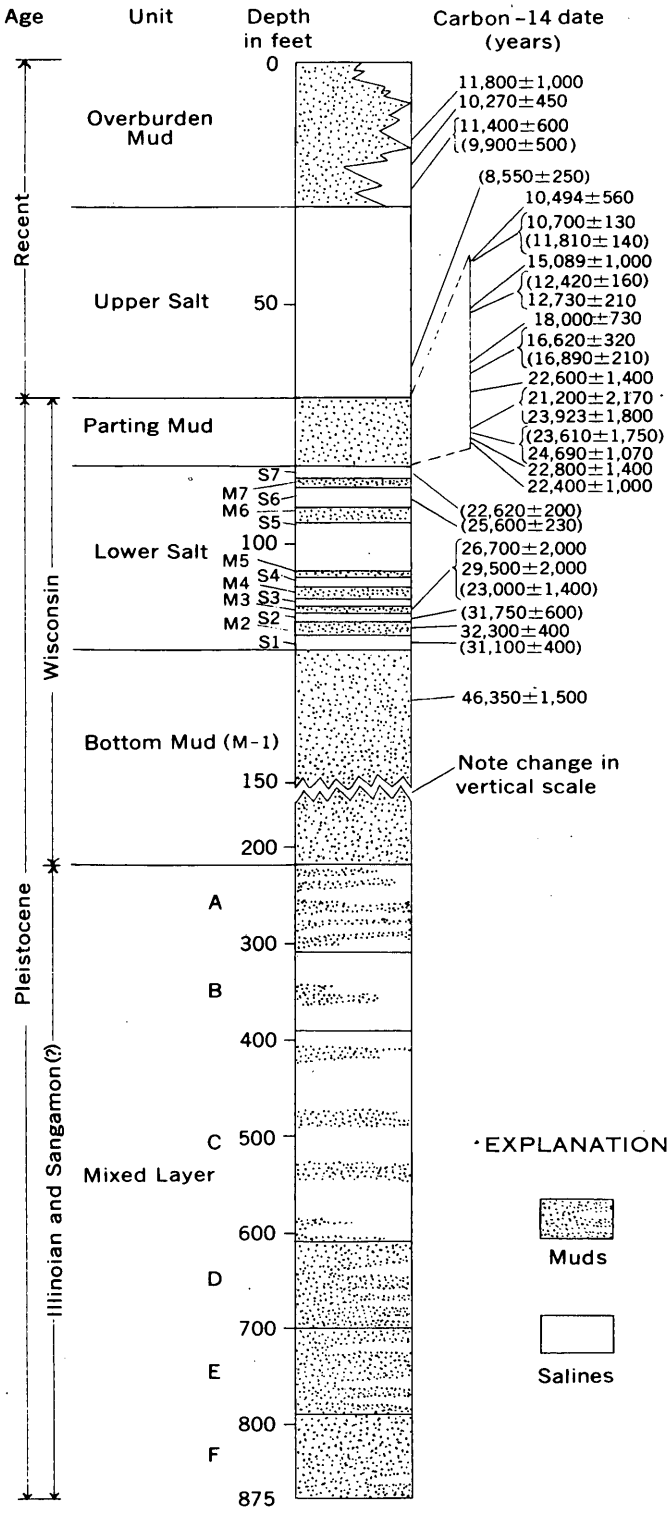

FIGURE 82.1.—Diagrammatic section of Searles Lake evaporites showing position and name of stratigraphic units and carbon-14 dates. Of the carbon-14 dates, 18 are based on carbon in disseminated organic material, 1 (26,700 years) on wood, and 11 (shown in parentheses on the illustration) on carbon in recrystallized carbonate minerals (probably not reliable for dating). Uppermost date (11,800 years) is from the U.S. Geological Survey laboratory (Meyer Rubin, written communication, 1961, sample W–942); all others are as listed by Flint and Gale (1958, table 2).

The relation between the Upper Salt and Overburden Mud is here modified from the usage of previous workers (Flint and Gale, 1959, fig. 3; Haines, 1959, p. 144, and fig. 7). They restricted the term Overburden Mud to the layer of solid mud that overlies the Upper Salt around the edge of the deposit, and they considered the interbedded muds and salines that lie near the surface in the central part of the deposit to be part of the Upper Salt. Cross sections constructed from Haines' core log data (1959), however, show that these interbedded muds and salines are lateral equivalents of the solid mud around the edge and were formed during the same episode. For this reason, they are here considered a facies of the Overburden Mud, and the two are combined into one stratigraphic unit. The term Upper Salt is restricted to the relatively mud-free salines that underlie them. In the central part of the deposit, the contact between the Upper Salt and Overburden Mud is gradational, but the two zones are distinct.

LITHOLOGY AND COMPOSITION

The muds in this deposit are mostly dark green to brown, soft, and impervious. They are chiefly combinations of Ca, Na, and Mg with CO_3, precipitated as fine-grained aragonite and dolomite, and as both fine- and coarse-grained gaylussite and pirssonite. A few mud layers have a large percentage of clay-sized halite, or a small percentage of fine- to coarse-grained borax or northupite. Clastic silt and clay are generally subordinate. Searlesite, galeite, schairerite, and tychite occur in traces.

The salines are mostly white to gray, hard, and somewhat porous. They consist chiefly of combinations of Na, K, and Mg with CO_3, HCO_3, SO_4, Cl, or B_4O_7, precipitated as coarse-grained halite and hanksite, and both coarse- and fine-grained trona, nahcolite, burkeite, borax, mirabilite, thenardite, northrupite, and aphthitalite. Small quantities of sulfohalite and tincalconite are reported.

The average evaporite-mineral composition of each stratigraphic unit has been estimated from the core logs of Smith and Pratt (1957) and Haines (1959), and from data obtained during subsequent microscopic and X-ray studies of the cores. The table below summarizes this information. The minerals are listed approximately in order of abundance. Many cores penetrate the Lower Salt and younger units, and estimates of the composition of both edge and central facies have been made. The composition of units at lower levels is much less accurately known; the descriptions in the table are as reported in the log of an 875-foot core (Smith and Pratt, 1957, p. 25–51).

Description and evaporite mineralogy of subsurface stratigraphic units in Searles Lake, California

[Compiled chiefly from Smith and Pratt (1957) and Haines (1959)]

Unit	Typical depth from top to base (feet)	Typical thickness (feet)	Evaporite-mineral components				Color and texture	Remarks
			Major		Minor (and trace)			
			Central facies	Edge facies	Central facies	Edge facies		
Overburden Mud	0–30	30	Halite	Halite Pirssonite Trona	Hanksite Borax Trona Pirssonite	Gaylussite	Dark brown, massive, grades centerward to interbedded brown muds and impure gray-green salines.	In central facies, beds of salines alternate with beds of muds; in edge facies, evaporite minerals all at base of unit, upper part mostly clastic sand, silt, and clay.
Upper Salt	30–70	40	Halite Trona Hanksite	Trona	Borax Aphthitalite	Halite Burkeite Borax Thenardite	White to light gray; trona finely granular in lower part, grades to bladed or fibrous in upper part; halite coarsely granular; hanksite as large euhedral crystals.	Trona most abundant in bottom 10 ft; hanksite most abundant in top 10 ft; halite most abundant in middle.
Parting Mud	70–84	14	Gaylussite Pirssonite Halite		Aragonite Borax Dolomite		Dark green to black, prominently laminated in upper two-thirds.	Aragonite most abundant in upper two-thirds of unit; pirssonite and gaylussite most abundant in upper and lower thirds of unit; dolomite most abundant near top and bottom contacts; borax mostly in top few inches.
Lower Salt:								
S-7	84–87	3	Trona Halite	Trona	Burkeite Borax	Halite Thenardite Borax	White; trona finely granular, fibrous, or bladed; halite coarsely granular.	
M-7	87–89	2	Gaylussite Pirssonite Northupite		Borax Northupite Aphthitalite (Trona)		Dark green to black, massive.	Megascopic gaylussite more abundant where unit nearest present surface, pirssonite more common where unit deepest.
S-6	89–93	4	Trona Halite	Trona	Burkeite	Borax Halite Nahcolite	White; trona fibrous to granular; halite coarsely granular.	
M-6	93–96	3	Pirssonite Gaylussite		Borax Halite Trona Thenardite (Burkeite) (Aphthitalite)		Dark green to black, massive.	Megascopic gaylussite more abundant where unit nearest present surface, pirssonite more common where unit deepest.
S-5	96–106	10	Trona Halite	Trona	Burkeite Borax (Hanksite)	Halite Burkeite Borax Thenardite Northupite Sulfohalite	White; trona granular to bladed; halite coarsely granular.	
M-5	106–107	1	Gaylussite		Borax Northupite Pirssonite (Tychite) (Sulfohalite)		Dark green to black, faintly laminated.	Unit locally has thin interbed of halite, trona, burkeite, and borax. Pirssonite near edges of unit.
S-4	107–109	2	Trona Halite	Trona Burkeite	Burkeite Borax	Halite Borax Northupite	White; trona finely granular, some fibrous or bladed; halite and burkeite granular.	
M-4	109–111	2	Gaylussite		Northupite Borax Halite Aphthitalite (Pirssonite?)		Dark green to black, faintly laminated.	
S-3	111–112	1	Trona	Trona	Burkeite Northupite Borax	Northupite Burkeite Hanksite Halite	White; trona is bladed, granular, or fibrous.	
M-3	112–113	1	Gaylussite		Northupite Thenardite Halite Aphthitalite (Borax) (Tychite)		Dark green to black, prominently laminated.	
S-2	113–115	2	Trona	Trona	Northupite Burkeite Borax	Northupite Borax (Tychite)	White; trona mostly bladed, some fibrous or granular.	
M-2	115–117	2	Gaylussite		Northupite Halite Thenardite Trona Burkeite (Tychite) (Schairerite) (Aphthitalite)		Dark green to black, prominently laminated.	Northupite most common near edge of deposit.

Description and evaporite mineralogy of surface stratigraphic units in Searles Lake, California—Continued

[Compiled chiefly from Smith and Pratt (1957) and Haines (1959)]

Unit	Typical depth from top to base (feet)	Typical thickness (feet)	Evaporite-mineral components				Color and texture	Remarks
			Major		Minor (and trace)			
			Central facies	Edge facies	Central facies	Edge facies		
Lower Salt—Con.								
S-1	117–120	3	Trona	Trona	Borax	Borax Thenardite Northupite Nahcolite (Tychite)	White; trona mostly bladed, some fibrous or granular.	
Bottom Mud (M-1)	120–220	100	Gaylussite		Dolomite Calcite Halite Thenardite Mirabilite Trona Borax		Dark green to black in upper part, more brown in lower part. Prominently laminated in lower 40 ft; beds and pods of mirabilite, white.	Mirabilite forms several thin beds at about 135 ft.
Mixed layer:								
A	220–310	90	Trona Gaylussite Nahcolite		Pirssonite Northupite Tychite		Salines white to light gray; muds dark brown, massive.	Nahcolite chiefly between 220 and 245 ft; pirssonite chiefly between 290 and 310 ft.
B	310–390	80	Trona Halite		Nahcolite Gaylussite Pirssonite Northupite Sulfohalite		Salines white, light gray, or clear; muds dark brown, massive.	
C	390–610	220	Halite Pirssonite		Trona Nahcolite Gaylussite Thenardite Northupite Burkeite Sulfohalite Tychite		Salines white, light gray, or clear; muds dark brown, massive.	
D	610–700	90	Pirssonite Halite Trona		Nahcolite Northupite Tychite Sulphohalite Calcite(?)		Salines white; muds dark brown, massive.	
E	700–790	90	Halite Pirssonite		Northupite Sulfohalite		Salines white, light gray, or clear; muds dark green to brown, faintly laminated in lower part.	
F	790–875+	85+	Pirssonite		Trona Halite Northupite		Muds dark green, faintly laminated; thin saline beds white to clear.	

AGE

Figure 82.1 shows the age of many of these layers as indicated by carbon–14 dates (Flint and Gale, 1958, table 2). Eighteen are based on carbon from disseminated organic material; most of this probably came from the decayed remains of plants and animals that lived in the lake, although a small part may have been reworked from older lakebeds exposed around the edge of the basin. One date is based on carbon from wood. The remaining 11 dates, shown in parentheses on figure 82.1, are based on carbon from partially or totally recrystallized carbonate minerals; they are less reliable than the dates from organic material.

These carbon–14 dates indicate that the approximate age of three contacts, in years before the present, is as follows (Flint and Gale, 1958, p. 703–707):

Upper Salt–Parting Mud	10,000
Parting Mud–Lower Salt	23,000
Lower Salt–Bottom Mud	34,000

The base of the Bottom Mud is too old for carbon–14 dating. The rate of mud deposition indicated by carbon–14 dates of the Parting Mud averages about 1 foot per 1,000 years. The Bottom Mud consists of similar material and probably was deposited at about the same rate as the Parting Mud. The Bottom Mud is about 100 feet thick, and it seems fair to assume that there were no significant periods of erosion or nondeposition. The age of the contact between the Bottom Mud and Mixed Layer can thus be estimated at between 100,000 and 150,000 years.

The carbon–14 dates of 9,900 years, and more, from samples of the Overburden Mud are surprisingly old for the most recent unit in the stratigraphic section, and it may be that large quantities of carbonate and organic carbon were washed into the lake from older lakebeds exposed around the edge of the basin. Mapping in progress shows that the lake in which these sediments were deposited was smaller than most of the earlier lakes occupying the basin, and that larger volumes of older lakebeds were removed by erosion during this period than during previous periods dated by the carbon–14 method.

The Overburden Mud and Upper Salt are probably of Recent age; the Parting Mud, Lower Salt, and Bottom Mud, of Wisconsin age; and the Mixed Layer, of pre-Wisconsin (possibly Sangamon and Illinoian) age.

REFERENCES

Flint, R. F., and Gale, W. A., 1958, Stratigraphy and radiocarbon dates at Searles Lake, California: Am. Jour. Sci., v. 256 p. 689–714.

Gale, H. S., 1914, Salines in the Owens, Searles, and Panamint basins, southeastern California: U.S. Geol. Survey Bull. 580–L, p. 251–323.

Haines, D. V., 1959, Core logs from Searles Lake, San Bernardino County, California: U.S. Geol. Survey Bull. 1045–E, p. 139–317.

Smith, G. I., and Pratt, W. P., 1957, Core logs from Owens, China, Searles, and Panamint basins, California: U.S. Geol. Survey Bull. 1045–A, p. 1–62.

METAMORPHIC GEOLOGY

83. STAUROLITE ZONE NEAR THE ST. JOE RIVER, IDAHO

By Anna Hietanen, Menlo Park, Calif.

This paper gives new information on metamorphic facies in the Belt Series of Precambrian age northwest of the Idaho batholith. In a recent summary (Hietanen, 1961, p. 84) I stated: "It is not known whether staurolite without kyanite occurs north of the kyanite-staurolite schists. Reconnaissance showed diopside gneiss and quartzite just north of the kyanite-staurolite schists, and farther north almandite-biotite schist." During the summer of 1961, fieldwork was extended northeast of the area previously mapped, and abundant large staurolite crystals without kyanite were found in the schist of the Wallace Formation exposed southwest of the St. Joe River between Bluff Creek and Beaver Creek (fig. 83.1). The southwestern part of this schist area contains kyanite as well as staurolite. Near Peggy Peak both of these minerals are altered: kyanite to muscovite, staurolite to chlorite and muscovite. Easily recognized pseudomorphs after kyanite are as much as 15 inches long. Toward the northeast they become smaller and less frequent. On the other hand, the size and abundance of pseudomorphs after staurolite increase toward the northeast, until in the central part of the schist area large unaltered staurolite crystals are embedded in fine-grained garnet-mica schist. This staurolite schist is exposed for more than a mile on three ridges that extend eastward and northeastward from Peggy Peak (fig. 83.1). On all three ridges the large staurolite crystals probably are in the same stratigraphic horizon. Little or no staurolite was found beneath the staurolite-rich layers in schist exposed along the creeks and on the slopes between the three ridges. The three occurrences lie in a narrow zone extending northwestward, which thus represents the staurolite zone in this neighborhood.

The staurolite schist is light brown to silvery gray, with distinct bedding and cleavage. In some outcrops north and northeast of Peggy Peak, cleavage is nearly parallel to the bedding, as is common where folding is very gentle. West of Angle Point, however, the cleavage is normal to the bedding and the schist breaks into shiny thin slabs parallel to the cleavage (fig. 83.2). In all outcrops staurolite is concentrated in thin beds separated by layers of mica schist containing abundant tiny almandite crystals.

The major constituents of the staurolite schist, in order of abundance, are: quartz, muscovite, biotite, staurolite, plagioclase, and almandite. Magnetite, apatite, and tourmaline are common accessory minerals. The staurolite crystals are much larger than the other minerals. In some outcrops of fine-grained garnet-mica schist, for example, staurolite crystals as much as 5 cm long are sparsely distributed throughout certain beds which contain garnets only 1 to 2 mm in diameter and mica flakes only about ½ mm long. In the staurolite zone, muscovite is more abundant than biotite; however, in some thin laminae, biotite is the major constituent. In many outcrops these biotite laminae, as well as muscovite laminae, cross the staurolite crystals, showing that the staurolite crystallized later than the micaceous minerals (fig. 83.2).

The staurolite zone, only about 1 mile wide, is much narrower than any of the other metamorphic zones northwest of the Idaho batholith. The zone in which kyanite accompanies staurolite is about 5 miles wide. In the schist 3 miles southeast of Bathtub Mountain abundant kyanite crystallized without staurolite. The schist northeast of the staurolite zone was crystallized to the biotite-almandite subfacies, indicating a lower-

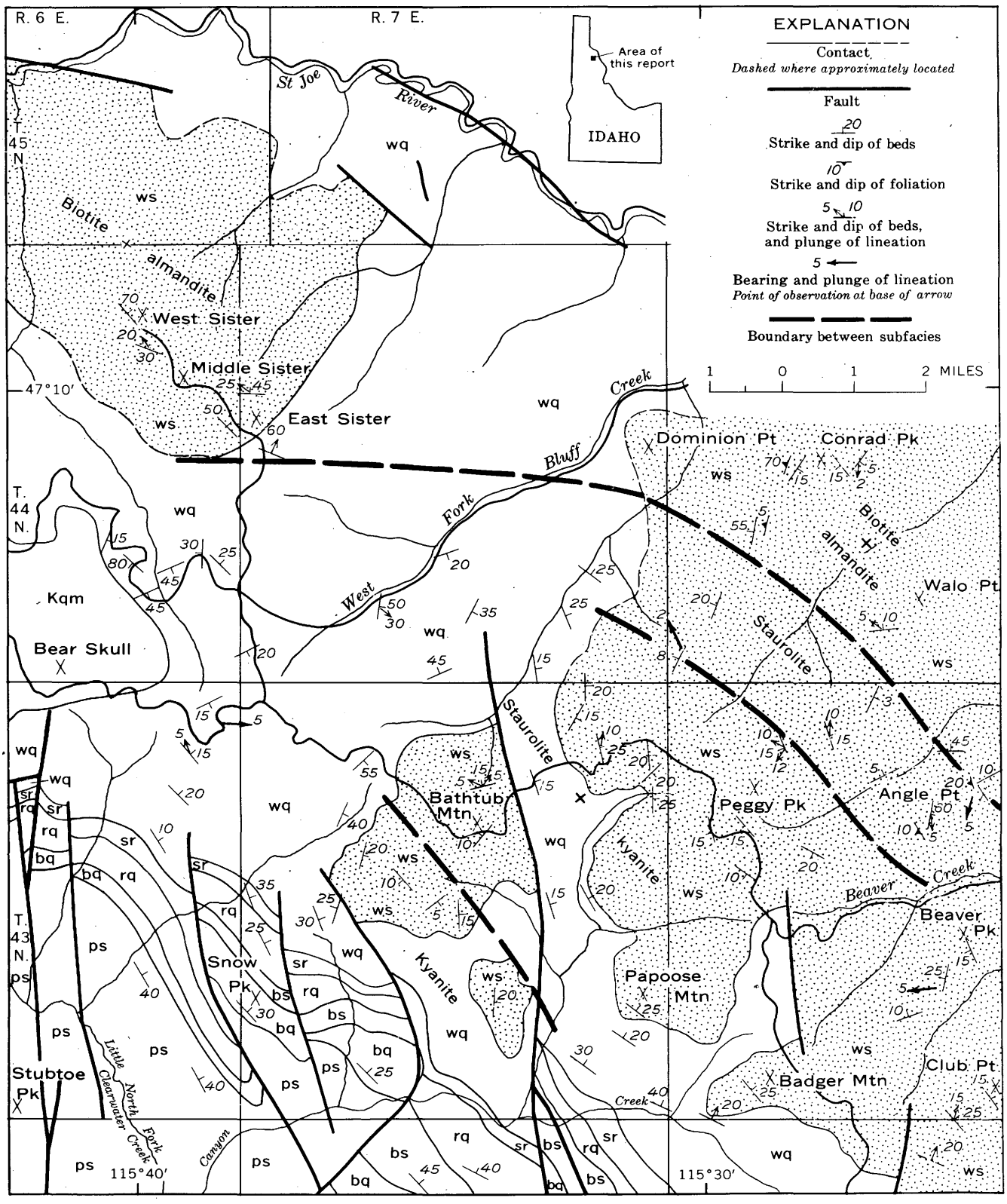

FIGURE 83.1.—Geologic sketch map showing the major rock units and the distribution of metamorphic index minerals between St. Joe River and the Little North Fork of the Clearwater River. The rocks of the Belt Series of Precambrian age, listed in order of deposition, are as follows: ps, schist of the Prichard Formation; bq, quartzite of the Burke Formation; bs, schist of the Burke Formation; rq, Revett Quartzite; sr, St. Regis Formation; wq, quartzite of the Wallace Formation; ws (stippled), schist of the Wallace Formation. Quartz monzonite (Kqm) of Cretaceous age cuts the rocks of the Belt Series discordantly.

FIGURE 83.2.—Slab of staurolite schist and crystals of staurolite. Cleavage in the schist is parallel to the photographed surface and bedding is at right angles to it. Mica flakes are well oriented parallel to the cleavage; staurolite is concentrated along the bedding. Sample is from 1 mile west of Angle Point. Note relict bedding in the crystal second from top. Crystals are from the ridge 3 miles southwest of Conrad Peak.

ing of the grade of metamorphism toward the northeast. Thus the field evidence shows that staurolite started to crystallize farther from the batholith and at lower temperature than the kyanite. Probable temperature ranges for the crystallization of these minerals northwest of the Idaho batholith are as follows: staurolite alone, 400°C–425°C; staurolite and kyanite together, 425°C–475°C; kyanite alone 475°C–500°C (Hietanen, 1961, fig. 3).

Pressure during crystallization was estimated to be about 5,000 atm (atmospheres) or slightly higher on the basis of the absence of wollastonite in the rocks studied (Hietanen, 1961). Wollastonite was found, however, during the field season of 1961 in lime-silicate rock near Dent, in the high-grade zone closest to the quartz dioritic and quartz monzonitic batholith. This confirms the inference that the pressure during the crystallization did not exceed by much, if any, the estimated 5,000 atm. The rocks in which kyanite, andalusite, and sillimanite occur together are in the same metamorphic zone as the wollastonite-bearing rocks (Hietanen, 1956), and were most likely recrystallized at the same pressure. Thus it seems that the pressure of the triple point in this area was close to 5,000 atm, and therefore much lower than recently suggested by Miyashiro (1961).

The occurrence of a staurolite zone outside the staurolite-kyanite zone near the St. Joe River suggests that staurolite started to crystallize at a lower temperature than kyanite. A similar relation occurs in the Dalradian rocks in Scotland (Barrow, 1893; Harker, 1939; Williamson, 1953); in the Sulitelma area, Norway (Vogt, 1927); and locally in the Appalachian area (Cloos and Hietanen, 1941). In lower grade rock, chloritoid takes the place of staurolite. In some areas where kyanite occurs with chloritoid, as for instance in Unst, Shetland Islands (Reed, 1934), there have been several episodes of metamorphism or a retrograde alteration during which kyanite has been preserved as an unstable relict. It seems therefore that in normal progressive metamorphism, staurolite crystallizes at a lower temperature than kyanite. The reaction 5 kyanite + 4 chloritoid $\rightarrow$ 2 staurolite + quartz + $3H_2O$ (Harker, 1939, p. 225), however, suggests that a "wet" environment would favor the formation of a kyanite-chloritoid assemblage instead of staurolite. This may have been the case for example, in the Hyde Park quadrangle, Vermont (Albee, 1957), where chloritoid and kyanite occur together.

REFERENCES

Albee, A. L., 1957, Bedrock geology of the Hyde Park quadrangle, Vermont: U.S. Geol. Survey Geol. Quad. Map GQ–102.

Barrow, G., 1893, On an intrusion of muscovite-biotite gneiss in the southeast Highlands of Scotland: Geol. Soc. London Quart. Jour., v. 49, p. 330–358.

Cloos, Ernst, and Hietanen, Anna, 1941, Geology of the "Martic overthrust" and the Glenarm series in Pennsylvania and Maryland: Geol. Soc. America Spec. Paper 35, 205 p.

Harker, A., 1939, Metamorphism: New York, E. P. Dutton & Co., 362 p.

Hietanen, Anna, 1956, Kyanite, andalusite, and sillimanite in the schist in Boehls Butte quadrangle, Idaho: Am. Mineralogist, v. 41, p. 1–27.

——— 1961, Metamorphic facies and style of folding in the Belt Series northwest of the Idaho batholith: Comm. geol. Finlande Bull. 196, p. 73–103.

Miyashiro, Akiho, 1961, Evolution of metmorphic belts: Jour. Petrology, v. 2, no. 3, p. 277–311.

Reed, H. H., 1934, The metamorphic geology of Unst in the Shetland Islands: Geol. Soc. London Quart. Jour. 90, p. 637–688.
Vogt, Th., 1927, Sulitelma feltets geologi og petrografi: Norges Geol. Undersokelse Skrifter 121, p. 1–560.
Williamson, D. H., 1953, Petrology of chloritoid and staurolite rocks north of Stonehaven, Kincardineshire: Geol. Mag., v. 90, p. 353–361.

GEOCHEMISTRY

84. ZINC IN MAGNETITE FROM ALLUVIUM AND FROM IGNEOUS ROCKS ASSOCIATED WITH ORE DEPOSITS

By P. K. Theobald, Jr., and C. E. Thompson, Denver, Colo.

Preliminary study of the trace-element content of heavy minerals in alluvium established that detrital magnetite derived from zinc-rich mineralized areas has a high zinc content (Theobald and Thompson, 1959). Later work here summarized shows that magnetite in intrusive rocks associated with zinc deposits also has a high zinc content and may be the principal source of the zinc-rich detrital magnetite in the alluvium.

The zinc content of alluvial magnetite concentrates ranges from less than 25 to more than 4,000 ppm (parts per million) in the samples studied. Individual areas are characterized by smaller ranges, as is shown in figure 84.1.

The Clear Creek drainage basin in the Front Range mineral belt of central Colorado, the only area that includes a zinc-producing mining district, has a higher mean value than any of the other areas sampled. Samples that contain more than 1,000 ppm of zinc are from streams draining directly from the productive part of the mining district. Virtually all samples from the Clear Creek drainage basin are richer in zinc than the averages of samples from the other areas shown in figure 84.1, suggesting to us that the zinc enrichment at Clear Creek extends considerably beyond the bounds of the ore-producing district.

Alluvial samples from the inner piedmont belt of North and South Carolina have a generally lower zinc content than those from Clear Creek. The majority contain less than 100 ppm of zinc, but some contain 100 to 1,000 ppm. We know of no zinc deposits in this area, but the depth of weathering, infrequent exposures, and the poor state of present geologic information cannot exclude the possibility of small or lean deposits. The samples that contain 100 to 1,000 ppm suggest that at least a few small deposits may exist. These above-average samples are clustered into geographically distinct zones that seem to parallel changes in metamorphic grade of the rocks.

In the Concord quadrangle, North Carolina, the mean and maximum values are the lowest of the three largest groups of samples. Even here, however, the

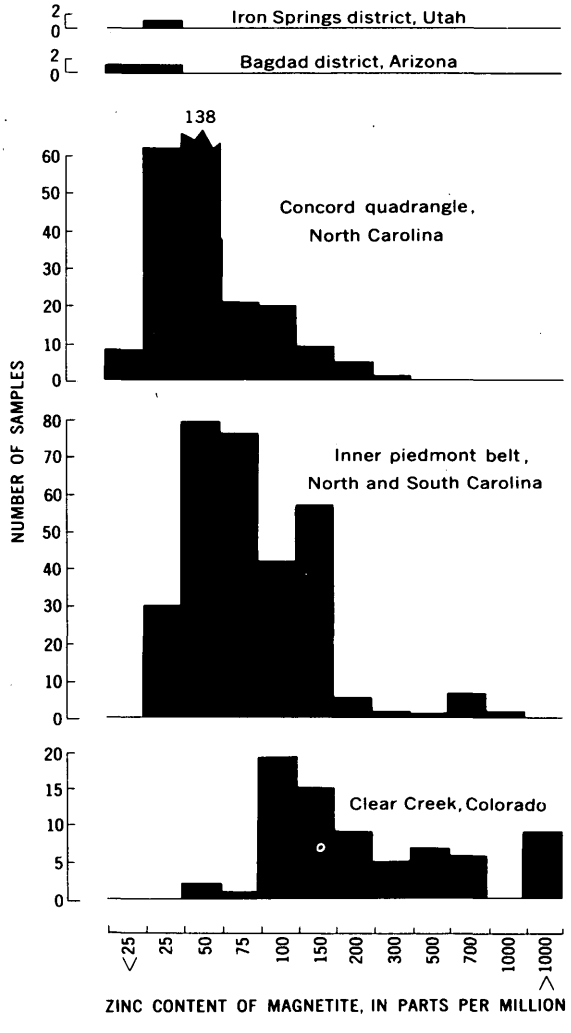

Figure 84.1.—Histograms showing zinc content of alluvial magnetite concentrates from five places in the United States.

few samples that contain more than 100 ppm of zinc appear to correlate with a syenite complex that intrudes older rocks (Bell, 1960). The syenite complex is inferred to be genetically related to minor zinc mineralization (W. C. Overstreet, written communication, 1959).

The two samples from Arizona and the one from Utah were separated from alluvium of small washes whose drainage basins were entirely within barren intrusive rocks.

The range in zinc content of magnetite concentrates from alluvium is large, and the variation is systematic. Three general subranges are recognized: (1) below 100 ppm, an overall average range that may be defined as background; (2) 100 to about 300 ppm, the range of samples peripheral to ore-bearing areas or to low-grade zinc mineralization; (3) above 300 ppm, potential association with zinc mineralization of ore grade.

Magnetite was concentrated from several suites of igneous rocks and analyzed in an effort to locate the source of the zinc-rich alluvial magnetite; the results are presented in the table. The zinc content of magnetite from rocks of the Front Range parallels that of the alluvium. Quartz monzonite of Precambrian age serves as a host rock to zinc ore, but contains considerably less zinc than quartz monzonite of Tertiary age that is several miles from ore deposits to which it is genetically related (Lovering and Goddard, 1950, p. 43–47).

The magnetite in most rocks of an extensive suite found in the Isenhour quarry near Concord, N.C., contains little zinc, but that from northeast-trending basic dikes contains large amounts. These dikes are inferred to be genetically associated with zinc mineralization (Overstreet, written communication, 1959). Nearby syenite also contains zinc-rich magnetite.

At Butte, Mont., magnetite from rocks presumably associated with copper deposits has little zinc, whereas magnetite from rocks associated with zinc mineralization at Hanover, N. Mex., and in the Illinois-Kentucky fluorite-sphalerite district contains abundant zinc (A. V. Heyl, oral communication, 1961).

Present information suggests that zinc-rich magnetite is derived from igneous rocks that are genetically related to ore deposits. The zinc-rich magnetite may be detected in alluvium miles downstream from the source rocks. This apparent relationship, if supported by continued work, could provide a powerful means for geochemical prospecting and another tool for the study of ore genesis.

Zinc in magnetites separated from igneous rocks

[Analyses by C. E. Thompson]

Rock type	Zinc-ore association	Number of samples	Zinc content (ppm)	
			Median	Range
Front Range, Colo.				
Quartz monzonite (Precambrian).	Unrelated zinc deposits in immediate vicinity.	2	400	150–700
Quartz monzonite (Tertiary).	Genetically related zinc deposits several miles to the south.	12	1,600	860–2,500
Isenhour quarry, Cabarrus County, N. C.[1]				
Miscellaneous inclusions in country rock.	No known association	4	50	<25–500
Granodiorite country rock	do	10	<25	<25–50
Mylonite zones in country rock.	do	3	<25	<25
Northwest-trending basic dikes.	do	8	50	<25–250
Epidotized, sheared granodiorite.	do	3	25	25–50
Pyroxenite	do	3	250	75–250
Young granite	do	15	25	<25–25
Pegmatite	do	7	50	25–75
Quartz vein	do	1	50	50
Syenite dike	Possible association with minor zinc mineralization.	10	40	25–50
Northeast-trending basic dikes.	Possible association with minor zinc mineralization as a late stage of syenite.	4	1,500	50–4,000
Syenite complex, Cabarrus County, N. C.[1]				
Syenite	Inferred association with minor zinc mineralization.	1	700	700
Minette	do	1	125	125
Southwest of Butte, Mont.[2]				
Butte Quartz Monzonite	Probable association with copper and associated mineralization at Butte.	7	25	25
Granodiorite	15 to 20 miles from mineralization.	30	50	25–200
Hanover district, New Mexico				
Replacement magnetite deposit.	Zinc deposits in mutual association with adjacent intrusive.	1	700	700
Hicks dome, Hardin County, Ill.[3]				
Lamprophyre	Abundant sphalerite with fluorite in same structure.	1	1,500	1,500

[1] Samples from W. C. Overstreet and Henry Bell III.
[2] Samples from George Neuerburg.
[3] Sample from R. D. Trace.

REFERENCES

Bell, Henry, III, 1960, A synthesis of geologic work in the Concord area, North Carolina: Art. 84 *in* U.S. Geol. Survey Prof. Paper 400–B, p. B189–B191.

Lovering, T. S., and Goddard, E. N., 1950, Geology and ore deposits of the Front Range, Colorado: U.S. Geol. Survey Prof. Paper 223, 319 p.

Theobald, P. K., Jr., and Thompson, C. E., 1959, Reconnaissance exploration by analysis of heavy mineral concentrates [abs.]: Mining Eng., v. 11, no. 1, p. 40.

85. METAL CONTENT OF SOME BLACK SHALES OF THE WESTERN CONTERMINOUS UNITED STATES—PART 2

By D. F. Davidson and H. W. Lakin, Denver, Colo.

In this article are presented partial analyses of samples from shale beds in nine Paleozoic formations in the Western Conterminous United States (see table). Sample localities are shown in figure 85.1. Samples of black shale beds of high metal content from six other geologic formations were described and partial analyses were given by the authors in a previous paper (Davidson and Lakin, 1961).

The samples were collected during reconnaissance investigations for uranium in black shale deposits of the Western United States, and their description and uranium content published previously (Duncan, 1953). All samples are of carbonaceous marine shale and most probably represent parts of shelf facies of marine sediments.

FIGURE 85.1.—Map of Western Conterminous United States showing locations at which samples were collected. 1, Custer County, Idaho; 2, Fergus County, Mont.; 3, 4, Gallatin County, Mont.; 5, Nye County, Nev.; 6, White Pine County, Nev.; 7, 8, Elko County, Nev.; 9, Utah County, Utah.

REFERENCES

Davidson, D. F., and Lakin, H. W., 1961, Metal content of some black shales of the Western United States: Art. 267 *in* U.S. Geol. Survey Prof. Paper 424–C, p. C329–C331.

Duncan, D. C., 1953, Reconnaissance investigations for uranium in black shale deposits of the Western States during 1951 and 1952: U.S. Geol. Survey TEI–381, 89 p.

Partial analyses of carbonaceous marine shale samples from nine geologic formations of the Western Conterminous United States

[Semiquantitative spectrographic analyses by E. F. Cooley and Uteana Oda; chemical analyses by H. L. Neiman]

Location on fig. 85.1	Sample	Formation	Age	Locality	Thickness (feet) [1]	Semiquantitative spectrographic analysis (parts per million)										Chemical analysis (parts per million)
						Pb	Mn	Cu	Zn	Ni	V	Mo	Ag	Cr	Fe	Se
1	74139	Milligen Formation.	Mississippian	Custer County, Idaho.	4	70	200	150	<200	100	3,000	100	2	300	30,000	32
2	66707	Heath Formation.	do	Fergus County, Mont.	4	15	100	70	1,000	150	1,000	150	5	200	15,000	----------
2	66711	do	do	do	5	20	300	70	1,500	200	1,000	300	2	150	15,000	----------
3	66763	Madison Limestone.	do	Gallatin County, Mont.	2.7	10	150	70	<200	100	1,000	2	<1	70	15,000	----------
4	66759	Three Forks Shale.	Devonian and Mississippian.	do	1.5	10	200	70	300	100	1,000	<2	<1	70	20,000	----------
5	53645	Unnamed shale	Mississippian	Toquima Range, Nye County, Nev.	7	20	100	150	2,000	50	3,000	50	2	150	5,000	28
6	53636	Chainman Shale	do	White Pine County, Nev.	5	20	150	700	3,000	200	3,000	150	15	200	30,000	20
7	73107	Unnamed shale	Carboniferous(?)	Taylor Canyon, Elko County, Nev.	4	20	200	700	2,000	200	3,000	150	15	200	30,000	30
8	76326	Unnamed shale	do	Goose Creek valley, Elko County, Nev.	(2)	10	500	100	700	70	2,000	20	<1	70	30,000	2
9	52075	Manning Canyon Shale.	Late Mississippian and Pennsylvanian.	Utah County, Utah	5	15	100	150	200	150	1,500	200	5	500	30,000	75

[1] Thickness of unit sampled.
[2] Grab sample.

86. CHEMICAL COMPOSITION OF PRECAMBRIAN PELITIC ROCKS, QUADRILÁTERO FERRÍFERO, MINAS GERAIS, BRAZIL

By NORMAN HERZ, São Paulo, Brazil

Work done in cooperation with the Departamento Nacional da Produção Mineral do Brasil

Chemical analyses of Precambrian pelitic rocks obtained in the course of the geologic study of the Quadrilátero Ferrífero, State of Minas Gerais, Brazil (Departamento Nacional da Produção Mineral, 1959) provide an opportunity for comparison with pelitic rocks elsewhere. The geochemistry of such rocks is of especial interest because it offers an approach to hypotheses regarding the primitive atmosphere and ocean (Pettijohn, 1957, p. 682).

The stratigraphic section in the Quadrilátero Ferrífero includes at least three series. The oldest series, the Rio das Velhas, is presumed to range from 1,350 to 2,400 million years in age; the younger two, the Minas and the Itacolomí Series, range from 500 to 1,350 million years (Herz and others, 1961). Pelitic rocks are the most common in the stratigraphic section.

Quartz, muscovite, and chlorite comprise the most common mineral assemblage in these pelitic rocks, and chloritoid also is present in rocks that have a low potassium content compared to aluminum. Magnetite, hematite, and limonite are the most common accessory minerals, but tourmaline, carbonates, and graphite are also present in some rocks.

Most rocks are dark green or gray and are fine grained. They are deformed to various degrees of intensity, but most commonly not to any severe degree, and the younger rocks still show good bedding. Many older rocks have undergone both retrogressive metamorphism and a mechanical reduction in grain size, so that bedding planes have been obliterated. In well-foliated rocks, muscovite, chlorite, and quartz grains, either equant or elongated, are alined parallel to foliation. In laminated rocks, alternate layers are rich in either chlorite-sericite or quartz.

The Nova Lima Group of the Rio das Velhas Series is the oldest mappable unit of the area (Dorr *in* Departamento Nacional da Produção Mineral, 1959, p. 71–72). The group consists largely of mica schist, phyllite, and quartz-mica schist but includes subordinate iron formation, graywacke, metavolcanics, and similar rocks, and it is presumably underlain by metasedimentary gneiss and granodiorite 2,400 million years of age. Sample Z–842 (table 86.1) is slate thought to come from the upper part of this sequence.

TABLE 86.1.—*Chemical analyses of pelitic rocks of low metamorphic grade, Quadrilátero Ferrífero, Minas Gerais, Brazil*

[Locations from quadrangles on map in Departamento Nacional da Produção Mineral (1959)]

	1	2	3	4	5	6	7
SiO_2	56. 1	61. 6	62. 4	57. 3	58. 6	61. 9	68. 8
Al_2O_3	18. 8	24. 5	19. 2	20. 4	22. 1	19. 7	17. 0
Fe_2O_3	3. 5	1. 0	1. 7	10. 1	2. 7	1. 7	3. 9
FeO	6. 6	. 1	3. 1	1. 2	5. 8	2. 4	. 34
MgO	5. 0	1. 7	2. 8	. 66	2. 2	3. 9	. 49
CaO	0	0	. 12	. 18	. 13	. 03	. 01
Na_2O	. 1	. 2	. 32	. 40	. 26	. 20	. 18
K_2O	4. 2	6. 2	4. 9	5. 7	3. 2	5. 4	3. 6
TiO_2	. 3	. 4	. 62	. 70	. 75	. 24	. 63
P_2O_5	. 06	. 09	. 06	. 16	. 09	. 05	. 05
MnO	. 03	0	. 02	. 02	. 16	. 02	. 02
H_2O	5. 0	3. 8	3. 9	2. 8	4. 1	4. 4	3. 6
CO_2			<. 05	<. 05	<. 05	<. 05	<. 05
Total	99. 7	99. 6	99. 1	99. 6	100. 1	99. 9	[1] 100. 1

[1] 1.5 percent organic matter.

1. Sample Z–842. Rio das Velhas Series (Nova Lima Group?), slate. Opaque in thin section except for fine-grained angular quartz (<0.01 mm). Gandarela quadrangle, 11,100 N., 5,300 E. Analyzed by Cassio Pinto Departamento Nacional da Produção Mineral, Belo Horizonte, M. G., Brazil; collected and described by J. E. O'Rourke.
2. Sample Z–597. Batatal Formation, slate. Opaque in thin section except for fine-grained quartz (<0.01 mm). Gandarela quadrangle, 9,950 N., 5,700 E. Analyzed, collected, and described by same persons as sample Z–842.
3. Sample J–84b. Moeda Formation, quartz-sericite phyllite. Coarse muscovite and sericite, 57 percent; quartz, 33 percent; limonite, 5 percent; chlorite, 2 percent; tourmaline, etc., 3 percent. Cachoeira do Campo quadrangle, 500 N., 12,600 E. Analyzed by P. L. D. Elmore, S. D. Botts, M. D. Mack, and H. W. Thomas, U.S. Geological Survey, Washington, D.C. (rapid rock analysis); collected and described by R. F. Johnson and Norman Herz.
4. Sample J–211. Piracicaba Group, quartz-sericite phyllite. Quartz, 40 percent (<0.1 mm); sericite, 45 percent (<0.2 mm); chlorite, 5 percent; magnetite, apatite, tourmaline. Dom Bosco quadrangle, 7,400 E., 11,700 N. Analyzed, collected, and described by same persons as sample J–84b.
5. Sample J–341. Piracicaba Group, quartz-sericite-chloritoid phyllite. Quartz, 40 percent (0.02–0.04 mm); sericite, 30 percent; chloritoid (late in paragenesis), 25 percent; chlorite, 5 percent; muscovite (1.5 mm, late in paragenesis), magnetite. Dom Bosco quadrangle, 11,500 E., 11,600 N. Analyzed, collected, and described by same persons as sample J–84b.
6. Sample J–682B. Piracicaba Group, quartz-sericite phyllite. Quartz, sericite, chlorite, muscovite, limonite (near granitized rock). Dom Bosco quadrangle, 3,250 N., 10,500 E. Analyzed, collected, and described by the same persons as sample J–84b.
7. Sample BP–1. Piracicaba Group, Barreiro Formation, fine-grained graphitic phyllite. Ibirite quadrangle. U.S. Geological Survey, Washington, D.C. (rapid rock analysis); collected and described by G. C. Simmons.

The Minas Series includes the Caraça Group overlain successively by the Itabira and Piracicaba Groups (Dorr and Simmons *in* Departamento Nacional da Produção Mineral, 1959, p. 72–81). The Moeda Formation, the basal unit of the Caraça Group, overlies the Rio das Velhas Series with profound unconformity. The formation consists largely of quartzite and associated rock types, including sericite-rich beds (table 86.1, sample J–84b). The Batatal Formation

639466 O - 62 - 6

(sample Z–597) overlies the Moeda and consists largely of phyllite and mica schist. The Batatal is overlain by the Itabira Group consisting of chemical sediments: a lower iron formation and an upper dolomite.

The Piracicaba Group, which overlies the Itabira in a disconformable relation, consists of a variety of metasedimentary rocks including ferruginous quartzite, phyllite, mica schist, graywacke, and metavolcanics. The upper part of the group at least represents a change from shelf to eugeosynclinal deposition, with an increase in clastic sediments. The other analyses of table 86.1 are from the lower part of this group.

The mineralogy of each sample is shown in table 86.1. An apparent composition (epinorm) was calculated using the average of the five analyses of quartz-sericite-chlorite rocks, excluding sample J–341, which contains chloritoid, and sample BP–1, which contains abundant organic matter. The epinorm (table 86.2), figured according to the system of Barth

TABLE 86.2.—*Epinormative minerals of average of analyses of samples Z–597, Z–842, J–211, J–682b, and J–84b (table 86.1)*

	Percent		Percen
Quartz	42. 6	Chlorite:	
White mica:		Amesite	13. 6
Muscovite	40. 0	Antigorite	0. 7
Paragonite	2. 0	Ilmenite	1. 0
		Apatite	0. 1

(1959), agrees with the actual minerals found and shows that the white mica is essentially muscovite and that the chlorite is magnesia rich. Paragonite was looked for by X-ray diffractometer analysis in 12 phyllitic rocks and was not found, suggesting that the paragonite shown in the epinorm is present only as a solid-solution phase in muscovite.

Sample J–341, which is chloritoid bearing, is from the basal part of the Cercadinho Formation, the basal part of the Piracicaba Group; it may represent, in part, a reworked regolith in which an abundance of alumina was preserved. The sample meets all the chemical conditions for chloritoid-bearing rocks found by Halferdahl (1961, p. 109–111), whereas the average of the chlorite-muscovite-quartz rocks does not (table 86.3). Apparently alumina in excess of that

TABLE 86.3.—*Molecular chemical ratios of chloritoid-bearing phyllite (sample J–341) compared with average of table 86.2*

	Sample J–341	Average of table 86.2
Al_2O_3: $Fe_2O_3+FeO+MnO+MgO$.	1.4	1.5
$Al_2O_3>Fe_2O_3+FeO+MnO+MgO>K_2O+Na_2O+CaO$.	15.5>11.1>2.9	14.4>9.3>4.3
Al_2O_3 excess after deducting micachlorite.	3.7	Deficient
$FeO+MnO>MgO$	6.0>3.9	2.7<5.0
$FeO+MnO>Fe_2O_3$	6.0>1.2	2.7>1.6

needed to make mica and chlorite, and less magnesia than ferrous iron were the critical factors for the development of chloritoid in these rocks.

The chemical composition of pelitic rocks of low metamorphic grade is considered by most workers to be due to variations in the original sedimentation. A reduction of iron, if organic matter is initially present, and a loss of hygroscopic water are the only certain changes due to metamorphism.

The average chemical composition of the Quadrilátero Ferrífero pelitic rocks is shown in table 86.4, and

TABLE 86.4.—*Average chemical composition of pelitic rocks*

	A	B	C	D	E	F
SiO_2	61. 1	56. 30	62. 58	60. 15	55. 43	59. 93
Al_2O_3	20. 3	17. 24	18. 09	16. 45	13. 84	16. 62
Fe_2O_3	3. 5	3. 83	1. 60	4. 04	4. 00	3. 03
FeO	2. 8	5. 09	5. 07	2. 90	1. 74	3. 18
MgO	2. 4	2. 54	2. 18	2. 32	2. 67	2. 63
CaO	. 07	1. 00	. 16	1. 41	5. 96	2. 18
Na_2O	. 24	1. 23	. 81	1. 01	1. 80	1. 73
K_2O	4. 8	3. 79	3. 68	3. 60	2. 67	3. 54
TiO_2	. 5	. 77	. 87	. 76	. 46	. 85
P_2O_5	. 08	. 14	. 10	. 15	. 20	------
MnO	. 04	. 10	. 04	Tr.	Tr.	------
H_2O	[1] 3. 8	3. 69	4. 18	4. 71	5. 56	4. 34
CO_2	[1] <. 05	. 84	. 3	1. 46	4. 62	2. 31

[1] Average of 5 analyses.

A. Average of 7 analyses, low-grade pelitic rocks, Quadrilátero Ferrífero.
B. Average of 33 analyses, Precambrian slates, Lake Superior district (Nanz, 1953, p. 57). Includes 1.98 percent FeS_2, 1.18 percent C, 0.28 percent SO_3.
C. Average of 7 analyses, low-grade pelitic rocks. Devonian Littleton Formation, New Hampshire (Shaw, 1956, p. 929).
D. Average of 51 analyses, Paleozoic shales (Clarke, 1924).
E. Average of 27 analyses, Meso-Cenozoic shales (Clarke, 1924).
F. Average of 85 analyses, low-grade pelitic rocks (Shaw, 1956, p. 928).

for comparison averages are shown for Precambrian rocks of the Lake Superior district, the Devonian Littleton Formation of New Hampshire, Paleozoic and Meso-Cenozoic shales, and low-grade pelitic rocks. In table 86.5 various chemical ratios for these rocks

TABLE 86.5.—*Chemical ratios for pelitic rocks*

Averages	CaO/MgO	Al_2O_3/Na_2O	SiO_2/Al_2O_3	FeO/Fe_2O_3	SiO_2/K_2O
A	0. 03	84. 2	3. 0	0. 8	12. 7
B	. 39	14. 0	3. 3	1. 3	14. 9
C	. 07	22. 3	3. 5	3. 2	17. 0
D	. 61	16. 3	3. 7	. 7	16. 7
E	2. 2	7. 7	4. 0	. 4	20. 8
F	. 83	9. 6	3. 6	1. 0	16. 9
R–1	. 24	24. 1	3. 2	[1]	14. 7
R–2	1. 4	24. 3	3. 4	[1]	12. 9
R–3	2. 2	20. 4	3. 2	[1]	13. 6
R–4	2. 7	12. 3	3. 4	[1]	19. 9
R–5	2. 7	11. 6	4. 8	[1]	22. 6

[1] All Fe reported as Fe_2O_3.

A–F. Same as table 86.4.
R–1—R–5. Averages of "clays" of the Russian platform (Vinogradov and Ronov, 1956),
R–1. Precambrian "Sinian," 17 analyses.
R–2. Lower Paleozoic, 45 analyses.
R–3. Middle and upper Paleozoic, 158 analyses.
R–4. Mesozoic, 32 analyses.
R–5. Cenozoic, 17 analyses.

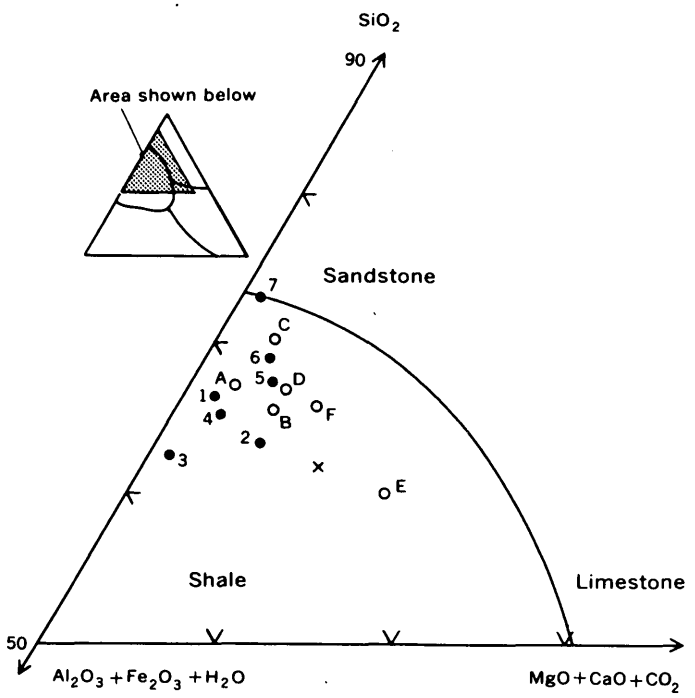

FIGURE 86.1.—Comparison of analyses of pelitic rocks. Dots, analyses 1–7, table 86.1 Quadrilátero Ferrífero. Circles analyses A–F, table 86.4. X, Clarke's (1924) average shale. (After Mason *in* Pettijohn, 1957, p. 106.)

and also for pelitic rocks of the Russian platform (Vinogradov and Ronov, 1956) are shown.

The individual and average analyses from the Quadrilátero Ferrífero are compared to the averages of table 86.4 and to Clarke's (1924) average shale on figure 86.1, a triangular diagram with apices SiO_2, $Al_2O_3+Fe_2O_3+H_2O$, and $MgO+CaO+CO_2$. All the analyses of table 86.4 fall within the shale field shown in figure 86.1. The average Meso-Cenozoic shale (E, fig. 86.1) is strongly displaced towards the $CaO+MgO+CO_2$ apex compared to the other rocks due to its comparatively high CaO content.

The CaO content is lowest in the Quadrilátero Ferrífero rocks and increases with geologic time. This is also shown by the CaO/MgO ratio of 2.2 (table 86.5) for the Mesozoic and Cenozoic rocks compared with values below unity for older rocks. The Russian-platform data also bear out this increase of CaO with time. This increase can be attributed to the appearance of lime-secreting invertebrates and a consequent fixing of lime and CO_2 in the Paleozoic and younger rocks (Pettijohn, 1957, p. 684).

Of the rocks compared in tables 86.4 and 86.5, the Quadrilátero Ferrífero pelites have the highest Al_2O_3/Na_2O ratio. The highest Na_2O content for any Quadrilátero Ferrífero rock is only 0.40 (sample J–211, table 86.1) which is still lower than all the other rock averages shown in table 86.4. Vinogradov and Ronov (1956) also show a high for this ratio in lower Paleozoic and Precambrian rocks of the Russian platform (table 86.5).

The Al_2O_3/Na_2O ratio should be a good measure of the maturity of the sedimentary source because sodium is easily leached from soils, whereas aluminum is generally not, and neither is likely to be added or subtracted after deposition (Pettijohn, 1957, p. 103). From this we can tentatively conclude that a plant cover of some kind may have been present in this area in Precambrian time to allow weathering to a mature stage. As a contrast, a low Al_2O_3/Na_2O ratio of 11 has been found by Nanz (1953) in a graywacke suite, a product of rapid uplift and erosion.

Abundant alumina in the Quadrilátero Ferrífero rocks is also reflected in their low SiO_2/Al_2O_3 ratio. This ratio is generally taken as an index of grain size in original sediments, with the ratio increasing in coarser grained material that is presumably more salt-rich and clay impoverished (Pettijohn, 1957, p. 101).

The FeO/Fe_2O_3 ratio does not vary in any systematic way in table 86.5. Apparently local conditions in the original basin of deposition exerted the greatest influence on this ratio and nothing of a temporal nature can be deduced from the data.

The Quadrilátero Ferrífero rocks are the most enriched in K_2O of all those compared. One may see in table 86.5 that the SiO_2/K_2O ratio does diminish in older rocks. In the Russian-platform data, the maximum for this ratio is in the most recent rocks, although the minimum is in Paleozoic rather than Precambrian rocks.

Some writers have maintained that the potassium content does diminish in younger rocks and have attributed this to a changing composition of ocean water (Conway, 1945). Exactly what the mechanism was for a higher potassium removal from early sea water cannot be deduced from the data alone, although at least in the rocks compared, the earlier sediments are clearly enriched in potassium compared to the later.

REFERENCES

Barth, T. F. W., 1959, Principles of classification and norm calculations of metamorphic rocks: Jour. Geology, v. 67, p. 135–152.

Clarke, F. W., 1924, The data of geochemistry (fifth edition): U.S. Geol. Survey Bull. 770, 841 p.

Conway, E. J., 1945, Mean losses of Na, Ca, etc. in one weathering cycle and potassium removal from the ocean: Am. Jour. Sci. v. 243, p. 583–605.

Departamento Nacional da Produção Mineral, 1959, Esbôço Geológico do Quadrilátero Ferrífero de Minas Gerais, Brasil (Outline of the Geology of the Quadrilátero Ferrífero, Minas Gerais, Brazil): Publicação Especial 1, p. 1–62 (Portuguese), p. 63–120 (English).

Halferdahl, L. B., 1961, Chloritoid: its composition, x-ray and optical properties, stability, and occurrence: Jour. Petrology v. 2, p. 49–135.

Herz, N., Hurley, P. M., Pinson, W. H., and Fairbairn, H. W., 1961, Age measurements from a part of the Brazilian Shield: Geol. Soc. America Bull., v. 72, p. 1111–1119.

Nanz, R. H. Jr., 1953, Chemical composition of Pre-Cambrian slates with notes on the geochemical evaluation of lutites: Jour. Geology, v. 61, p. 51–64.

Pettijohn, F. J., 1957, Sedimentary rocks: New York, Harper, 718 p.

Shaw, D. M., 1956, Geochemistry of pelitic rocks, Part 3—Major elements and general geochemistry: Geol. Soc. America Bull., v. 67, p. 919–934.

Vinogradov, A. P., and Ronov, A. B., 1956, Evolution of the chemical composition of clays of the Russian Platform: Geochemistry (Geokhimiya), no. 2, p. 123–139.

GEOCHRONOLOGY

87. AGE OF LARIMIDE PORPHYRIES NEAR LEADVILLE, COLORADO

By Robert C. Pearson, Ogden Tweto; Thomas W. Stern, and Herman H. Thomas: Denver, Colo.; Washington, D.C.

In the Leadville area, Colorado, the Laramide orogeny began with homoclinal tilting of sedimentary strata on the eastern flank of a great anticline now marked by the Sawatch Range to the west (fig. 87.1). Some faults formed during the stage of tilting and accompanying uplift, but most of the numerous faults of the area formed later, during a stage characterized by intrusion of porphyries and by uplift of the fault block Mosquito Range to the east. Of some 30 varieties of porphyries intruded during this stage, about 15 fall into a well established sequence(Tweto, 1958; 1960). Many faults can be dated geologically by their relation to this porphyry sequence. Age determinations on selected porphyries therefore serve to date events in the stage of faulting that marks the structural climax of the Laramide orogeny in this area, and also to measure the duration of this climax.

Exploratory age determinations were made on three of the porphyries and on a possible deep-seated equivalent of one of them, using K-Ar and lead-alpha techniques. The determinations were made on: (1) the Pando Porphyry, the oldest porphyry known in the region; (2) Johnson Gulch Porphyry, intermediate rock of the porphyry sequence; (3) Lincoln Porphyry, one of the youngest rocks of the sequence; and (4) granodiorite that is petrographically similar to, and tentatively correlated with, the Pando Porphyry. The Pando Porphyry (Tweto, 1951, p. 510) includes the rocks known as White and Mt. Zion Porphyries of the Leadville district and Mosquito Range (Emmons, Irving, and Loughlin, 1927, p. 43, 50; Behre, 1953, p. 42–45), and is the most widespread of all the porphyries. The Johnson Gulch Porphyry is restricted to the Leadville mining district, where it is the chief component of what has there been called the Gray Porphyry Group (Emmons, Irving, and Loughlin, 1927, p. 46–50). The Lincoln Porphyry occurs in many bodies in an area extending from Leadville northward and eastward about 20 miles. The granodiorite occurs principally in a small pluton intruded into the Precambrian rocks of the Sawatch Range near Missouri Creek, 14 miles northwest of Leadville. All four of the rocks tested are granodioritic to quartz monzonitic in composition, and all except the granodiorite in the Sawatch Range occur as sills, dikes, and small, partly concordant stocks. Except in a few small areas, the porphyries were deuterically altered throughout the region, and in many places they were further altered hydrothermally during the mineralization stage.

Results of the age determinations are given in the table below. The K-Ar determinations on biotite yielded values of about 70 m.y. (million years) for both the granodiorite and the Pando Porphyry, and about 64 m.y. for the Lincoln Porphyry. Of two samples of the freshest Johnson Gulch Porphyry obtainable, the biotite in one was too altered for analysis and the other yielded an age figure of 41 m.y. As the Johnson Gulch Porphyry is known geologically to be Laramide and intermediate in age between the Pando and Lincoln Porphyries, this unexpectedly low figure is not regarded as an indication of the real age.

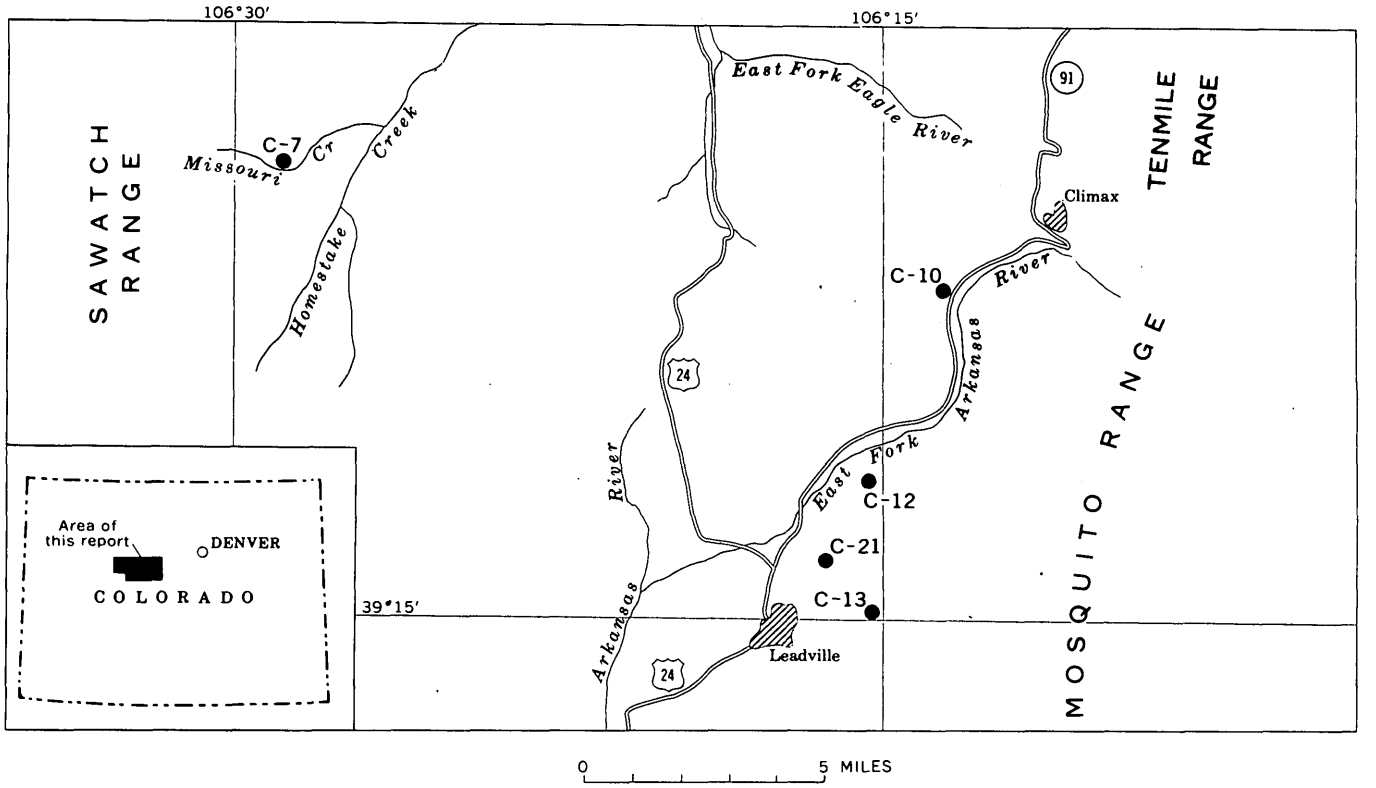

FIGURE 87.1.—Index map of Leadville area, Colorado, showing sampled localities and numbers of the samples used for age determinations.

Assuming the figure to be analytically correct, it probably reflects a stage of heating, during which argon was liberated from biotite. Such heating may have occurred locally during a younger stage of intrusion, when agglomeratic rhyolite pipes and dikes were formed (Emmons, Irving, and Loughlin, 1927, p. 55), or during one of the two or more stages of mineralization. As the Johnson Gulch Porphyry is

Potassium-argon and lead-alpha ages and analytical data on rocks of Laramide age, Leadville area, *Colorado*

Sample No.	Rock type or name	Potassium-argon data on biotite					Lead-alpha data on zircon		
		K_2O (percent)[1]	K^{40} (ppm)	Ar^{40} (ppm)	Ar^{40}/K^{40}	Calculated age (millions of years)[2]	Alpha counts per milligram per hour	Pb (ppm)[3]	Calculated age (millions of years)[4]
C-7	Granodiorite	8.11	8.13	0.0339 [5] (.0336)	0.00417 [5] (.00413)	70 [5] (69)	----------	----------	----------
C-10	Lincoln Porphyry	8.92	8.94	.0344	.00385	64	108	24	530±60
C-12	Pando Porphyry	7.84	7.86	.0328	.00417	70	----------	----------	----------
C-13	Johnson Gulch Porphyry	----------	----------	----------	----------	----------	371	19.7	130±20
C-21	Johnson Gulch Porphyry	9.02	9.04	.0223	.00247	41	367	17.2	120±20

[1] Potassium determinations made with a Perkin-Elmer flame photometer with Li internal standard by P. L. D. Elmore and Ivan Barlow, U.S. Geological Survey.

[2] Constants: $\lambda_\epsilon = 0.589\times10^{-10}$/yr, $\lambda_\beta = 4.76\times10^{-10}$/yr, $K^{40} = 1.21\times10^{-4}$ gm per gm K.

[3] Lead determinations by Charles Annell and Harold Westley, U.S. Geological Survey. All values are averages of duplicate determinations.

[4] Lead-alpha ages (rounded to nearest 10 million years) were calculated from the equation:

(1) $t = \frac{C\,Pb}{\alpha}$, where t is the calculated age in millions of years, C is a constant based upon the U/Th ratio and has a value of 2,485, Pb is the lead content in parts per million, and α is the alpha counts per milligram per hour; and

(2) For age in the range 200–1,700 m.y. an additional equation is used: $T = t - 1/2\ Kt^2$ where T is the age in millions of years corrected for decay of uranium and thorium, and K is the decay constant based upon the U/Th ratio and has a value of 1.56×10^{-4}.

The U/Th ratio was assumed to be 1.0. The error quoted is due only to uncertainties in analytical techniques.

[5] Based on a replicate argon determination.

C-7. Granodiorite from first switchback on Missouri Creek trail above junction of Missouri Creek and Sopris Creek, alt. 10,340 ft., Holy Cross quadrangle.

C-10. Lincoln Porphyry from large erratics of local origin under powerline on west side of Leadville-Climax highway (State route 91) at second gulch south of Chalk Creek, Mt. Lincoln quadrangle.

C-12. Pando Porphyry from cut on old railroad grade at base of northwest slope of Prospect Mountain; approximately 1,600 ft. N. 15° E. of BM 10,415 on modern railroad grade, Holy Cross quadrangle.

C-13. Johnson Gulch Porphyry from dump of Fairmount shaft, east of mouth of Johnson Gulch, Leadville district, Holy Cross quadrangle.

C-21. Johnson Gulch Porphyry from dump of Price shaft on north side of Evans Gulch north of East Fryer Hill. Leadville district, Holy Cross quadrangle.

almost entirely restricted to the intensely mineralized Leadville mining district, it is everywhere highly altered and is nowhere far distant from agglomeratic rhyolite.

Ages determined on zircon by the lead-alpha method are much greater than those determined by the K-Ar method and are widely disparate. Tentatively, they are assumed to reflect the presence in the porphyries of zircon derived from Precambrian rocks. Such zircon may exist as small xenocrysts caught up in the porphyry magmas (fragments of Precambrian rocks are abundant in some porphyry bodies), or it may represent a refractory residue in porphyry magma formed by melting of Precambrian rocks. Similarly disparate and generally high lead-alpha age values were obtained by Jaffe and others (1959, p. 72) for the porphyritic intrusive rocks of the La Sal Mountains, Utah. The magma from which these rocks crystallized was judged on geologic evidence by Waters and Hunt (Hunt, 1958, p. 348–354) to have formed by melting of Precambrian rocks.

Although there can be no assurance that the K-Ar ages of 64 and 70 m.y. for the Lincoln and Pando Porphyries are unequivocally correct, they are of the right relation to each other to fit the geologic evidence, and they fall within the age range of the Laramide as currently accepted (Holmes, 1959). Moreover, they are of the same order as ages of other Laramide intrusive bodies and ores in the Front Range part of the Colorado mineral belt. These include the Audubon stock, 66.3±1.1 m.y.; the Caribou stock, about 68 m.y. (Hart, 1960, p. 141, 147); and pitchblende from the post-porphyry veins. Various determinations give an age of 59±5 m.y. for the pitchblende of Central City and Larimer County (Eckelmann and Kulp, 1957, p. 1128), but a more nearly concordant age of 73±5 m.y. was obtained recently by the lead-uranium method from pitchblende from the Mena mine, Jefferson County, Colorado (D. M. Sheridan, oral communication, 1962).

If the 64- and 70-m.y. ages of the Lincoln and Pando Porphyries are tentatively accepted, they suggest that most of the faulting and intrusion that marked the climax of the Laramide orogeny in the Leadville area took place in the relatively brief span of roughly 6 m.y. This span of time represents only some unevaluated fraction of the total time occupied by the Laramide orogeny in this area. Uplift, the development of regional folds, and much erosion occurred before the stage of faulting and intrusion; mineralization and waning fault movement continued after. If correct, the figures here reported would place the climax of Laramide faulting and intrusion in early Paleocene time according to the most recent time scale of Holmes (1959), and in late Cretaceous time according to the time scale of Kulp (1961). Pebbles of porphyries occur in sedimentary rocks along the flanks of the Colorado mountains, principally in strata of Paleocene and Eocene age, but excepting one variety studied by Lovering and Goddard (1938) and by Wahlstrom (1940, p. 1817, 1818), not enough work has yet been done on these pebbles, nor on volcanic debris at somewhat lower stratigraphic levels, to correlate them with specific porphyries of the mountains.

REFERENCES

Behre, C. H., Jr., 1953, Geology and ore deposits of the west slope of the Mosquito Range: U.S. Geol. Survey Prof. Paper 235, 176 p.

Eckelmann, W. R., and Kulp, J. L., 1957, Uranium-lead method of age determination: Geol. Soc. America Bull., v. 68, p. 1117–1140.

Emmons, S. F., Irving, J. D., and Loughlin, G. F., 1927, Geology and ore deposits of the Leadville mining district, Colorado: U.S. Geol. Survey Prof. Paper 148, 368 p.

Hart, S. R., 1960, A study of mineral ages in a contact metamorphic zone, *in* Variation in isotopic abundances of strontium, calcium, and argon and related topics: Mass. Inst. Tech., Eighth Annual Progress Report for 1960, U.S. Atomic Energy Commission, NYO–3941, p. 131–154.

Holmes, Arthur, 1959, A revised geological time-scale: Edinburgh Geol. Soc. Trans., v. 17, pt. 3, p. 183–216.

Hunt, C. B., 1958, Structural and igneous geology of the La Sal Mountains, Utah: U.S. Geol. Survey Prof. Paper 294–I, p. 305–364.

Jaffe, H. W., Gottfried, David, Waring, C. L., and Worthing, H. W., 1959, Lead-alpha age determinations of accessory minerals of igneous rocks (1953–1957): U.S. Geol. Survey Bull. 1097–B, p. 65–148.

Kulp, J. L., 1961, Geologic time scale: Science, v. 133, p. 1105–1114.

Lovering, T. S., and Goddard, E. N., 1938, Laramide igneous sequence and differentiation in the Front Range, Colorado: Geol. Soc. America Bull., v. 49, p. 35–68.

Tweto, Ogden, 1951, Form and structure of sills near Pando, Colorado: Geol. Soc. America Bull., v. 62, p. 507–532.

——— 1958, Time relations of intrusion, faulting, and mineralization at Leadville, Colorado [abs.]: Geol. Soc. America Bull., v. 69, no. 12, pt. 2, p. 1656.

——— 1960, Pre-ore age of faults at Leadville, Colorado: Art. 5 *in* U.S. Geol. Survey Prof. Paper 400–B, p. B10–B11.

Wahlstrom, E. E., 1940, Audubon-Albion stock, Boulder County, Colorado: Geol. Soc. America Bull., v. 51, no. 12, pt. 1, p. 1789–1820.

88. LEAD-ALPHA AGES OF ZIRCON FROM NORTH AND SOUTH CAROLINA

By W. C. Overstreet; Thomas W. Stern, Charles Annell, and Harold Westley: Beltsville, Md.; Washington, D.C.

Lead-alpha ages were determined for zircon from North and South Carolina localities that have been previously dated by the lead-alpha method (Overstreet and others, 1961). Close agreement exists between the new determinations and those previously published.

Three new samples were collected to test the reproducibility of such dates. Some uncertainty always exists in the reliance that can be placed on a single sample collected from a geologic unit, and on the effect of changes in laboratory personnel and procedures. The new zircon samples described here were collected by different people from different parts of the dikes previously sampled, and in part they were processed in the laboratory by different personnel. Thus both sources of uncertainty are included in this test, and their combined effect is measured in the result.

Data on the new samples of zircon crystals and the lead-alpha ages determined for them are given in the table.

Analyses of the new specimens show greater alpha activity and more lead than was found for the original samples, but the newly determined lead-alpha ages have the same range in value as the original determinations. Apparently the zircon varies in composition in different places in the same geologic unit, but the variation makes little difference in the age. The new analyses support a previous conclusion (Overstreet and others, 1961, p. B105) that lead-alpha ages of minerals from the youngest plutonic rocks in the Piedmont are consistent with each other and with field data.

Description and lead-alpha ages of zircon crystals from rocks in North and South Carolina

	1	2	3	4	5
	Zirconia, Henderson County, N.C.		Tigerville, Greenville County, S.C.		
	1961 report [1]	This report	1961 report [1]	This report	
Alpha counts [2] per milligram per hour	439	756	269	430	443
Average lead content from duplicate determinations [3] parts per million	51	95	28	47	46.5
Calculated age [4] millions of years	280±30	300±45	255±30	270±30	260±30

[1] Overstreet and others (1961).
[2] Alpha-activity measurements, this report, by T. W. Stern.
[3] Spectrographic analyses of lead, this report, by Charles Annell and Harold Westley.
[4] Lead-alpha ages(rounded to nearest 10 million years, this report, and nearest 5 million years, 1961 report) were calculated from the equations:
(1) $t=C\ Pb/\alpha$, where t is the calculated age in millions of years, C is a constant based upon the U/Th ratio and has a value of 2485, Pb is the lead content in parts per million, and α is the alpha count per milligram per hour; and
(2) $T=t-1/2kt^2$ where T is the age in millions of years corrected for decay of uranium and thorium, and k is a decay constant based upon the U/Th ratio and has a value of 1.56×10^{-4}. U/Th ratio assumed 1.0.
1. USNM 80114. See Overstreet and others (1961) for description.
2. Sample 60-0T-1000. Large zircon crystals collected by J. W. Whitlow from syenite pegmatite at Jones mine. Locality 2 on fig. 45.1 of Overstreet and others (1961); same source as sample USNM 80114.
3. USNM 105674. See Overstreet and others (1961) for description.
4. Sample 60-0T-1001. Large zircon crystals collected by J. W. Whitlow from vermiculite quarry near Tigerville. Locality 1 on fig. 45.1 of Overstreet and others (1961); same source as USNM 105674.
5. Sample 60-0T-1002. Large zircon crystals collected by H. S. Johnson, Jr., from same locality as sample 60-0T-1001.

REFERENCE

Overstreet, W. C., and others, 1961, Recent lead-alpha age determinations on zircon from the Carolina Piedmont: Art. 45 *in* U.S. Geol. Survey Prof. Paper 424-B, p. B103-B107.

PALEONTOLOGY

89. A MIOCENE POLLEN SEQUENCE FROM THE CASCADE RANGE OF NORTHERN OREGON

By Jack A. Wolfe, Washington, D.C.

A succession of volcanic rocks including the entire Miocene Series crops out in an area of about 1,000 square miles in the Clackamas, Molalla, and Sandy River basins of northern Oregon. Beds at several localities within this succession contain abundant pollen and spores associated with well-preserved leaves (fig. 89.1). With the assistance of D. L. Peck in determining field relations of the rock units, the rela-

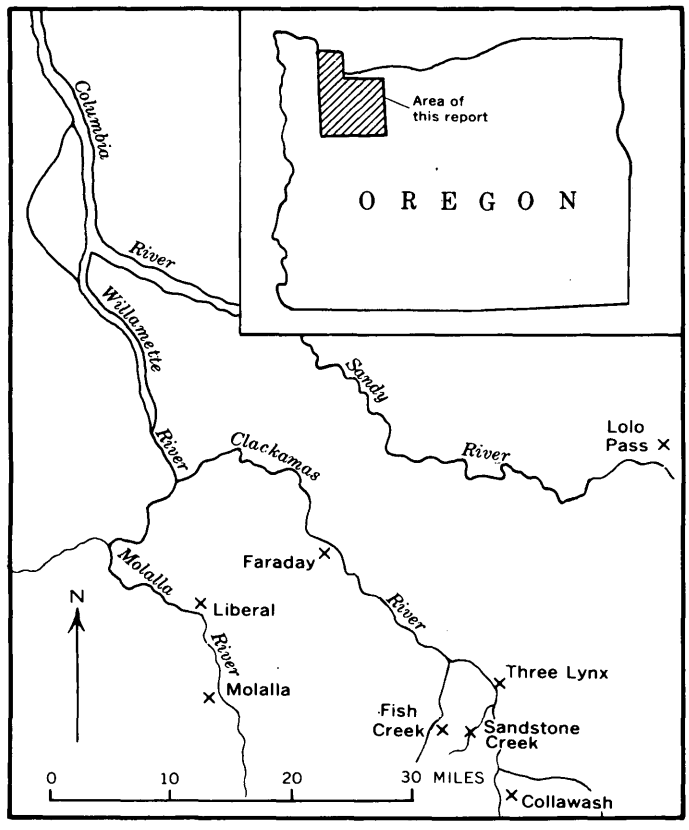

FIGURE 89.1.—Sketch map of part of northwest Oregon showing plant localities (×) of Miocene age.

tive stratigraphic positions of most of the plant localities have been established (Peck, 1961). Plant fossils are lacking in one major part of the section in the Clackamas, Molalla, and Sandy basins; however, rocks equivalent to this interval contain fossil plants to the south in the Santiam and McKenzie basins. Consequently a series of floras ranging in age from early to late Miocene is represented.

Study of both plant microfossils and megafossils from this stratigraphic sequence has furnished a more complete concept of floral composition and alteration in the region during the Miocene than could be obtained from either type of fossil alone. Six floral zones have been recognized within this sequence of rocks. Miocene floras from certain localities elsewhere in Oregon and Washington can be placed in these floral zones (table 89.1). Leaf floras from the Columbia Plateau equivalent to zones 4, 5, and 6 have been discussed by Chaney (1959); microfossils associated with these leaves were listed generically by Gray (*in* Chaney, 1959).

The present preliminary report is based on a completed study of the megafossils by the author, the results of which will be published soon, and on a nearly completed study of the microfossils begun in 1953. The completeness of this Cascade Miocene sequence and the abundance of pollen have since attracted other palynologists to investigate this area (Jane Gray, written communication, 1960). Certain data from my studies were included in a previous paper on generic change in western Tertiary floras (Wolfe and Barghoorn, 1960).

Significance of the plant microfossils in the Cascade Miocene sequence has three major aspects: corroboration of genera determined from foliage and seeds, recognition of genera and families not represented as megafossils, and elucidation of proportional changes in the flora as represented by regional pollen rain during the Miocene Epoch.

Identified pollen and spores are listed in table 89.2; those forms marked with an asterisk are also represented as megafossils. Correspondence between the plant megafossils and microfossils is great, although a number of genera are known from only one type of fossil. Taxa represented only by palynomorphs are primarily those of presumed herbaceous habit: *Galium*-type (fig. 89.2, *s*, *t*), *Valeriana* (fig. 89.2, *u*), Chenopodiaceae-type, Compositae (fig. 89.2, *o-r*,), Malvaceae (fig. 89.2, *g*, *h*). Of special interest in the Collawash flora (zone 2) is pollen representing *Securidaca* (fig. 89.2, *e*), *Xanthophyllum* (fig. 89.2, f), and *Xylonagra* (fig. 89.2, *v*); these genera are woody members of predominantly herbaceous families. There is a pronounced increase in percentage and taxonomic diversity of probable herbaceous pollen types during the Miocene Epoch.

EXPLANATION OF FIGURE 89.2

a. *Schoepfia*-type. Loc. D1736 (Collawash), slide 75.
b, c. *Caesalpinia*. Loc. D1569 (Three Lynx), slide 1.
d. *Pachysandra*. Loc. D1736 (Collawash), slide 57.
e. *Securidaca*. Loc. D1736 (Collawash), slide 46.
f. *Xanthophyllum*. Loc. D1736 (Collawash), slide 68.
g, h. Malvaceae, gen. indet. Loc. 1528–2 (Faraday), slides 1, 2.
i–m. *Lagerstroemia*-type. Loc. D1526 (Molalla), slide 3.
n. *Liquidambar*. Loc. D1526 (Molalla), slide 3.
o, p. Astereae, gen. indet. Loc. D1736 (Collawash), slide 62.
q, r. Cichoreae, gen. indet. Loc. D1528–18 (Faraday), slide 18.
s, t. *Galium*-type. Loc. D1528–1 (Faraday), slide 1.
u. *Valeriana*. Loc. D1736 (Collawash), slide 56.
v. *Xylonagra*. Loc. D1736 (Collawash), slide 68.

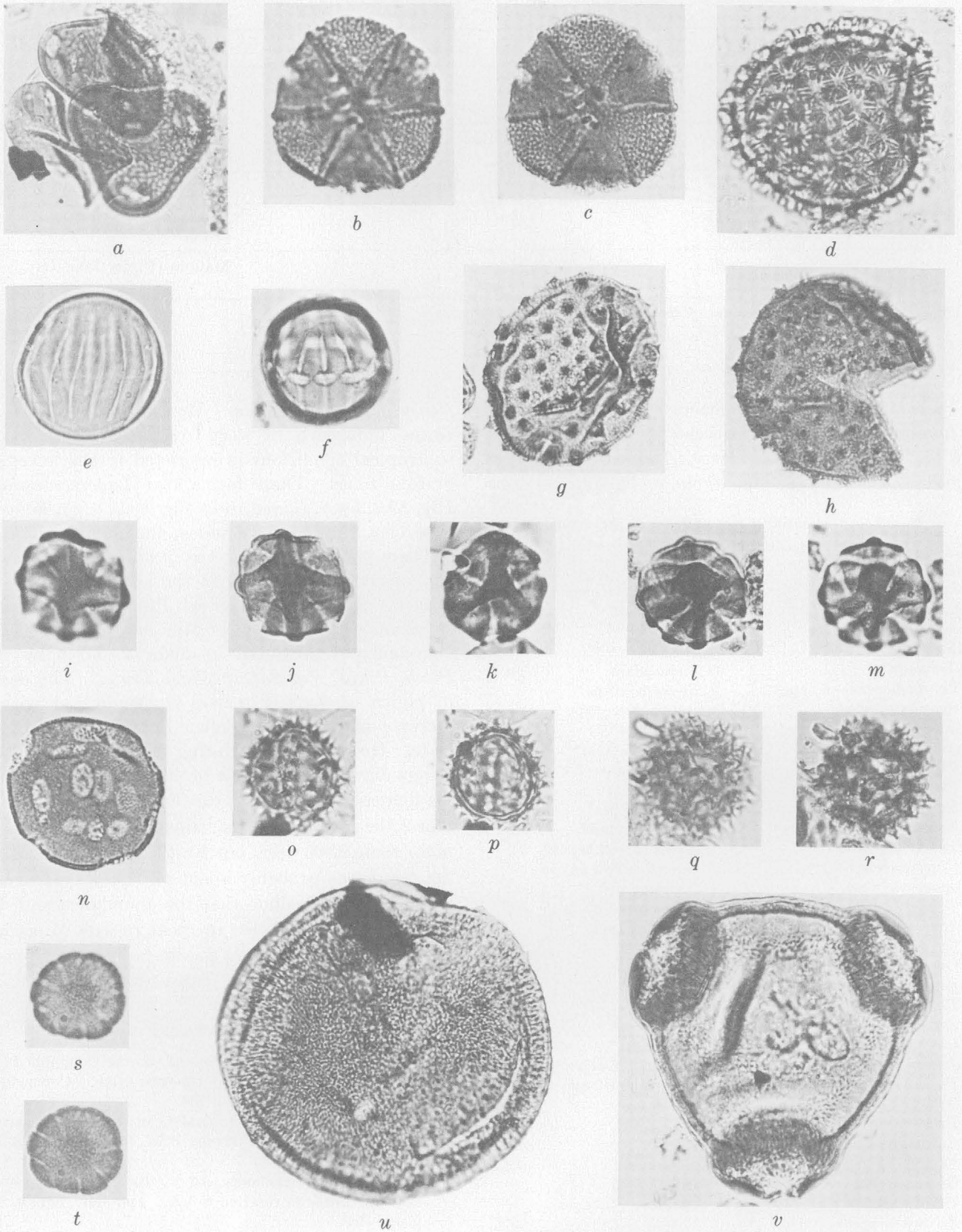

FIGURE 89.2—Miocene pollen from the Cascade Range of northern Oregon.

[All specimens × 600. Numbers are USGS paleobotanical locality and slide numbers]

TABLE 89.1—*Correlation of some Miocene floras*

	Floral zone	Clackamas, Sandy, and Molalla basins	Santiam and McKenzie basins	Columbia Plateau
Miocene Series	6	Faraday Lolo Pass		Stinking Water
	5		Hidden Lake	Blue Mountains Succor Creek
	4		Fern Ridge	Mascall
	3	Fish Creek		Monument Latah
	2	Collawash Molalla		Maupin (Upper John Day)
	1	Sandstone Creek Three Lynx Liberal	Cascadia	

Pollen of a number of genera is found uniformly throughout the Cascade Miocene section. These genera include: *Carya*, *Pterocarya*, *Alnus*, *Betula*, *Fagus*, *Quercus*, *Ulmus*-type, *Liquidambar* (fig. 89.2, *n*), *Ilex*, *Nyssa*, and *Symplocos*. However, pollen of some forms indicative of very warm-temperate or even subtropical conditions is restricted to the lower three or four zones. These forms are: *Lagerstroemia*-type (fig. 89.2, *i-m*), *Caesalpinia* (fig. 89.2, *b*, *c*), *Schoepfia*-type (fig. 89.2, *a*), *Securidaca*, and *Xanthophyllum*.

There is a notable increase in abundance and diversity of coniferous pollen in the upper part of the sequence. Although pollen of Pinaceae is present in small amounts in the lower Miocene beds, Pinaceae are abundantly represented in zones 5 and 6 by *Abies*, *Picea*, *Pinus*, *Pseudotsuga*, and *Tsuga*. The decrease in pollen of warmer genera concommitant with this increase in coniferous pollen indicates a cooling climate. However, the elevating of the western Cascade Range during the Miocene probably also contributed to the increasing coniferous element. During the time of zone 2, the relief in the Clackamas basin was probably no more than 2,000 feet, but by the end of the Miocene the relief was probably about 4,000 feet. Hence, it is reasonable to conclude that the abundance and diversity of pinaceous pollen in rocks of late Miocene age in northern Oregon were due to both regional cooling and uplift of the western Cascade Range.

TABLE 89.2—*Partial list of pollen and spore types*

[Taxa marked by an asterisk are also found as megafossils]

Lycopodiales
Lycopodium
Selaginellales
Selaginella
Filicales
*Osmunda**
Polypodiaceae—6 types
Sporites arcifer
Coniferales
Abies—2 types*
*Picea**
Pinus—2 types*
Pseudotsuga
*Tsuga**
Taxodiaceae*
Cupressaceae*
Monocotyledones
*Typha**
*Sparganium**
Cyperaceae*
Gramineae
Dicotyledones
*Populus**
*Salix**
Carya—2 types*
Juglans—2 types*
*Pterocarya**
Alnus—2 types*
*Betula**
Castanea—type*
**Fagus*—2 types
Quercus—2 types*
Ulmus—type*
Zelkova—type*
Schoepfia—type
Chenopodiaceae—type
*Liquidambar**
*Platanus**
*Prunus**
Caesalpinia
Sophora—type*
Astragalus—type
*Securidaca**
*Xanthophyllum**
Pachysandra—2 types*
Celastraceae
Ilex—2 types*
Acer—2 types*
Rhamnus—2 types*
Lagerstroemia—type
Xylonagra
Onagraceae
Galium—type
Malvaceae
*Tilia**
*Nyssa**
*Cornus**
*Symplocos**
*Halesia**
Ericales—2 types*
Viburnum—2 types*
*Fraxinus**
Cornutia
**Vitis*
Valeriana
Chichoreae
Astereae—3 types

REFERENCES

Chaney, R. W., 1959, Miocene floras from the Columbia Plateau, Part I: Composition and interpretation: Carnegie Inst. Washington Pub. 617, p. 1–134.

Peck, D. L., 1961, Cenozoic volcanism in the Oregon Cascades: Art. 144 *in* U.S. Geol. Survey Prof. Paper 400–B, p. B308–B310.

Wolfe, J. A., and Barghoorn, E. S., 1960, Generic change in Tertiary floras in relation to age: Am. Jour. Sci., v. 258–A, p. 388–399.

90. *CLIOSCAPHITES SAXITONIANUS* (McLEARN), A DISCRETE AMMONITE ZONE IN THE NIOBRARA FORMATION AT PUEBLO, COLORADO

By GLENN R. SCOTT and WILLIAM A. COBBAN, Denver, Colo.

The Late Cretaceous scaphite, *Clioscaphites saxitonianus* (McLearn), can be regarded now as a guide fossil for a distinct range zone immediately underlying that of *Clioscaphites vermiformis* (Meek and Hayden) and overlying that of *Scaphites depressus* Reeside at Pueblo, Colo. This relationship was discovered by Scott from fieldwork on the Niobrara Formation during the summer of 1961.

Clioscaphites saxitonianus (McLearn, 1929, p. 77, pl. 18, figs. 1–3; pl. 19, figs. 1, 2) is a tightly coiled cephalopod recorded in the United States from only three localities (Cobban, 1951, p. 37). At these localities the stratigraphic position of *C. saxitonianus* in regard to other ammonite occurrences was not known, but from its moderately large size, dorsum of adult body chamber entirely in contact with the last septate whorl, and suture pattern with trifid lobes, *C. saxitonianus* was believed to lie at the level of *C. vermiformis* (Meek and Hayden) (Cobban, 1951, fig. 1).

Clioscaphites saxitonianus was found by Scott at eight localities near Pueblo in the Niobrara Formation. Here the Niobrara Formation is about 745 feet thick and can be divided into 2 members, the 40-foot-thick Fort Hays Limestone Member at the base and the overlying Smoky Hill Shale Member. The specimens occur undistorted in limestone concretions and as flattened impressions in calcareous shale of the Smoky Hill. The stratigraphic position of the fossils can be determined best along Dry Creek in the NE¼SW¼ sec. 10, T. 20 S., R. 65 W., just north of Pueblo. The Smoky Hill contains, slightly above the middle, a yellowish-gray thin-bedded ledge-forming chalky limestone 28 feet thick underlain by a 280-foot unit of sandy and silty calcareous shale. The bottom of this shale unit lies about 115 feet above the base of the Smoky Hill. *Scaphites depressus* var. *stantoni* Reeside and *S. binneyi* Reeside were found in the lower 30 feet of the shale unit. *Clioscaphites saxitonianus* was found from 30 feet above the base of the shale unit to 31 feet below the top for a total range of nearly 220 feet. *Clioscaphites vermiformis* was found 20 feet below the top of the shale unit.

REFERENCES

Cobban, W. A., 1951, Scaphitoid cephalopods of the Colorado Group: U.S. Geol. Survey Prof. Paper 239, p. 1–42 [1952].

McLearn, F. L., 1929, Cretaceous invertebrates, *in* Mesozoic paleontology of Blairmore region, Alberta: Canada Nat. Mus. Bull. 58, p. 73–79.

SEDIMENTATION

91. ROLL IN A SANDSTONE LENTIL OF THE GREEN RIVER FORMATION

By JOHN R. RAPP, Green River, Wyo.

A sandstone lentil in the Laney Shale Member of the Green River Formation exhibits a variety of depositional and postdepositional structural features. The formal designation Tower Sandstone Lentil as applied to this sandstone was recently abandoned by W. C. Culbertson (Art. 78). The sandstone usually is massive to highly cross bedded and may be highly contorted. Local channeling and rapid lensing within beds of oil shale are common features. The sandstone is best exposed along the inner valley of the Green River near the town of Green River, Wyo., where it caps the vertical to steep valley walls and the erosional outliers, the "Towers."

The effect of differential compaction on the oil shale of the Green River Formation has been discussed by Bradley (1931). It is suggested herein that contortions in at least some of the beds of the sandstone lentil can also be attributed to differential compaction.

The sandstone lentil consists of a group of lenticular sandstones in a sequence of beds of oil shale. The relative position of two bodies of sandstone within

beds of oil shale can be seen in figure 91.1. The difference in stratigraphic position of the two adjacent sandstones (Ss–1, the lower, and Ss–2, the upper) is marked by the intervening bed of rich oil shale (OS–r). On the left side of the photograph this oil shale merges with the main bed of rich oil shale, which appears to split over and under Ss–1. This apparent split is interpreted to be the result of compaction of the oil shale and resultant settling of the sandstone. Note also that the rich oil shale (OS–r) is missing under the main part of the roll and that it reappears as a distorted mass under the massive part of Ss–1 on the right side of the photograph. The bed is continuous both to the right and left of the photograph. The underlying, leaner oil shale (OS–l), which is more compact and tougher than OS–r, shows very little distortion or thinning. The rolled form of the sandstone is well displayed in the left center of the photograph.

The following discussion of the origin of the roll is based on the relation of the exhibited features to the adjustment of sediments in response to differential compaction. Depositional environment, therefore, is

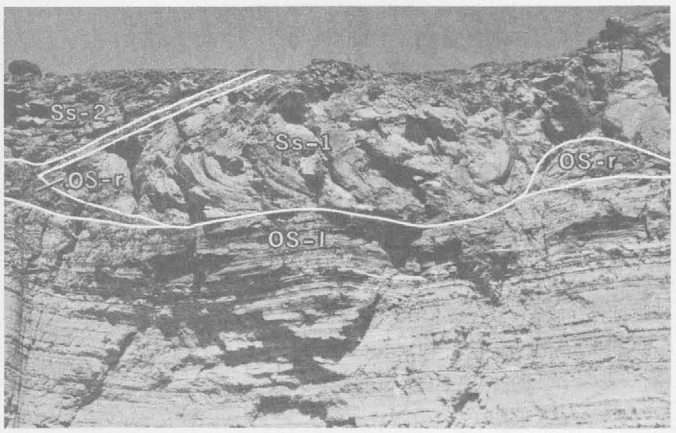

FIGURE 91.1.—Photograph showing a roll in the sandstone lentil about 1½ miles northwest of Green River, Wyo. Ss–1 and –2, sandstone; OS–r, rich oil shale; OS–l, lean oil shale.

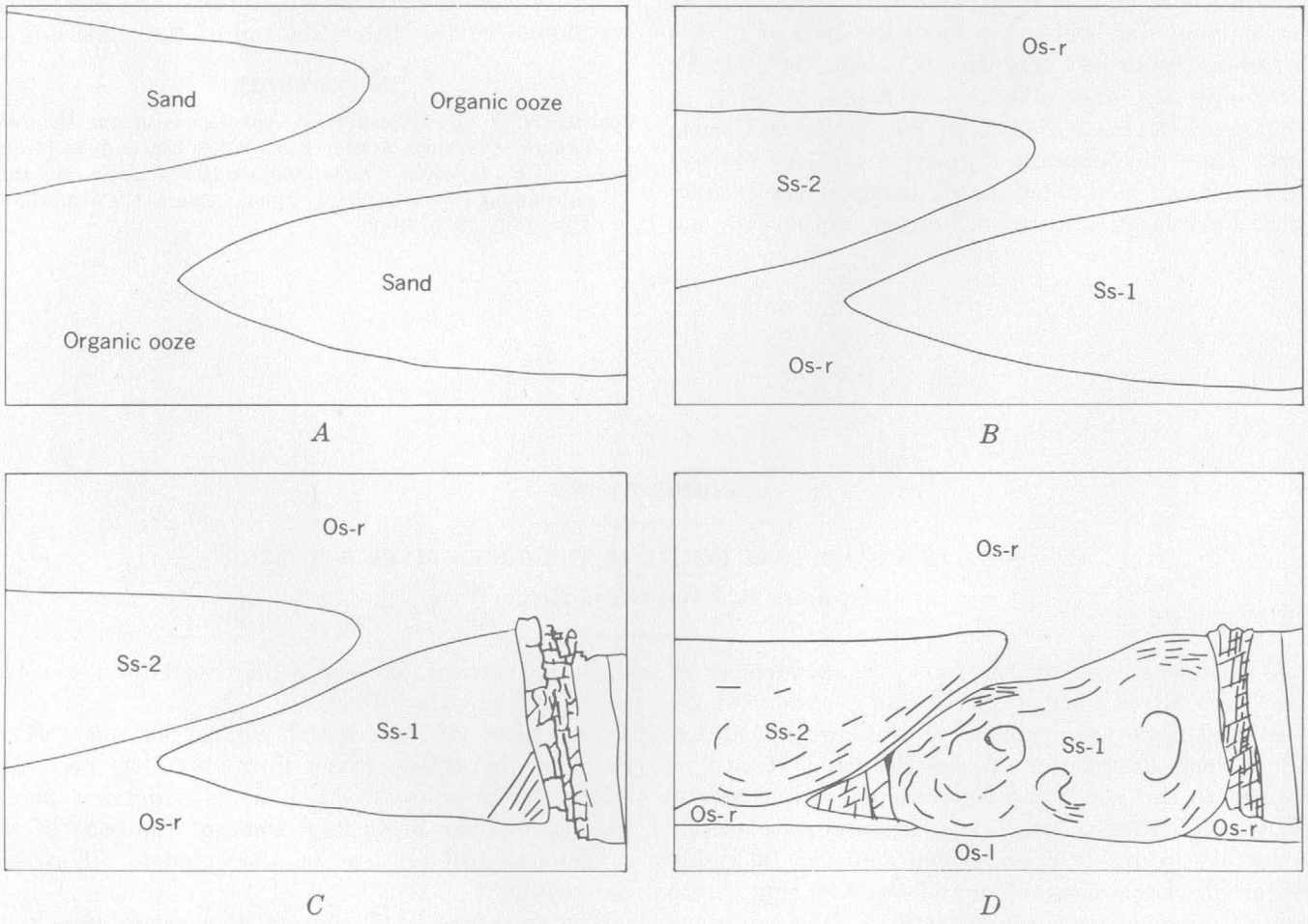

FIGURE 91.2.—Evolution of a roll in the sandstone lentil: *A*, sand bodies in organic ooze; *B*, initial stage in compaction of sediments; *C*, rupturing and rotation of sandstone; *D*, structure after final adjustment of sediments and prior to denudation.

a primary consideration. At the beginning of Laney time an accumulation of organic ooze began within the Eocene lake Gosiute, which was reverting from a saline to a fresh-water lake. During this interval, when the lake level was fluctuating rapidly, lake and stream currents scoured channels that subsequently were filled with sand and volcanic ash. As newer sediments accumulated, the earlier sediments were compressed. The beds of sand probably were somewhat distorted by gravity flowage and by relief of hydraulic pressure through rupturing of confining beds or materials. However, on the basis of the features shown on figure 91.1, it is believed that the major cause of the deformation was differential compaction. It also is possible that some of the conspicuous fold in the left end of Ss–1 was caused by slumping of the plastic sand body, the movement being downward and to the left.

The mechanics involved in the development of the roll pictured on figure 91.1 are shown by stages in figure 91.2. In figure 91.2*A*, sand lenses lie within a body of organic ooze. As newer sediments accumulated, compaction of the older sediments began (fig. 91.2*B*). The body of sand was compacted only a small amount because it was only slightly compressible, whereas the organic ooze was compacted greatly owing to its high initial porosity and great compressibility. According to Bradley (1929, p. 97), organic ooze compacts into oil shale having a thickness one-tenth or less of the original thickness under a load of 1,000 to 2,000 feet of rocks. Thus, for illustration, a 20-foot bed of ooze would be reduced to a 2-foot bed of oil shale, but the thickness of a bed of sandstone would not differ appreciably from that of the sand as deposited. As shown in figure 91.2*C*, the wing of the sandstone body (Ss–1) could have broken off as a result of unequal, downward stresses exerted both by the lowering of the body and by the loading effects of Ss–2. As Ss–2 continued to lower in response to compaction, the settling was unequal. That part of Ss–2 overlying Ss–1 was supported, but the main part of the body, underlain entirely by oil shale, settled more. As the body tilted it began to slide off Ss–1. The resultant forces were sufficient to cause the broken section of Ss–1 to rotate. Aiding this rotation were the lubricated surfaces of the enclosing oil shale and, to some extent, the bedding planes and the seams and inclusions of oil shale within the sandstone body. As rotation continued, the underlying OS–r was dragged along and piled behind the rotating sandstone and against the "stable" main part of Ss–1 (fig. 91.2*D*).

At least some of the contorted beds of sandstone in the sandstone lentil may therefore be attributed to differential compaction of sediments. As the oil shales compacted, the lenticular beds of sandstone settled unevenly. The resulting forces accounted for the breaking off and rotation of sections of sandstone. During these processes the sandstone must have been sufficiently consolidated to retain the bedding planes and general original structure, yet plastic enough to bend considerably without completely shattering.

REFERENCES

Bradley, W. H., 1929, The varves and climate of the Green River Epoch: U.S. Geol. Survey Prof. Paper 158–E, 110 p., 4 pls.

——— 1931, Origin and microfossils of the oil shale of the Green River Formation of Colorado and Utah: U.S. Geol. Survey Prof. Paper 168, 56 p., 28 pls.

GEOMORPHOLOGY

92. THE CAROLINA BAYS AND EMERGENCE OF THE COASTAL PLAIN OF THE CAROLINAS AND GEORGIA

By Eugene C. Robertson, Silver Spring, Md.

The origin of the Carolina Bays, the thousands of oval depressions extending across the Atlantic Coastal Plain from Virginia to Florida, has been a subject of much controversy. Discussions of previous studies and hypotheses are given in Prouty (1952), Schriever (1951), and Johnson (1942). The segmented-lagoon hypothesis of Cooke (1934), which was discredited early (Melton, 1934), seems now to deserve renewed consideration in the light of recent studies by Zenkovich (1959) of existing lagoons and by Carson and Hussey (1960) and others of elliptical lakes.

Cooke's (1934) explanation for the segmentation of a lagoon differs from that of Zenkovich by requiring that wind-driven elliptical currents move and deposit

sediment at regular intervals across the lagoon, perpendicular to the lagoon shore, rather than along the shore. Zenkovich does not specifically apply his hypothesis for the development of shore embankment features to the origin of the Carolina Bays, but he does describe an applicable process in which cuspate spits form behind barrier bars: wind-driven waves cause long-shore currents which move the shore debris so as to form spits at fairly regular intervals that are determined by the wave fetch length, which in turn is determined by the width of the lagoon; this is shown diagrammatically in figure 92.1*A*. Half-moon bays are scoured from the shore as the spits are extended, and finally oval lakes are formed by joining of spits across the lagoon; a late stage in this process is shown in figure 92.1*B*.

The formation of the elliptical shape of the lakes presumably is part of the same littoral process, but final shaping of the lakes could also occur later. Preferred orientation of lakes in other localities has been described in detail by Black and Barksdale (1949), Livingstone (1954), Zenkovich (1959, p. 274–275), Carson and Hussey (1960), and Rex (1961). These authors describe how lakes with banks moderately susceptible to erosion are made elliptical if the prevailing winds are from one direction or from two opposing directions: long-shore currents remove and deposit sediment, smoothing irregularities of the shores and shaping the lakes; the final shape of the lakes is elliptical, with the short axis of the ellipse parallel to the direction of the dominant wind.

The conspicuous en echelon arrangement and northwest orientation (Cooke, 1954) of the Carolina Bays can thus be explained if a southwest or northeast wind prevailed during their late history. Odum (1952) reconstructed a mean atmospheric-pressure map for the Pleistocene epoch, and from it he deduced that a northwest wind prevailed then. However, his assumptions of the temperature distribution and the persistence of ice throughout the epoch are rather arbitrary, and the actual wind direction may have differed considerably from the inferred one, especially during interstadial and post-Wisconsin time when the ice was gone. As the orientation of the bays may be due to winds prevailing at some time after the segmentation of the lagoons, the wind direction is not critical to the argument that the bays originated as shoreline features.

Zenkovich (1959, pl. 1) observed present-day oval lakes and cuspate spits forming behind barrier beaches on Chukotsky Peninsula (fig 92.1*C*) Similar spits have been observed by Fisher (1955) on St. Lawrence Island, Alaska (fig. 92.1*D*). These modern spits and lakes are similar in shape to some of the Carolina Bays (fig 92.1*E*), and may be compared with the bays described by Cooke (1934), Melton (1934), Johnson (1942), and Prouty (1952); their similarity is evident in the alternating beach ridges, swales, and chains of lakes, and in the shape and size of the lakes and bays.

Cooke's original hypothesis does not explain the overlapping of the bays on each other and on beach ridges (Prouty, 1952, p. 198, pls. 8, 9). This overlapping, however, can be explained under a modified Cooke-Zenkovich hypothesis as interference resulting from the erosion of the old and the formation of new bars, spits, lagoons, and lakes in response to small changes in sea level and to changes in the groundwater table controlled by base level and sea level. A sequence of rising and falling of sea level coupled with warping of the land surface may be necessary to explain certain overlaps, but in the many examples that appear in available aerial photographs, a simple emergence of the land relative to the sea would seem capable of producing the observed configurations of features.

According to the studies in Maryland and Virginia by Hack (1955, p. 26–40) and of the whole Atlantic Coastal Plain by Flint (1940), it is difficult to identify erosion surfaces above an altitude of 100 feet, and more difficult to identify marine-cut terraces, but this does not mean that the bays were nonmarine; it merely means that the relation, if any, of the bays to adjacent geomorphic surfaces is not known.

The most plausible genesis of the bays seems therefore to be that they formed by segmentation of marine lagoons and are thus linked to the sea in origin. It follows that the succession of bays, beach ridges, and swales, extending about 150 miles inland from the present shore, represent landforms developed in chronologic sequence during stillstands of the sea in the Pleistocene and possibly earlier epochs. These features could be used as evidence of geologic events in the geomorphologic history of the coastal plain. Furthermore, if the sequence of deposits associated with the bays in the coastal plain of the Carolina's and Georgia can be dated, it will be possible to determine not only the Pleistocene chronology but also the rate of emergence of the land relative to sea level. The half-lives of carbon-14 and uranium-lead isotopes do not cover all the Pleistocene epoch, but chlorine-36 or ionium might be used, if reliable source materials can be found.

A palynological study by Frey (1953) offers the best data available so far on the history of the Carolina Bays during Wisconsin and Recent time. Using a peat borer and sediment sampler, he obtained cores

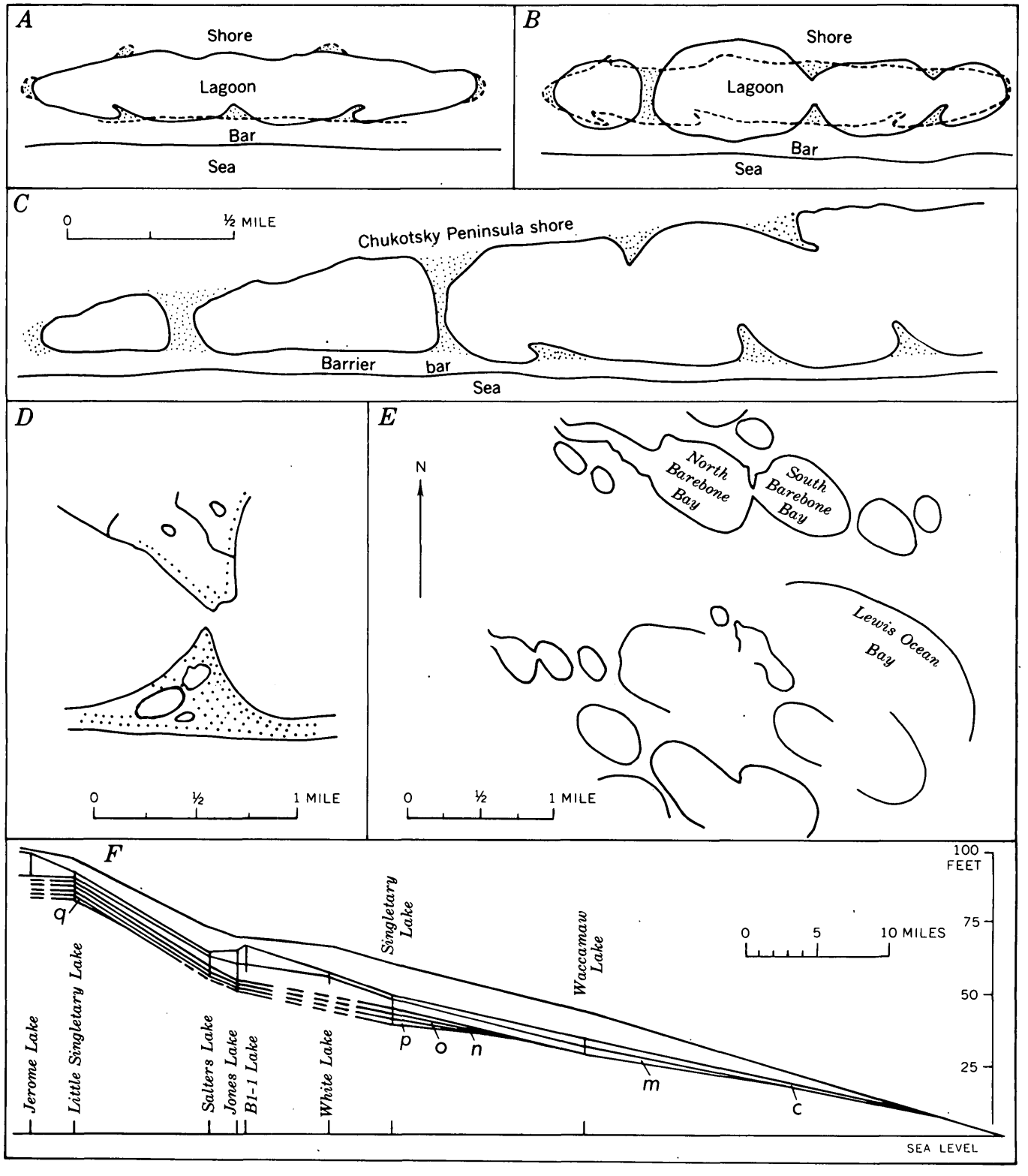

FIGURE 92.1.—Carolina Bays, segmented lagoons, and cuspate spits. *A*, Segmentation of a lagoon by cuspate spits, after Zenkovich (1959, fig. 2). *B*, Late stage in the evolution of a lagoon, after Zenkovich (1959, fig. 2). *C*, Lagoons in the Chukotsky Peninsula region, from an aerial photomosaic of Zenkovich (1959, pl. 1, A). *D*, Cuspate spits of St. Lawrence Island, Alaska, after Fisher (1955, fig. 3). *E*, Outlines of Carolina Bays near Myrtle Beach, S.C., from an aerial photomosaic of Johnson (1942, fig. 7). *F*, Correlation of late Quaternary deposits in eight North Carolina lakes on a N. 45° W. profile, from Frey (1953); see text for explanation of letters.

from eight water-filled bays in southeastern North Carolina. Frey divided the sediments into zones by making pollen counts; and by correlating pine-spruce, broadleaf, and grass maxima with similar vegetation fluctuations in North America and northern Europe, he assigned the zones to glacial and interglacial stages.

Frey (1955) obtained carbon-14 dates for three organic-silt layers in Singletary Lake and gave ages to the zones and the stages. Analyzing the data from Frey and various other sources, Karlstrom (1961, fig. 2, p. 298–299) tentatively assigned glacial events and ages to Frey's pollen zones as follows (fig. 92.1*F*): *q*, Illinoian glacial stage; *p*, 85,000 years old, Sangamon interglacial stage; *o*, Iowan glacial stage; *n*, 45,000 years old, Iowan-Wisconsin interglacial stage; *m*, Wisconsin glacial stage; and *c*, 10,000 years old (at the bottom of the zone), postglacial stage.

Profiles of the zones at the lakes (fig. 92.1*F*) show a pinching out of the pollen-correlated sedimentary layers, progressing southeast from Little Singletary Lake to Waccamaw Lake. As Frey's cores bottomed in sand containing little or no pollen, presumably the full record of limnological deposits was sampled, except in Jerome Lake, B1–1 Lake, and White Lake, which had incomplete cores because the lakes were dry for some period or were sampled inadequately (Frey, 1953, p. 294, 296, 299).

The implications of these data and interpretations are that the bays increase in age northwestward from the coast and that the coastal plain has been rising since Illinoian time. Using the ages listed and the present heights of the deposits, the rate of emergence of land would be 0.01 to 0.1 cm per yr. Basically, however, the evidence proves only that sea level was not successively higher than the bottom of the interglacial zones, *p* at 46 feet, *n* at 28 feet, and *c* at about sea level. Either eustasy or tectonism could reasonably account for these facts.

Additional pollen and geologic studies, especially for evidence of marine deposition in the sand below the pollen-bearing sediments, are needed to determine the geologic history of the Carolina Bays.

H. W. Coulter and T. N. V. Karlstrom were most helpful in clarifying unfamiliar concepts during preparation of this paper.

REFERENCES

Black, R. F., and Barksdale, W. L., 1949, Oriented lakes of northern Alaska: Jour. Geology, v. 57, p. 105–118.

Carson, C. E., and Hussey, K. M., 1960, Hydrodynamics in three Arctic lakes: Jour. Geology, v. 68, p. 585–600.

Cooke, C. W., 1934, Discussion of the origin of the supposed meteorite scars of South Carolina: Jour. Geology, v. 42, p. 88–96.

——— 1954, Carolina Bays and the shapes of eddies: U.S. Geol. Survey Prof. Paper 254–I, p. 195–207.

Fisher, R. L., 1955, Cuspate spits of St. Lawrence Island, Alaska: Jour. Geology, v. 63, p. 133–142.

Flint, R. F., 1940, Pleistocene features of the Atlantic Coastal Plain: Am. Jour. Sci., ser. 5, v. 238, p. 757–787.

Frey, D. G., 1953, Regional aspects of the late-glacial and postglacial pollen succession of southeastern North Carolina: Ecol. Monographs, v. 23, no. 3, p. 289–313.

——— 1955, A time revision of the Pleistocene pollen chronology of southeastern North Carolina: Ecology, v. 36, no. 4, p. 762–763.

Hack, J. T., 1955, Geology of the Brandywine area and origin of the upland of southern Maryland: U.S. Geol. Survey Prof. Paper 267–A, p. 1–44.

Johnson, D. W., 1942, The origin of the Carolina Bays: New York, Columbia Univ. Press, 341 p.

Karlstrom, T. N. V., 1961, The glacial history of Alaska—its bearing on paleoclimatic theory, *in* Fairbridge, R. W., ed., Solar variations, climatic change, and related geophysical problems: New York Acad. Sci. Annals, v. 95, Art. 1, p. 290–340.

Livingstone, D. A., 1954, On the orientation of lake basins: Am. Jour. Sci., v. 252, p. 547–554.

Melton, F. A., 1934, Reply to "Discussion of the origin of the supposed meteorite scars": Jour. Geology, v. 42, p. 97–104.

Odum, H. T., 1952, The Carolina Bays and a Pleistocene weather map: Am. Jour. Sci., v. 250, p. 263–270.

Prouty, W. F., 1952, Carolina Bays and their origin: Geol. Soc. America Bull., v. 63, p. 167–224.

Rex, R. W., 1961, Hydrodynamic analysis of circulation and orientation of lakes in northern Alaska, *in* Raasch, G. O., ed., Geology of the Arctic: Toronto, University Press, v. 2, p. 1021–1043.

Schriever, W., 1951, On the origin of the Carolina Bays: Am. Geophys. Union Trans., v. 32, p. 87–95.

Zenkovich, V. P., 1959, On the genesis of cuspate spits along lagoon shores: Jour. Geology, v. 67, no. 3, p. 269–277.

93. DEFLATED MARINE TERRACE AS A SOURCE OF DUNE CHAINS, ATACAMA PROVINCE, CHILE

By KENNETH SEGERSTROM, Santiago, Chile

Work done in cooperation with the Instituto de Investigaciones Geológicas, Santiago

Most of the coast of Chile is bordered by a mountain range, but this is low or absent for about 25 miles south of lat 27° S. In that area the Llano de Caldera occupies a marine terrace 3½ to 12 miles wide, with an average altitude of about 350 feet above sea level. The prevailing wind from the southwest, whose direction at the surface of the ground is modified by irregularities in the topography, has transported clastic material inland from the terrace in two major sand streams or dune chains (fig. 93.1). The region is one of great aridity and very little vegetation.

The uneven surface of the llano reflects the changes that have taken place since the marine terrace was formed. The Río Copiapó, whose present course has been superposed on a high surface of marine deposits containing fossils of Quaternary age, cuts the southern part of the terrace, passing through La Angostura, a narrow granite gorge more than 300 feet deep. A granite ridge at La Angostura and other similar ridges to the north have been partly exhumed from their former cover of marine sediments. Outcrops of granite bedrock and exfoliated blocks have been etched, pitted, undercut, and hollowed out by the abrasive action of windblown sand (figs. 93.2–93.4). Some of the sand has been trapped by desert shrubs and by the granite outcrops, but there are no large dune areas in the Llano de Caldera.

Arcuate ridges on the terrace represent strand lines where coarse beach gravels were deposited. Large areas of the Llano de Caldera are covered with a desert pavement of pebbles and cobbles of many exotic rock types, including welded tuff. Many of these clasts are polished and faceted. Other areas of the llano are floored with lime-cemented shell beds. The western and northern edges of the terrace, and parts immediately adjacent to the gorge of the Río Copiapó,

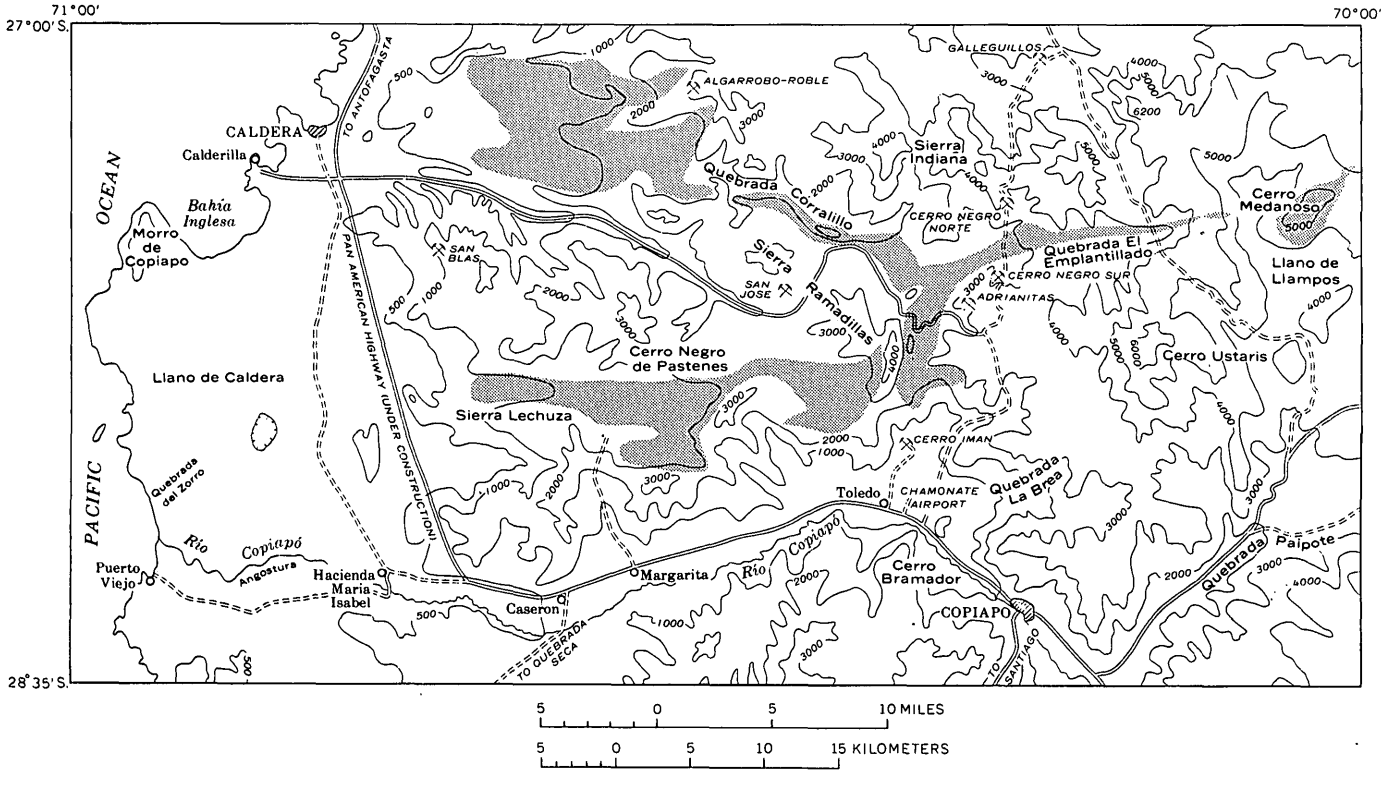

FIGURE 93.1.—Map of the area north and west of Copiapo, Atacama Province, Chile, showing principal areas of sand dunes (stippled). Base map from World Aeronautical Chart 1317, Point Morro.

639466 O - 62 - 7

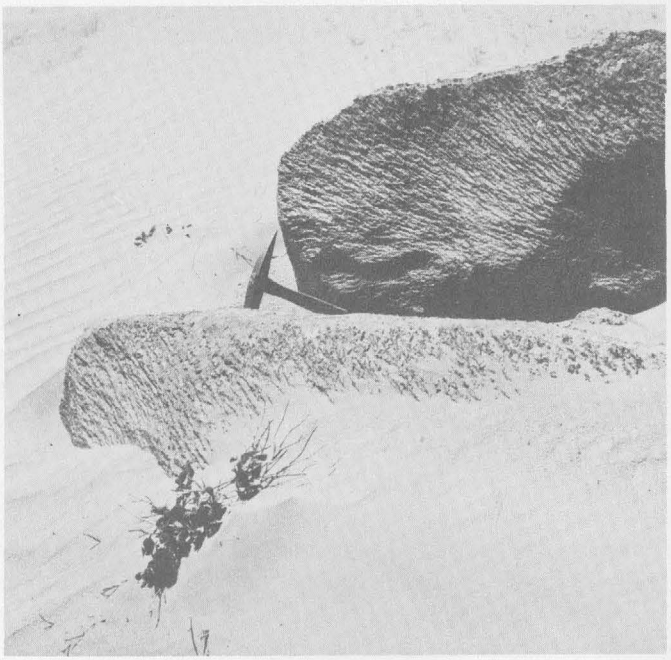

FIGURE 93.2.—Outcrop of granite that has been etched and pitted by the abrasive action of windblown sand, Llano de Caldera.

have been eroded by exterior drainage, but most of the area is one of interior drainage. Several of the undrained depressions are over a mile long and are rimmed by steep escarpments 10 to 15 feet high. The floors are partly covered with cracked mud of ephemeral lake deposits. The deepest part of the largest undrained area (shown in fig. 93.1 with a depression contour line) reaches the water table; ground water that emerges on the surface has a high brine content.

The sand streams, made up of chains and colonies of dunes, begin a little east of the llano, attain widths of as much as 6 miles, and extend inland through gaps between the hills, joining near the Adrianitas mine, about 35 miles inland and 2,800 feet above sea level. From there the sand extends in a narrow stream up the valley of Quebrada El Emplantillado about 12 miles farther east, dies out at the head of the valley, and reappears on Cerro Medanoso, over 5,000 feet above sea level. The sand probably attains a maximum thickness of 1,000 feet on the bedrock-cored Cerro Medanoso and 750 feet in a dune in the valley of Quebrada Corralillo, at the northeast base of Sierra Ramadillas. The major dunes are longitudinal and are as much as 3 miles long and 750 feet thick. Smaller, transverse dunes abound on the crests and flanks of many of the longitudinal dunes (fig. 93.5). The transverse dunes are chiefly barchans that have been modified by joining and by the action of offshore winds, which are weaker than the prevailing wind from the southwest. The sand is chiefly composed of well-rounded and well-sorted grains of feld-

FIGURE 93.3.—Outcrop of granite that has been undercut by the abrasive action of windblown sand, Llano de Caldera.

FIGURE 93.4.—Exfoliation block of granite that has been hollowed out by the abrasive action of windblown sand, Llano de Caldera.

FIGURE 93.5.—Large longitudinal dunes and small transverse dunes on east slope of Sierra Ramadillas.

spar, quartz, and magnetite. Amphibole, epidote, biotite, and fine-grained rock clasts are also present. Less than 1 percent of the sand is larger in diameter than 0.5 mm or smaller than 0.05 mm.

The source of at least part of the dune sand is the Llano de Caldera, which is swept daily by strong wind from the southwest. Millions of cubic feet of fine-grained material have been removed from the terrace and redeposited to the east. Before the process of sand removal took place, the bedrock was sufficiently buried for the superposed Río Copiapó to flow over it, but now the exhumed and sand-blasted outcrops of bedrock are higher than the surrounding areas of deflation. The intervening lower areas are occupied, for the most part, by closed basins. After allowing for the natural westward slope of the terrace, differences in altitude of 100 feet or more between the topographic highs and lows can be attributed only to wind action (deflation) that is retarded in places by exposure of granite, resistant shell beds, shingled strand lines, and proximity of the water table.

GLACIOLOGY AND GLACIAL GEOLOGY

94. GRAVIMETRIC DETERMINATIONS OF ICE THICKNESS OF JARVIS GLACIER, ALASKA

By NED A. OSTENSO and G. WILLIAM HOLMES, University of Wisconsin, Madison, Wis., and Washington, D.C.

Jarvis Glacier, in central Alaska (fig. 94.1), is about 5 miles long and ½ mile wide and lies in a deep U-shaped valley on the north flank of the Alaska Range. Surface elevations range from about 4,000 feet at the snout of the glacier to 6,000 feet in the cirque. The glacier is well suited to glaciological study because of its small size and relatively smooth surface. It is accessible by trail along Jarvis Creek, and by light aircraft, which can land almost anywhere on the glacier.

In conjunction with other glaciological studies, 76 gravity stations were established on the glacier during the period March 30 to May 1, 1955. Ice thickness was determined by the difference in the density of the glacial ice and the underlying rock. Although ice-thickness determinations made by gravimetric observations are less accurate than those made by seismic measurements or by borings, the method has the advantage of speed and ease of operation, and requires a minimum of equipment and logistics support. Moreover, crevasses, basal roughness, or extreme slopes, common in mountain glaciers, frequently preclude the use of seismic soundings.

These studies were conducted as a private project by Ostenso in cooperation with general investigations in the area by Holmes that were sponsored by the U.S. Army Corps of Engineers Waterways Experiment Station. The work was generously supported by Prof. G. P. Woollard, University of Wisconsin, who supplied the gravimeter. Major James R. Evans, U.S. Air Force, flew the aircraft and provided valuable field assistance. Daniel Sokol, of the U.S. Geological Survey, assisted in the fieldwork.

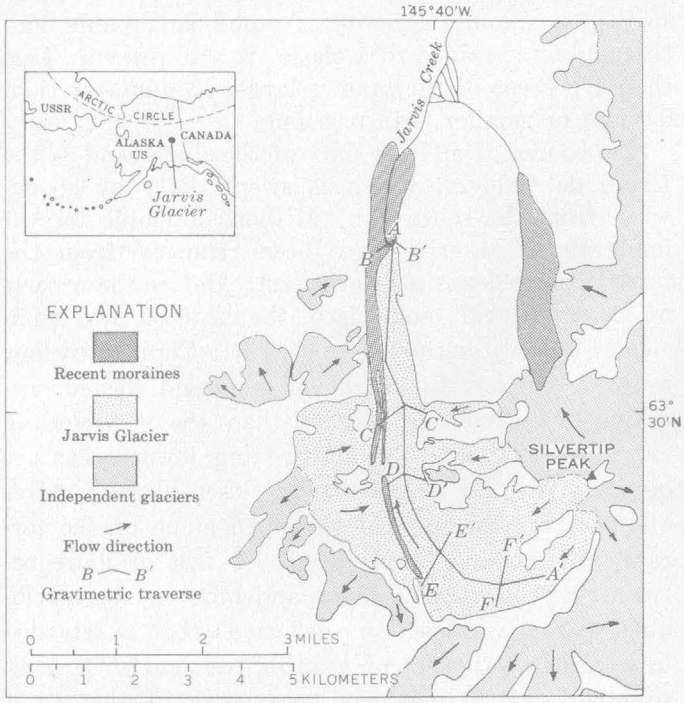

FIGURE 94.1.—Map of Jarvis Glacier, Alaska Range, showing principal features, direction of flow, and location of gravity traverses.

This part of the Alaska Range is composed of the early Precambrian Birch Creek Schist series, a complex unit of metasedimentary rocks including quartzite, quartzite schist, sericite schist, and gneiss (Wahrhaftig and Hickcox, 1955, p. 354; Capps, 1940, p. 97).

Jarvis Glacier is nourished chiefly by firn fields on the flanks of the mountain locally known as Silvertip Peak and on the cirque wall to the south. Three small hanging glaciers on the west wall of the valley may have nourished the glacier during recent glacial advances. Like many other glaciers in the area, Jarvis Glacier has recently retreated and decreased in volume. The firn limit is normally high in the cirque; in 1955 it was at an elevation of approximately 5,700 feet. Well-developed lateral moraines with relief of 20 to 30 feet lie along most of the lower two-thirds of the glacier. The outer moraine is slightly weathered, and the inner moraine is fresh. Both lateral moraines converge into a poorly defined end moraine, which has been partly breached by melt water. This pattern of two moraines, considerably smaller and younger than the massive late Pleistocene Donnelly moraines to the west in the Delta River valley, is typical of glaciers in this section of the Alaska Range.

A Worden geodetic gravimeter (No. W14), calibrated against the Gulf-Wisconsin pendulum station network, was used because of its light weight, ruggedness, and independence of external power source.

Five gravity traverses were made across Jarvis Glacier and one the length of the glacier (fig. 94.1). The location of the stations was determined by triangulation on mountain peaks using a telescopic alidade; the distance between individual stations was chained. All elevations were determined with the alidade; their relative accuracy is estimated to be within 2 feet. The entire survey network was reduced to sea level by multiple ties to a U.S. Coast and Geodetic Survey benchmark by altimeter, with a probable accuracy of ± 10 feet.

The gravity method for determining ice thickness assumes that variations in the Bouguer anomaly over the glacier surface are primarily a function of the thickness of the underlying ice. If the difference in the density of the ice and the country rock is known, the ice thickness may be estimated by considering it proportional to the Bouguer anomaly. In practice, however, this correlation is complicated by the fact that the gravimeter measures the strength of a potential field, and readings are influenced by a large mass of glacier ice rather than the small column of ice directly beneath it. This results in an "averaging" effect which is a function of the irregularity of the ice–rock interface, the ice thickness, the proximity to valley walls, and the density differential between ice and rock. Variation in the density of the ice and the rock also complicates the relationship, but the contrast is large and a density change of 0.1 gm per cm^3 for either rock or ice will cause an error in ice thickness of less than 3 feet per milligal. Isostatic effects and variation in bedrock density may also cause gravity anomalies which might be interpreted as changes in ice thickness. However, the gravitational effect of these deeper, bedrock variations can usually be eliminated by measurements along the margin of the glacier. In general the gravity method for determining ice thickness is rapid and reasonably accurate.

Theoretical sea-level gravity was obtained from tables based upon the International Gravity Formula. The simple Bouguer correction was applied to the free-air gravity by assuming a density of 2.67 gm per cm^3 for the country rock, primarily schist and quartzite. As Jarvis Glacier is situated in a deep mountain valley, terrain corrections had to be applied to all reductions of observed gravity. These corrections were determined by the zone chart and tables computed by Hammer (1939). The magnitude of these corrections varied from 1.34 mgal (milligal) for a central station to 5.87 mgal for a station at the edge of the glacier.

The corrected observed gravity was subtracted from the theoretical gravity for each station to give the

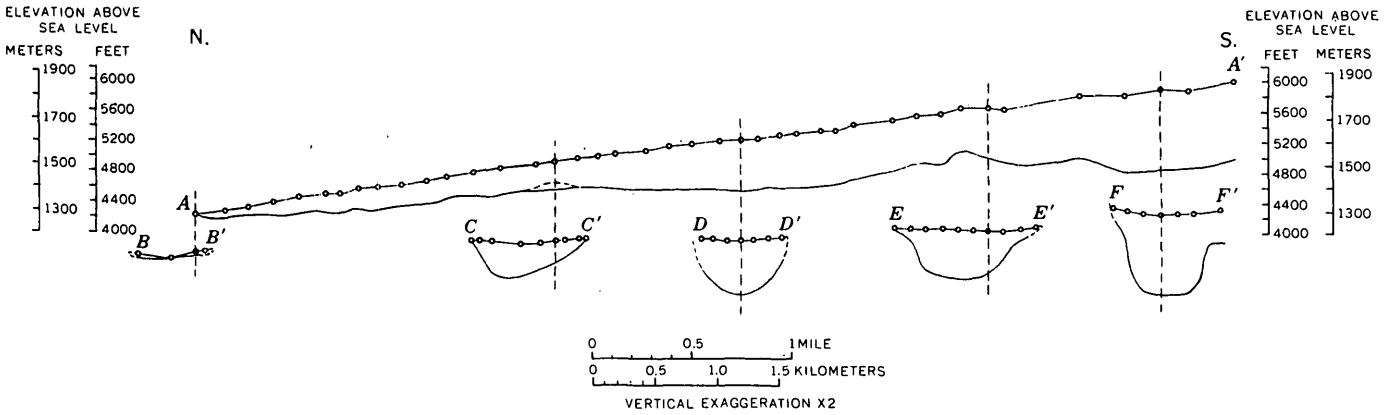

FIGURE 94.2.—Profiles of the Jarvis Glacier, Alaska Range, Alaska. Gravimetric stations are shown by dots; location of traverses is shown on figure 94.1.

Bouguer anomaly. The Bouguer anomalies showed an inverse correlation with elevation because of the effect of isostatic compensation and geologic structure. In order to compensate for this regional gradient, the traverses extended beyond the edge of the glacier wherever possible, and interpolations for the intermediate points were made where crevassing prevented extending the profiles to bedrock. The observed gravity at the stations on bedrock were set equal to the theoretical gravity at these points, and appropriate regional corrections were applied to all of the stations on the glacier. These stations then showed residual Bouguer anomalies which were a function of the deficiency in mass of the ice column between the instrument and the underlying rock.

For convenience in calculating ice thickness from the residual Bouguer anomalies, a simple geometric model was constructed with the glacier represented as an infinite slab. The total gravitational effect, g, at any point over such a slab can then be represented as: $g=2\pi\gamma\rho t$ mg, where γ is the gravitational constant, 6.67×10^{-8} cgs units; ρ is the density differential between the ice and the rock; and t is the ice thickness, in centimeters. Assuming a density of 0.89 g per cm^3 for the glacial ice and 2.67 g per cm^3 for the country rock, ρ would equal 1.78 g per cm^3, and a Bouguer anomaly of 1.0 mgal would be equivalent to 44 feet of ice. After the approximate ice thickness was calculated, a refined determination of the glacier profile was obtained by using a line integral method described by Hubbert (1948).

The results of the gravity traverses on Jarvis Glacier are shown as profiles in figure 94.2. Unfortunately, part of the fieldwork was conducted during a period of poor visibility, and the longitudinal traverse deviated from the central axis of the glacier, resulting in an apparent thinning of the ice (dashed on profile A–A'). This discrepancy was adjusted by substituting the greatest ice thickness along transverse profile C–C' where it crossed the point of deviation. The presence of crevasses made it impossible to extend some traverses beyond the glacier.

The valley of Jarvis Glacier has a pronounced U-shaped transverse profile and a relatively smooth bottom. A maximum ice thickness of 1,055 ft was found in the center of the cirque. Transverse profile F–F' (fig. 94.2) through the cirque shows a small tributary glacier joining it from the southwest slope of Silvertip Peak. Of particular interest is the sill on the down-glacier end of the cirque (west of profile E–E', fig. 94.2). Ice must flow uphill in moving from the cirque into the glacial valley. The overdeepened cirque can be explained by erosional mechanisms such as rotational slip (Lewis, 1949) or perhaps by increased erosion under conditions of compressive flow (Nye, 1952), or by a combination of the two. The longitudinal profile in figure 94.2 shows that the glacier is at present too thin and without sufficient surface slope for rotational slip to occur and cause abnormal cirque scouring. During earlier advances, however, the glacier originated higher in the cirque and rotational slip may have occurred. Once the sill started to form, the process could be continued according to the theory of Nye (1952) and Sheidegger (1961). The cirque floor would have a concave profile over which glacial flow would be compressive and erosion would be intensified.

The abrupt change in surface slope over the cirque sill is in qualitative agreement with Nye's hypothesis (1959) which states that the surface slope is inversely proportional to the ice thickness. Paucity of data along this critical portion of the profile, the lack of precision of subice topographic measurements by the

gravity method, and the effect of side friction preclude a quantitative testing of Nye's general law.

REFERENCES

Capps, S. R., 1940, Geology of the Alaska Railroad region: U.S. Geol. Survey Bull. 907, 201 p.

Hammer, Sigmund, 1939, Terrain corrections for gravimeter stations: Geophysics, v. 4, p. 184–194.

Hubbert, M. K., 1948, A line-integral method of computing the gravimeter effects of two-dimensional masses: Geophysics, v. 13, p. 215–225.

Lewis, W. V., 1949, Glacial movement by rotational slipping: Geog. Ann. Stockh., v. 31, p. 146–58.

Nye, J. F., 1952, The mechanics of glacier flow: Jour. Glaciology, v. 2, p. 82–93.

——— 1959, Motion of ice sheets and glaciers: Jour. Glaciology, v. 3, p. 493–507.

Scheidegger, A. E., 1961, Theoretical geomorphology: Berlin, Springer-Verlag, 264 p.

Wahrhaftig, Clyde, and Hickcox, C. A., 1955, Geology and coal deposits, Jarvis Creek coal field, Alaska: U.S. Geol. Survey Bull. 989–G, p. 353–366.

95. MULTIPLE TILLS OF END MORAINES

By George W. White, Columbus, Ohio

Work done in cooperation with the Ohio Department of Natural Resources, Division of Water

In stratigraphic studies facilitated by deep road cuts recently made for superhighways, several till sheets have been traced for considerable distances at and below the surface in northeastern Ohio. Also, some end moraines are composed of three or more tills, of which the uppermost is only a few feet thick and forms a veneer upon the underlying material that makes up the bulk of the moraine. These moraines therefore antedate the last ice advance.

The tills in the end moraines vary in texture, composition, permeability and engineering properties. Silt, sand, and gravel—at many places water-bearing—occur not only as sheets between the tills, but also at some places as channel and valley fillings in the lower till (Norris and White, 1961).

The Kent moraine (fig. 95.1), at the margin of the Grand River lobe, is composed of till knolls and large gravel kames. Locally, the Kent Till overlies older drift. The Kent moraine is overlain by the Hiram Till of the Cuyahoga sublobe in northeastern Summit, northwestern Portage, and southwestern Geauga Counties, but the characteristic morainic topography is preserved. Gravel pits in the moraine show 1 to 15 feet of the Hiram Till overlying gravel of Kent age, which is being excavated. The sequence of three tills, once well exposed at the Ohio Turnpike interchange at Streetsboro, Portage County, is illustrated in figure 95.2.

The Wabash moraine extends from the till plain in western Ohio eastward into the Allegheny plateau, to about the Medina-Summit County line west of Akron, where it becomes obscure (Goldthwait, White, and Forsyth, 1961). In almost every cut made in this moraine more than one till can be identified. In Wayne and much of Ashland Counties the Hiram Till margin lies at the Wabash moraine, but the Hiram Till is generally so thin—2 to 10 feet—that it adds little to the volume of the moraine. The Wabash moraine formed a barrier over which the Hiram ice did not advance.

The Ft. Wayne moraine, which lies 2 to 5 miles south of the Defiance moraine in the western part of the Allegheny plateau, extends across Richland, Huron, and Ashland Counties into south-central Medina County where it joins the Wabash moraine (fig. 95.1). In Medina County the Hiram Till, 5 to 15 feet thick, overlies prominent kames associated with an earlier moraine. The sand and gravel deposits of the buried kames are an important source of ground water in southern Medina County. They are being excavated in several large gravel pits in southwestern Medina County where the overlying Hiram Till has been removed by stripping.

The Defiance moraine extends eastward from the till plain to the Allegheny plateau and loops southward in the Grand River lowland in Ashtabula, Trumbull, and Geauga Counties, where 5 to 15 feet

of the Hiram Till overlies the Lavery Till. A layer of silt ranging from a fraction of an inch to several inches in thickness generally separates the two tills. At a few places this separating layer is 2 or more feet thick and is sandy. The Hiram Till extends only to the eastern (outer) margin of the Defiance moraine on the eastern side of the Grand River basin in Trumbull and Ashtabula Counties, but it extends as much as 25 miles south of the southern part of the Defiance moraine.

The Ashtabula morainic system (Shepps and others, 1959, p. 45), called the Lake Escarpment morainic system by Leverett (1902, p. 651), is a few miles south of Lake Erie and extends from Cleveland eastward across Pennsylvania into New York as a series of 2 to 4 prominent parallel ridges. In Ohio, cuts made in the Ashtabula moraine for superhighway construction in 1959, 1960, and 1961, showed that the uppermost Ashtabula Till ranges in thickness from 10 to

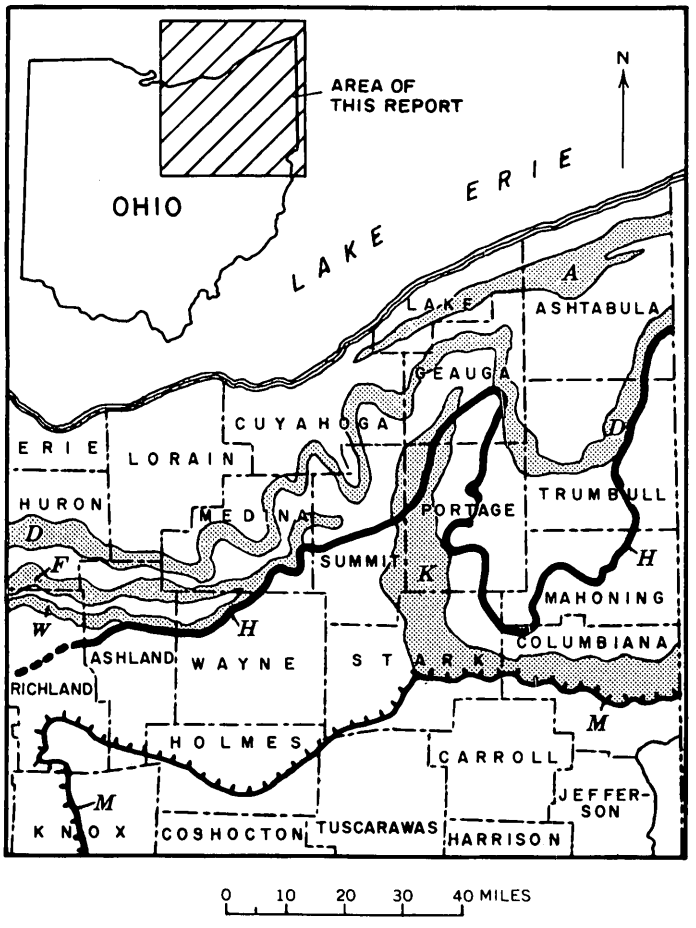

FIGURE 95.1.—Map showing end moraines and drift borders in northeastern Ohio. (*A*) Ashtabula moraine, (*D*) Defiance moraine, (*F*) Ft. Wayne moraine, (*W*) Wabash moraine, (*K*) Kent moraine, (*H*) outer limit of Hiram Till, (*M*) margin of Wisconsin Drift.

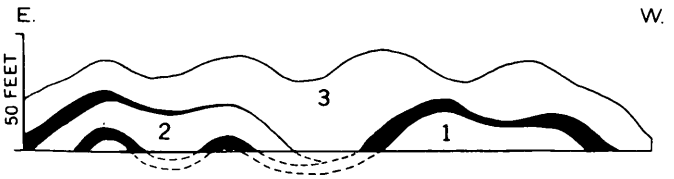

FIGURE 95.2.—Sketch of south side of cut in Kent moraine for Ohio Turnpike interchange 1½ miles northwest of Streetsboro, Portage County. (1) Mogadore Till, (2) Kent Till, (3) Hiram Till; sand and gravel shown by solid pattern; length of section 1,500 feet.

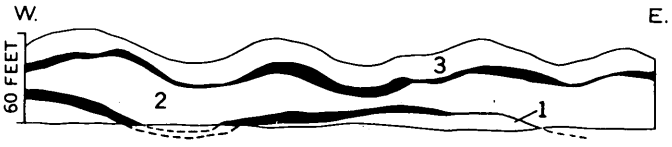

FIGURE 95.3.—Sketch of north side of road cut in outer member of Ashtabula moraine; view northeast from interchange in northwestern Leroy Township, Lake County, 4 miles east-southeast of Painesville. (1) Lavery Till, (2) Hiram Till, (3) Ashtabula Till; sand and gravel shown by solid pattern; length of section 1,200 feet.

30 feet. It is separated from the underlying Hiram Till by a sand and gravel deposit ranging in thickness from a few inches to more than 10 feet that can be traced in the cuts for half a mile or more (fig. 95.3). The deposit generally is water bearing and has presented problems in excavation and slope stabilization in highway construction. Well records show that the sand and gravel layer is many tens of square miles in extent (J. L. Rau, oral communication, 1961). In some of the deepest cuts the Lavery Till underlies the Hiram Till, and the two tills are separated by sand or gravel.

Moraines of multiple character have been reported from other areas. The massive Valparaiso moraine in northeastern Illinois owes its form to earlier, underlying material in the Grays Lake quadrangle (Powers and Ekblaw, 1940, p. 1332) and in the Chicago region (Bretz, 1955, p. 710). End moraines near Ellesmere in northeastern Wales reportedly belong to an earlier ice advance than does the surface till, which forms a capping on the strongly morainic topography (E. G. Poole and A. J. Whiteman *in* Peake, 1961, p. 364 and 365, respectively).

Most end moraines in northeastern Ohio owe neither their form nor most of their volume to the deposits of the last readvance of the ice sheet. The uppermost till is the last record, but the earlier records below it may be read much as a "palimpsest," or "codex rescriptus," may be read from an ancient manuscript on which two or more writings are superimposed.

SELECTED REFERENCES

Bretz, J H., 1955, Geology of the Chicago region; part 2—The Pleistocene: Illinois Geol. Survey Bull. 65, pt. 2.

Goldthwait, R. P., White, G. W., and Forsyth, J. L., 1961, Glacial map of Ohio: U.S. Geol. Survey Misc. Geol. Inv. Map I-316.

Leverett, Frank, 1902, Glacial formations and drainage features of the Erie and Ohio basins: U.S. Geol. Survey Mon. 41, 802 p.

Norris, S. E., and White, G. W., 1961, Hydrologic significance of buried valleys in glacial drift: Art. 17 *in* U.S. Geol. Survey Prof. Paper 424-B, p. B34-B35.

Peake, D. S., 1961, Glacial changes in the Alyn River system and their significance in the glaciology of the north Welsh border: Geol. Soc. London Quart. Jour., v. 117, p. 335-366.

Powers, W. E., and Ekblaw, G. E., 1940, Glaciation of the Grays Lake, Illinois, quadrangle: Geol. Soc. America Bull., v. 51, p. 1329-1336.

Shepps, V. C., and others, 1959, Glacial geology of northwestern Pennsylvania: Pennsylvania Geol. Survey Bull. G-32.

White, G. W., 1960, Classification of Wisconsin glacial deposits in northeastern Ohio: U.S. Geol. Survey Bull. 1121-A, 12 p.

——— 1961, Classification of glacial deposits in the Killbuck glacial lobe: Art. 176 *in* U.S. Geol. Survey Prof. Paper 424-C, p. C71-C73.

ANALYTICAL TECHNIQUES

96. DISSOLVING FLUORITE WITH SOLUTIONS OF ALUMINUM SALTS

By R. E. Stevens, C. L. Sainsbury, and A. C. Bettiga, Menlo Park, Calif.

The purpose of this article is to point out to mineralogists the effectiveness of solutions of aluminum salts in dissolving fluorite. Although Feigl (1929) used aluminum chloride to dissolve fluorite more than 30 years ago, modern textbooks on mineralogy do not mention the effectiveness of this solvent for fluorite. Previously, deBoer and Basart (1926) had used zirconium chloride for the same purpose. The seventh edition of Dana's System of Mineralogy (1951) does not mention aluminum salt solutions as solvents for fluorite, although cryolite is stated as being easily soluble in $AlCl_3$ solutions.

Feigl (1958) in his book on spot tests tells of this method of dissolving fluorite. Calcium fluoride is slightly soluble in water in accordance with the following reaction:

$$CaF_2 \rightleftarrows Ca^{+2} + 2F^{-1}.$$

Many metal ions in the solution shift this equilibrium to the right by removing the fluoride ion to form soluble metal-fluoride complex ions, for example $[AlF_6]^{-3}$, $[FeF_6]^{-3}$, $[ZrF_6]^{-2}$, $[TiF_6]^{-2}$, and $[BeF_4]^{-2}$. The calcium fluoride is caused to dissolve to an extent dependent upon the quantity of aluminum or other metal ion in the solution.

Neuerburg (1961) separated beryllium minerals, anatase, barite, bastnaesite, carbon, graphite, rutile, topaz, zircon, and others from rock fragments "by repeated application of hydrofluoric acid over a period of several weeks. Water-insoluble reaction products are removed by boiling in a solution of aluminum chloride."

We have tested 50 percent w/v solutions of $AlCl_3 \cdot 6H_2O$, $Al(NO_3)_3 \cdot 9H_2O$, and $Al_2(SO_4)_3 \cdot 18H_2O$ as solvents for calcium fluoride. One hundred milliliters of the boiling acidified aluminum chloride solution dissolved 17.5 grams of calcium fluoride, added in small increments, before a residue not readily dissolved was obtained; 100 ml of the aluminum nitrate solution dissolved over 9 grams of calcium fluoride. Four grams of calcium fluoride added to 100 ml of the 50 percent w/v solution of $Al_2(SO_4)_3 \cdot 18H_2O$ was entirely altered to gypsum ($CaSO_4 \cdot 2H_2O$), showing that all of the fluoride ion had been dissolved. The gypsum was identified by its birefringence and indexes of refraction under the microscope and by its X-ray pattern. No evidence of fluorite was found in the insoluble material.

The action of aluminum solutions in dissolving or decomposing fluorite may have important industrial application to the recovery of fluoride from low-grade fluorspar ore and to the making of artificial cryolite. As many beryllium ores occur intergrown with fluorite, a chemical treatment of such ores might be developed which could produce artificial cryolite as a byproduct. The action of aluminum sulfate would seem to be particularly interesting for the recovery

of fluoride from low-grade fluorspar because the calcium is left with the residue as gypsum.

The following procedure has been used to remove fluorspar from samples from Alaska which contain phenacite, beryl, chrysoberyl, and tourmaline in order to obtain clearer X-ray patterns for identification and confirmation of the beryllium minerals:

1. The ore is crushed and sized to 150–200 mesh.
2. The sample is digested in a boiling 50 percent w/v $AlCl_3 \cdot 6H_2O$ solution to remove fluorite (about 10 ml of $AlCl_3$ solution for a gram of sample).
3. The sample is washed with water repeatedly, and dried.
4. Sized material is passed through the Frantz isodynamic separator at 1.5 amperes, which usually separates the beryl and chrysoberyl from the tourmaline.
5. The nonmagnetic fraction containing the beryl and (or) chrysoberyl is centrifuged in heavy liquid with a specific gravity of 3.28–3.3, which separates beryl and chrysoberyl. In our experience with the Alaska ores, we found that very fine-grained chrysoberyl seemed to display a specific gravity lower than that quoted in mineralogy books for well-crystallized chrysoberyl (3.5–3.84), and hence a liquid of 3.28–3.3 specific gravity was used; this liquid also floats any remaining tourmaline.

By this method, X-ray patterns which indicate pure chrysoberyl have been obtained on fractions separated from ores containing as little as 0.425 percent BeO.

Aluminum chloride solution is also useful for etching rock specimens in order to bring out in relief the silicates and beryllium minerals by removing the fluorite.

REFERENCES

deBoer, J. H., and Basart, J., 1926, A rapid volumetric determination of fluorine even in complex and insoluble fluorides: Z. anorg. allgem. Chem., v. 152, p. 213.

Feigl, F., 1929, Quantitative microanalysis. III. Detection of thiocyanate, fluoride and copper, two methods of distinguishing between tap water and distilled water, detection of alkali in water, and a drop reaction for ammonia: Mikrochemie, v. 7, p. 10–20.

——— 1958, Spot tests: Elsevier, New York, p. 270.

Neuerburg, G. J., 1961, A method of mineral separation using hydrofluoric acid: Am. Mineral., v. 46, p. 1498–1501.

97. SYNTHESIS OF LARGE CRYSTALS OF SWARTZITE

By Robert Meyrowitz, Washington, D.C.

Swartzite, $CaMgUO_2(CO_3)_3 \cdot 12H_2O$, is a rare secondary uranium mineral that was first synthesized by Axelrod and others (1951), who found it necessary to seed the solution (containing uranyl nitrate, potassium carbonate, magnesium nitrate, and calcium nitrate) to obtain crystal growth. The present paper notes the unusual solution behavior of swartzite in the system $Ca_2UO_2(CO_3)_3$–$Mg_2UO_2(CO_3)_3$–$Ca(NO_3)_2$–$Mg(NO_3)_2$, and describes a technique for preparing large crystals of swartzite.

The phases liebigite ($Ca_2UO_2(CO_3)_3 \cdot 10H_2O$) and bayleyite ($Mg_2UO_2(CO_3)_3 \cdot 18H_2O$) crystallize readily from solutions on evaporation of the water in the system $Ca_2UO_2(CO_3)_3 - Mg_2UO_2(CO_3)_3 - Ca(NO_3)_2 - Mg(NO_3)_2$, and the fields of liebigite plus solution and bayleyite plus solution occupy such a large part of the boundary of the quaternary solution field that the growth of swartzite crystals requires a careful control of solution composition. If the Ca-Mg mole ratio is 7:8 or greater, liebigite is the initial precipitate; ratios of 5:8 or less yield bayleyite; and a ratio of 3:4 gives swartzite.

Large crystals (3 × 10 mm) of swartzite, identified by their powder X-ray diffraction pattern (Axelrod and others, 1951), can be prepared as follows:

An aqueous solution (13.5 ml) containing 2.7 g of $Ca(NO_3)_2 \cdot 4H_2O$ (¾ × 0.015 mol CaO) is added slowly with constant stirring (magnetic stirrer) to an aqueous solution (60 ml) of 12.4 g of synthetic bayleyite ($Mg_2UO_2(CO_3)_3 \cdot 18H_2O$) (0.015 mol) prepared according to the procedure described by Meyrowitz and Lindberg (1960). The solution is allowed to stand for 24 hours. It is filtered and the filtrate is allowed to evaporate at room temperature. In approximately 2 weeks clusters of swartzite crystals form. These clusters are detached from the beaker, quickly washed with water, and allowed to air dry.

REFERENCES

Axelrod, J. M., and others, 1951, The uranium minerals from the Hillside Mine, Yavapai County, Arizona: Am. Mineralogist, v. 36, p. 1–22.

Meyrowitz, R., and Lindberg, M. L., 1960, Synthetic bayleyite: Art. 201 *in* U.S. Geol. Survey Prof. Paper 400–B, p. B440–B441.

98. APPARATUS FOR RAPID DETERMINATION OF FOAM HEIGHT

By C. H. Wayman, J. B. Robertson, and H. G. Page, Denver, Colo.

Work done in cooperation with the Federal Housing Administration

A simple apparatus designed to determine the foaming characteristics of dilute aqueous solutions is shown in figure 98.1. The unit consists of a large chromatographic column (outside diameter, 5.8 cm, and length, 30.0 cm, graduated to 0.5 cm) connected to a lower tube (outside diameter, 1.0 cm, and length, 18.5 cm) by a 55/35 tube-socket ground-glass joint; a coarse-porosity fritted disc is sealed to the upper end of the lower tube.

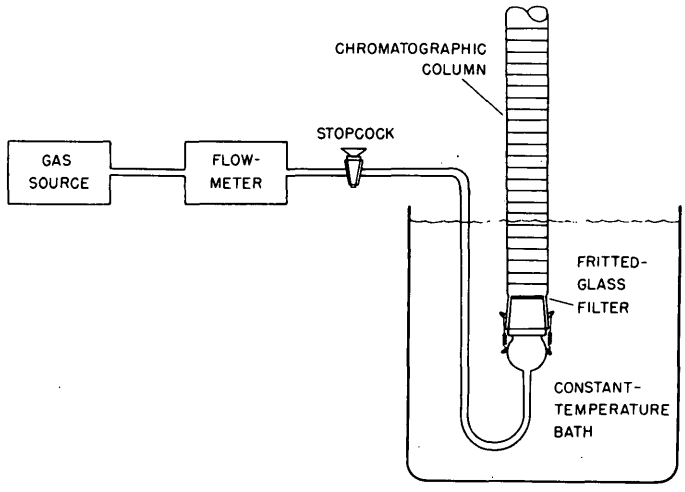

FIGURE 98.1.—Apparatus for study of foaming characteristics.

The apparatus can be operated by releasing air or nitrogen at a constant flow rate into a solution containing a surface-active agent in the chromatographic column and observing the height of foam formation as a function of time. The stability of the foam can be determined by interrupting the gas flow through the system and observing the decrease in foam height as a function of time. The portion of the apparatus containing the liquid can be immersed in a constant-temperature bath to evaluate the influence of temperature on these characteristics.

The table below shows the rate at which a solution containing 1,000 parts per million of alkylbenzenesulfonate foams at two different flow rates for 20°C. The foam height varies directly with the flow rate of the gas.

This method can be used to evaluate the foaming characteristics of other surface-active agents and might also be used, after possible modification, to study drainage rates of foams and foam fractionation.

Variation of foam height with changes in flow rate of gas and in time

Time (sec)	Foam height (cm) at indicated flow rate	
	280 cc gas per minute	720 cc gas per minute
20	4.5	10
50	10	26
100	21	54

99. COMPARISON OF THREE METHODS FOR ESTIMATING DENSITY OF *ESCHERICHIA COLI* IN LABORATORY PREPARATIONS

By H. G. Page, C. H. Wayman, and J. B. Robertson, Denver, Colo.

Work done in cooperation with the Federal Housing Administration

Investigation of physicochemical properties of chemically and biologically polluted water requires a rapid and accurate method for counting bacteria in laboratory preparations. Commonly used methods for counting coliform bacteria include the gas-generation (MPN), photometer, membrane-filter (MF), and plate-count techniques. Previous work has not compared the relative merits of all the techniques; therefore, an attempt was made to evaluate the accuracy of bacterial count per milliliter and the influence of volumetric dilution in the MPN and photometer methods, using the plate count as a referee method (Mc-

Carthy and others, 1958; Levin and others, 1961). Because of its inherent difficulties and lack of precision (McCarthy and others, 1958; Malaney and others, 1961; Levin and others, 1961), the MF method was not evaluated.

The popular MPN and MF methods are approved by the American Public Health Association and others (1960), but many references indicate serious deficiencies in obtaining an accurate bacterial count by these methods (McCarthy and others, 1958; Malaney and others, 1961; Levin and others, 1961). In the examination of natural and waste waters (American Public Health Association and others, 1960), the MPN and MF methods apparently serve their primary purpose of identifying and determining semiquantitatively the density of coliform bacteria. For such waters, the photometer method is deficient because of the many constituents, other than colifrm, that cause turbidity in the solution. However, for laboratory preparations requiring a known concentration of pure-culture bacteria, the photometer method produces results much superior to the other methods in combined accuracy and rapidity.

In evaluating the photometer method, a calibration curve was prepared using McFarland standard solutions of barium sulfate. These solutions representing a range of bacteria concentration from 0 to 30 $\times$ 10^8 bacteria per milliliter (Kolmer and Boerner, 1945) are commonly used to determine bacterial density by visual comparison. Before measuring the transmittance value, each solution was shaken vigorously about 25 times and allowed to settle for about 20 seconds. The calibration curve is shown in figure 99.1, where percent transmittance is plotted against equivalent concentration of bacteria per milliliter. Use of this curve and the photometer measurements eliminates deficiencies of the human eye in visual comparisons and permits many concentration determinations between the points on the curve. Nonlinearity of the calibration curve is indicated by two inflection points, at about 1 $\times$ 10^8 and 10 $\times$ 10^8 bacteria per milliliter. These points are in satisfactory agreement with the work of Jennison (1934) and Mestre (1935), respectively. The technique is most reliable in the range 1 $\times$ 10^8 to 10 $\times$ 10^8 bacteria per milliliter.

For each of several experiments, a stock solution was prepared by mixing a pure culture of *Escherichia coli* in a 0.85-percent sodium chloride solution. The bacterial concentration of the stock solution was determined by comparing its transmittance to the calibration curve. Serial dilutions were made from the stock solution, and bacteria concentrations for each

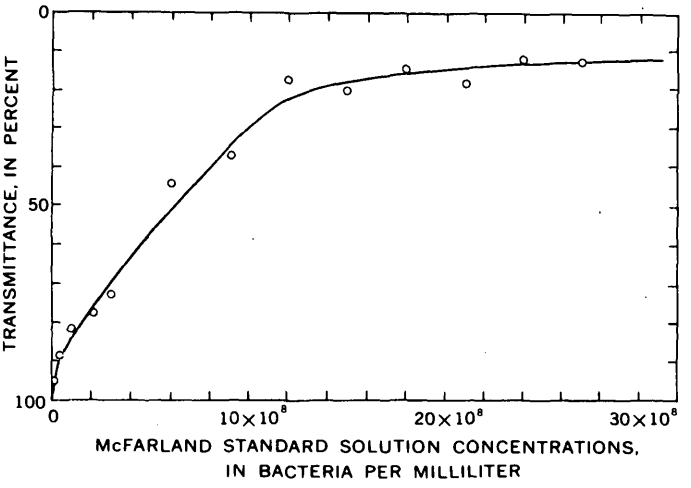

FIGURE 99.1.—Calibration curve, showing relationship between McFarland standard-solution concentrations (equivalent to *Escherichia coli*) and percent transmittance at 500 millimicrons wavelength; distilled-water blank.

dilution were determined from photometer readings. Any desired concentration can be prepared using this technique. In each experiment, one dilution calculated to have the desired bacterial concentration was used to inoculate fermentation tubes and agar pour plates. Standard incubation and counting procedures were followed.

After 48 hours incubation, the MPN in all experiments indicated a count of 24+ bacteria per milliliter, with a general range in the 95-percent confidence limits from about 7 to 700 bacteria per milliliter (American Public Health Association and others, 1960, p. 503–506; Malaney and others, 1961). The same dilution concentrations used for the MPN method produced plate counts ranging from 28 to 9,000 bacteria per milliliter (see table). After some

Comparison of bacteria counts obtained by plate count and photometer methods. All experiments using MPN method indicated a count of 24+ bacteria per milliliter

Experiment	Volume of solution (ml)	Pour plate count per milliliter [1]	Photometer count per milliliter [2]
1	10	100	5, 600
2	10	9, 000	300
8	100	230	150
4	100	390	100
11	100	100	80
6	500	28	100
7	500	65	100
12	500	95	100
3	1, 000	223	100
9	1, 000	120	190
10	1, 000	100	150

[1] Considered correct count for solution used. Average of 5 plates, each experiment.
[2] Calculated for dilution used, from stock-solution concentration determined with photometer.

experience with the photometer technique, reasonable agreement was obtained between plate and photometer counts. For equal-volume test solutions, the best comparative bacteria counts per milliliter for plate and photometer methods respectively were: 100-ml test solutions, 100 and 80; 500-ml test solutions, 95 and 100; and 1,000-ml solutions, 100 and 150. The table indicates the apparent influence of volumetric dilution on the method. Preparations using at least 100 milliliters are important; the use of smaller volumes results in large errors.

These results indicate the limited value and the variability of the MPN method for quantitative determinations. For pure-culture bacteria, the photometer method produces highly accurate and reproducible estimates within minutes as compared to about 48 hours by other methods.

REFERENCES

American Public Health Association and others, 1960, Standard methods for the examination of water and wastewater: 11th ed., New York, Am. Public Health Assoc., 626 p.

Jennison, M. W., 1934, A note on the Richards-Jahn photoelectric nephelometer: Jour. Bacteriology, v. 28, no. 1, p. 107–109.

Kolmer, J. A., and Boerner, F., 1945, Approved laboratory technic: 4th ed., New York, Appleton-Century, 1017 p.

Levin, G. V., Stauss, V. L., and Hess, W. C., 1961, Rapid coliform organism determination with C–14: Rudolfs Research Conference, Rutgers University, 21 p. [duplicated].

McCarthy, J. A., Thomas, H. A., Jr., and Delaney, J. E., 1958, Evaluation of the reliability of coliform density tests: Am. Jour. Public Health, v. 48, no. 12, p. 1628–1635.

Malaney, G. W., and others, 1961, Evaluation of methods for coliform counts in farm pond waters: Am. Water Works Assoc. Jour., v. 53, no. 1, p. 43–48.

Mestre, Harold, 1935, A precision photometer for the study of suspensions of bacteria and other microorganisms: Jour. Bacteriology, v. 30, no. 4, p. 335–358.

100. A SEQUENTIAL HEATING DEVICE FOR FeO DETERMINATIONS

By Leonard Shapiro and Fred Rosenbaum, Washington, D.C.

The Geological Survey's laboratory for rapid rock analyses has been able to reduce considerably the time and energy spent in the determination of ferrous iron by the use of a sequential heating apparatus.

The procedure described by Shapiro and Brannock (1962) specifies that solutions prepared by boiling samples with HF and H_2SO_4 be titrated with a standard dichromate solution, using diphenylamine sulfonic acid as the indicator. The apparatus to be described accommodates 15 100-ml platinum crucibles at one time. It automatically controls the 10-minute boiling time and delivers a solution ready for titration every 3 minutes. Additional platinum crucibles can be placed into holes as they become vacated, so that the number of samples that can be handled in one sequence is limited only by the number of crucibles available.

The device, as shown in figure 100.1, consists of a circular Transite board (*a*) 19 inches in diameter and ½ inch thick, mounted on a shaft, which is rotated continuously by a small 1½-rpm motor (*b*) through a worm and spur-gear combination having a 100:1 ratio. Twenty 2-inch holes are drilled near the periphery of the board to carry the platinum crucibles. Two 200-watt heating strips (*c*), 7 inches long and 1¼ inches wide, are mounted below 5 of the holes at such a height that they are just cleared by the platinum crucibles as they move past. The heating strips and the motor are controlled by a single toggle switch (*d*), and they run continuously when the device is in operation. A pointer (*e*) at the end of the heating element

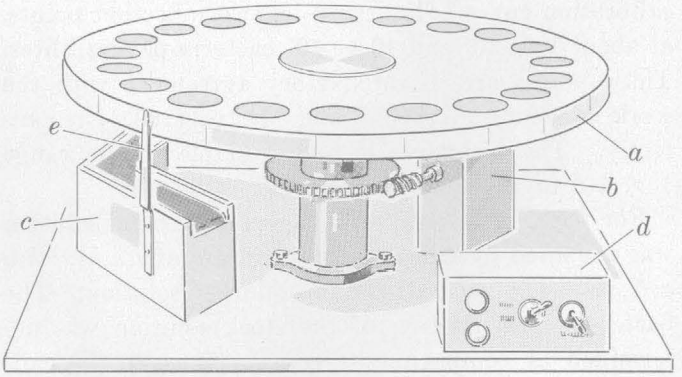

Figure 100.1.—Diagram of the sequential heater. Letters are referred to in text.

conveniently indicates the position for removal of the samples. By experiment it was determined that each sample is boiled for about 10–12 minutes.

The advantage arising from this arrangement is that a reproducible heating time can be obtained semi-automatically for a series of samples. Greater speed is also obtained in that 20 samples per hour can be conveniently titrated.

REFERENCE

Shapiro, Leonard, and Brannock, W. W., 1962, Rapid analysis of silicate, carbonate, and phosphate rocks: U.S. Geol. Survey Bull. 1144–A. (In press.)

101. GEOCHEMICAL FIELD METHOD FOR BERYLLIUM PROSPECTING

By L. E. Patten and F. N. Ward, Denver, Colo.

A quick, reliable analytical method for determining beryllium in soils and rocks is needed to aid in the search for new deposits of the metal. The procedure described below is suitable for determining as little as 1 ppm (part per million), does not require special equipment or highly trained personnel, and is effective on minerals containing beryllium as an accessory constituent as well as on beryllium minerals such as beryl, chrysoberyl, phenakite, bertrandite, beryllonite, and helvite.

The fluorescent complex formed by the reaction of beryllium with morin (3,5,7,2′,4′–pentahydroxyflavone) is often used as a basis of beryllium determinations (Sandell, 1959). The reaction is highly selective and, in the presence of a suitable buffer and chelating agent, is almost specific (Sill and Willis, 1959). Silver and copper in amounts as great as 1 percent are complexed by EDTA (disodium ethylenediaminetetraacetate) or DPTA (diethylenetriaminepentaacetic acid) and do not show any tendency to catalyze the oxidation of the morin. Calcium, aluminum, and lithium form fluorescent compounds with morin and may interfere with the procedure if present in more than the following percentages: calcium (30), aluminum (30), lithium (10). Hydroxides of certain rare earth elements, such as yttrium, also form fluorescent compounds with morin.

The beryllium determinations can be made under field conditions or in a mobile laboratory. The procedure is suitable for determining from 1 to 100 ppm of beryllium in the sample, but with proper adjustment of the sample size or volume of solution taken for analysis, the range is expandable. An analyst experienced with the method can analyze 60 or more samples per day.

REAGENTS

All stock solutions are made with demineralized water and reagent-grade chemicals unless otherwise indicated. The commercial grades of piperidine and DTPA contain fluorescent impurities and need to be purified for acurate work. The piperidine is purified by distillation and the DTPA by recrystallization from water. A high-quality morin should be used.

Ammonium bifluoride, flake.

Beryllium standard solution, 0.01 percent, w/v solution. Dissolve 0.1968 gm of beryllium sulfate tetrahydrate in 100 ml of (1 + 99) sulfuric acid. This solution contains 100 μg of beryllium per ml. This is diluted with (1 + 99) sulfuric acid to make solutions less concentrated in beryllium.

Morin, 0.01 percent. Dissolve 50 mg of morin in about 400 ml of 95 percent ethyl alcohol by heating over a steam bath. Cool and dilute to 500 ml with alcohol.

Morin, 0.0015 percent. Prepare fresh daily by mixing 15 ml of the 0.01 percent solution with 85 ml of water.

Nitric acid, 0.1 *N*. Dilute 3.2 ml of concentrated nitric acid to 500 ml with water.

Piperidine buffer. Weigh 30 gm of DTPA and transfer to a 1-liter flask containing 200 ml of water. Add 150 ml of piperidine, shake contents to mix, and allow the solution to cool. Dissolve 40 gm of anhydrous sodium sulfite in 300 ml of water and combine with DTPA-piperidine mixture. Dilute mixture to 1 liter. The pH of the buffer is about 11.8.

TEA-EDTA solution. Dissolve 5 gm of EDTA and 3 ml of colorless TEA (2,2′, 2″-trinitriloethanol) in 100 ml of water.

EQUIPMENT

The following list does not include items of regular chemical equipment, such as pipets and volumetric flasks, that are required to prepare reagents and standards.

Scoop, calibrated to contain about a quarter of a gram of the sample material.

Mortar and pestle.

Glass test tubes, 25- × 30-mm. Not commercially available; prepare by cutting a 25- × 100-mm culture tube.

Gas burner or propane torch.
Centrifuge tubes or extraction sticks (see Sandell, 1959, p. 735, for description of filter sticks).
Centrifuge (optional).
Test tubes, 22- × 175-mm, marked at 25-ml volume.
Porcelain crucibles, 00 size (optional).
Ultraviolet light, long or short wavelength, battery operated for field use.

PROCEDURE

In a mortar, mix intimately 0.25 gm of finely ground sample with about 0.5 gm of ammonium bifluoride and transfer the mixture to a 25- × 30-mm test tube. Heat the mixture in a sand bath or directly over a gas burner until dense white fumes cease evolving (the sand bath provides even heating). Break up the fused mass with a stirring rod and reheat to a temperature just below red heat until fuming ceases, leaving a dark, usually red, powder in the tube. The ammonium bifluoride is preferable to other fluxes because the low fusion temperature permits the use of glass test tubes that are etched only slightly by the fusion and may be used repeatedly.

Add 5 ml of 0.1*N* nitric acid to the tube and heat to incipient boiling (90°–94°C). Use a polyethylene stirring rod to police down the edges of the test tube. Decant the solution to a centrifuge tube and centrifuge for 5 minutes. If a centrifuge is not available, allow the solution to settle or filter through an extraction stick or filter paper.

Pipet a 2-ml aliquot of the supernatant liquid or filtrate into a calibrated 22- × 175-mm test tube. Add 3ml of TEA-EDTA solution, 5 ml of the piperidine buffer, and 10 ml of the 0.0015 percent morin, in that order. Dilute to mark with water. Stopper, and mix contents.

Estimate the beryllium content of the sample by comparing its fluorescence with that of a series of standard solutions. Prepare the following recommended series of standards for 0.0, 0.1, 0.2, 0.5, 1.0, 2.0, and 5.0 μg of beryllium by transferring appropriate aliquots of the beryllium standard solution to each of a series of 22- × 175-mm test tubes and then adding the TEA-EDTA, piperidine buffer, and morin in the same manner as with the samples. Better comparisons of fluorescence result if small volumes of sample and standard solutions are placed in nonreflecting containers such as small porcelain crucibles.

In the above procedure calculate the beryllium content of a sample in parts per million by multiplying by 10 the number of micrograms of beryllium in the standard. With an aliquot or sample weight differing from that recommended, calculate the beryllium content as follows:

$$\text{Beryllium (ppm)} = \frac{\text{Be } (\mu g)}{\text{sample (g)}} \times \frac{\text{volume of dilute acid}}{\text{volume of aliquot}}$$

RESULTS

This field method has been used to analyze a series of samples with a large range in beryllium content, and the results of one such study are shown in the following table. The results obtained by the proposed field method compare favorably with those obtained by quantitative and semiquantitative spectrographic procedures.

Beryllium content of samples

[Spectrographic analyses by A. W. Helz and E. F. Cooley, U.S. Geological Survey]

Sample	Beryllium (parts per million)		
	Spectrographic		Fluorescent (field method)
	Quantitative	Semiquantitative	
CR–1058–67	<2	15	2
68	7	30	7
69	120	150	80
70	52	70	25
71	29	15	25
72	90	200	50
73	30	70	25
74	<2	2	2
75	460	500	500
76	98	100	85
77	230	500	200
78	100	70	100
79	84	70	75
80	56	50	40
81	16	3	15
82	<2	<1	3

REFERENCES

Sandell, E. B., 1959, Colorimetric determination of traces of metals: New York, Interscience Publishers, 1032 p.
Sill, C. W., and Willis, C. P., 1959, Fluorometric determination of submicrogram quantities of beryllium: Anal. Chemistry, v. 31, p. 598–608.

102. TWO IMPLEMENTS FOR HANDLING SMALL QUANTITIES OF LIQUID

By FRANK C. CALKINS, Menlo Park, Calif.

Although the loop and pipet here described have been found by experience to be the most useful of several implements that were dealt with in earlier papers (Calkins, 1934, 1946a, 1946b), they were treated most fully in the last, which is the least accessible. I have also improved the methods of making and using these implements, and have amplified the data relating to volumes of charges in loops.

UNCLOSED LOOP

The form of the unclosed loop, and a way to fashion a small one, are shown in figure 102.1*A* and *B*. The cut to form the gap can be made with a knife or a dental chisel while the loop rests on a glass slide. The shank may either be wedged into a wooden handle or fused into a piece of Pyrex tubing (fig. 102.1*C*). The loop may be made of platinum wire, but platiniridium has the advantage of being stiffer, and a cheaper material such as Nichrome will often serve the purpose.

The width of the gap should be adjusted as follows: Hold the loop horizontal, dip it in water, and then twitch it upward just far enough to raise it clear of the surface. If the loop is empty, make the gap narrower. If it carries a lens of water, gently bring the wire in contact with a slide; if the water is not all released, make the gap wider. The difficulty of making this adjustment increases with the diameter of the loop, especially if it is made of thin wire; it is rarely worth while, however, to make a loop over 4 mm in outer diameter—and difficult to make one less than 1 mm in outer diameter.

The "quick-horizontal" method of dipping described above gives these desirable results: the charge of a given liquid brought up by a given loop is nearly constant, and it is the largest charge of closely predictable volume that can readily be put into that loop. The amount of a given liquid taken up in this way by a given loop may therefore be called the "normal charge" for that loop and that liquid. Although a larger quantity of liquid can be fed in with a dropping rod (Short, 1931, p. 52), its volume cannot be controlled. A nearly normal charge can be obtained by inserting the loop in liquid hanging from the end of a dropping rod and then drawing it aside, but the quick horizontal dip gives the most nearly uniform results, and it can be used, if due care is exercised, in taking liquid from the neck of a tilted bottle.

In figure 102.1*D*, approximate volumes of normal charges of water at room temperature are plotted against *outer* diameters of loops. The reason for using outer instead of inner diameter is indicated in figure 102.1*E* and *F*. These are merely sketches, but they bring out the readily observed fact that the liquid wets all the inner surface of the wire, and show that if two loops having the same inner diameter are made of different-sized wire, the one made of the thicker wire may take up considerably more liquid

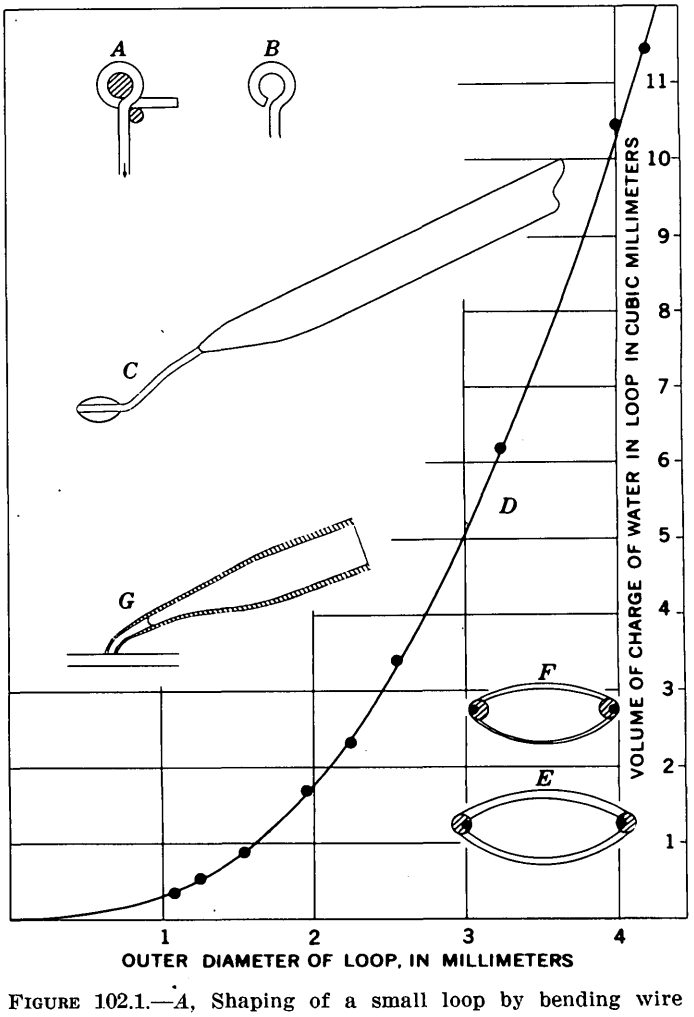

FIGURE 102.1.—*A*, Shaping of a small loop by bending wire around needles driven into a board. *B*, Plan of finished loop, showing gap. *C*, Profile of mounted loop carrying normal charge (× ½). *D*, Normal charges of water in loops, plotted against outer diameters of loops. *E*, Cross sections of normal charges in loops having the same inner diameter but made of thick and thin wire. *F*, As in *E* except that the loops have the same outer diameter. *G*, Longitudinal section of contact pipet carrying normal charge (× ½).

than the other, whereas two loops of the same outer diameter will take up nearly the same amount regardless of the thickness of the wire. Figure 102.1*D* was constructed by determining the aggregate weight of several droplets deposited from each loop tested. The variation in size between individual droplets was not determined, but from visual comparison I judge that it will rarely exceed 10 percent. We can therefore assume that normal charges of similar liquids in a given loop are at least roughly equal; we can expect, for example, that if a normal charge of oil having n 1.546 is added to one of oil having n 1.544, both from the same loop, the n of the mixture will be close to 1.545.

The liquid in a normal charge forms a biconvex lens, and when one lowers a charged loop, under the microscope, toward a small grain for example, the grain presently comes into focus, magnified by this lens. One then instinctively retards the downward motion and centers the loop on the grain. When the liquid reaches the slide it is released very gently, and spreads over a nearly circular area that is as small as the surface tension of the liquid will permit; its diameter has been found to be, on the average, about 1.6 the outer diameter of the loop.

An unclosed loop can thus be made to deliver a droplet of closely predictable size, which can be accurately placed under the microscope and which when released will occupy a small area relative to its volume. These results are all useful in microchemical work, and they cannot be so well attained by using the closed loops figured in laboratory-supply catalogs. A closed loop given a quick horizontal dip brings up as much liquid as an unclosed loop of the same diameter and made of the same wire. It does not release all of its charge, however, when brought in contact with a slide. The amount of liquid it retains depends in part on the thickness of the wire, whose effect is sufficiently allowed for in unclosed loops by measuring outer diameter; but it also varies to an unpredictable extent with the way in which the loop is applied to the slide. The liquid retained, moreover, will sometimes bring up small solid particles from a sample of powder, which cannot happen when the liquid is all deposited.

The mode of dipping is important. My experience indicates that the one described not only gives the best results but is the easiest one to practice consistently. An unclosed loop dipped slowly will usually come up empty. A closed loop held horizontal and raised slowly will aways bring up a charge, but it brings up a smaller one than if it is raised quickly; and when held vertical and raised slowly, as is sometimes advised, it brings up a concave lens of liquid—a mere film if the loop is made of thin wire—which is hard to release on a slide and impossible to place accurately.

Very small loops are most likely to be used on polished sections, but a droplet laid down with a 1-mm loop will spread over a circle about 1.6 mm in diameter, and as its volume is only about 0.3 mm^3 it may dry up before doing its work. It can be held in place almost indefinitely, however, by covering it with oil, which can be gently deposited from a large unclosed loop, and it can then be kept at a fairly high temperature as long as it is not made to vaporize. The same procedure may be applied to grains, which can most readily be kept in place by putting them in the hollow on a culture slide.

CONTACT PIPET

Two pipets of the form shown in figure 102.1*G* can be made by heating the middle of a piece of glass tubing, drawing the two halves apart, and gently reheating the tapered end of each until it bends downward. A plane surface must then be ground on the tip. A tip of relatively large diameter can be ground by rubbing it on fine sandpaper or abrasive cloth, but for one of very small diameter it is better to use a carborundum hone, over which the small end of the tube, after being dipped in water, is repeatedly drawn a short distance toward the right (if the operator is right-handed). The ground surface should be at such an angle with the axis of the tube that it can readily be brought in close contact with a slide under the microscope—hence the term "contact pipet." This angle is about 25°, but its correctness should be tested by charging the pipet with water and then seeing whether, under the microscope, it readily deposits a droplet when brought in contact with a slide; if not, its tip must be reground at such an angle that it will. The ground surface need not be very smooth and must not be fire-polished. A tip as little as 0.5 mm in outer diameter can be finished in this way.

The pipet is given what may be called its "normal charge" by immersing its tip while the tube slopes about 25°, and letting the liquid rise as far as capillary action will take it. (It can be "supercharged" by holding it level.) The first droplet deposited from a normal charge on contact with a slide has about 1.3 the volume of the normal charge in a loop of the same outer diameter as the tip of the pipet, but if several droplets are deposited from the same charge each one is a trifle smaller than the last, which makes the pipet less useful than the unclosed loop as a measuring implement. It can be used, however, for

transferring liquid from one place to another. When, for example, one or more small mineral grains have been covered with an immersion oil that is found not to have the desired index of refraction, this oil can be removed as follows: (a) mix the oil with xylene by putting a droplet of xylene beside it with a pipet (about 1½ mm in tip diameter)—which can supply several droplets from one supercharge; (b) take up the mixture with a smaller pipet; and (c) drain this pipet by touching its tip to absorbent paper. Repeat these operations until the grain is sufficiently clean to be covered with another oil; if a cover glass is not used, time as well as material can be saved by applying the oil with a loop rather than a dropping rod.

REFERENCES

Calkins, F. C., 1934, Transfer of grains from one liquid to another: Am. Mineralogist, v. 19, no. 4, p. 143–149, 1 fig.

——— 1946a, Picking up grains: Am. Mineralogist, v. 31, nos. 9–10, p. 503–506, 1 fig.

——— 1946b, Simple devices for measuring out small quantities of liquid: Jour. Chemical Education, v. 23, p. 604–608, 2 figs.

Short, M. N., 1931, Microscopic determination of the ore minerals: U.S. Geol. Survey Bull. 825, 204 p.

103. USING A BRUNTON COMPASS AND A SPRING WIRE FOR WEIGHING SMALL SAMPLES

By Lyman C. Huff, Denver, Colo.

Geochemical-prospecting tests commonly require many repetitive weighings of samples in makeshift field laboratories. To make these weighings the field analyst must either transport an analytical balance to the field laboratory or resort to a volumetric scoop. The spring balance described here is easier to transport than a standard analytical balance and is much more accurate than a volumetric scoop.

The balance consists of a 12-inch length of springy wire such as piano wire mounted on a wood box such as that used for holding analytical weights (fig. 103.1). One end of the wire is held between two rubber washers on a small round-headed wood screw in the side of the box. After the wire is placed between the rubber washers, the screw is tightened so that the wire is held firmly at an angle of about 30° from horizontal.

The balance pan on the opposite end of the wire is folded from a thin aluminum sheet and is mounted on a small cork. The wire goes through the center of the cork, and a right angle bend at the end of the wire is imbedded firmly in a razor cut in the end of the cork. The edge of the balance pan is imbedded in the same razor cut.

To use this balance, the analyst views the wire against a reference mark centered on the mirror of the Brunton compass. The Brunton compass, with the mirror vertical, is placed on a thick book or brick so that it is slightly higher than the weight box. The analyst places the desired weight in the pan and levels the sighting arm tip of the Brunton compass so that when sighting from the tip the wire is near the reference mark and the reflection of the wire in the mirror shows no parallax. The final adjustment to bring the wire exactly over the mark is made by gently sliding the compass back and forth. A pipe cleaner mounted vertically on a suitable base can be pressed gently against the middle of the spring wire to dampen its vibrations.

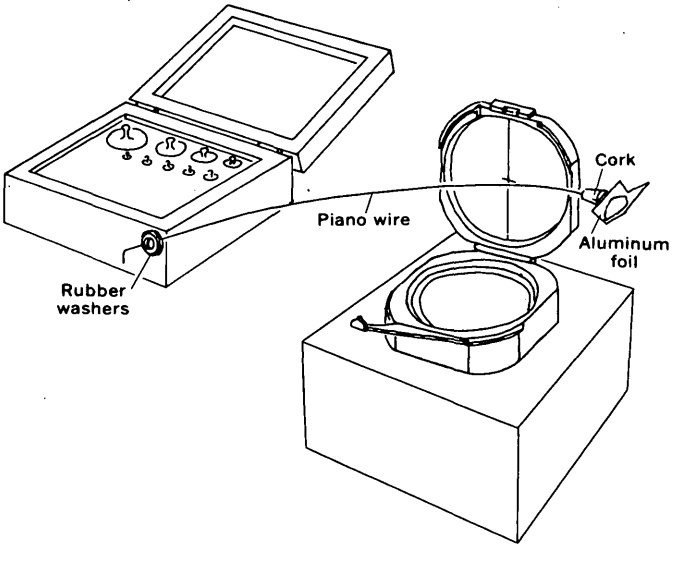

Figure 103.1.—Spring balance and Brunton compass used in weighing small samples.

639466 O - 62 - 8

After the balance is adjusted, samples are weighed by replacing the known weight on the pan with the amount of sample that returns the spring wire to the reference mark. The pan can be emptied into a digestion t· be by holding the cork and gently twisting. If the pan is mounted securely, the wire should return to the reference mark when tested with the known weight.

The wire for the balance can be selected according to the weight to be measured. A 12-inch length of 0.030-inch-diameter steel piano wire is convenient for weighing 1.0-g samples, and a similar length of No. 26 Nichrome wire is convenient for weighing 0.05-g samples. Other wires can be used for intermediate weights. Normally, samples to be weighed in geochemical prospecting are in the range from 0.05 to 1.0 g.

To compare the results obtained with a spring balance and with a scoop, 5 analysts each measured ten 50-mg portions of plant ash by both methods and then weighed the measured portions with an analytical balance. The spring used in the spring balance was a 12-inch length of No. 26 Nichrome wire; when in adjustment with 50 mg on the balance pan, an increase of 5 mg caused a 2.5-mm deflection of this wire from the reference mark. The scoop used was a small cavity drilled in a plastic strip and designed to hold 50 mg of plant ash. The true weight of the scooped portions shows that, for all analysts, scooping yielded too little leaf ash and too much twig ash (see table). The deviation or error for each measured portion of ash was calculated in terms of the overall average weight of 49.0 mg for scooped portions and 49.7 mg for portions measured with the spring balance. Errors for samples measured by the spring balance amount to 1 percent on the average, whereas errors for samples measured by the scoop amount to 16 percent. None of the analysts found that weighing of samples by spring balance took significantly longer than measuring by scoop.

Weight, determined by analytical spring balance, of measured portions of 10 plant ashes. Portions were measured by scoop and by spring balance to equal 50 milligrams

[Samples from 5 mesquite trees]

Analyst	Scoop				Spring balance			
	Average weight (mg)			Average deviation (mg) [1]	Average weight (mg)			Average deviation (mg) [2]
	Leaf	Twig	Both		Leaf	Twig	Both	
A	42.1	55.6	48.9	7.0	49.2	50.1	49.6	0.8
B	43.9	57.2	50.6	7.3	49.6	49.9	49.8	.4
C	38.1	52.5	45.3	9.5	49.9	50.1	50.0	.3
D	40.5	54.6	47.6	8.4	49.5	49.6	49.5	.5
E	44.8	60.0	52.4	7.9	50.0	49.2	49.6	.5
Average	41.9	55.9	49.0	8.0	49.6	49.8	49.7	0.5

[1] From 49.0 mg, the average weight of both types of sample.
[2] From 49.7 mg, the average weight of both types of sample.

HYDROLOGIC STUDIES

ENGINEERING HYDROLOGY

104. INTERBASIN MOVEMENT OF GROUND WATER AT THE NEVADA TEST SITE, NEVADA

By Isaac J. Winograd, Las Vegas, Nev.

Work done in cooperation with the U.S. Atomic Energy Commission

Hunt and Robinson (1960) have suggested that ground water may be moving through ridges of Paleozoic carbonate rocks that separate Death Valley from the flanking intermontane basins. Their argument is based upon chemical analyses of spring water. Hydraulic evidence for interbasin circulation of ground water through carbonate rocks of Paleozoic age at the Nevada Test Site is presented in this paper, which is a byproduct of studies to evaluate the potential risk of contamination of ground water by underground nuclear testing at the test site.

The Nevada Test Site is in the Basin and Range physiographic province in south-central Nevada, just north of the California State line and northeast of

Death Valley and the Amargosa Desert (fig. 104.1), and includes three large intermontane basins—Yucca Flat, Frenchman Flat, and Jackass Flats (fig. 104.2).

Paleozoic sedimentary rocks, totaling more than 22,000 feet in thickness, have been intensely deformed by thrust and high-angle faulting (Johnson and Hibbard, 1957, p. 335–336, 369–380). These strata are overlain unconformably by welded and semiwelded ash-flow and ash-fall tuffs of Tertiary age that generally are less than 5,000 feet thick. Block faulting has displaced both the Paleozoic strata and the Tertiary pyroclastic rocks as much as 2,000 feet, creating troughlike depressions. Valley fill washed into these troughs is as much as 1,900 feet thick in south-central Yucca Flat.

When this study was started in 1960, only 8 wells had been drilled to the regional water table beneath the 3 basins of major interest. Five of the 8 wells tapped water in tuffaceous aquifers and 3 tapped water in the valley fill at depths ranging from 700 to 1,700 feet.

The altitudes of the static water levels in these wells ranged only from about 2,390 to 2,440 feet above

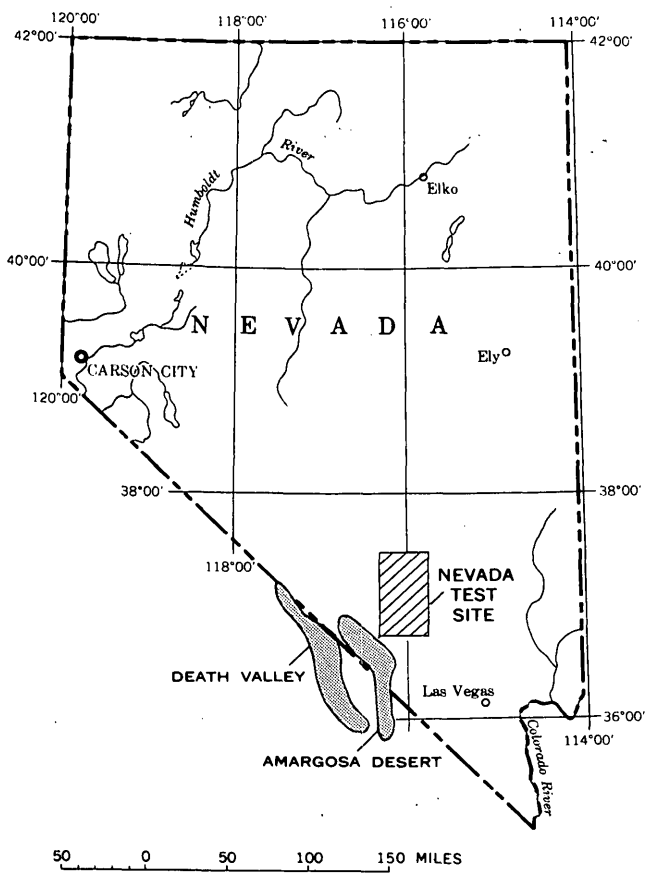

FIGURE 104.1.—Map of Nevada showing the Nevada Test Site, Death Valley, and the Amargosa Desert.

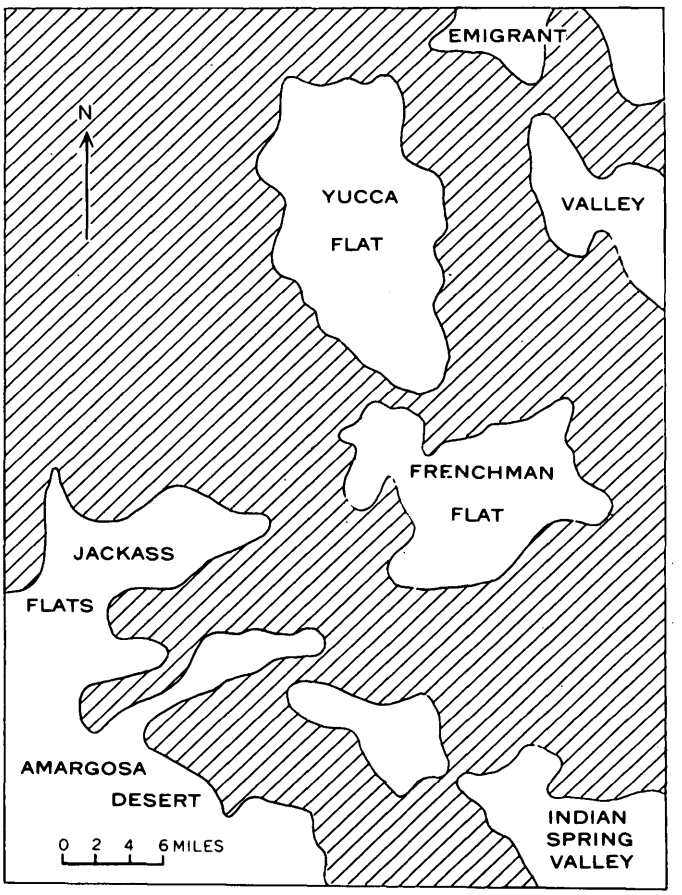

FIGURE 104.2.—Map of the Nevada Test Site showing the major intermontane basins and the intervening mountains (shaded).

sea level. This similarity in altitudes suggested a hydraulic connection between the three basins; this was supported to a degree by the diversity in altitudes of the piezometric surfaces beneath adjacent basins. The water-level altitudes in Gold Flat, Kawich Valley, and Emigrant Valley, northwest, north, and northeast respectively of Yucca Flat, ranged from 1,100 to 2,500 feet higher than those within the test site, and those in the southern half of Indian Spring Valley to the southeast were 800 to 900 feet higher. Thus, water levels in wells in the three basins on the site were close to a common altitude, but were much lower than levels in adjacent basins.

The available control indicated no hydraulic gradient between the basins. Moreover, the range in water-level altitudes within the individual basins was 15 to 40 feet, almost as great as the range between the basins.

Test drilling done in Yucca Flat in 1960–61 supplied answers for many of the questions that had arisen. Six test holes penetrated aquifers in valley fill, tuff, and Paleozoic strata, and a thick, relatively

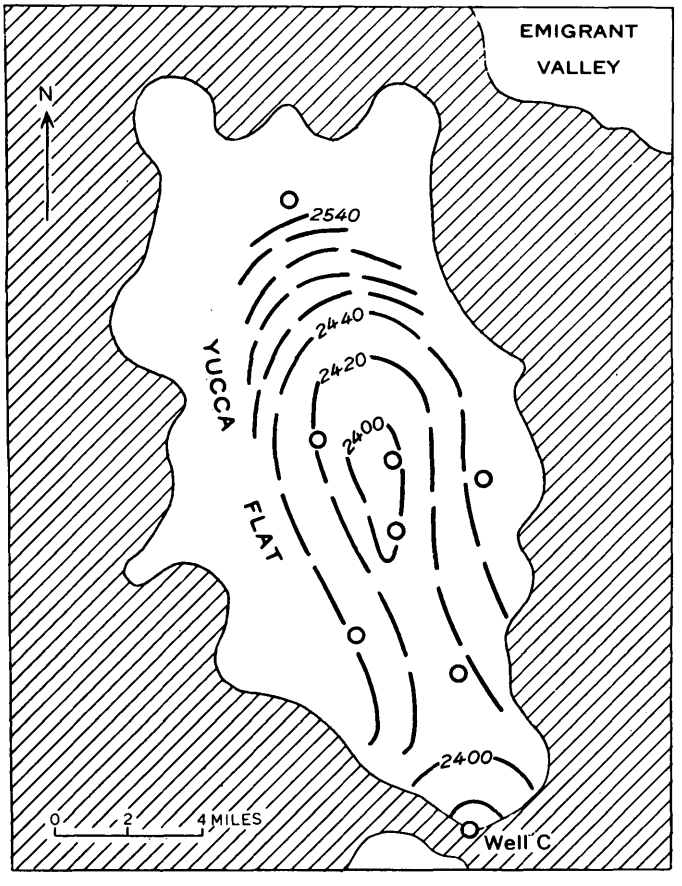

FIGURE 104.3.—Configuration of the piezometric surface, Yucca Flat, Nevada Test Site. Contours represent altitude of water levels in wells penetrating 50 feet or less of saturated rocks. (Datum, mean sea level; interval, 20 feet.)

impermeable zeolitized tuff. Hydraulic tests of the aquifers indicate that the Paleozoic carbonate rocks locally have the greatest transmissibility, the Paleozoic clastic rocks the least, and the tuff and valley fill intermediate values. The coefficients of transmissibility range from less than 1,000 gallons per day per foot for some tuffs and the Paleozoic clastic aquifers, to more than 100,000 for some carbonate strata.

Intensely zeolitized or clayey tuffs form the lower part of the section of Tertiary pyroclastic rocks; they range in thickness from 200 to more than 1,500 feet, and they separate the relatively permeable tuff or valley-fill aquifers from the Paleozoic carbonate-rock aquifers, which locally are of greater permeability.

Periodic measurements of water level were made in each test well as the saturated zone was penetrated. In 3 wells in zeolitized tuff, a drop in head of 20 to 50 feet was noted in drilling through the tuff. In one of these, the head dropped just before or immediately after drilling into Paleozoic dolomite.

The relative permeabilities of the valley fill, the tuff, and the carbonate-rock aquifers, and the decline in head as the zeolitized tuff was penetrated indicate that water in the Cenozoic aquifers of Yucca Flat moves vertically by drainage into the locally more permeable underlying Paleozoic carbonate and then laterally out of the area. Thus, the water in the Cenozoic rocks is semiperched with respect to water in the Paleozoic carbonate rocks.

The vertical drainage is illustrated on figure 104.3 by piezometric contours based on water levels in eight wells. Five of the wells tap tuff, 1 taps valley fill, 1 taps dolomite, and 1 taps interbedded argillite and dolomite. The water-level measurements used in constructing the map were, with one exception, made before more than 50 feet of the aquifer had been penetrated. The sink, or depression, near the center of the valley strongly suggests that drainage of the Cenozoic rocks is into the underlying strata. Only the horizontal component of the hydraulic gradient is portrayed on the map; other data collected during the study suggest that the vertical component may be several times greater than the horizontal.

The semiperched conditions observed in Yucca Flat, and suggested by data from 3 wells in Frenchman Flat, afford an explanation for the apparent absence of a hydraulic gradient between the 3 basins. The eight wells drilled in earlier investigations all tapped water in Cenozoic aquifers. In any of these wells the water-level altitude probably was affected by the depth of penetration into the zone of saturation, the thickness and degree of fracturing of the relatively impermeable zeolitized tuff, and the permeability of the underlying Paleozoic strata; thus it is not surprising that the water-level altitudes in adjacent wells differed considerably. When taken together these eight altitudes seemingly fitted no pattern and afforded no clue to the direction of ground-water flow.

The similarity in the altitude of the piezometric surface of the semiperched aquifers in Yucca Flat, Frenchman Flat, and Jackass Flats is best explained by assuming that the three basins are hydraulically connected by tortuous movement of ground water along fracture zones in carbonate strata. This assumption is supported by the locally great permeability of the carbonate rocks and by their widespread subsurface distribution.

Data from test well C, which taps highly fractured limestone, indicate that such circulation of ground water is both possible and probable (fig. 104.3). The static water level is 10 to 170 feet lower than the static water level in all wells within a 25-mile radius that tap water in Cenozoic rocks or Paleozoic clastic strata, but it is 15 to 20 feet higher than the highest

known water level at Ash Meadows in the eastern part of the Amargosa Desert.

Ash Meadows, about 35 miles southwest of Yucca Flat, is an important area of natural ground-water discharge. Some of the discharge, which is estimated to exceed 18,000 acre-feet annually (Loeltz, 1960, p. 1917), issues from Paleozoic carbonate rocks. As Ash Meadows is the nearest point of large natural discharge and the hydraulic gradient suggests movement of ground water in that direction, presumably the discharge consists in part of water from the test site area.

In summary, the movement of ground water in the valley fill and the tuffs beneath the bolsons of the Nevada Test Site is vertically downward into the Paleozoic carbonate rocks. The ground water moves laterally in the carbonate rocks, though probably circuitously, beneath all three basins toward discharge areas, presumably to the southwest.

The present study, plus the work of Hunt and Robinson, and of Loeltz, indicates that ground-water flow beneath some intermontane basins in south-central Nevada differs significantly from that previously reported, in which ground-water flows either down the axis of a bolson to a spill point at one end of the basin, or toward discharge areas within the basin, such as playas or springs.

The present studies suggest that future appraisals of the ground-water resources of some valleys should take into account possible underflow through the consolidated rocks flanking and underlying the valley fill. They suggest further that an evaluation of the suitability of bolsons for the disposal of radioactive wastes may require a thorough study of the hydrology of the flanking basins.

REFERENCES

Hunt, C. S., and Robinson, T. W., 1960, Possible interbasin circulation of ground water in the southern part of the Great Basin: Art. 123 *in* U.S. Geol. Survey Prof. Paper 400–B, p. B273–B274.

Johnson, M. S., and Hibbard, D. E., 1957, Geology of the Atomic Energy Commission Nevada proving grounds area, Nevada: U.S. Geol. Survey Bull. 1021–K.

Loeltz, O. J., 1960, Source of water issuing from springs in Ash Meadows Valley, Nye County, Nevada [abs.]: Geol. Soc. America Bull. v. 71, p. 1917.

105. POTENTIAL AQUIFERS IN CARBONATE ROCKS, NEVADA TEST SITE, NEVADA

By Stuart L. Schoff and Isaac J. Winograd, Denver, Colo., and Las Vegas, Nev.

Work done in cooperation with the U.S. Atomic Energy Commission

Carbonate rocks at many places yield moderate to large quantities of water to wells, but until recently the carbonate rocks at the Nevada Test Site had not been tapped, although they constitute about three-fourths of the 22,000 feet of Paleozoic strata described by Johnson and Hibbard (1957, p. 335–369). Their ground-water potential is suggested by springs that issue from limestone at Ash Meadows, 55 miles southwest of the test site, and Indian Springs, 50 miles southeast. Their permeability probably results from fractures, because carbonate rocks generally have but little interstitial permeability and those at the test site seem not to have large or extensive solution openings.

Six core holes were drilled in 1959–60 in the northern part of Yucca Flat, Nevada Test Site; two of them are described in this article. The core-hole records give some indication of the permeability of the carbonate rocks penetrated, and a pumping test of a well in the southern part of Yucca Flat, also described in this article, gives further indication. The location of the core holes and the tested well is shown on figure 105.1.

Core hole U12e.M–1 penetrated dolomite, probably the undifferentiated Devils Gate Limestone and Nevada Formation of Devonian age. The hole was drilled vertically from a drift nearly a mile from the portal and a quarter of a mile below the land surface. The hole began in tuff, entered dolomite at 974 feet, and ended in the dolomite 1,501 feet below the drift and 2,870 feet below the land surface. Casing and cementing operations probably sealed the upper part of the hole, so that the water-injection test reported here applies only to the 507.5 feet of uncased, uncemented hole in the dolomite (fig. 105.2).

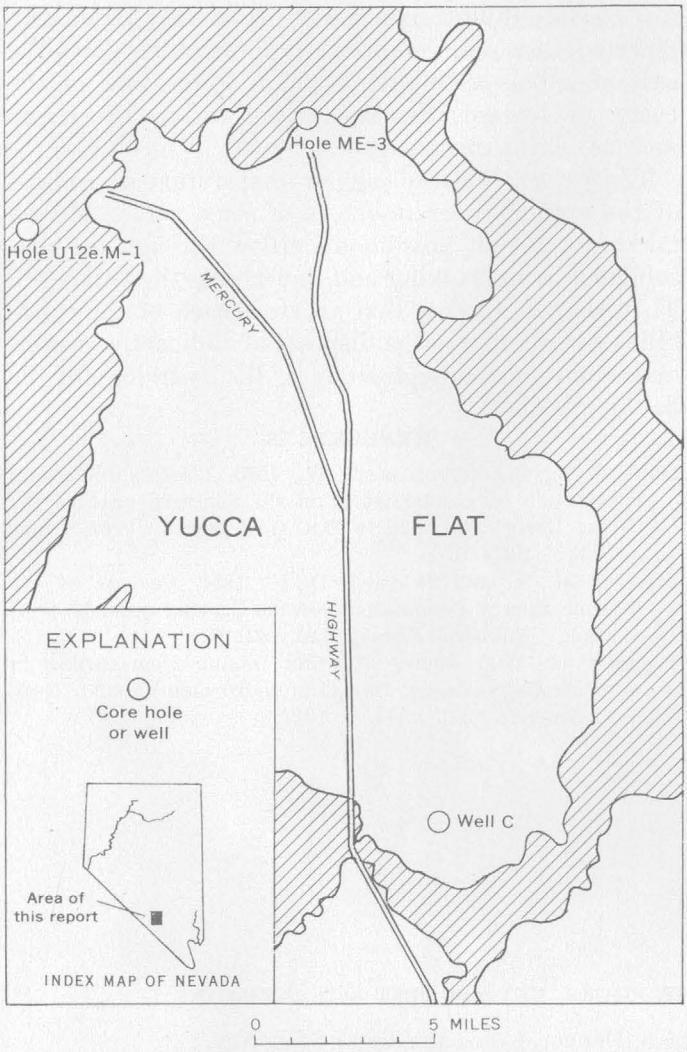

FIGURE 105.1.—Map of Yucca Flat, Nevada Test Site, showing location of core holes and tested well. Shaded areas are mountains.

The permeability of the rocks was demonstrated qualitatively during drilling operations by the loss of large volumes of drilling fluid into the hole, despite the use of bentonite in the fluid and the addition of bagasse when fluid losses were unusually severe. The quantity of water used in drilling was not measured, but it probably paralleled the use of bentonite, which was substantially greater in the dolomite than in most of the tuff (fig. 105.2).

The permeability of the rocks was demonstrated also by a water-injection test in which 785 gallons of water was pumped into the hole and the ensuing decline of water level was observed. An average of 6.3 gallons per minute entered the rock opposite the uncased, uncemented section of the hole while the water level declined the first 100 feet. The uncased, uncemented section of the hole was 3 inches in diameter, and if the diameter were uniform about 0.78 square foot of rock surface per foot of depth would have been exposed, or a total of about 400 square feet. The rock, therefore, received an average of 0.016 gallon of water per minute per square foot of rock surface. The hydrostatic pressure ranged from 650 pounds per square inch at the bottom of the open section at the beginning of the decline, to 357 pounds per square inch at the top of the open section, when the water level reached a depth of 100 feet.

The rock took in water despite bentonitic mud and bagasse that probably remained on the walls of the hole and in the fractures and other possible openings. The dolomite, therefore, probably contains open fractures, perhaps to the bottom of the hole, although it seems to have been unsaturated. Periodic measurements in the hole showed a decline of fluid level to within 15 feet of the bottom of the hole, the greatest depth at which the measurements were successful. The fluid probably was only drilling mud or mud filtrate.

Core hole ME–3 (fig. 105.1) penetrated 951 feet of

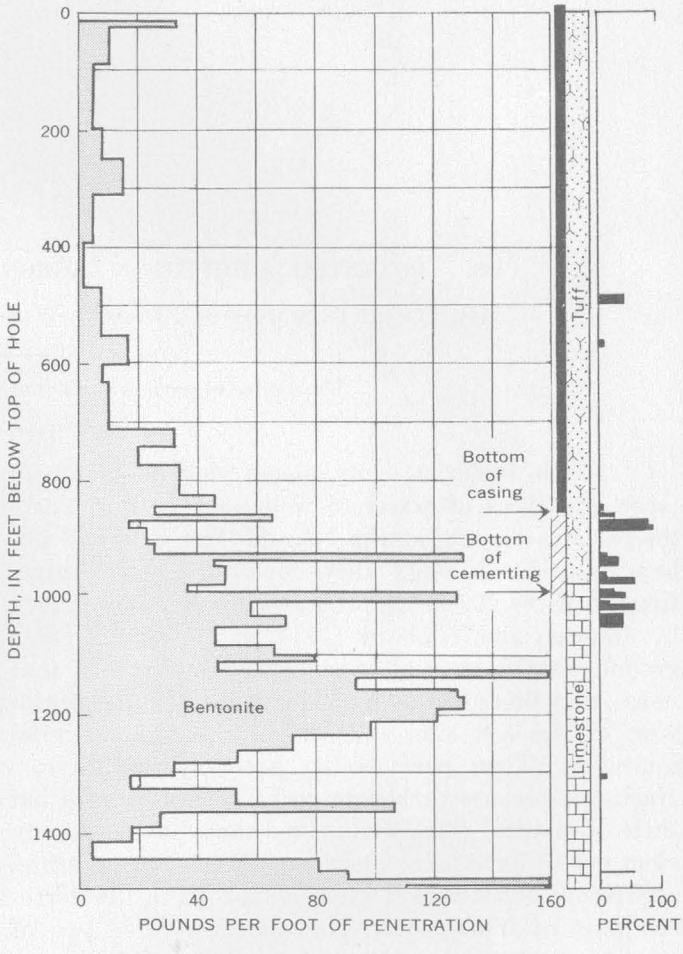

FIGURE 105.2.—Amount of bentonite used per foot of penetration and percentage of core not recovered, core hole U12e.M–1.

marble of the Pogonip Group of Ordovician age and 27 feet of underlying granodiorite. The hole probably entered a saturated zone. A total of 243,000 gallons of water was used in drilling operations, and the average per foot of penetration, nearly 250 gallons, indicates a moderate rate of infiltration. A plunger pump was installed in the hole, and water was pumped continuously for about a week at an average rate of about 6 gallons per minute. The drawdown resulting from this pumping could not be detected in measurements of water level made by the airline method, indicating significant permeability.

The total pumpage from hole ME–3, about 60,000 gallons, was only about one-fourth the quantity of water put into the hole during drilling operations, but part of the pumped water probably was formation water because (1) drawdown should have increased progressively during pumping if only drilling fluid had been pumped, but, actually, drawdown was not detectable by the airline method; (2) chemical analyses show that a magnesium bicarbonate water was pumped from the hole, whereas a sodium bicarbonate water had been introduced as drilling fluid; (3) the fluid level in the hole rose slightly for 7 months, beginning 3 months before pumping started, whereas the level probably would have declined if only drilling fluid had been in the hole and had been draining into unsaturated rock; (4) the altitude of the static fluid level is within 40 feet of that in another core hole 900 feet distant, suggesting that the 2 holes penetrate a common zone of saturation.

Well C is one of several test wells drilled for the Atomic Energy Commission. Completed in 1961, it tapped water only in limestone of Paleozoic age between depths of 1,543 and 1,701 feet. The well was pumped for 5 hours at 212 gallons per minute, but the drawdown, measured with an electrical sounder, was so small that it was largely obscured by water-level fluctuations due to changes in barometric pressure. The data from this test indicate that the coefficient of transmissibility is more than 100,000 gallons per day per foot for the 158 feet of saturated limestone penetrated by the well. The limestone has not been identified as to formational unit.

The Pogonip Group and the undifferentiated Devils Gate and Nevada Formations, together with the unidentified limestone in well C, may be aquifers worth further exploration. Where saturated they may be capable of yielding substantial quantities of water to wells.

The core holes and the well provide data on only a few of many carbonate-rock formations at the Nevada Test Site. The other carbonate-rock formations, however, are highly fractured in many exposures, and, therefore, they too may be worthwhile aquifers.

REFERENCE

Johnson, M. S., and Hibbard, D. E., 1957, Geology of the Atomic Energy Commission Nevada proving grounds area, Nevada: U.S. Geol. Survey Bull. 1021–K, p. 333–384.

106. HYDROLOGY OF RADIOACTIVE WASTE DISPOSAL IN THE MTR-ETR AREA, NATIONAL REACTOR TESTING STATION, IDAHO

By Paul H. Jones and Eugene Shuter, Idaho Falls, Idaho

Work done in cooperation with the U.S. Atomic Energy Commission

Aqueous low-level radioactive waste of the Materials Testing Reactor-Engineering Test Reactor (MTR–ETR) facility at the National Reactor Testing Station (NRTS) has been discharged to a leaching pond since operations began in 1952. The discharge has been less than 10^{-3} μc per ml (microcuries per milliliter); the annual rate reached about 1,000 c (excluding tritium) in 100 million gallons of water by 1955, and has averaged about 3,700 (excluding tritium) in about 220 million gallons of water annually since 1957 (B. L. Schmalz, written communication, 1962). The radioactive waste discharged has included as many as 40 to 60 radioactive isotopes, about 90 percent of which have a half life of less

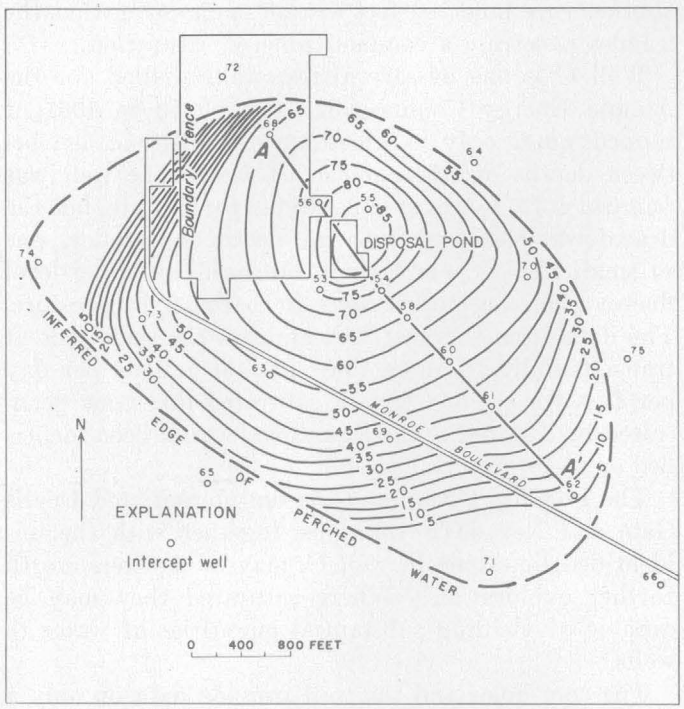

FIGURE 106.1.—Lines of equal thickness and areal extent of the perched-water zone in basalt beneath the alluvium of the Big Lost River in the MTR–ETR area in March 1961, and location of section *A–A'* (fig. 106.2). (Interval, 5 feet.)

than 100 days. About 50 percent of the water discharged to the pond was nonradioactive waste from water-treatment facilities, cooling-tower purge lines, and other sources. The pH of the water ranged from less than 3 to more than 9 over a period of a few weeks, the temperature was above 60°F on the average, and the dissolved-solids content was generally more than double that of the ground water of the regional ground-water reservoir. The tritium content of the waste water during the period 1952–60 is not known, but recent analyses indicate a concentration in the magnitude of 10^{-4} μc per ml. There is no evidence that the concentration has varied during recent operations.

The disposal pond occupies an L-shaped excavation about 460 feet from north to south and 300 feet from east to west (fig. 106.1). It is about 11 feet deep, and the water level is generally 5 to 7 feet below its rim. The alluvium of the Big Lost River, in which the pond is excavated, is locally composed of sand, gravel, and small cobbles. It ranges in thickness from about 40 to 60 feet and is underlain by Snake River Basalt. (R. L. Nace and others, unpublished data, 1956; R. L. Nace and others, unpublished data, 1959). Locally the regional water table is about 460 feet below the land surface, and the natural moisture content of the rocks above the water table ranges from about 8 to 11 percent.

Seepage from the pond has moved downward through the alluvium of the Big Lost River, entered the underlying basalt, and become perched on an extensive sedimentary bed that lies 110 to 160 feet below the land surface (fig. 106.2). A thin zone of perched water that occurs in fine-grained sediments at the base of the alluvium of the Big Lost River immediately above the basalt extends about 400 feet southeastward from the pond. The underlying zone of perched water in the Snake River Basalt is roughly elliptical in shape, more than 1 mile long, and ½ mile wide (Schmalz, 1961) (fig. 106.1). Beneath the vicinity of the pond the water body perched in basalt is more than 85 feet thick. The sedimentary bed that underlies the perched zone in the basalt has become wetted to a depth of several feet, and this bed, only,

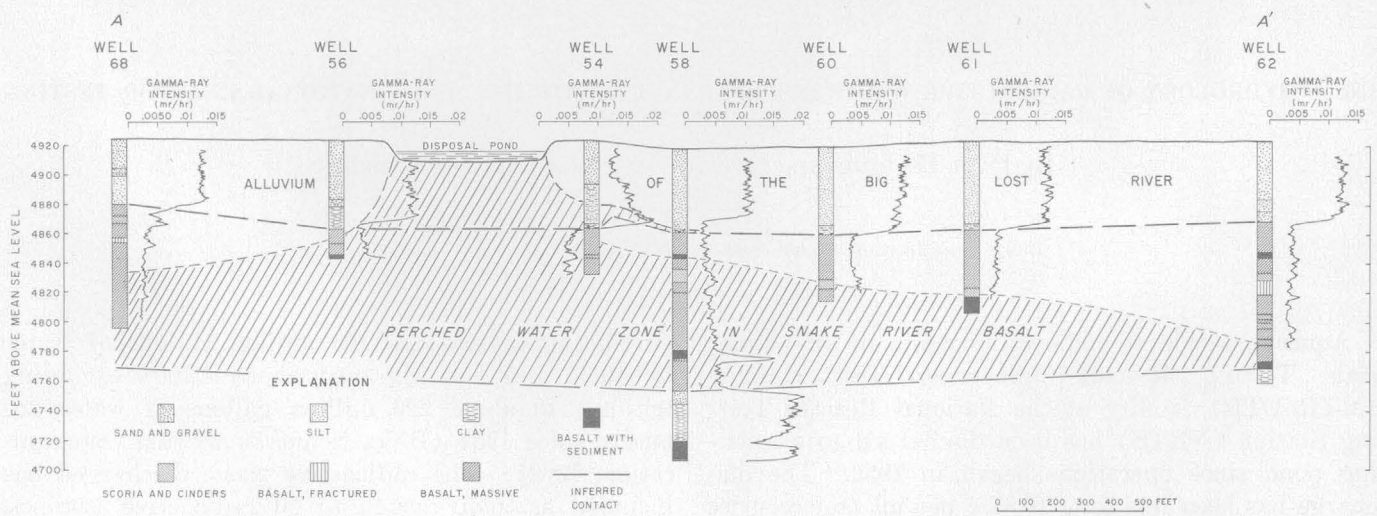

FIGURE 106.2.—Section in the vicinity of the MTR–ETR disposal pond along line *A–A'* (fig. 106.1).

is saturated at the extreme edges of the perched-water zone near wells 71 and 74 (fig. 106.1). The base of this zone of perched water is more than 300 feet above the regional water table, which in this area slopes southwestward about 2.5 feet per mile.

The size of the body of perched water beneath the MTR–ETR area is great enough to contain all waste water discharged to the pond since operations began in 1952 if the average effective porosity of the rock is about 25 percent. Losses to evaporation and to unsaturated and saturated flow laterally in the alluvium of the Big Lost River are not considered in this estimate. Radioactive-waste liquids are believed to have reached the regional ground-water reservoir only down the bores of test wells.

Records of the temperature of waste water discharged to the pond do not exist, but the temperature now is generally above 60°F and probably has not differed greatly from year to year. The temperature of the perched water (fig. 106.3) ranges from 60°F to 49°F, decreases with distance from the pond, as might be expected, and is coldest southward and southeastward from well 61. Restriction of flow through the vicinity of well 61, or a change in the texture, type, or porosity of the rock, may be responsible. Such differences are indicated elsewhere by the contrast of thermal gradients in different directions from the pond. It may be inferred that preferred directions of flow are westward, southwestward, and south-southeastward from the pond. The thermal conductivity of the rock, its structure and natural moisture content, and the heat of wetting (Hogentogler, 1937, p. 385) must also be considered in a flow analysis based on the temperature map.

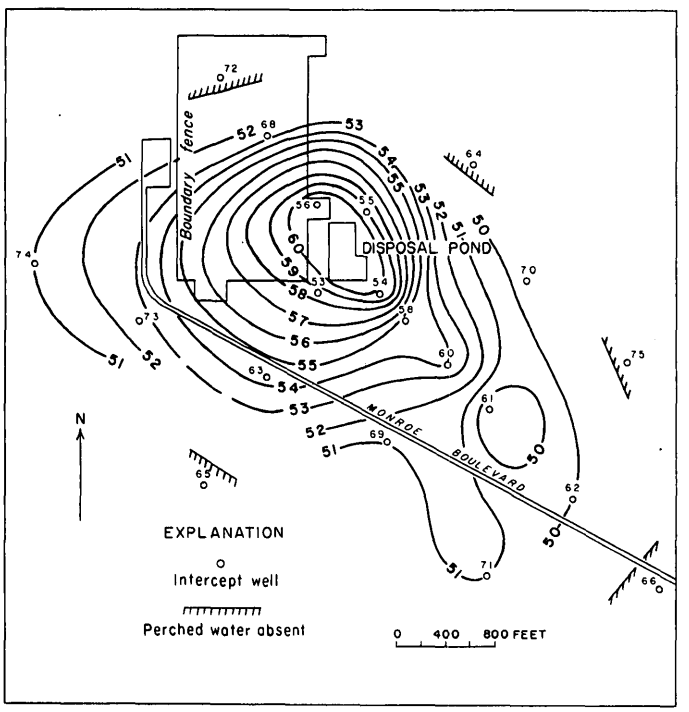

FIGURE 106.3.—Temperature of perched water underlying the alluvium of the Big Lost River in the MTR–ETR area in late January and early February 1961. (Interval, 1°F.)

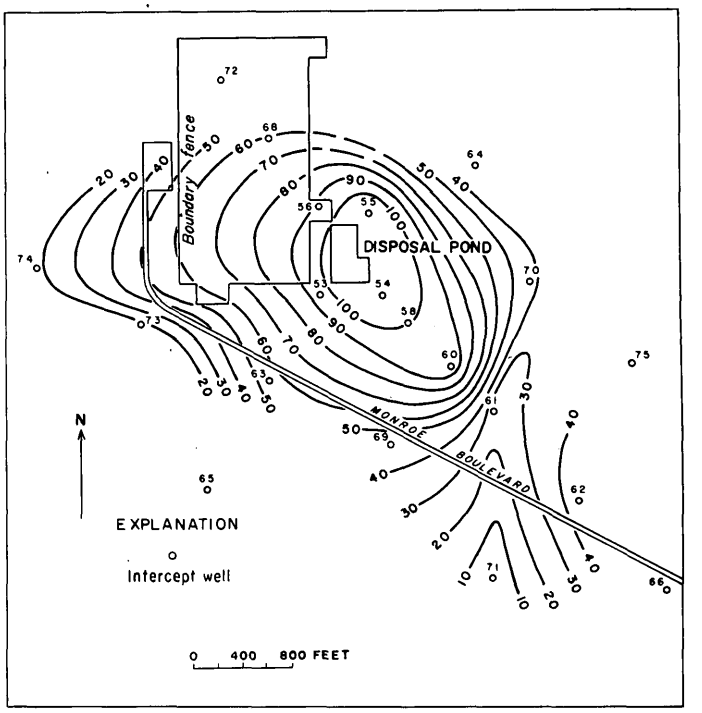

FIGURE 106.4.—Lines of equal tritium content of perched water underlying the alluvium of the Big Lost River in the MTR–ETR area on July 14, 1961. (Interval, 10 μc per ml $\times$ 10^{-5}.)

The tritium content of the perched water ranged from about 10×10^{-5} μc per ml to 100×10^{-5} μc per ml on July 14, 1961 (fig. 106.4). The natural tritium content of the water in the zone now occupied by perched water before waste disposal began is not known, but presumably it was less than 1.6×10^{-7} μc per ml. The tritium content of the perched water decreases with distance from the pond (fig. 106.4) except southeastward from well 61. This tends to confirm inferences regarding the flow of perched water based on the temperature map (fig. 106.3), although the tritium content of water from well 61 is not the lowest in the area and the concentration gradient southward from it is not analogous to the thermal gradient. Nevertheless the isopleths of tritium content form a pattern very similar to that of the isotherms. Possibly the tritium content of discharged waste water has increased progressively with time,

or there may be more dilution by preexisting water than has been supposed. If the tritium content of waste water has been relatively uniform since discharge to the pond began in 1952, which seems likely, and if the water at the outer edge of the perched-water body is indeed water discharged in 1952, the tritium content now observed is much too low.

REFERENCES

Hogentogler, C. A., 1937, Engineering properties of soils: New York, McGraw-Hill.

Schmalz, B. L., 1962, Waste disposal practices and programs at the National Reactor Testing Station, Idaho: Atomic Energy Commission Working Conference on Ground Disposal of Radioactive Waste, 2d, Chalk River, Ontario, Proc. (in press).

107. ARTIFICIAL RECHARGE OF BASALT AQUIFERS, WALLA WALLA, WASHINGTON

By ARTHUR A. GARRETT, Tacoma, Wash.

Work done in cooperation with the State of Washington, Department of Conservation, Division of Water Resources

Data from a recent series of artificial-recharge tests on a well tapping the Columbia River Basalt at Walla Walla suggest that a schedule of short periods of recharge followed by immediate surging may eliminate the reduction in well yield that resulted during earlier testing. The first attempt at artificially recharging the ground-water reservoir at Walla Walla through wells was made late in 1957 and early in 1958 (Price, 1961). During a 28-day period, 71.3 acre-feet of stream water was injected into Walla Walla city well 3, which was drilled 1,169 feet into basalt aquifers.

The artificial-recharge experiment was not entirely successful. Before injection, the well yielded 1,630 gpm (gallons per minute) with a drawdown of 45 feet; indicating a specific capacity (yield divided by drawdown) of 36 gpm per foot of drawdown. After completion of the artificial-recharge experiment, the yield of the well was 1,540 gpm and the drawdown was 67 feet; the specific capacity had dropped to 23 gpm per foot. The deterioration in yield and specific capacity probably was the result of partial clogging of the aquifer by air dissolved or entrained in the recharge water.

Subsequently, some construction work was done in anticipation of further artificial-recharge experiments. The pump was removed from the well, the well was cleaned, more turbine stages were added to the pump, and several additional air-relief valves were installed in the pipeline transporting the water to the injection well. After the construction work, the yield of the well was 1,760 gpm at a drawdown of 56 feet and the specific capacity was 31 gpm per foot, on the basis of a pumping test on October 16, 1961. The addition of the air-relief valves was not effective in decreasing the amount of air carried in the pipeline.

The water supply for both series of tests was from Mill Creek, which is the principal source of water for the city of Walla Walla. The water injected was similar in chemical character to the ground water, although the dissolved-solids content of the injection water (about 60 ppm) was less than half that of the ground water (Price, 1961, p. A13). The injected water had a low sediment content and a generally low bacteria content. The one notable feature of the injected water with respect to its suitability for recharge was its relatively high air content during both series of tests.

Ground water occurs in the Columbia River Basalt chiefly in contact zones between individual flows. According to Newcomb (1951, p. 41) the water-bearing openings are mainly cracks or crevices produced by incomplete closure of one flow over another and by fragmentation of the basalt at the tops of some of the flows. Walla Walla city well 3, where the principal tests were made, penetrates 145 feet of unconsolidated material, which is cased off, and 1,024 feet of the Columbia River Basalt. The basalt section is uncased from 178 to 1,063 feet and from 1,102 to 1,169 feet.

Artificial recharge was resumed on November 14, 1961. Because a large quantity of air still was being carried in the surface-water supply, injection was restricted to short periods so that any deterioration in yield or in specific capacity could be detected while in

Test results for Walla Walla well 3

Run No.	Water level before recharge (feet below land surface)	Duration of recharge (days)	Average recharge rate (gpm)	Maximum water-level buildup during recharge (feet)	Specific capacity during recharge (gpm per ft)	Water level about 24 hours after recharge stopped (feet below land surface)	Yield after recharge (gpm)	Drawdown (feet)	Specific capacity during pumping (gpm per ft)
1	191	1.01	561	31	18.1	189	1,840	62	29.7
2	(1)	2.00	605	(1)	----------	162	1,840	(1)	----------
3	(1)	2.92	547	(1)	----------	156	1,810	(1)	----------
4	186	3.92	589	(1)	----------	190	1,810	65	27.8
5	190	5.02	550	52	10.6	185	1,780	67	26.6
6	186	4.07	647	66	9.8	184	1,830	69	26.5
7	187	4.20	629	63	10.0	182	1,840	71	25.9
8	185	1.01	638	59	10.8	(1)	(1)	(1)	----------
9	184	.28	720	29	24.8	183	1,850	66	28.0
10	183	3.05	592	32	18.5	179	1,850	[2] 81	22.8
11	188	4.98	649	50	13.0	182	1,850	71	26.0

[1] Not measured.
[2] After pumping 3.14 days. Level affected by pumping of 2 nearby wells.

the incipient stage. A schedule was set up to recharge for a short time, to surge the well immediately after cessation of recharge, to let the well remain idle for 1 day, and then to pump for 1 hour to test for any change in specific capacity. As of January 16, 1962, 11 of these cycles had been completed. About 23.5 million gallons of water (72 acre-feet) was injected. Of this amount, about 1.5 million gallons was removed during the pumping and surging intervals that followed each of the 11 runs. This pumpage represents a loss of about 6 percent of the water injected.

The results of the 11 short-term runs, ranging in length from less than 1 day to more than 5 days, are shown in the above table. The data presented therein were collected by the personnel of the City of Walla Walla Water Department, who ran the tests under the direction of Mr. Paul Meyer, Director of Utilities.

No decrease in yield resulted from addition of water to the well. Except for test 5, the yield remained above 1,800 gpm. However, a slight decrease in specific capacity occurred during pumping. This decrease is considerably less than was expected, taking into consideration the difference in temperature between the native ground water and the surface water used for injection. The temperature of ground water from the injection well is about 59°F. The temperature of the water from the well after pumping for about 1 hour after each injection period was about 41°F, only 1° or 2° higher than that of the surface water injected. The apparent coefficient of permeability, taking this decrease of 18° into consideration, would be about 1/1.33 that of the permeability at 59°F. (Wenzel, 1952, p. 62.) On the basis of the relation between permeability and specific capacity, the specific capacity could be reduced to 23.6—from its prerecharge value of 31.5—without indicating incipient aquifer clogging. Although the specific capacity for run 10 was 22.8, this is not considered significant inasmuch as the pumping level in the recharge well was being affected by the operation of two nearby wells at the time of measurement.

The specific capacity of the well during recharge (injection rate divided by rise in water level) for the 11 runs was less than the specific capacity during pumping, and ranged from 9.8 to 24.8. A possible cause of the difference in specific capacity during recharge and during pumping is the formation of a partial screen of bubbles at the well–aquifer interface.

It is tentatively concluded that the series of short-term tests has been successful in providing a means of injecting water containing air into basalt aquifers without loss in yield or significant loss in well efficiency.

REFERENCES

Newcomb, R. C., 1951, Preliminary report on the ground-water resources of the Walla Walla basin, Washington-Oregon: U.S. Geol. Survey open-file report, 203 p., 9 pls.

Price, C. E., 1961, Artificial recharge through a well tapping basalt aquifers, Walla Walla area, Washington: U.S. Geol. Survey Water-Supply Paper 1594–A, 31 p.

Wenzel, L. K., 1942, Methods for determining permeability of water-bearing materials, with special reference to discharging-well methods: U.S. Geol. Survey Water-Supply Paper 887, 192 p.

108. EFFECT OF THE HAIKU TUNNEL ON KAHALUU STREAM, OAHU, HAWAII

By GEORGE T. HIRASHIMA, Honolulu, Hawaii

Work done in cooperation with the Hawaii State Division of Water and Land Development—Department of Land and Natural Resources

The rapid development of the communities of Kailua and Kaneohe across the Koolau Range from Honolulu (fig. 108.1) has prompted an intensive study of the low-flow characteristics of the streams on the windward or northeast side of the island of Oahu. Analysis of stream-gaging records in the area revealed that the base flow of Kahaluu Stream decreased at about the same time that a water-development tunnel was bored in Haiku Valley, 2½ miles away. This article explores the possibility that the decrease was due to withdrawal of ground water by the tunnel, and appraises quantitatively the decrease of the annual runoff of Kahaluu Stream.

Rainfall in the Koolau Range is the source of water in Haiku and Kahaluu Streams, as well as in other streams in the area (fig. 108.2). Part of the rainfall runs off quickly as surface flow, part evaporates or is transpired by vegetation, and the remainder percolates into the ground. Of the amount that percolates into the ground, only the small part that reaches the stream channels in a day or two moves through the soil mantle as shallow subsurface runoff; the larger part percolates deeply to become ground water.

Numerous springs at high altitude indicate the existence of high-level ground-water reservoirs. These reservoirs are bounded by intrusive dikes cutting the lava flows that make up the Koolau Range. These dikes are less permeable than the lava flows; therefore, they are effective in channeling the movement of ground water along their trends. The predominant strike of the individual dikes is roughly parallel to the Koolau Range. This, together with the fact that the axes of Haiku and Kahaluu Streams and others

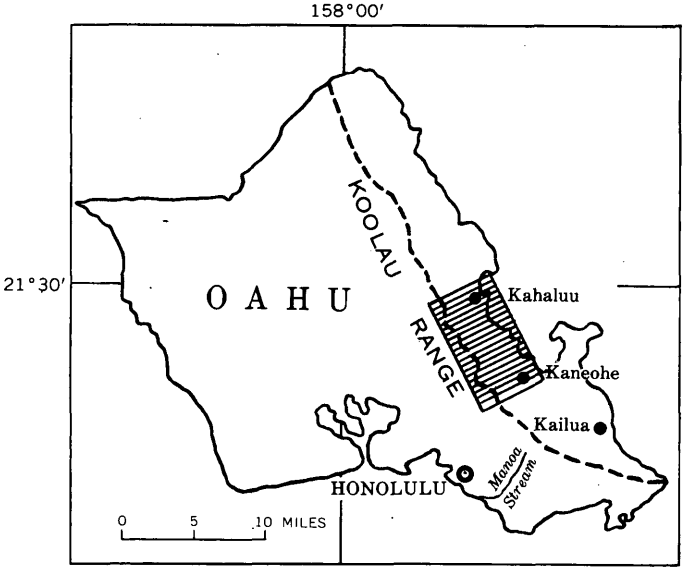

FIGURE 108.1.—Map of Oahu showing area of study.

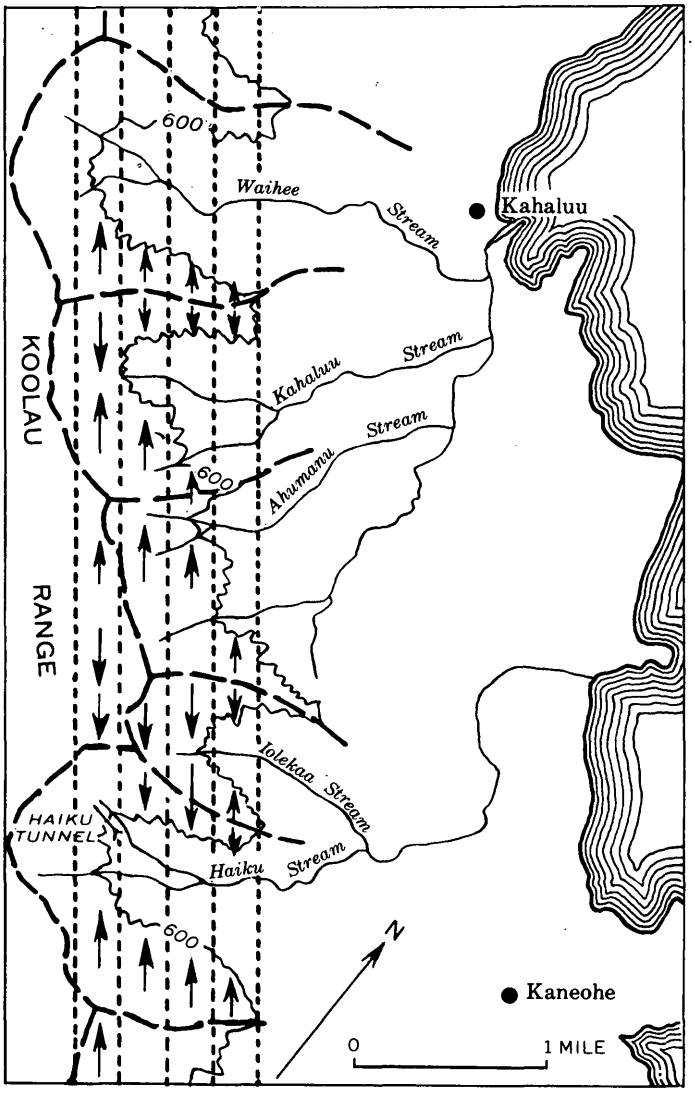

FIGURE 108.2.—Map of study area showing location of streams. Short dashed lines show schematically the arrangement of dikes. Long dashed lines show surface divides. Arrows indicate deduced direction of flow in ground-water reservoirs.

in the area are transverse to the Koolau Range, suggests that the spring-fed flow of these streams is sustained by interconnected ground-water reservoirs (fig. 108.2).

The first indication of a change in the flow regimen of Kahaluu Stream was given by the shape of the flow-duration curve. For most streams on Oahu, flow-duration curves are normally smooth and concave upward from about 10- to 80-percent duration, when plotted on logarithmic probability paper. For Kahaluu Stream, however, the shape of the flow-duration curve for the period July 1936 to June 1946 was found to differ from that of the normal. This difference appeared to be more than could be accounted for merely by combining a series of low-flow years with some high-flow years. A further indication of a change in regimen was given by a change in the runoff relationship between Waihee and Kahaluu Stream after the 1941 fiscal year. For the period July 1936 to June 1940, the runoff of Kahaluu Stream averaged 52 percent of that of Waihee Stream, while for the period July 1941 to June 1946 it dropped to 40 percent. This change is equivalent to a 23 percent decrease in streamflow of Kahaluu Stream.

The streamflow records for Kahaluu Stream were reviewed to eliminate the possibility of the change being due to errors in the record or to changes in the location of the gage. This review showed no change in location and no errors sufficient to change appreciably the shape of the flow-duration curve or the amount of the annual discharges. It was thus concluded that there was a real decrease in the flow of Kahaluu Stream and that further investigation should be made to establish the amount of the change and the reason for it.

The most logical cause of the change of the flow regimen of Kahaluu Stream appears to be the withdrawal of ground water by the Haiku tunnel, which was bored in 1940. This tunnel, which was bored at an altitude of 550 feet, was the first of three water-development tunnels in the area between Haiku and Waihee Valleys. (The second tunnel was bored in Kahaluu Valley in 1946 and the third was bored in Waihee Valley in 1955). The Haiku tunnel is 1,200 feet long and cuts through 4 dikes that range from 1 to 10 feet in thickness. Holes drilled into the 10-foot dike at a distance of 1,200 feet from the portal tapped water under considerable pressure. During the construction of the tunnel in November and December 1940 and for several months in 1941, a large quantity of water with flow rates up to 11 mgd (million gallons per day) was drained from the ground-water reservoirs.

After the completion of the tunnel, ground water continued to be withdrawn by the distribution system, at a rate less than the free-flow rate but greater than the average recharge rate of 2 mgd. (The average recharge rate was determined from the yield of the tunnel for the 6-year period 1953 to 1958, inclusive, during which there was little or no change in storage.) This withdrawal of water lowered the water level in the ground-water reservoirs and possibly shifted the ground-water divide toward Kahaluu Valley, thereby causing some water that previously fed Kahaluu Stream to move toward Haiku Valley.

A plot of the monthly mean discharges of Kahaluu Stream against those of Waihee Stream shows that August 1941 gave the first indication of a change in relationship. Thus, the period from January 1936 (the first complete month of record for Waihee Stream) to July 1941 was taken as the one before the change in relationship. The period after the change was taken from August 1941 to June 1946 (the Kahaluu tunnel was bored beginning in July 1946, so that the "after" period necessarily stops in June 1946).

An analysis of covariance made by using the above-mentioned periods shows that the change in relationship was highly significant at the 1-percent level.

A similar analysis using the records for Kahaluu Stream and for East Branch Manoa Stream, which is hydrologically similar to Kahaluu Stream but on the other side of Koolau Range, showed that the change in relationship between these two streams was also highly significant at the 1-percent level.

As the change in relationship was probably not due to chance, the regression equation for the "before" period (Kahaluu versus Waihee) was used to estimate the monthly discharge of Kahaluu Stream for the "after" period. The regression equation was computed by the least squares method and found to be $\log y = -0.14 + 0.84 \log x$. The standard error of the estimate is 0.02 log units or 7 percent, and the coefficient of correlation is 0.94.

The computation shows that the decrease in Kahaluu streamflow averaged 0.81 mgd over the period August 1941 to June 1946—a decrease of about 26 percent.

In summary, the flow of Kahaluu Stream after July 1941 was about 26 percent less in relation to that of Waihee Stream than it was before that date. In view of the favorable opportunity for ground wa-

ter trapped behind intrusive dikes to move parallel to the Koolau Range and the fact that the change occurred soon after the Haiku tunnel was bored, it is concluded that the decrease in flow of Kahaluu Stream is due to withdrawal of ground water by the Haiku tunnel, 2½ miles away.

GROUND WATER

109. GROUND-WATER SHADOWS AND BURIED TOPOGRAPHY, SAN XAVIER INDIAN RESERVATION, PIMA COUNTY, ARIZONA

By L. A. Heindl, Washington, D.C.

Work done in cooperation with the U.S. Bureau of Indian Affairs

The yield and specific capacity of wells vary considerably from place to place in alluvial deposits. Adjacent to mountain fronts, the yield and specific capacity of wells may vary markedly within short distances. Commonly such variations have been ascribed rather vaguely to the heterogeneity of alluvial deposits. However, such variations in ground-water occurrence probably reflect specific geologic and climatic controls or local depositional environments. Thus, the distribution of general quantitative well characteristics, such as yield and specific capacity, and of aquifer characteristics, such as transmissibility, may serve as clues to the geometry of the alluvium and the geomorphology during its deposition.

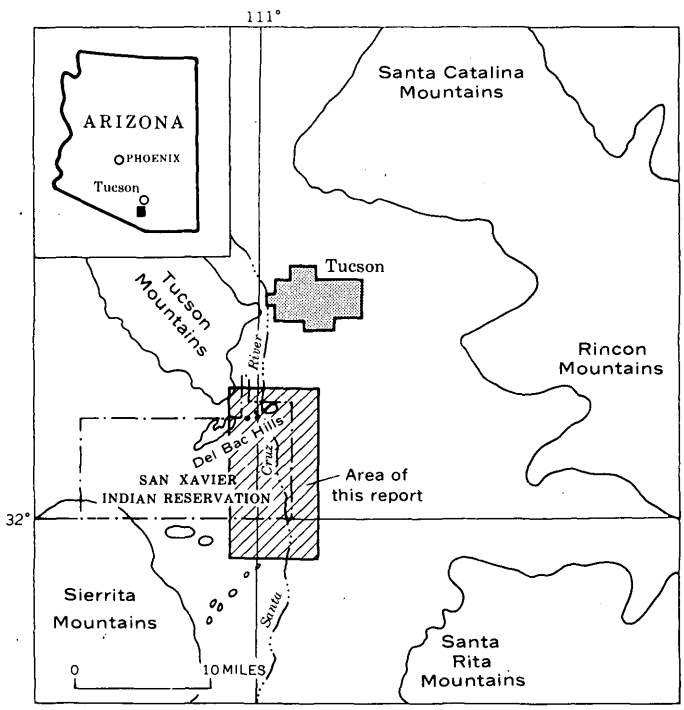

FIGURE 109.1.—Map showing location of the report area.

The areas of low yield commonly are moderately well defined. Areas of low yield have been identified in interstream areas between large alluvial fans along mountain fronts in the San Joaquin Valley in California (Davis and others, 1959, p. 83) and in the Willcox basin in Arizona (Heindl, 1961). Areas of low yield, however, occur in other geologic situations, and the general term "ground-water shadows" has been used to describe them, by analogy with rain shadows on the lee sides of mountains (Heindl, 1961).

Several ground-water shadows occur along the Santa Cruz River in and adjacent to the San Xavier Indian Reservation south of Tucson, Ariz. (fig. 109.1). The river channel here traverses the west margin of a broad alluvial basin between the Sierrita and Tucson Mountains on the west and the Santa Catalina, Rincon, and Santa Rita Mountains on the east. The channel is about 2 miles from bedrock hills on the northeast slope of the Sierritas (fig. 109.2, Hills A and B) and skirts bedrock at several places along the west side of the Tucson Mountains. Within the San Xavier Indian Reservation, the Santa Cruz River passes through a gap in the Del Bac Hills, where its flood plain, elsewhere about 1½ miles wide, is constricted to about a quarter of a mile.

Most of the wells of large yield, drilled for irrigation, municipal, and industrial supply, are in or near the flood plain of the Santa Cruz River. A few, however, are as much as 2 miles away from the flood plain, and some wells in the flood plain yield only small

amounts of water. The ground-water shadows shown on figure 109.2 are based on specific-yield data from different sources. The specific yields were computed from pumping rates ranging from 250 to 2,000 gpm (gallons per minute), however, except for one well, and probably indicate reasonably well the water-yielding characteristics of the materials penetrated. The distribution of ground-water shadows and corollary areas of high yield is at least partly substantiated by other subsurface and surface information, although the areas of low and high yield are not closely defined in most places because pertinent data are available only from the few wells shown on figure 109.2.

The three geologic units shown on figure 109.2 are: (1) bedrock, composed of Paleozoic to middle(?) Tertiary sedimentary and volcanic rocks; (2) older alluvium, consisting of stream and sheetwash deposits of late Tertiary and probable Quaternary age; and (3) younger alluvium, consisting of late Pleistocene and Recent flood-plain and channel deposits (Heindl, 1959; Cooper, 1960). The bedrock, with the exception of probable equivalents of the Helmet Fanglomerate (Cooper, 1960), generally is nearly impermeable. The older alluvium is the principal water-bearing formation in the area. The younger alluvium is too fine grained to be considered an aquifer and, in addition, is above the water table except when the Santa Cruz River flows.

The bedrock units were deformed into high and low areas and extensively eroded before the older alluvium was deposited. Preceding and contemporaneous with the deposition of the older alluvium, the ancient Sierrita and Tucson Mountains were sculptured into valleys and ridges trending about N. 60° E. This trend is more or less parallel to the Del Bac Hills (fig. 109.1) and is probably controlled largely by faults. Hills A and B, in the southwest corner of the area (fig. 109.2), are the northeasternmost surface expressions of two partly buried ridges of similar trend, which have been substantiated by exploratory borings west and southwest of the Del Bac Hills and Hills A and B. These ridges, and a third smaller one between the Del Bac Hills and Hill A, probably extend northeastward. This probability is substantiated at least in part by the distribution of specific capacities along the Santa Cruz River. The buried valley north of the Del Bac Hills is substantiated by drillers' logs and supports the likelihood of similar valleys to the south.

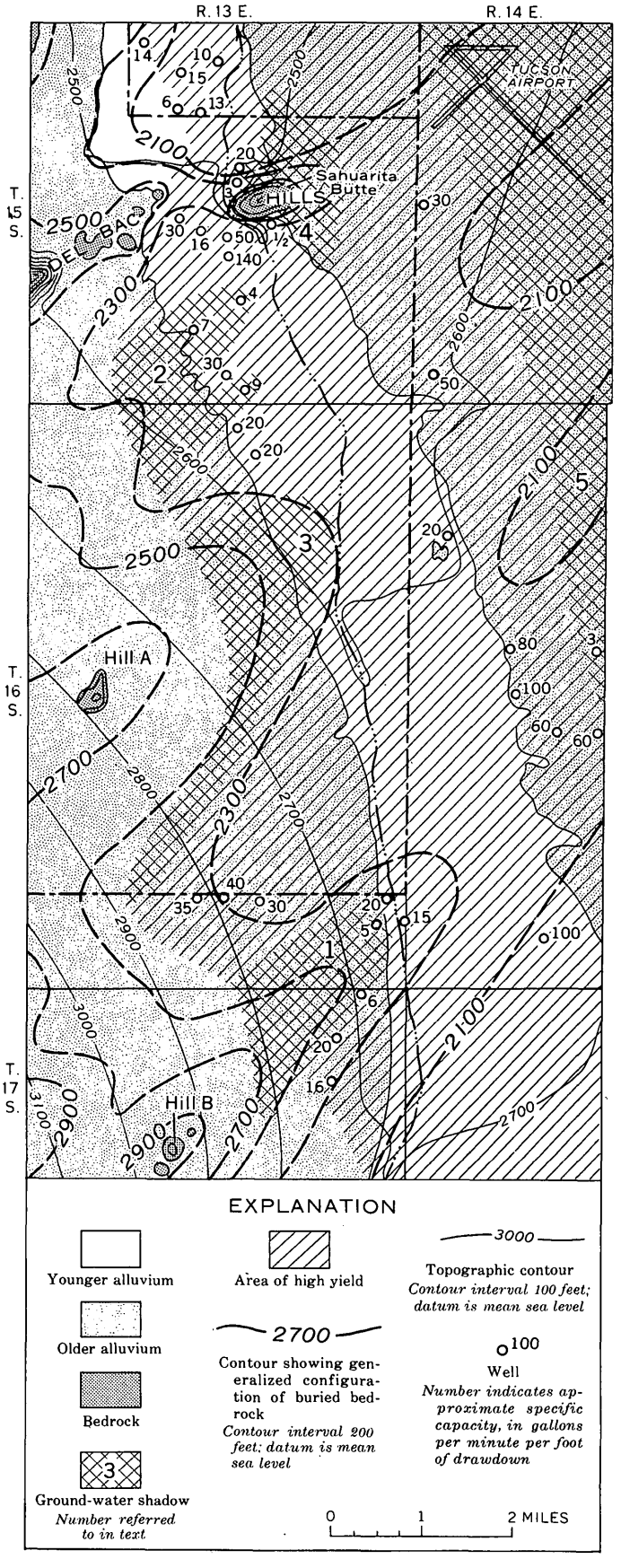

FIGURE 109.2.—Generalized geologic map along the Santa Cruz River in the vicinity of San Xavier Indian Reservation showing the approximate configuration of buried bedrock topography and areas of ground-water shadows and high yields.

The base of the older alluvium at two well-field sites east of the river appears to be between 500 and 600 feet below the present surface (Schwalen and Shaw, 1957, p. 22; Kidwai,[1] 1957, p. 40, 43; S. F. Turner, oral communication, 1960). The configuration of the bedrock surface east of the river shown on figure 109.2 is an extrapolation of these depths and the trends of the buried ridges and valleys.

Ground-water shadows and areas of high yield occur in three general geologic situations in the area of this report.

In the first geologic situation, ground-water shadows and areas of high yield seem to be related to buried ridges and valleys. Ground-water shadows 1 and 2 (fig. 109.2) and the areas of high yield north of shadows 1 and 3 aline with buried ridges and valleys indicated by drill-hole data to the west. This relationship reflects conditions observable in recent sediments—the better sorted and more permeable materials are deposited in the central parts of valleys where trunk-stream flow is concentrated, whereas the less well sorted and hence less permeable materials are deposited adjacent to and across the noses of the ridges by less competent streams. Ground-water shadow 3 is not substantiated by any specific-capacity data but is presumed because of the buried ridge extending east of Hill A.

The second general situation is illustrated by data from where the Santa Cruz River passes through the gap at the east end of the Del Bac Hills. Here the specific capacity ranges from ½ to 140 gpm per ft of drawdown within less than a mile. Wells of low specific capacity are close to Sahuarita Butte, whereas wells of high specific capacity are farther away from the bedrock ridges or are in the Santa Cruz River channel. The west side of ground-water shadow 4 seems to represent areas of predominantly fine grained material deposited outside the main course of the channel. The eastward extension of shadow 4, postulated by analogy to shadows 1, 2, and 3, is restricted by the high-capacity well 1½ miles east of Sahuarita Butte.

The third general situation is illustrated by the distribution of specific capacity along the east side of the Santa Cruz River. About 6 miles south-southeast of Sahuarita Butte, a well which has a specific capacity of only 3 gpm per ft is flanked on the west by a group of wells of high specific capacity. Ground-water shadow 5 is shown extending northward from these wells, and its limits are based on the specific capacity of wells 1½ miles east and 2 miles southeast of Sahuarita Butte and on data north of the area of figure 109.2. Driller's logs and well cuttings indicate that coarse gravel beds underlie the river channel in the gap west of Sahuarita Butte and in the area east of the butte at about the same altitudes. The well with a specific capacity of 3 gpm per ft does not penetrate prominent gravel beds at this general level, although it penetrates a thin gravel deposit at a greater depth. The data suggest that the ancient Santa Cruz River at some time flowed both east and west of the butte. Ground-water shadow 5 presumably represents less permeable deposits laid down by tributary streams from the distant Santa Rita Mountains (fig. 109.1), whereas the area of high yield represents more permeable deposits laid down along the channel of the ancient Santa Cruz River.

Evidence for the local environmental control of deposits of varying permeability is fragmentary and the conclusions drawn for this area are necessarily tentative. These conclusions remain to be tested by drilling east of Sahuarita Butte and along the west side of the Santa Cruz River. In general, however, this study indicates that the heterogeneity of alluvial deposits is not random but reflects the local environment of deposition, and that a synthesis of the environment of deposition, based even on limited geologic and hydrologic data, may suggest the local distribution of areas of greater and lesser permeability.

[1] Kidwai, Z. U., 1957, Relationship of ground water to alluvium in the Tucson area, Arizona: Univ. of Arizona M.S. thesis, 55 p.

REFERENCES

Cooper, J. R., 1960, Some geologic features of the Pima mining district, Pima County, Arizona: U.S. Geol. Survey Bull. 1112–C, p. 63–103.

Davis, G. H., and others, 1959, Ground-water conditions and storage capacity in the San Joaquin Valley, California: U.S. Geol. Survey Water-Supply Paper 1469, 287 p.

Heindl, L. A., 1959, Geology of the San Xavier Indian Reservation, Arizona *in* Arizona Geol. Soc. Southern Arizona Guidebook II, p. 152–159.

——— 1961, Ground-water shadows: U.S. Geol. Survey open-file rept., presented at joint meeting of Southwestern and Rocky Mountain Div. Am. Assoc. Adv. Sci. and Arizona Acad. Sci., Arizona State Univ., April 1961, 2 p.

Schwalen, H. C., and Shaw, R. J., 1957, Ground water supplies of the Santa Cruz Valley of southern Arizona between Rillito Station and the International Boundary: Arizona Univ. Agr. Expt. Sta. Bull. 288, 119 p.

110. WATER-BEARING CHARACTERISTICS OF THE LOCKPORT DOLOMITE NEAR NIAGARA FALLS, NEW YORK

By Richard H. Johnston, Albany, N.Y.

Work done in cooperation with the New York Water Resources Commission

Ground water in the Niagara Falls area occurs principally along seven prominent zones of jointing parallel to bedding in the Lockport Dolomite. These zones have much higher permeability than the surrounding rock and are, in effect, separate and distinct artesian aquifers. An opportunity to observe these zones and other water-bearing openings was provided by the excavation of two 4-mile long conduits in the Lockport. The conduits, part of the Niagara Power Project, were built to divert water from the upper Niagara River, around Niagara Falls, to the Robert Moses Generating Plant below the falls.

The Lockport Dolomite is the youngest bedrock and the only important aquifer in the Niagara Falls area. It consists of thin to massive beds of dark-gray to brown dolomite except near the base, where the section contains light-gray limestone and shaly dolomite beds. Small irregular masses of gypsum are disseminated throughout the formation. The Lockport forms the resistant lip of the falls and the rims of the Niagara River Gorge and the Niagara Escarpment. The formation ranges in thickness from about 20 feet along the escarpment to over 140 feet along the upper Niagara River above the falls; the difference in thickness is due to erosion. The beds dip southward about 30 feet per mile. The Lockport is underlain by the Rochester Shale and is overlain by a 5- to 20-foot cover of glacial till and lacustrine deposits.

The Lockport Dolomite derives its permeability from three types of openings: (1) bedding joints, which constitute the 7 important water-bearing zones of the formation; (2) vertical joints; and (3) to a small degree, irregular cavities (generally 1 to 3 inches in diameter) from which gypsum has been dissolved. The seven water-bearing zones are the most permeable parts of the formation and transmit nearly all the water moving through it. These water-bearing zones most commonly occur within very thin-bedded intervals of the section that are immediately overlain by massive beds. Although vertical joints are prominent locally where they have been widened by solution, they generally are tight and yield little water. Most joints in the upper 10 to 15 feet of the rock have been widened by solution, but these enlarged openings are usually filled with mud.

One of the most striking features of the 4-mile long conduit excavations was the almost continuous line of seepage along the water-bearing zones parallel to bedding (fig. 110.1). The greatest amount of seepage occurred where open vertical joints intersected the bedding joints, or where cavities were formed by solution of gypsum within the seepage zone. At a few such places, water was observed squirting from the openings.

The stratigraphic position of the seven water-bearing zones that are believed to be areally extensive in the Niagara Falls area is shown in figure 110.2. These zones have been numbered 1 to 7 from bottom to top. Zones 4 through 7, which are in the upper and middle parts of the Lockport, appear to transmit most of the water. The most extensive seepage observed in the conduits was from zone 4, a bedding joint which is open $\frac{1}{16}$ to $\frac{1}{8}$ inch locally.

Because the seven water-bearing zones are in otherwise relatively impermeable rock, they act as virtually separate aquifers within the formation. A series

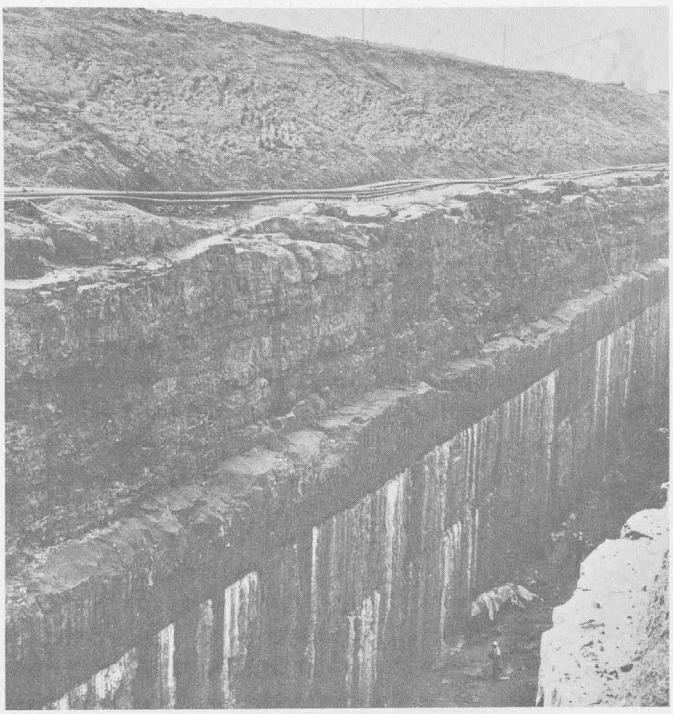

Figure 110.1.—Seepage from two water-bearing zones parallel to bedding in the Lockport Dolomite. The zones are marked by precipitation of mineral matter from the ground water. (Photograph by the Power Authority of the State of New York.)

639466 O - 62 - 9

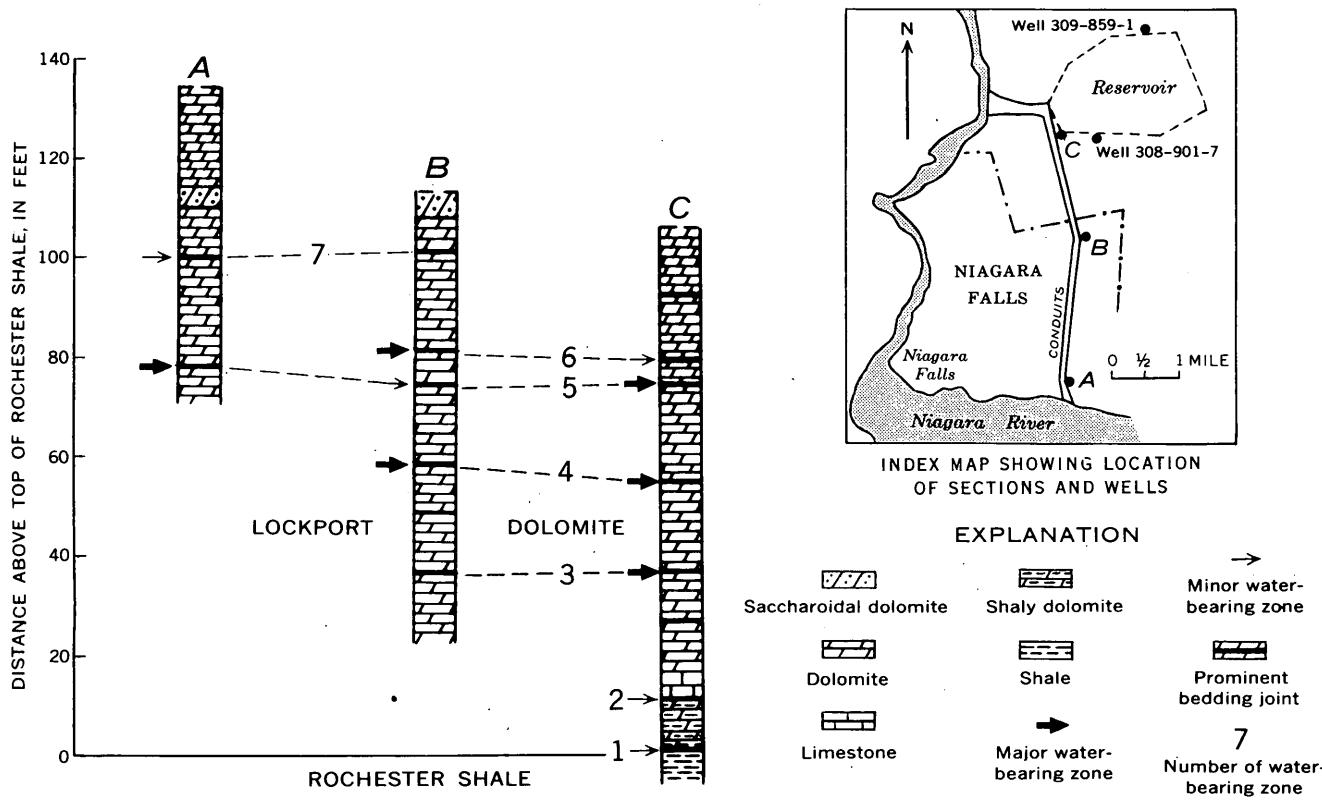

FIGURE 110.2.—Sections showing position of water-bearing zones in the Lockport Dolomite in the vicinity of Niagara Falls, N.Y.

of observation wells, drilled by the Power Authority of the State of New York, provided an opportunity to observe the hydraulic effect of these individual zones or aquifers on the water-bearing characteristics of the formation as a whole.

The piezometric level in each successively lower water-bearing zone is progressively lower in most of the wells drilled, owing to drainage by the open conduits. The piezometric level progressively declines in a steplike sequence as the wells are drilled deeper; that is, when a well has been drilled through the uppermost water-bearing zone, the water level in the well remains approximately the same until the next lower zone is penetrated, at which time the water level abruptly declines to the piezometric level of the next lower zone. At the same time, the rate at which water can be bailed from the well usually increases. In some wells the increase is very marked. For example, during the drilling of well 308–901–7 (fig. 110.2) the bailing rate increased abruptly from 12 to 50 gpm (gallons per minute) when water-bearing zone 5 (fig. 110.2) was tapped.

Packers were installed upon completion of the well so that the difference in piezometric levels between the individual water-bearing zones could be measured. The difference in piezometric levels usually was large and between some zones was comparable to the distance between the zones.

The yield of wells in the Lockport generally depends upon which water-bearing zones are penetrated. The average yield of 56 wells tapping the upper and middle Lockport (water-bearing zones 4 through 7) was 31 gpm. In contrast, 15 wells tapping only the lower 40 feet of Lockport (water-bearing zones 1, 2, and 3) have an average yield of 7 gpm. These averages do not include a few wells along the Niagara River which yield more than 1,000 gpm through infiltration from the river.

A pumping test of well 309–859–1 (fig. 110.2) indicates the very permeable nature of water-bearing zone 3 as compared with the remainder of the formation. Figure 110.3 shows the recovery curve of the water level in the well following the cessation of pumping. The water level rose 3 feet in the first 5 minutes and then was almost stationary for 7.5 minutes. The ini-

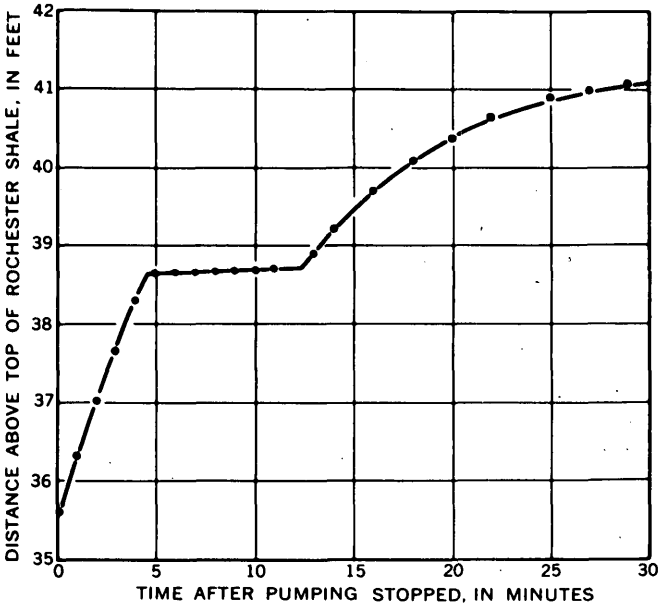

FIGURE 110.3.—Recovery curve of water level in well 309–859–1 following cessation of pumping.

tial rise reflects the time required to fill the well below the level of water-bearing zone 3; the step in the recovery curve between 5 and 12.5 minutes reflects the time required to replace the water drawn from water-bearing zone 3 (which at this well is about 39 feet above the Rochester). The coefficient of transmissibility for the lower 42 feet of the Lockport, as determined by this test, was about 300 gallons per day per foot. It is unrealistic to convert this value to an average coefficient of permeability for the section of the formation penetrated, however, because most of the water came from the single water-bearing zone, and the remainder of the saturated portion of the formation contributed little to the yield of the well. The average coefficient of transmissibility of the Lockport as a whole is about 2,000 gallons per day per foot.

The author wishes to thank the members of the Geology Section of Uhl, Hall, and Rich, Engineers for the Power Authority of the State of New York, who provided valuable data and assistance.

111. EFFECT OF STREAM INFILTRATION ON GROUND-WATER TEMPERATURES NEAR SCHENECTADY, NEW YORK

By JOHN D. WINSLOW, Albany, N.Y.

Work done in cooperation with the city of Schenectady, New York, and the New York Water Resources Commission

Study of ground-water temperatures along the flood plain of the Mohawk River in the vicinity of the well fields of the city of Schenectady and the town of Rotterdam, N.Y., has (1) demonstrated that the river recharges the sand and gravel aquifer underlying the flood plain, and (2) indicated the principal paths of flow between the Mohawk River and the well fields. In addition, the variation of ground-water temperature with depth suggests wide differences in permeability between different beds within the aquifer. The aquifer is so permeable that the usual methods of hydrologic analysis, based on changes of water level, cannot be used.

Ground-water temperatures were measured in about 60 wells. During the period of temperature measurements (1960–61), the average combined pumping rate at the well fields was about 20 mgd (million gallons per day); the city of Schenectady pumped about 90 percent of this amount.

The Schenectady and Rotterdam well fields are on the flood plain of the Mohawk River about 4,000 feet downstream from lock 8, a dam and navigation lock of the New York State Barge Canal (fig. 111.1). In the Schenectady area, the Mohawk River cut into the relatively impermeable shale and siltstone of the Schenectady Shale, of Ordovician age, during the Pleistocene epoch, and subsequently the river valley was partly filled with glacial drift and alluvium. The valley-fill deposits overlying the bedrock consist of till overlain by 20 to more than 100 feet of sandy gravel and sand (the principal aquifer), which in turn is overlain by about 30 feet of flood-plain deposits. The upper surface of the till is uneven, but generally it slopes away from the valley walls. The thickness of the sand and gravel aquifer is about 30 feet at the Schenectady well field, more than 50 feet at the Rotterdam well field, and more than 100 feet at lock 8. South of the Schenectady well field the

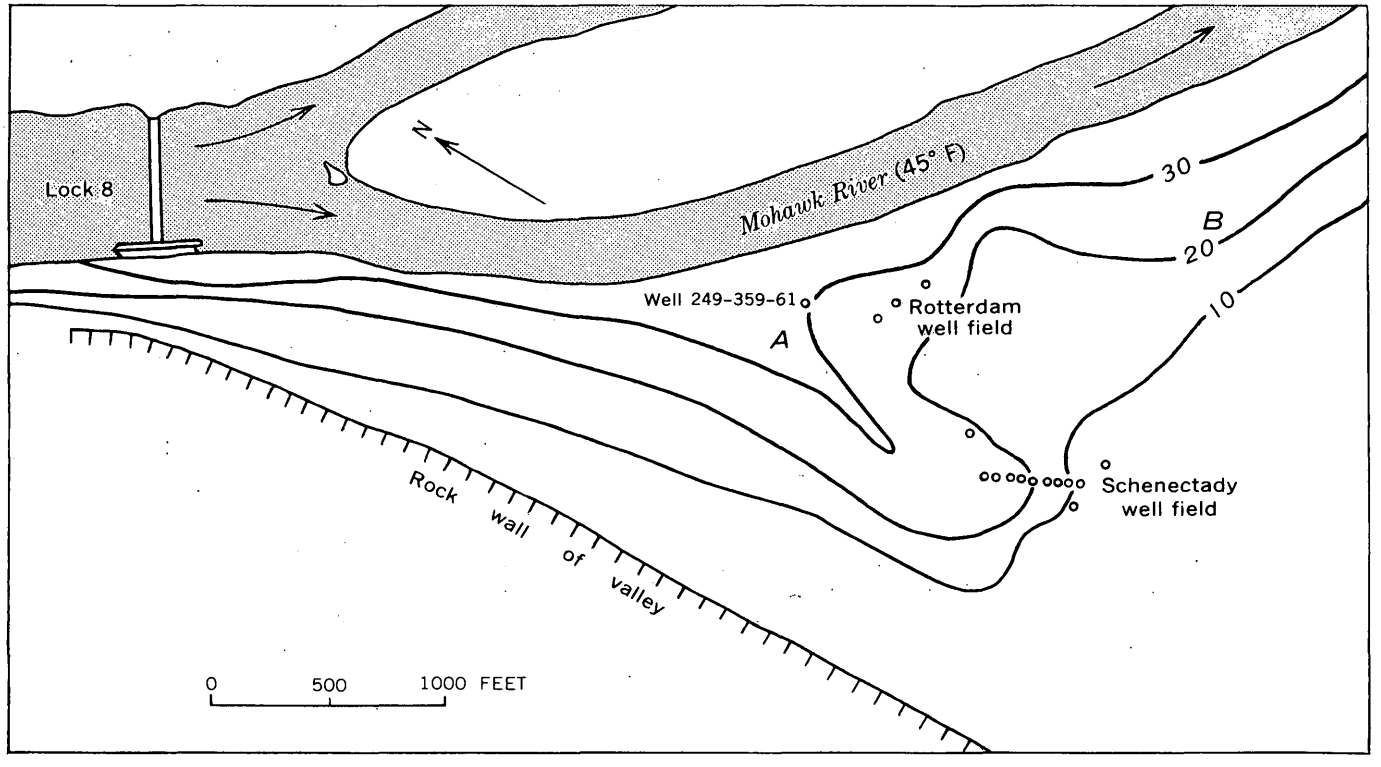

FIGURE 111.1.—Isallotherms (°F) showing the annual variation of ground-water temperatures in the vicinity of the Schenectady and Rotterdam well fields near Schenectady, N.Y. (1960–61). Annual temperature variation of the river water was 45°F.

sand and gravel grade abruptly to a medium- to fine-grained sand.

The present Mohawk River channel is cut through the flood-plain deposits into the top of the sand and gravel aquifer, but because the river is pooled for navigation purposes, organic silty clay, generally 2 to 4 feet thick, has been deposited on the river bottom. This material, relatively impermeable though thin, acts as a partial barrier that hampers infiltration from the stream into the underlying very permeable sand and gravel aquifer. The coefficient of permeability of the aquifer is on the order of 100,000 gpd (gallons per day) per square foot, and that of the organic clay is less than 1 gpd per square foot.

Operation of the barge canal affects the areal extent of the cone of depression about the well fields. During the navigation season (April-December) the upper pool at lock 8 is about 14 feet higher than the lower pool. During the non-navigation season, when the dam is removed, the difference between upper and lower pools is about 1 foot. The cone of depression does not extend as far upstream as lock 8 during the navigation season because the underflow (resulting from the difference in pool elevations) around the dam is more than sufficient to stabilize the cone of depression below the dam. During the non-navigation season the amount of underflow around the dam is slight and the cone of depression extends above lock 8. A second reason for the larger cone of depression during the winter months is that the viscosity of the river water at 32°F is nearly double that during the summer, when the temperature of the river water is about 75°F. Thus, the effective permeability of the river-bottom material in winter is only about half that during the summer.

Interpretation of the ground-water temperature data is based on the following premises: 1) that the temperature of ground water in natural transit from a point of recharge to a point of discharge has a small annual variation and approximates the annual mean air temperature; and 2) that river temperatures approximate the weekly average air temperature (except when the air temperature is below 32°F). Therefore, if substantial amounts of water infiltrate from the stream, a considerably greater variation in ground-water temperature in the vicinity of a well field should result. If the variation of ground-water temperatures correlates with the variation of river temperature, it indicates that a considerable amount of the water pumped at the well field is infiltrating from the river.

Isallotherms (lines of equal temperature change) in the vicinity of the well fields are shown in figure 111.1. The sharp deflection of the 30°F isallotherm away from the river just above the well fields (*A*,

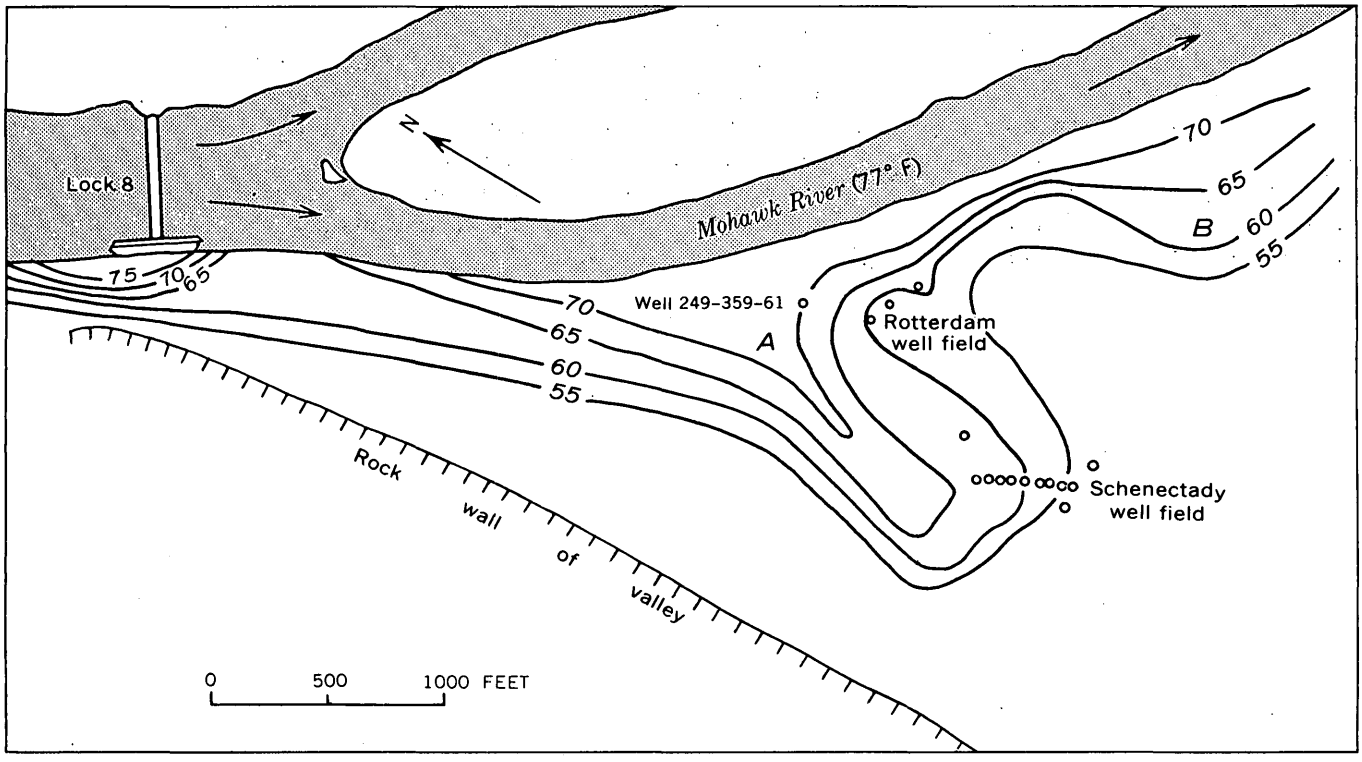

FIGURE 111.2.—Isotherms (°F) showing ground-water temperatures in the vicinity of the Schenectady and Rotterdam well fields on September 7, 1961. Temperature of the river water was 77°F.

fig. 111.1) indicates the principal flow path of ground water from the river to the Schenectady well field. It is a relatively narrow path through coarse sand and gravel beds that are much more permeable than the aquifer elsewhere in the well-field area. A second, but less permeable, major flow path is at *B* (fig. 111.1). Of course, infiltration occurs along the entire reach of the river within the cone of depression, and as the water moves from the river to the well fields there is some mixing of the water infiltrating from the river at different places, times, and temperatures. The resulting averaging of temperatures causes the annual variation of ground-water temperature to decrease progressively away from the river. The ground-water isotherms on September 7, 1961, shown in figure 111.2, form a pattern similar to that of the isallotherms in figure 111.1.

The general pattern of the isallotherms and isotherms will remain the same from year to year, but will vary in detail because of the following factors: (1) variation in the annual range of river temperature; (2) variation in the amount of pumpage, which determines the amount of infiltration; (3) differential changes in transmissibility resulting from fluctuations of water level; and (4) periodic dredging of the river for navigation purposes, which removes, or partly removes, the organic clay bed on the river bottom, thus increasing the infiltration rate in particular areas and thereby changing the flow pattern within the aquifer.

Temperature measurements made at various depths in a well may indicate differences in permeability between strata penetrated by the well. Figure 111.3

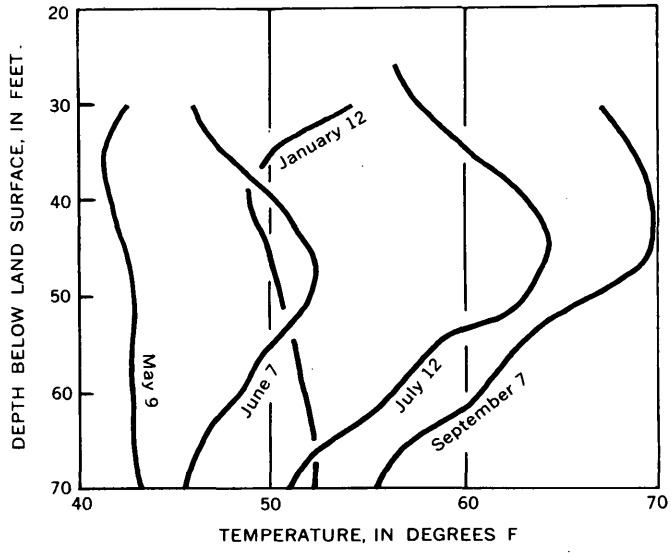

FIGURE 111.3.—Variation of ground-water temperature with depth in well 249–359–61 near flow path *A* at different dates in 1961.

shows the variation of ground-water temperature with depth in well 249–359–61, located along flow path *A*, about 500 feet from the river. The well is 70 feet deep and the aquifer lies between depths of 25 and 70 feet. The annual variation of ground-water temperature is about 20°F at 25 feet, 25°F at 30 feet, 28°F at 40 feet, 22°F at 50 feet, and 12°F at 70 feet. The deflection of the July temperature line to the right at a depth of about 50 feet indicates a zone that is more permeable than average. On the other hand, in fall and winter (January temperature line) ground water appears to move through the aquifer most rapidly at a depth of about 40 feet. Judging from the annual variation of ground-water temperature with depth in the well, the most permeable zone lies between depths of 30 and 50 feet.

SURFACE WATER

112. A RELATION BETWEEN FLOODS AND DROUGHT FLOWS IN THE PIEDMONT PROVINCE IN VIRGINIA

By Ennio V. Giusti, Washington, D.C.

Some streams show an exceptionally large variation between their extremes of flow. Others show a more moderate variation and have relatively higher sustained flows and relatively lower flood peaks. The differences in these extremes of flow is investigated here for the Piedmont province in Virginia.

All unregulated streams in this area that have at least 10 years of hydrologic record were selected for this study. The median annual flood and 7-day drought flow were used as indices of the extremes of flow. These median values were related to drainage area as shown in figure 112.1 to account for differences in the size of the basins. The computed regression equations are

$$Q_f = 181A^{0.56} \quad (1)$$

$$Q_d = 0.51A^{1.10} \quad (2)$$

where Q_f is the median annual flood, in cubic feet per second, Q_d is the median annual drought, in cubic feet per second, and A is the drainage area, in square miles.

The annual flood is defined as the instantaneous maximum discharge during the hydrologic year ending September 30; the annual drought is defined as the minimum average flow for 7 consecutive days during the climatic year ending March 31.

For each stream, the ratio of the observed median annual flood to the value computed from equation 1 was plotted in figure 112.2 against a similar ratio for drought values from equation 2. The apparent relationship (shown in fig. 112.2) indicates that streams which yield below-average droughts have above-average floods and conversely, that streams having above-average droughts have below-average floods. Equations 1 and 2, modified to include stream slope as an index of physiographic factors, yield ratios of observed to computed values that would not significantly alter the relationship shown in figure 112.2.

The inverse relationship shown in figure 112.2 may be reasoned intuitively in terms of differences in the

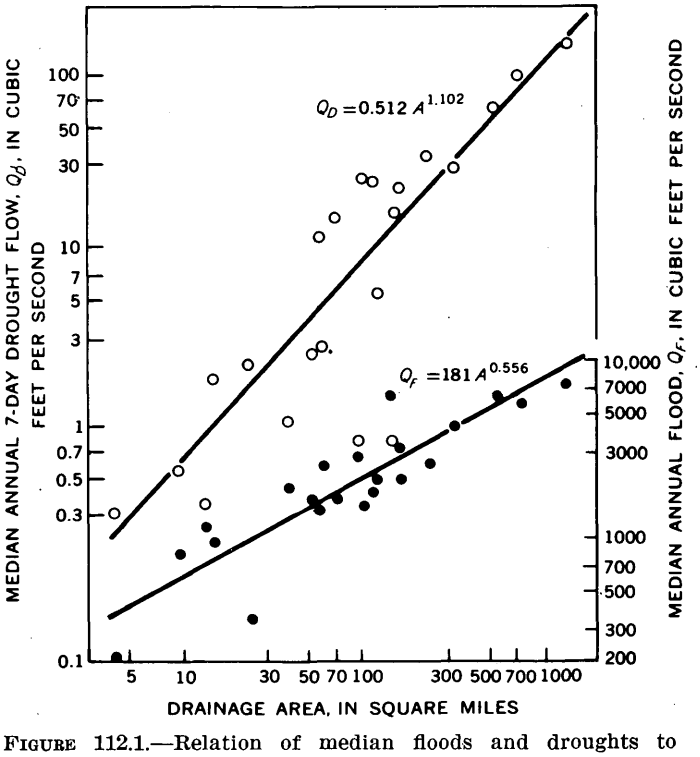

FIGURE 112.1.—Relation of median floods and droughts to drainage area. Dots represent floods, open circles droughts.

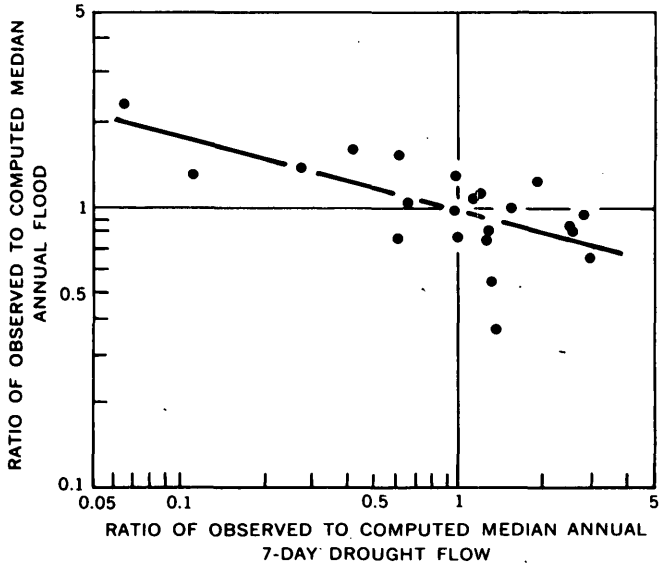

FIGURE 112.2.—Relation between floods and droughts expressed as the ratio of observed to computed values for comparable size of drainage area. Lower right quadrant represents above-average droughts and below-average floods; upper left quadrant represents the opposite.

subsurface rocks. Rain falling on a basin underlain by relatively impermeable crystalline rocks will flow readily into the stream channels; relatively little will percolate into the ground. Floods will be high in volume and short in duration. During periods of little or no rainfall, streamflow will be deficient because of the low permeability of the rocks and small ground-water supply. In contrast, rain falling on a similar basin underlain by permeable sedimentary rocks will more readily percolate into the ground. Floods will be lower. During periods of little or no rainfall, flow will be sustained because of the permeability of the rocks and the more abundant ground-water supply.

As the streams analyzed here are all underlain by metamorphosed crystalline rocks, variation in flow cannot be attributed to differences in type of rock. The variations between streams are more likely due to differences in storage capacity of the rocks caused by variations in the decomposition of the rocks by weathering, or by differences in the degree of fracturing and jointing, both of which influence storage and movement of water.

113. EFFECT OF URBAN GROWTH ON SEDIMENT DISCHARGE, NORTHWEST BRANCH ANACOSTIA RIVER BASIN, MARYLAND

By FRANK J. KELLER, Rockville, Md.

Work done in cooperation with the U.S. Army Corps of Engineers

During the transition period from rural to urban land, erosion of denuded areas increases the sediment discharged by the receiving streams. With all other factors remaining constant, sediment discharge will change with changes in land use. Land with good vegetal cover is less subject to soil erosion than land that is denuded for agricultural crops and urban development. A recent investigation provided an opportunity to measure, in a limited way, the effect of urban growth on sediment discharge.

The drainage basin of the Northwest Branch Anacostia River is in Prince Georges and Montgomery Counties, Md. The principal soil types throughout the basin are Manor and Glenelg silt loams (U.S. Dept. of Agriculture, 1961). This basin is in the path of the rapidly expanding Washington metropolitan area. The upper 40 percent of the basin is considered rural in character [1960], but does contain some urban development.

The drainage area of the Northwest Branch Anacostia River at the stream-gaging station near Hyattsville is 49.4 square miles and at the upstream gage near Colesville is 21.3 square miles. The relation of sediment discharge to water discharge for the two stations is illustrated in figure 113.1. Some of the sediment measurements are not shown in this figure, but all of them were used in determining the position of the average curves.

The difference between the suspended-sediment discharge at the two stream-gaging stations was greater than could be attributed to the larger drainage area at Hyattsville. For example, with a water discharge

of 4 cubic feet per second per square mile, the approximate sediment discharge at Colesville and at Hyattsville would be 3 and 11 tons per day per square mile, respectively. This is 64 tons per day of sediment from above the Colesville station compared to 543 tons per day from the entire basin above Hyattsville. If we assume that all the sediment passing the Colesville station also passes the Hyattsville station, the area undergoing urban growth between these 2 stations contributed 479 tons per day or 17 tons per day per square mile. This is nearly a sixfold increase in suspended-sediment discharge from an urban growth area compared to that from a rural area. If the undetermined amount of sediment that was trapped by the Burnt Mills storage reservoir located on the river between the two stations were included, this increase would be even greater.

The sediment discharged by a stream is a function of all factors that cause streamflow and the concentration of sediment in this streamflow. Sediment concentrations can be very high in runoff water draining directly from lands denuded by construction. During September 11 and 12, 1960, a hurricane produced a uniform rainfall of about 2.5 inches throughout the basin. Sediment concentrations at the two stations during this storm are plotted in figure 113.2 with

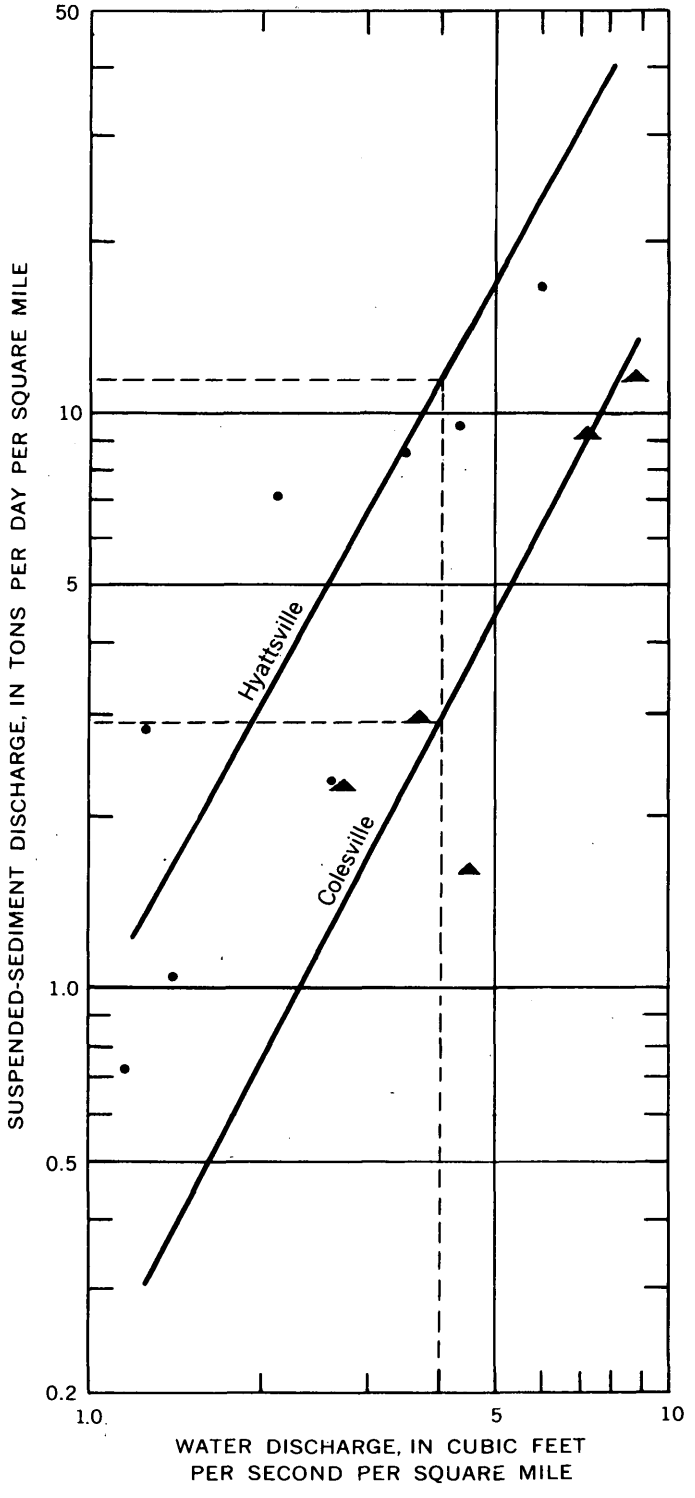

FIGURE 113.1.—Comparison between the relation of sediment discharge to water discharge from an urban development area (Hyattsville, Md.) and a rural area (Colesville, Md.), Northwest Branch Anacostia River.

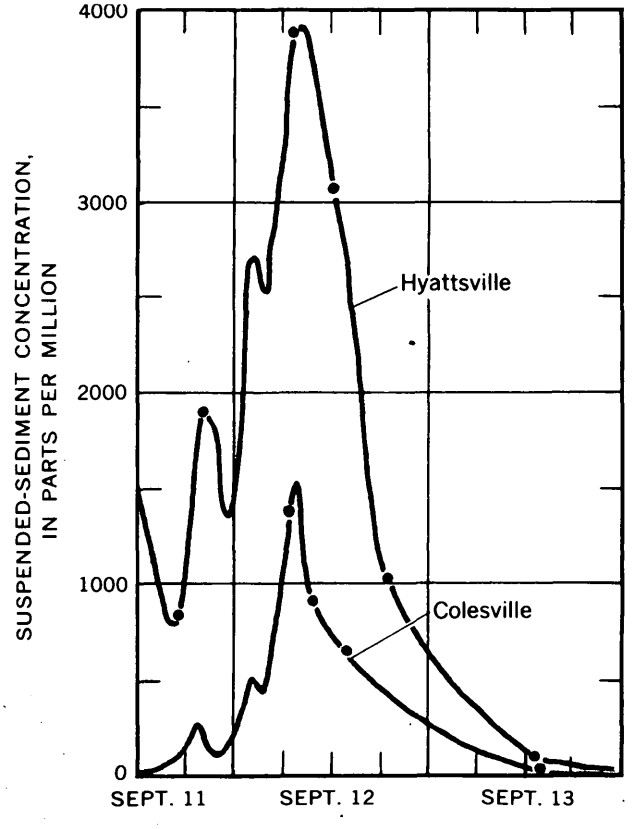

FIGURE 113.2.—Comparison between suspended-sediment concentration of runoff from an urban development area (Hyattsville, Md.) and a rural area (Colesville, Md.), Northwest Branch Anacostia River, Sept. 11–13, 1960.

smooth curves connecting the points. A comparison of these curves shows that suspended-sediment concentrations are 2 to 5 times higher and persist longer in water draining from urban-growth land than in water draining from rural land. Other measurements of runoff at these stations had similar differences in sediment concentrations; therefore the curves are considered typical for the period of study.

Unfortunately, high sediment discharge from urban-growth land continues for a long period of time. H. P. Guy and G. E. Ferguson (written communication, 1961) point out that such factors as intensity and dispersion of construction, construction methods, and street layout, as well as physiographic and meteorologic factors, affect the quantity of sediment eroded in urban development. Furthermore, water-discharge peaks are increased after rural land is changed to urban land (Carter, 1961). Therefore, a high sediment discharge can be expected until all major areas of construction are restabilized and the stream channels have adjusted to the more frequent high flows.

REFERENCES

Carter, R. W., 1961, Magnitude and frequency of floods in suburban areas: Art. 5 *in* U.S. Geol. Survey Prof. Paper 424–B, p. B9–B11.

U.S. Dept. of Agriculture, 1961, Soil Survey of Montgomery County, Maryland: U.S. Dept. of Agriculture, Soil Conservation Service.

QUALITY OF WATER

114. SOURCE OF SULFATE IN GROUND WATER OF THE TRUCKEE MEADOWS AREA, NEVADA

By Philip Cohen, Carson City, Nev.

Work done in cooperation with the Nevada Department of Conservation and Natural Resources

In many of the intermontane valleys in Nevada, the dissolved-solids content of ground water increases with increasing distance from recharge areas (for example, see Zones, 1961, p. 38). However, in the Truckee Meadows area the dissolved-solids content of the ground water tends to decrease with increasing distance from recharge areas largely because the recharge areas contribute water having a high dissolved-solids and a high sulfate content.

Figure 114.1, a trilinear diagram, shows the percentage of the major anions, CO_3+HCO_3, SO_4, and Cl (in equivalents per million) in 113 surface-water and ground-water samples from the Truckee Meadows area. The diagram is divided into three fields as follows: Field 1—chloride water, in which the percentage of Cl is greater than the percentage of SO_4, and the percentage of CO_3+HCO_3 is less than 80 percent of the major anions; field 2—sulfate water, in which the percentage of SO_4 is greater than the percentage of Cl, and the percentage of CO_3+HCO_3 is less than 80 percent of the sum of the major anions; field 3—carbonate-bicarbonate water, in which the per-

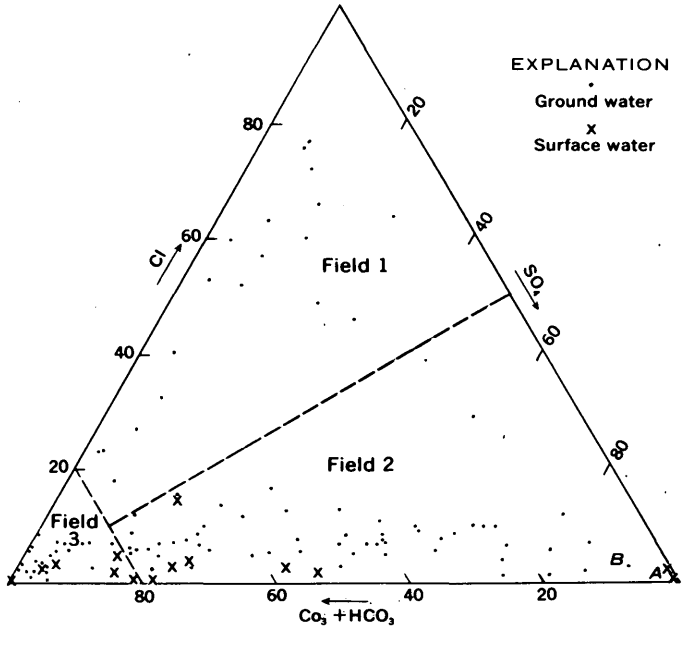

FIGURE 114.1.—Relative concentration of major anions in water of the Truckee Meadows area, Nevada.

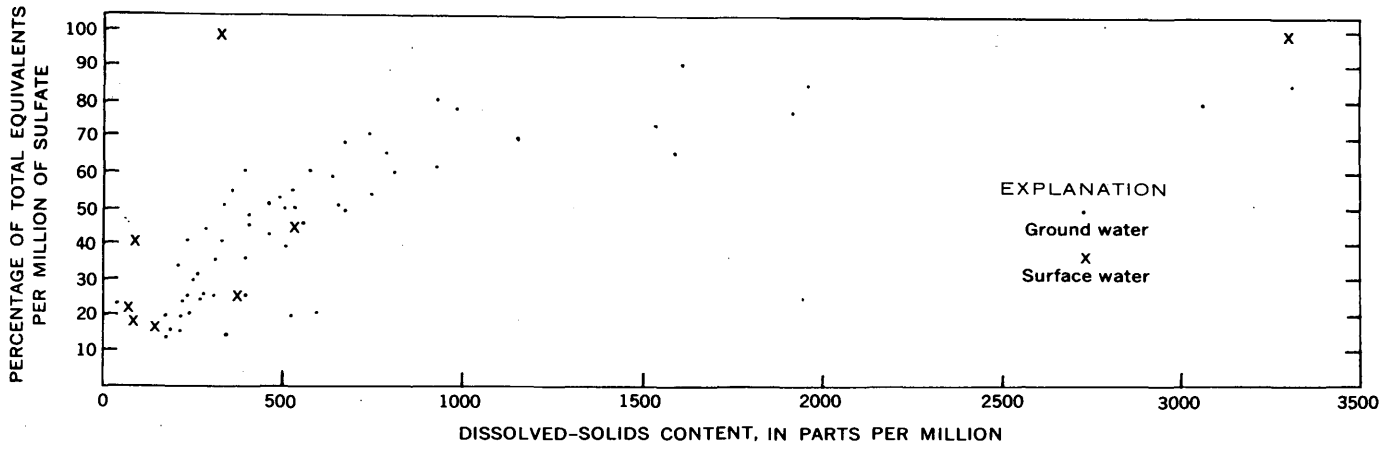

FIGURE 114.2.—Relation between the percentage of equivalents per million of sulfate and the dissolved-solids content in the sulfate water of the Truckee Meadows area, Nevada.

centage of CO_3+HCO_3 is greater than 80 percent of the sum of the major anions.

The consolidated rocks of the mountains bordering the area are dominantly basalt, andesite, and granodiorite, but include lesser amounts of metamorphic and sedimentary rocks. Hydrothermal alteration of these rocks has resulted in the formation of such minerals as chlorite, epidote, some zeolites, and pyrite and other metallic sulfides. Sulfurous and sulfuric acid and ferrous and ferric sulfate, which formed as a result of oxidation and hydration of the metallic sulfides, have bleached the hydrothermally altered rocks. The bleached rocks are rich in sulfate compounds and consist predominantly of clay, opal, and some quartz.

Areas of bleached rock occur locally in all the mountains bordering the Truckee Meadows area, and the dissolved-solids and sulfate content of the streams draining these areas is high. Also, the water from wells penetrating bleached rock has a high dissolved-solids and sulfate content. Samples A and B on figure 114.1 are from a stream draining an area of bleached rock and from a shallow well in bleached rock, respectively. The dissolved-solids content of the samples is 3,300 and 3,060 parts per million, and the sulfate content is 2,570 and 1,680 parts per million, respectively.

The sulfate-rich streams draining areas of bleached rock discharge onto the alluvial apron bordering the valley; part of the water recharges the alluvial deposits of the ground-water reservoir and moves downgradient toward the axis of the valley. As the sulfate-rich water moves downgradient, is is diluted by infiltration of irrigation water of low dissolved-solids content diverted into the basin from the Truckee River, which drains the Sierra Nevada west of the Truckee Meadows area.

Virtually all the carbonate-bicarbonate water is derived from the Truckee River or from streams draining areas of unbleached rock. All the water has a low dissolved-solids content, commonly less than 250 parts per million. The relatively continuous band of points along the base of the triangle represents samples that are mixtures of highly mineralized sulfate water and dilute carbonate-bicarbonate water. The percentage of sulfate decreases from right to left in the samples represented by the band of points. In addition, the dissolved-solids content decreases from right to left, as is shown on figure 114.2.

Although there are some exceptions, most of the samples that plot in field 2 are, from right to left, progressively farther downgradient from areas of bleached rock. This strongly suggests that most of the sulfate is derived from streams draining areas of bleached rock rather than from the solution of sulfate compounds in the alluvial deposits of the ground-water reservoir.

REFERENCE

Zones, C. P., 1961, Ground-water potentialities in the Crescent Valley, Eureka and Lander Counties, Nevada: U.S. Geol. Survey Water-Supply Paper 1581, 50 p.

115. DOWNDIP CHANGES IN CHEMICAL QUALITY OF WATER IN THE "500-FOOT" SAND OF WESTERN TENNESSEE

By GERALD K. MOORE, Memphis, Tenn.

Work done in cooperation with the Tennessee Division of Water Resources

The "500-foot" sand of the Memphis area (Klaer, 1940, p. 92) underlies more than half of western Tennessee and produces an estimated 75 percent of the ground water withdrawn in that area. This paper discusses the major downdip changes in chemical quality of water in this important aquifer and relates them to the geology of the aquifer.

The report area (fig. 115.1), which is drained by tributaries of the Mississippi River, lies on the eastern flank of the syncline that forms the Mississippi embayment.

The "500-foot" sand of Eocene age comprises the lower and middle units of the Claiborne Group in Tennessee. The top of this sand section seems to correlate with the top of the Sparta Sand in Mississippi, and the base with the base of the Claiborne Group in Mississippi, Arkansas, and Tennessee. The "500-foot" sand consists of thick beds of fine- to coarse-grained gray quartz sand containing a few thin lenses of clay or silt. Carbonaceous material is abundant in some zones and is characteristic of the unit. The base of the sand ranges in altitude from 600 feet above to 900 feet below mean sea level. The sand ranges in thickness from 0 to 750 feet. The beds strike north-northeast, roughly parallel to the Mississippi River, and dip toward the river 19 to 25 feet per mile.

The outcrop belt (fig. 115.1) is the principal recharge area for the "500-foot" sand, and ground water in this area is generally under water-table conditions. Artesian conditions exist west of the outcrop belt where the "500-foot" sand is overlain by younger formations. Water in the sand moves downdip to the axis of the Mississippi embayment and thence southward along the axis.

Regionally the "500-foot" sand is a hydrologic unit, although clay lenses locally separate the sand beds.

Ground water in most of the Mississippi embayment region is a sodium bicarbonate type (Stephenson and others, 1928; Foster, 1950; and Meyer and Turcan, 1955). Calcium, magnesium, and iron ions in the water have been replaced with equivalent amounts of alkali ions, chiefly sodium, probably through cation exchange. In the report area, however, all analyses show a high calcium–sodium ratio and a significant downdip increase in calcium, magnesium, and iron. This condition probably exists because the "500-foot" sand is lacking in minerals with significant exchange capacity.

As a means of comparing the chemical analyses of water from numerous wells in the "500-foot" sand, diagrams for the major constituents were plotted in the manner suggested by Stiff (1951, p. 15). Representative plots are shown on figure 115.2, and the location of the wells from which the water samples were taken is shown on figure 115.1.

The concentration of all chemical constituents in the water from well 1 was low, and the iron content was negligible. This analysis is typical of water samples from wells near the outcrop area of the "500-foot" sand. The median pH, measured in the field, of water samples from 12 wells near the outcrop area was 5.7.

The analysis of a water sample from well 2 is typical of the water farther west and downdip in the aquifer. The calcium, magnesium, and bicarbonate content was much greater than in the water from well 1. The iron content of the water from well 2 was 1.7 ppm (parts per million), sufficient to be objectionable for some purposes. The median pH, measured in the field, of 6 samples of water of this chemical type was 6.2.

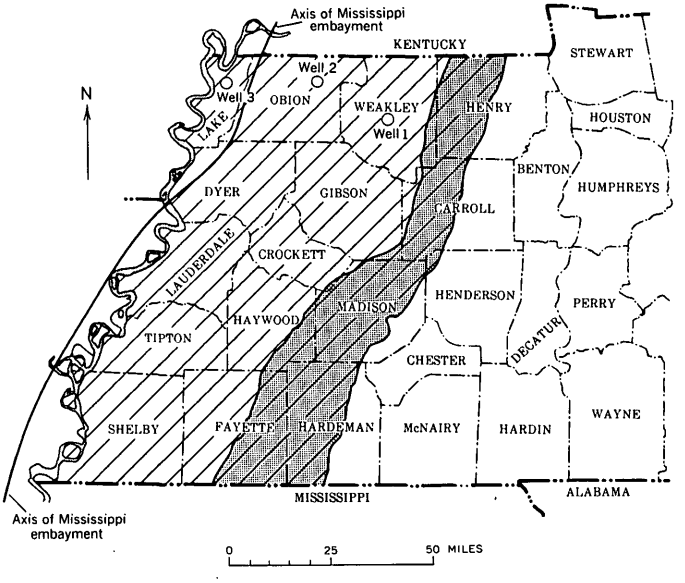

FIGURE 115.1.—Index map of western Tennessee showing area of this report (diagonal lines), outcrop area of "500-foot" sand (shaded), axis of Mississippi embayment, and location of wells.

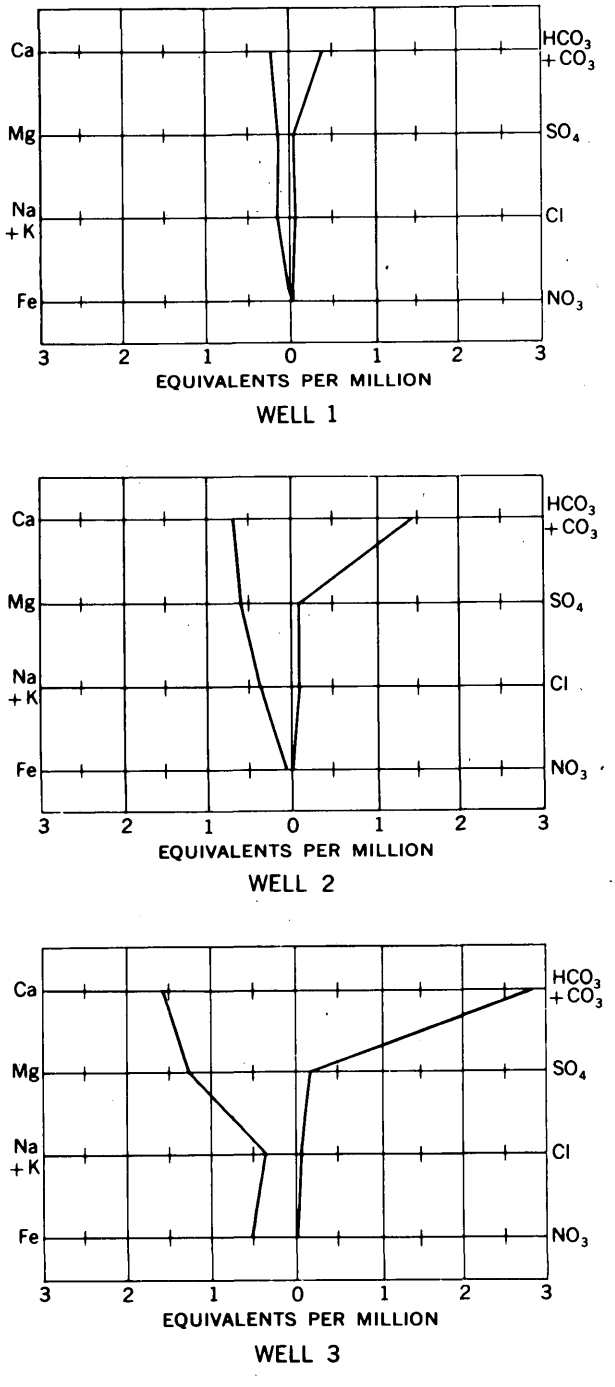

FIGURE 115.2.—Diagrams of analyses of water from wells 1–3.

Water from well 3 near the axis of the Mississippi embayment contained 15 ppm of iron and requires aeration for most uses. The content of bicarbonate, magnesium, and calcium also was greater than in samples from wells 1 and 2. The median pH, measured in the field, of water samples from 5 wells near the axis of the embayment was 6.7.

The increase in content of calcium, magnesium, and bicarbonate indicated by the water from wells 2 and 3 probably results from the slow solution of calcium and magnesium minerals as the ground water moves downdip. This process would account for the downdip increase in pH, assuming no addition of carbon dioxide to the water.

The increase in iron content of the water away from the outcrop area presumably is due to a shift from an oxidizing environment near the outcrop to a reducing environment near the axis of the embayment. Hem and Cropper (1959) indicate that, in the pH range of these waters, the solubility of iron is dependent upon the oxidation-reduction potential (Eh) of the water in the aquifer. The presence of hydrogen sulfide gas in the water from some wells tapping the "500-foot" sand near the axis of the embayment is evidence of a reducing environment in the aquifer.

The quality of water from the "500-foot" sand generally is very good; the only treatment given most municipal supplies taken from this sand is aeration and chlorination.

REFERENCES

Foster, M. D., 1950, The origin of high sodium bicarbonate waters in the Atlantic and Gulf Coastal Plains: Geochim. et Cosmochim. Acta, v. 1, p. 33–48.

Hem, J. D., and Cropper, W. H., 1959, Survey of ferrous-ferric chemical equilibria and redox potentials: U.S. Geol. Survey Water-Supply Paper 1459–A.

Klaer, F. H., 1940, Water levels and artesian pressure in wells in Memphis: U.S. Geol. Survey Water-Supply Paper 907, p. 92–101.

Meyer, R. R., and Turcan, A. N., Jr., 1955, Geology and groundwater resources of the Baton Rouge area, Louisiana: U.S. Geol. Survey Water-Supply Paper 1296, 138 p.

Stephenson, L. W., Logan, W. N., and Waring, G. A., 1928, The ground-water resources of Mississippi: U.S. Geol. Survey Water-Supply Paper 576, 515 p.

Stiff, H. A., Jr., 1951, The interpretation of chemical water analysis by means of patterns: Jour. Petroleum Technology, v. 3, no. 10, p. 15.

116. ESTIMATING WATER QUALITY FROM ELECTRICAL LOGS

By A. N. TURCAN, JR., Baton Rouge, La.

Work done in cooperation within Louisiana Department of Public Works and Department of Conservation, Louisiana Geological Survey

Electrical logs are extremely useful for correlating subsurface geologic formations and for determining the occurrence of fresh ground water. Fortunately, for many years electrical logs have been made of most oil- and gas-test holes and of many water wells in Louisiana. About 75,000 electrical logs of oil and gas wells are on file at the Louisiana Geological Survey. These logs and the availability of a large number of chemical analyses of water make it possible to estimate, for selected aquifers, the relation of the concentration of certain chemical constituents to the resistivity readings on electrical logs.

The possible development and use of an empirical method which does not involve extensive laboratory determinations or estimates based upon field examination of core samples was envisioned by Guyod (1957), who stated, "For example, inasmuch as the composition of the water of a given formation is relatively uniform over a large area, it is generally possible to calibrate, for the area, the readings of the electric log in terms of water salinity. If water samples and an electric log are available in a test hole, it is a simple matter to determine the limiting resistivity and potential values beyond which the water can be used for domestic or industrial purposes. This information can then be applied for all the wells drilled in the general area." Such an empirical relation has been established for some of the major aquifers in Louisiana. To demonstrate the method, deposits of the Wilcox Group in Bossier and Caddo Parishes are analyzed in this paper. Only the following equation (Archie, 1942, p. 2) for computing the formation resistivity factor, F, for a selected aquifer is needed to compute the concentration of the formation water.

$$F = \frac{R_o}{R_w}$$

where R_o is the resistivity of a saturated sand, and
R_w is the resistivity of the formation water.

Although ideal conditions, such as uniform porosity and uniform tortuosity, do not exist, conditions are sufficiently uniform so that the resistivity values on the long-normal curve usually approximate the resistivity (R_o) of the formation in place in Louisiana. Accordingly, the formation factors listed in the following table are representative of the formation in place and are not necessarily the same as those determined from laboratory-prepared and "clean" material. It should be noted that the field formation resistivity factor (F_f) used here differs from the apparent formation resistivity factor (F_a), which has been defined as the ratio of the resistivity of the flushed zone (R_{xo}) to the resistivity of the mud filtrate (R_{mf}) (Schlumberger Well Surveying Corp., 1957, p. C–12, and Patnode and Wyllie, 1950, p. 50). As shown in the table, the ratio of the resistivity reading (R_o) from electrical logs to the resistivity of the formation water (R_w) indicates field formation factors for deposits of the Wilcox Group that range from 1.7 to 3.0 and average 2.4.

Specific-conductance data used to make the calculations were obtained from chemical analyses of water from wells that tap the Wilcox Group. All resistivity readings were adjusted to resistivity at 77°F, the standard temperature at which laboratory tests of specific conductance of water generally are reported (see table).

Specific conductance of water and resistivity characteristics of deposits of the Wilcox Group, Bossier and Caddo Parishes, La.

Well	Specific conductance (μmhos per cm at 77 °F)	R_w[1] (ohms-m²/m at 77 °F)	R_o[2] (ohms-m²/m)	R_o (ohms-m²/m at 77 °F)	F_f[3]
Bo–137	605	16. 5	35	31	1. 9
173	2, 470	4. 0	12	11	2. 8
180	1, 360	7. 4	25	22	3. 0
200	1, 510	6. 6	18	17	2. 6
205	1, 080	9. 3	17	16	1. 7
Cd–360	953	10. 5	20	19	1. 8
362	1, 410	7. 1	20	19	2. 7
375	1, 800	5. 6	13	12	2. 1
428	1, 580	6. 3	18	17	2. 7

[1] R_w=1/specific conductance×10⁴.
[2] Resistivity reading from electrical log at field temperature.
[3] F_f (field formation resistivity factor)=R_o/R_w.

Following the U.S. Public Health Service (1946) drinking-water standards, ground water in Louisiana whose chloride content is 250 ppm (parts per million) or less is considered fresh (Rollo, 1960, p. 47). The relation of content of chloride and of dissolved solids to specific conductance in water from deposits of the Wilcox Group is shown in figure 116.1. The chloride curve indicates that water from sands of the Wilcox

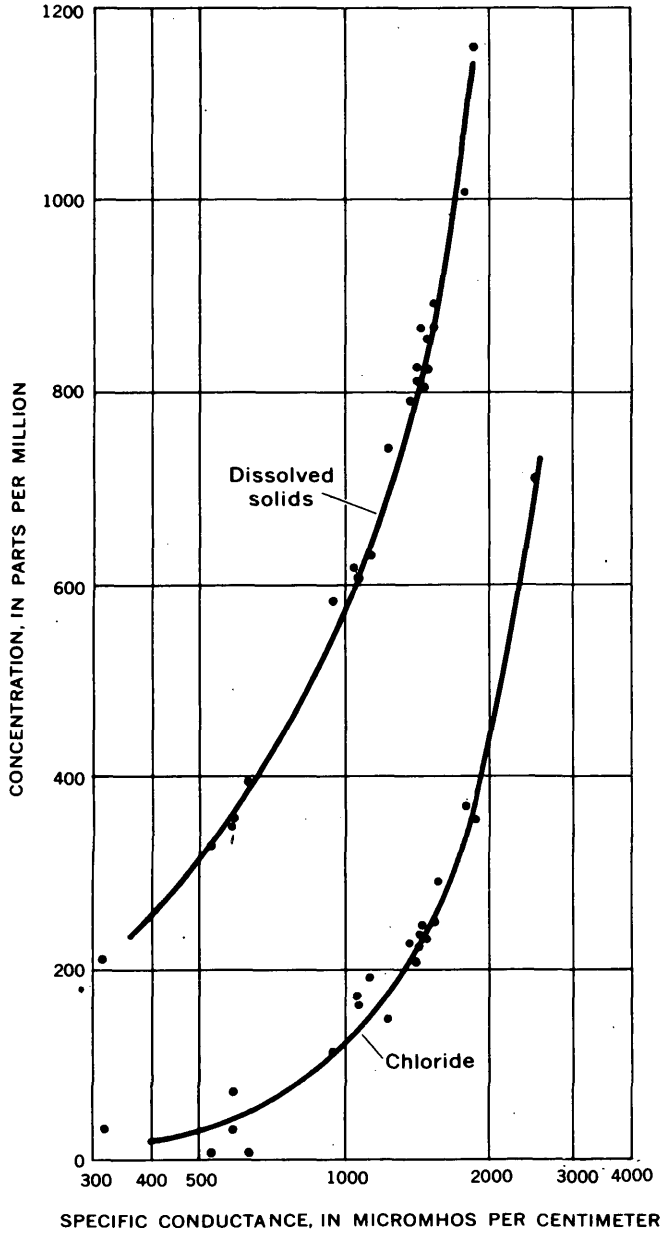

FIGURE 116.1.—Relation of specific conductance to chloride content and dissolved-solids content of water from sands of the Wilcox Group, Bossier and Caddo Parish, La.

Group having a chloride content of 250 ppm has a specific conductance of 1,560 μmhos per cm, which is equivalent to a formation water resistivity (R_w) of 6.4 ohms-m²/m. Thus, a resistivity (R_o) reading of about 15 ohms-m²/m indicates that the interstitial water has a chloride content of about 250 ppm. This "rule of thumb" of 15 ohms-m²/m or more for fresh water applies specifically to the sands of the Wilcox Group in Bossier and Caddo Parishes. However, where sufficient data are available, an empirical relation can be established between formation resistivity and chemical character in other aquifers and in other areas.

An example of this method and the calculations used to estimate the presence of fresh water is shown by means of a typical electrical log on figure 116.2.

REFERENCE

Archie, G. E., 1942, The electrical resistivity log as an aid in determining some reservoir characteristics: Am. Inst. Mining Metall. Engineers Tech. Pub. 1422, Petroleum Technology, 8 p.

Guyod, Hubert, 1957, Electric detective investigation of groundwater supplies with electric well logs: Water Well Jour., v. 11, nos. 3, 4.

Patnode, H. W., and Wyllie, M. R. J., 1950, The presence of conductive solids in reservoir rock as a factor in electric log interpretation: Am. Inst. Mining Metall. Engineers Tech. Pub. 2797, v. 189, p. 47–52.

Rollo, J. R., 1960, Ground water in Louisiana: Louisiana Dept. Conserv., Geol. Survey and Louisiana Dept. Public Works Water Resources Bull. 1.

Schlumberger Well Surveying Corp., 1957, Log interpretation charts.

U.S. Public Health Service, 1946, Drinking water standards: U.S. Public Health Service Repts., reprint 2697.

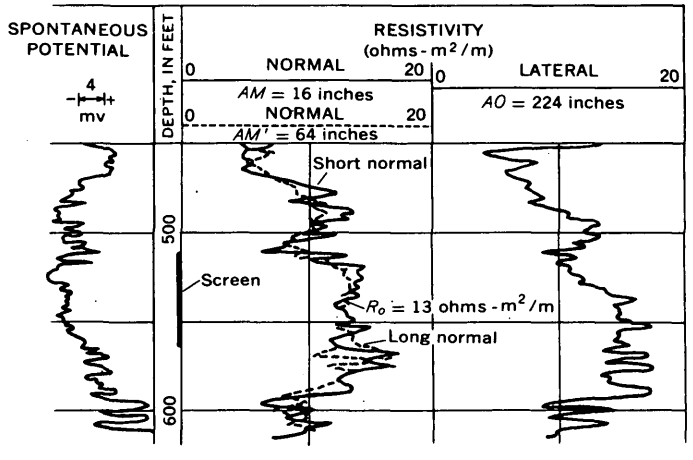

R_o = 13 ohms-m²/m at 70°F
R_o (adjusted) = 12.1 ohms-m²/m at 77°F
F_f (average) = 2.4 (from table)
$R_o/F_f = R_w$ = 5.1 ohms-m²/m or 1,950 μmhos per cm
Chloride content estimated from fig. 116.1 is 360 ppm
Chloride content from chemical analysis is 289 ppm

FIGURE 116.2.—Part of an electrical log of a water well screened opposite sand of the Wilcox Group, Caddo Parish, La.

EXPERIMENTAL HYDROLOGY

117. ADSORPTION OF ANIONIC DETERGENT ON SOLID MINERAL SURFACES

By Cooper H. Wayman, Denver, Colo.

Work done in cooperation with Federal Housing Administration

One of the chief components in commercial detergents is the anionic alkylbenzenesulfonate (ABS). This material is resistant to biological and chemical degradation and is adsorbed on solid mineral surfaces. Because of these properties ABS may persist in water supplies and contaminate ground-water aquifers. The behavior of detergent anions toward soil minerals is therefore of interest in pollution studies.

The adsorption of ABS by soil minerals has been described in other reports. Renn and Barada (1959) observed the amounts of adsorption given in table 117.1

Table 117.1.—*Adsorption of ABS on mineral surfaces*

Material	Adsorption capacity (μg ABS per g solid)
Natural stream silt	25, 000
Talc	2, 000
Precipitated $CaCO_3$	1, 400
China clay	1, 200
Diatomite	660
Silica gel	650

for solutions containing about 5.0 mg ABS per l (milligrams per liter) with the generalized formula $[C_{12}H_{25}\text{–}C_6H_4\text{–}SO_3]^{-1}$. Jenkins and Klein (1961) found that sands and sandy loams adsorbed from 1.4 to 22.1 μg ABS per g (micrograms ABS per gram) solid from a solution containing 1.0 mg ABS per l. Ewing, Lefke, and Banerji (1960) reported that "20–30 Ottawa Sand" adsorbed about 3.8 μg ABS per g sand from solutions containing 10 mg ABS per l and Robeck (1961) reported that similar sands having surface areas of 49 cm^2 per g (square centimeters per gram) and 110 cm^2 per g adsorbed 3.0 μg per g and 10–20 μg per g respectively from solutions containing 10 mg ABS per l. Actually the adsorption or desorption at a solid-liquid interface depends on a complex set of conditions. These conditions are influenced by (1) the composition of the solid mineral, (2) bulk composition of the solution, (3) surface area of the solid, (4) cross-sectional area of the solute, (5) crystalline nature of the solid and surface coatings, and (6) electrical properties of both the solid and solution. If these conditions are not well defined, the results of experiments cannot be compared.

Because few data are available on the adsorption of ABS by mineral surfaces as a function of surface area, an attempt was made to determine the adsorption of ABS on sized fractions of the "20–30 Ottawa Sand."

Theoretically, ABS is adsorbed as a monomolecular layer at the surface of sand grains. To calculate the area covered by a monomolecular layer of detergent, a molecular weight of 350 was assumed for ABS. The surface required per ion should be equivalent to the cross-sectional area of the detergent species, which has been indicated to be 20 A^2 (Meader and Criddle, 1953); A^2 represents 1 square angstrom or 10^{-16} cm^2. The number of ABS ions in 100 ml of an aqueous solution containing 10 mg ABS is

$$\frac{1 \times 10^{-2} g \times 6.02 \times 10^{23} \text{ ions per mole}}{350 \text{ g per mole}} = 1.72 \times 10^{19} \text{ ions.}$$

The surface area X, which would be covered by a monolayer of this number of ions, is the product of the number of ions and their cross-sectional area, or

$$X = \frac{20 \text{ A}^2 \times 1.72 \times 10^{19} \text{ ions}}{\text{ion}} = 34{,}400 \text{ cm}^2.$$

Thus, a total surface area of the solid (mineral) of about 34,000 cm^2, if completely covered with a monomolecular layer, can adsorb 10 mg ABS.

To determine whether theory could be correlated with experiment, the adsorption of ABS on sized fractions of the "Ottawa Sand" was investigated as a function of time. About 95 percent of this sand ranges in size from 20 to 30 mesh. After grinding and separation by screening, 25-gram samples of the original material, +140, −140 +270, −270 +325, and −325 mesh fractions, and a blank (no solid present) were agitated at room temperature (26°±1°C) with 100 ml of an aqueous solution containing 10 mg ABS. These solutions were sampled periodically and their ABS content was determined.

The surface area for each size fraction was calculated, assuming spherical particles and a median grain size between sieves; the results are given in table 117.2, where a value of 30 microns was assumed for the −325 mesh fraction. Bikerman (1958, p. 223) indicates that calculated surface areas and those measured by gase-

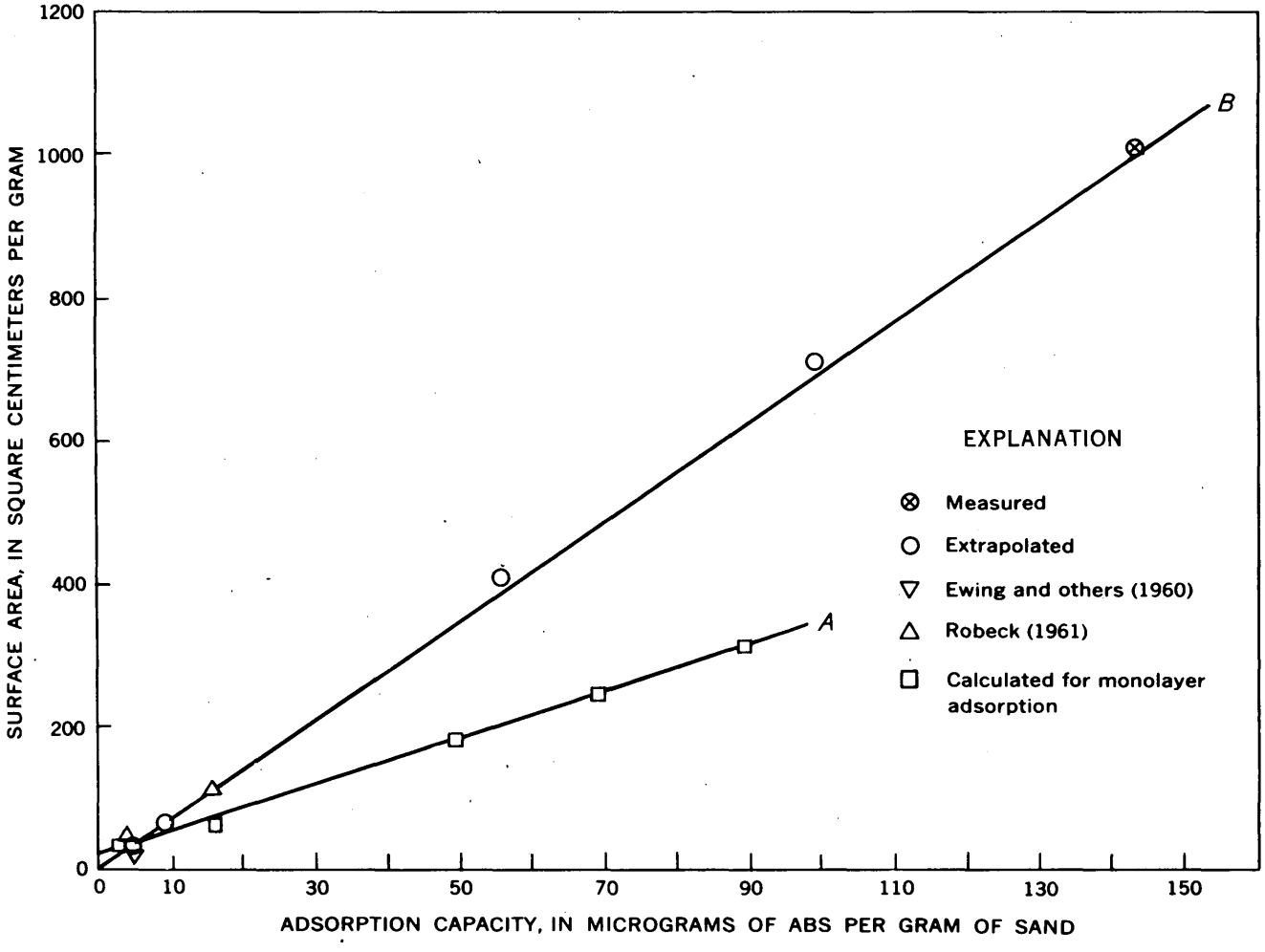

FIGURE 117.1.—Adsorption of ABS on "Ottawa Sand" as a function of surface area. *A*, adsorption capacity calculated for a monolayer; *B*, experimental results.

ous adsorption do not vary by more than a factor of 2 for silica sands of −270 mesh.

TABLE 117.2.—*Calculated surface areas and adsorption capacity of size fractions*

Mesh	Surface area (cm^2 per g)	A^2 per ion	Adsorption capacity (μg ABS per g solid)	
			Observed	Calculated
20–30	28	0.42	4	8
+140	60	.87	8	16
−140+270	400	5.78	56	112
−270+325	700	10.10	100	200
−325	1,000	14.42	144	288

The experimental results showed that an apparent equilibrium was established in about 40 hours for the −325 mesh fraction. For the amount of surface area available on 25 grams of this fraction (14.42 A^2 per ion or 25,000 cm^2), about 70 percent of the ABS could have been adsorbed assuming a monolayer of coverage. The measured adsorption was about 35 percent. In figure 117.1, the surface area is plotted against adsorption capacity for calculated monolayer adsorption (*A*) and for the experimental determination (*B*). Because equilibrium adsorption on fractions of +325 mesh was slow and because the analytical method was limited in both detection limit and reproducibility, no apparent adsorption on these fractions was observed; therefore, these fractions are shown as extrapolated values (open circles) on figure 117.1 and appear as observed values in table 117.2, where the observed and calculated adsorption capacities are compared. Data of figure 117.1 indicate that ABS in dilute solutions probably is adsorbed on coarse sand, like the "Ottawa Sand," at less than a monolayer of coverage.

The agreement between theory and experiment is considered reasonable. The proportion of surface that will be occupied by a monolayer is a function of the number of ions in solution, and other factors, and

complete coverage of the surface probably is not to be expected in this dilute system.

For sand particles having a surface area of 1,000 cm^2 per g, the observed adsorption capacity was 144 μg per g. This value is in reasonable agreement for the adsorption capacity of amorphous silica or silica gel (Ganguly, 1951). Grinding of the "Ottawa Sand" probably produced an amorphous silica layer, which has been observed by many investigators such as Gordon and Harris (1955).

Thus ABS adsorption on "Ottawa Sand" surfaces greater than 50 cm^2 per g probably takes place at less than a monolayer for dilute solutions containing up to 100 mg per l; experimental adsorption is equivalent to 50 percent of a monolayer of coverage.

REFERENCES

Bikerman, J. J., 1958, Surface chemistry: 2d ed., New York, Academic Press, 223 p.

Ewing, B. B., Lefke, L. W., and Banerji, S. K., 1960, Synthetic detergents in ground water and soils—Progress report, Sept. 1, 1959, to Nov. 30, 1960: Illinois Univ. Dept. Civil Eng.

Ganguly, A. K., 1951, Base-exchange capacity of silica and silicate minerals: Phys. Colloid Chemistry Jour., v. 55, p. 1417–1428.

Gordon, R. L., and Harris, G. W., 1955, Effect of particle size on quantitative determination of quartz by X-ray diffraction: Nature, v. 175, p. 1135.

Jenkins, D., and Klein, S. A., 1961, Sanitary Eng. Research Lab., California Univ. News Quarterly, v. 11, p. 9.

Meader, A. L., and Criddle, D. W., 1953, Force-area curves of surface films of soluble surface-active agents: Colloid Sci. Jour., v. 8, p. 170.

Renn, C. E., and Barada, M. F., 1959, Adsorption of ABS on particulate materials in water: Sewage and Indus. Wastes, v. 31, p. 850–864.

Robeck, G. G., 1961, Ground-water contamination studies at the Sanitary Engineering Center: U.S. Public Health Service Symposium on Ground-Water Contamination, Robert A. Taft Sanitary Engineering Center, Cincinnati, 1961. (Paper presented at meeting.)

118. RETENTION OF WATER IN SILTS AND SANDS

By A. Nelson Sayre and W. O. Smith, Washington, D.C.

The retention of water in soils or granular deposits such as sand, silt, or clay has been variously interpreted by scientists working in different fields. The ground-water hydrologist or the petroleum engineer desires a liquid retention as low as possible so that the maximum yield to wells may be obtained. The agronomist or forester, however, desires a high liquid retention, so that plants may draw water from the soil along with other nutrients for a long period after precipitation. The engineer concerned with the foundations for dams or the construction of levees requires a water retention high enough that the earth may be compacted, but a permeability low enough that water will move through the material slowly and thus avoid movement of the grains, which would eventually cause boils and channeling and destroy the structure. The purpose of this paper is to point out certain physical principles involved in the retention and movement of water in silts and sands.

Water may be retained in soil or granular materials by adsorption, by molecular attraction between the water and the material, and by capillarity. When water containing dissolved matter is adsorbed by a soil material, some of the dissolved material may enter into ionic exchange with some of the soil minerals, which may change the permeability of the soil. If a pebble is dipped into a tank of water, a thin film 1 or 2 molecules thick clings to the outer layer of the pebble and can be detached only by a force greater than the molecular force which causes the water to cling to the pebble. The water is not available to plants because the forces holding it to the granular material are greater than the forces exerted by the plants. The third force that causes retention of water in the soil is capillarity (Davies and Rideal, 1961, p. 1–5), which is exerted in the spaces adjacent to the points of contact between the grains of material. A part of this water is available to plants for their growth, but some is held too tightly to be moved downward by the force of gravity.

The retained water can be observed and the results can be easily photographed (figs. 118.1, 118.2). Uniform, opaque, ceramic spheres ½ inch in diameter arranged as closely as possible (in rhombohedral pattern) and only 1 layer in thickness were packed between 2 glass plates. The spheres had been cleaned

639466 O - 62 - 10

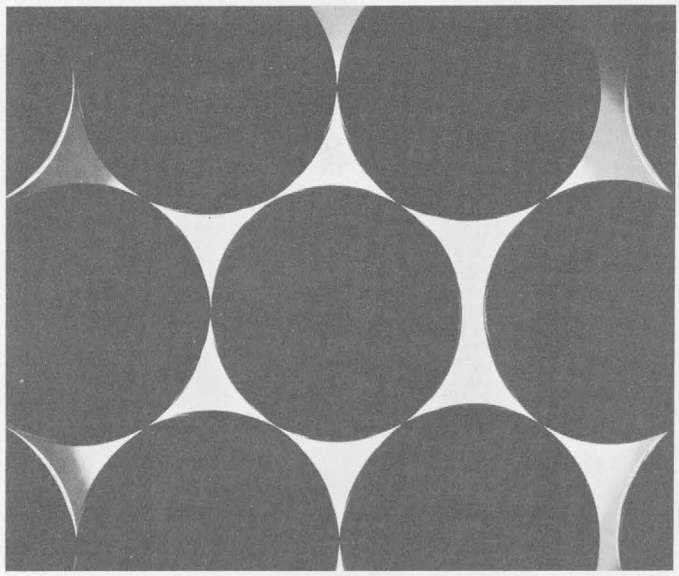

FIGURE 118.1.—Photograph of the rhombohedral packing of uniform ceramic spheres (½-inch-diameter) before wetting. There are no optical highlights at the contact points in the dry packing shown.

with a chromic acid mixture and thoroughly washed with grease-free distilled water and then dried. The model before wetting is shown in figure 118.1. The model was then immersed in water until all air was expelled. The water was then allowed to drain until no free water was apparent at the bottom of the model (fig. 118.2). The photographs were taken with lighting from the rear. Water is visible only in the areas where the spheres are in contact. The openings are triangular and the vertices of the triangles are rounded off by capillary surfaces. We conclude that the molecular pellicular water masses on the surface of the spheres as pictured by Briggs (1897) do not exist or are so thin that they are not visible in figure 118.2. This is contrary to the illustration presented by Briggs and copied by Meinzer (1923, fig. 9) and many other authors on hydrology.

This ideal soil, of course, does not exist in nature, but an approximation of an ideal soil was obtained by packing rounded grains of graded silica sand 20–24 mesh, between glass plates. This model, which would approximate the most uniform sands to be found in nature, was photographed in the same way (fig. 118.3). No pellicular layers can be seen around the individual grains of sand. In some areas where several grains of sand are closely packed, capillary water in funicular form (Versluys, 1917) remained with the sand, as shown in the circled area of figure 118.3. In other areas there were pendular rings of capillary water around the contacts between individual grains of sand as shown by the arrow in figure 118.3. However, the photograph demonstrates that even where sands are very uniform, the mathematical analysis of the geometry of pore space and of water retention is a very difficult problem that has not yet been completely solved.

REFERENCES

Briggs, L. T., 1897, The mechanics of soil moisture: U.S. Dept. Agriculture Bur. Soils Bull. 10.

Davies, J. T., and Rideal, E. R., 1961, Interfacial phenomena: New York, Academic Press.

Meinzer, O. E., 1923, The occurrence of ground water in the United States, with a discussion of principles: U.S. Geol. Survey Water-Supply Paper 489.

Versluys, J., 1917, Die Kapillarität der Boden: Inst. Mitti J. Bodenk, v. 7, p. 117–140.

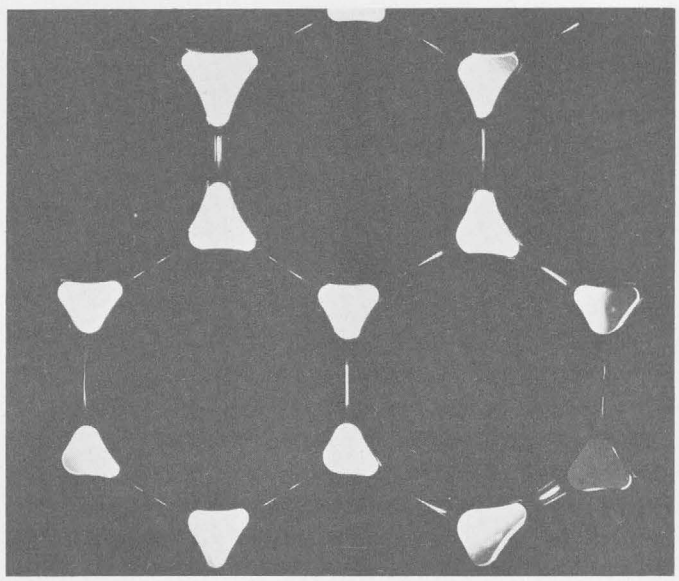

FIGURE 118.2.—Photograph of pendular water rings in the rhombohedral packing of figure 118.1. The model is freshly drained. The highlights shown in the rings are an optical effect. They arise from refraction of the light, which enters from the rear of the packing, by the pendular rings of liquid which approximate convex cylindrical lenses. The only water present is in the pendular rings surrounding the contact points, except for the uniform wetting layer a few molecules thick. Comparison with figure 118.1 indicates that thick wetting layers are not present on the grain surfaces of the freshly drained packing as shown in the drawings of Briggs (1897) and Meinzer (1923, fig. 9). Photographs by W. O. Smith, A. N. Sayre, and J. R. McKinney.

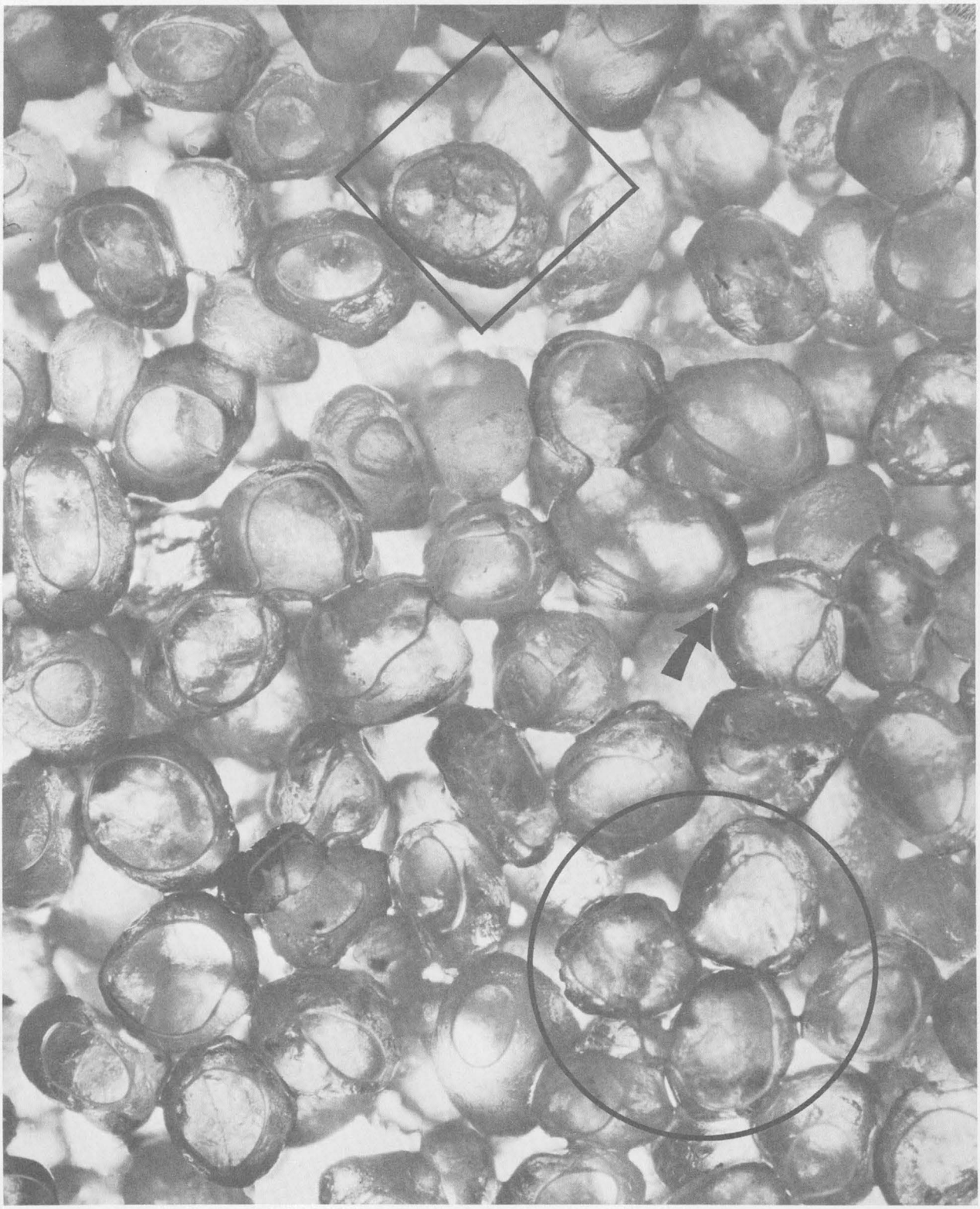

FIGURE 118.3.—Water retained in a packing of freshly drained, uniform silica sand. The sand is 20-24 mesh Standard Ottawa Silica Sand. The packing is contained between 2 glass plates about 2 mm apart. The arrow shows a pendular water ring around the contact of two adjacent grains. The circled area shows a funicular water body filling the pores between the three adjacent grains within the circle. The area within the square shows pendular water bodies retained around the contact between a grain and one of the glass plates of the containing cell. Photograph by W. O. Smith, A. N. Sayre, and J. R. McKinney.

119. VADOSE FLOW IN LAYERED AND NONLAYERED MATERIALS

By W. N. Palmquist, Jr., and A. I. Johnson, Denver, Colo.

Work done in cooperation with the U.S. Atomic Energy Commission

Water containing nuclear waste in solution is disposed of in open pits at some atomic-energy installations. The nuclear waste is free to move downward with the water to the water table, then laterally to pumping wells or streams. To protect water supplies obtained from wells or streams in the vicinity of such installations, the disposal pits must be located and operated so that either the radioactive waste will be absorbed by the granular materials beneath the pits or the length of time of travel of waste between the pit and water-supply sources will be great enough for the radioactivity of the waste to decay to harmless levels. Thus, knowledge of the rate of flow of water from disposal pits and the volume of rock encountered by the waste in its downward movement is needed for guiding disposal operations.

Studies of downward flow of water in two models of porous media were made in the Hydrologic Laboratory of the Geological Survey, Denver, Colo., to demonstrate the general patterns of flow and the volumes of material wetted beneath disposal pits.

The models were contained in a tank 5 feet high, 4 feet wide, and 3 inches thick between front and rear faces. The tank was constructed entirely of transparent acrylic plastic. Tap water from the Denver municipal supply, generally containing less than 200 parts per million of dissolved solids, was introduced into the models through a small crib 1 inch wide and 3 inches long that extended from the front to rear face of the model on the upper surface of the porous media. The water flowed at a rate sufficient to maintain the liquid pressure at 1 atmosphere across the entire area of the crib. Water flowed from the bottom of the model through 38 collector bins constructed with uniform spacing along the bottom of the tank. The shape of the wetted front at selected times of flow was marked on the plastic face of the model tank and photographed.

The first model (fig. 119.1) consisted of 1 homogeneous bed of initially dry glass beads 0.47 mm in diameter (medium-sand size). The permeability was 2,000 gpd per sq ft (gallons per day per square foot), the porosity averaged 40 percent, and the capillary rise was about 3 cm after 3 minutes elapsed time of imbibition vertically upward into an initially dry column. Water was introduced at an average rate of 50 ml per minute into the crib. After 40 minutes the flow beneath the crib had evidently reached the steady state. The wetted area was confined to a relatively narrow vertical column except near the bottom of the model, where restriction of outflow through the bins caused some lateral spread. The inflow was stopped after 55 minutes. At that time the shape of the wetted area was the same as that observed after 40 minutes.

The second model consisted of 3 beds (A, C, and E, fig. 119.2) of glass beads 0.036 mm in diameter (silt size, permeability 20 gpd per sq ft) separated by 2 beds (B and D) of beads 0.47 millimeters in diameter (medium-sand size, permeability 2,000 gpd per sq ft). Water was introduced through the top of the initially dry model at a rate of 15 ml per minute. The position

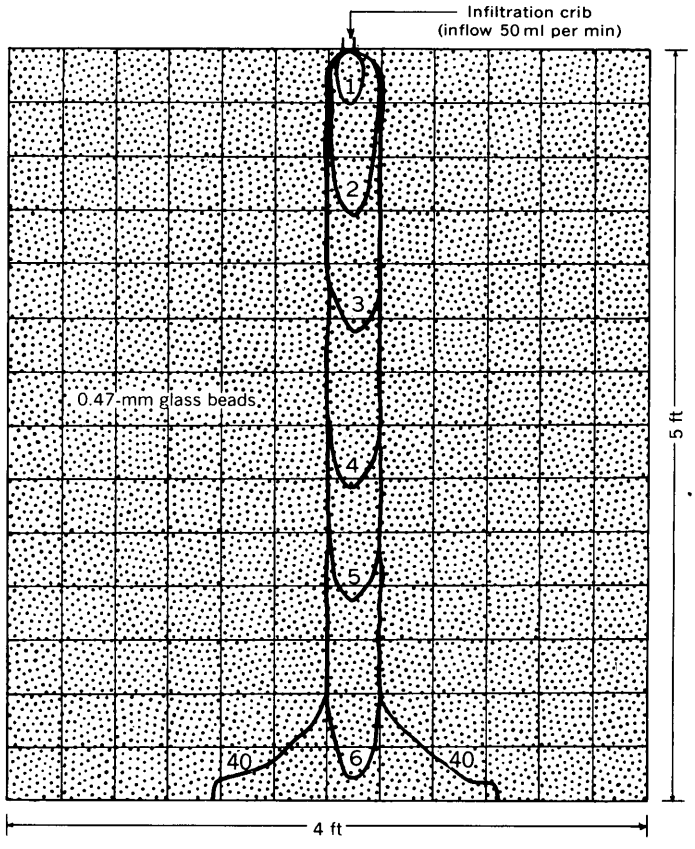

Figure 119.1.—Diagram of model tank used in first test. Heavy lines show positions of wetting front at the end of 1, 2, 3, 4, 5, 6, and 40 minutes of flow.

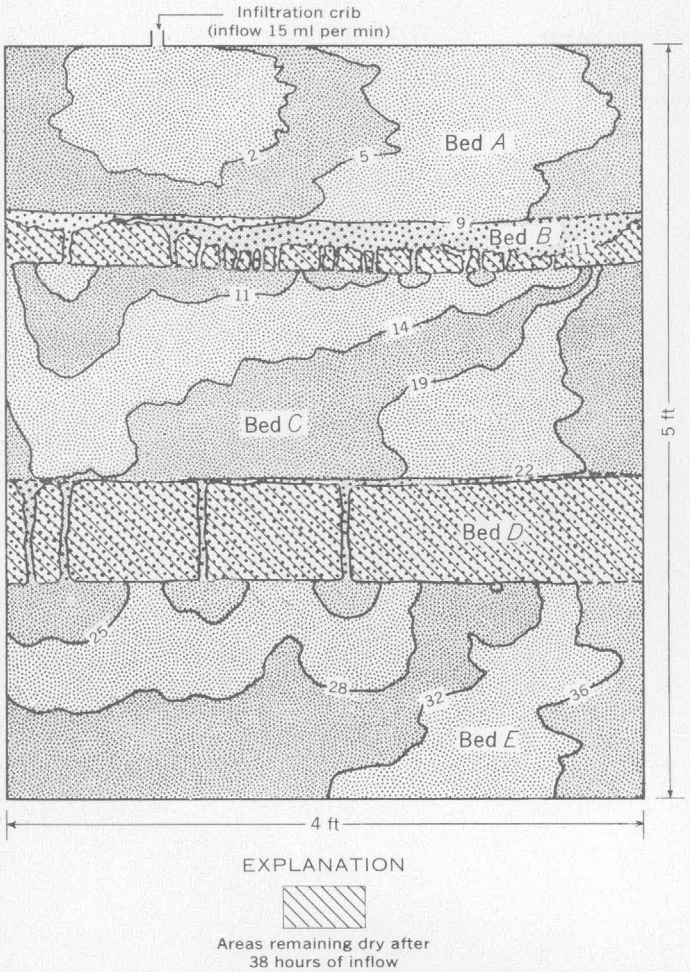

FIGURE 119.2.—Diagram of model tank used in second test. Lines show position of wetting front after selected times of infiltration, in hours. Beds *A*, *C*, and *E* are composed of 0.036-mm glass beads; beds *B* and *D* of 0.47-mm beads.

of the wetting front observed at selected times is shown in figure 119.2. The wetting front moved away from the inflow crib in bed *A* at nearly equal horizontal and vertical velocities until it reached the top of bed *B* at the end of 3 hours. Where the wetting front first reached the top of bed *B* the downward movement stopped and the front moved horizontally in bed *A*. At first water could not cross the interface between *A* and *B* because the water head in *A* was less than the value required to allow capillary flow into the pores of *B*. However, as inflow continued and the wetting front moved out laterally in *A*, the water head in *A* increased to a value high enough to allow capillary flow into *B* at a point vertically below the inflow crib. After about 8½ hours, flow from bed *A* was confined to a column 2½ centimeters wide through bed *B*. At this time about 85 percent of bed *A* was wetted and the water head had built up sufficiently so the liquid pressure was only slightly less than atmospheric at the *A*–*B* interface just below the crib.

The front moved generally into and through beds *C*, *D*, and *E* much as it had in beds *A* and *B*. After about 38 hours of inflow, bed *E* was completely wetted and water began to drain from the bottom of the model.

Under comparable hydraulic gradients, downward flow from the beds of fine beads would require only about one hundredth as much wetted area in order to pass through the beds of coarse beads. This fact accounts for the confinement of flow to relatively narrow columns in beds *B* and *D*. The spread of liquid throughout beds *B* and *D* would take place very slowly, by vapor diffusion, and ultimately these beds would have an almost uniform but much smaller liquid content than beds *A*, *C*, and *E*. After 30 days of inflow the visible water distribution in *B* and *D* was very nearly the same as that observed after 38 hours of inflow.

Although the flow tests described were not dimensionally modeled, the results indicate qualitatively that pits for the disposal of nuclear waste can be operated more safely where the underlying granular materials are highly stratified and have different grain sizes. These results apply chiefly to arid regions where the deposits above the water table contain very little moisture to great depths, and to disposal pits in which the distance across the pit surface is only a few tens of feet. At many places where the deposits in the unsaturated zone are naturally very moist, and the size of the disposal pits is of the order of hundreds of feet, lateral spread of the waste-carrying water may not be an important control on the movement of waste products.

SELECTED REFERENCES

Aronovici, V. S., 1955, Model study of ring infiltrometer performance under low initial soil moisture: Soil Sci. Soc. America Proc., v. 19, p. 1–6.

Hansen, V. E., 1955, Infiltration and soil water movement during irrigation: Soil Sci., v. 79, p. 93–105.

Richards, L. A., 1950, Laws of soil moisture: Am. Geophys. Union, v. 31, p. 750–753.

——— 1952, Water conducting and retaining properties of soils in relation to irrigation: Internat. Symposium on Desert Research, Jerusalem 1952, Proc., 22 p.

Taylor, S. A., 1957, Use of moisture by plants, *in* Soils, the 1957 yearbook of agriculture: U.S. Dept. Agriculture, p. 61–66.

SUBJECT INDEX

[For major topic headings such as "Economic Geology," "Stratigraphy," "Ground Water," see under State names or refer to "Table of Contents"]

Note—Numbers refer to articles.

Note—Numbers refer to articles.

AUTHOR INDEX

Note—Numbers refer to articles.

U. S. GOVERNMENT PRINTING OFFICE : 1962 O - 639466